THE UNIVERSITY *of* EDINBURGH

This thesis has been submitted in fulfilment of the requirements for a postgraduate degree (e.g. PhD, MPhil, DClinPsychol) at the University of Edinburgh. Please note the following terms and conditions of use:

This work is protected by copyright and other intellectual property rights, which are retained by the thesis author, unless otherwise stated.
A copy can be downloaded for personal non-commercial research or study, without prior permission or charge.
This thesis cannot be reproduced or quoted extensively from without first obtaining permission in writing from the author.
The content must not be changed in any way or sold commercially in any format or medium without the formal permission of the author.
When referring to this work, full bibliographic details including the author, title, awarding institution and date of the thesis must be given.

Cellular models to study the emergence, expansion and differentiation of pancreatic progenitor cells in vitro

Colin Plumb

THE UNIVERSITY
of EDINBURGH

Submitted for the degree of Doctor of Philosophy in Regenerative Medicine

The University of Edinburgh

2018

Lay summary

Diabetes is the disease caused when your body is no longer able to control the glucose levels in your blood. Normally, your pancreas is the organ responsible for regulating glucose. Within areas of the pancreas known as 'islets' reside highly specialised cells called β-cells; β-cells can detect high levels of glucose in the blood and release a hormone called insulin in response. Insulin acts as a chemical messenger to the rest of your body, instructing cells in the liver, fat, and muscle to absorb the excess glucose in the blood, which can then be stored or used for energy. Having persistently high blood glucose levels can lead to a whole host of complications and on average, people diagnosed with diabetes tend to lead shorter lives than people without diabetes.

Current treatments for diabetes are generally limited to insulin injections for Type 1 diabetics, and medication for Type 2 diabetics designed to increase the amount and effectiveness of the insulin released by their pancreas. However, there is another treatment option that is rarely used – the islet transplant. The islet transplant is an example of a 'cell therapy', where islets containing β-cells are taken from a donor pancreas and injected into a diabetic recipient. Once transplanted, β-cells can detect glucose and release insulin, as they do in a healthy pancreas. Islet transplants can be effective in improving the quality of life for severe Type 1 diabetics, and may even allow them to stop taking insulin injections altogether. The main barrier to making islet transplants more widely available has been a shortage of donor organs.

In an effort to bypass the reliance on pancreases from deceased donors, many scientists have been researching ways of generating insulin-producing β-cells in the lab. Human embryonic stem cells (hESCs) are viewed as the ideal alternative source of islet cells; hESCs are capable of generating every cell type of the body, but this depends on researchers providing hESCs with the right signals to tell them what to do. hESCs must first be instructed to produce pancreas stem cells, and then given further cues to become β-cells. Scientists have made considerable progress in discovering the correct cues to permit efficient production of pancreas stem cells, but we can only inefficiently generate insulin-producing β-cells.

To understand how to better induce this switch from pancreas stem cell to islet cell, it would be beneficial for researchers to have a consistent, unlimited supply of pancreas stem cells to study, without the need to make them fresh from hESCs every time. However, no simple, good quality supply of pancreas stem cells exists. In this thesis, WE describe simple methods for isolating and culturing large quantities of pancreas stem cells from the developing mouse and human foetal pancreas, as well as a hESC tool we have generated. These cellular models should provide a consistent source of cells for future researchers to work on in efforts to improve islet cell production in the lab. Eventually, these cells could be used to treat diabetes.

Abstract

Cell transplantation of pancreatic islets has been proven to be an effective long-term treatment for Type 1 diabetes. However, the lack of sufficient cadaveric donor tissue has prevented widespread clinical adoption of cell therapy. An alternative source of cells would be hugely beneficial in overcoming this donor shortage. Cells of the islets arise during development from a shared precursor cell – the $NGN3^+/NEUROD1^+$ pancreatic endocrine progenitor. Over the past decade, human embryonic stem cells (hESCs) and induced pluripotent stem cells (iPSCs) have been the main focus for providing an alternative source of pancreatic cell types for transplant. While differentiation to $PDX1^+/SOX9^+$ early pancreas progenitor cells has been successful, efficient differentiation to endocrine progenitors and mature islet cells has not been achieved. This suggests that we lack the knowledge to correctly and effectively specify an endocrine fate in hES-derived pancreas cells. It was the aim of this thesis to describe simple methods for culturing authentic pancreas progenitor cells from mouse and human foetal pancreas tissue, with which we could study the biology of these progenitor cells to ultimately inform better hESC differentiation protocols, and which may also be useful for cell therapy in their own right.

To achieve these aims, we have taken three approaches. First, we provide characterisation of early pancreas progenitors during human foetal pancreas development, and how expression of key markers changes over time. Second, we describe methods for isolating and expanding mouse and human foetal pancreas progenitors, producing new cellular models with which to investigate the specification of endocrine cell fate. Finally, we generated an hESC reporter line to allow for easier identification of conditions that induce hESC-derived pancreatic endocrine progenitors in vitro.

We have described the precise timing of the transition from early pancreas progenitor to endocrine progenitor in the developing human and mouse foetal pancreas. Using this information, we have pinpointed the stages of foetal development when mouse and human have the maximum potential proliferative capacity. Using samples from these developmental stages, we demonstrate that $PDX1^+/SOX9^+$ human and mouse foetal progenitors can be isolated and expanded long-term in monolayer in defined conditions. Cultured mouse foetal pancreas progenitors can be induced to differentiate to endocrine progenitors in vitro. We also generated a novel NGN3-GFP/CyclinB1-Cherry hESC reporter line, which allows identification of emerging endocrine progenitor cells and their proliferative capacity.

The new cellular models presented here are ideally suited for many downstream applications including high-throughput pharmacological screens and imaging assays. Studies using these systems will help improve our understanding of human pancreatic endocrine progenitor specification and harness these cells in new types of cell therapies for diabetes.

Acknowledgements

I would first like to acknowledge my supervisors Dr Gillian Morrison and Prof Steve Pollard for guiding me through this PhD. To Gillian, thank you for giving me the opportunity to start this journey, teaching me so many things, and for your continued help and advice, even when you had taken on new responsibilities. To Steve, thank you for generously agreeing to take me on and advising me when you didn't have to, so I could see the journey out to the end. I must also thank all members of the Pollard lab, who have been accommodating, supportive and most importantly provided a wonderful atmosphere to work in.

Projects rarely work out the way you planned, and PhDs are the greatest proof of that. It's been an exercise in how to cope with pressure and stress, and that has surely made me a better person. Still though, it helps to have good people around you when you're low, so I'm grateful to all the friends I've made in SCRM. I'll miss you all and our lunchtime laughs greatly.

Without my parents I would never have been in a position to do this PhD. They took a huge risk coming to the UK so many years ago to build a new life from nothing, so I owe all my success to their hard work. Finally, to Ashley – thanks for making Scotland feel like home, and for being the best adventure partner I could wish for. Here's to the next one.

Declaration of originality

I declare that this thesis has been composed solely by myself and that it has not been submitted, in whole or in part, in any previous application for a degree. Except where stated otherwise by reference or acknowledgment, the work presented is entirely my own.

Thursday, August 23 2018

List of abbreviations

A83	A83-01 (TGFβ receptor inhibitor)
AMY	amylase
ANOVA	analysis of variance
BMP	bone morphogenetic protein
CDB	cyclinB1 destruction box
CDK	cyclin dependent kinase
CDKN	cyclin dependent kinase inhibitor
cDNA	complementary deoxyribonucleic acid
CHIR	CHIR99021 (GSK3 inhibitor)
CPA	carboxypeptidase
CT	cycle threshold
DAPI	4',6-diamidino-2-phenylindole
DE	definitive endoderm
DNA	deoxyribonucleic acid
dpc	days post-conception
E-cad	E-cadherin
EDTA	ethylenediaminetetraacetic acid
EF2	EGF+FGF2
EF7	EGF+FGF7
EGF	epidermal growth factor
EMT	epithelial-to-mesenchymal transition
FACS	fluorescence-activated cell sorting
FGF	fibroblast growth factor
FGFR	fibroblast growth factor receptor
FOV	field of view
GDM	gestational diabetes mellitus
gDNA	genomic deoxyribonucleic acid
GFP	green fluorescent protein
GLU	glucagon
H&E	haemotoxylin and eosin
HDR	homology-directed repair
hESC	human embryonic stem cell
ICC	immunocytochemistry
IHC	immunohistochemistry

INS	insulin
iPSC	induced pluripotent stem cell
ITS-X	insulin-transferrin-selenium-ethanolamine
MODY	maturity onset diabetes of the young
LDN193	LDN193189 (BMP inhibitor)
mRNA	messenger ribonucleic acid
MS7	MasterShef7 hESCs
ND	not determined or not detectable
NS	neural stem
PB	PiggyBac
PBS	phosphate buffered saline
PFG	posterior foregut
PI103	PI3K family inhibitor
PI3K	phosphatidylinositol 3 kinase
PKC	protein kinase C
PP	pancreatic polypeptide
RA	retinoic acid
RNA	ribonucleic acid
ROCKi	Rho kinase inhibitor
RT-qPCR	reverse transcription quantitative polymerase chain reaction
SANT1	Hedgehog/Smoothened inhibitor
T1D	Type 1 diabetes
T2D	Type 2 diabetes
T3	triiodothyronine
TPB	(2S,5S)-(E,E)-8-(5-(4-(trifluoromethyl)phenyl)-2,4-pentadienoylamino)benzolactam (PKC activator)
VIM	vimentin
WT	wild type
ZFN	zinc finger nuclease
$ZnSO_4$	zinc sulphate

List of figures and tables

Figure 1. Mouse and human islet composition and cell distribution. 5

Figure 2. Inter-regulation of cells within the islet. 17

Figure 3. Overview of pancreas organogenesis. 20

Figure 4. Markers expressed by progenitor cell types during pancreas development. 28

Figure 5. Documented sources of multipotent pancreatic progenitor cells. 46

Figure 6. mRNA expression of *PDX1* and *SOX9* in whole human foetal pancreas. 69

Figure 7. mRNA expression of *NGN3* and *NEUROD1* in whole human foetal pancreas. 72

Figure 8. H&E staining of human foetal pancreas. 75

Figure 9. PDX1 and SOX9 expression in human foetal pancreas. 77

Figure 10. Total nuclei measured and example staining intensity cut-offs. 80

Figure 11. PDX1 and SOX9 positivity at the cellular level in human foetal pancreas at different stages of development. 82

Figure 12. PDX1 and SOX9 staining intensity in sections of human foetal pancreas at different stages of development. 84

Figure 13. NKX2.2 expression in foetal and adult human pancreas. 89

Figure 14. Proposed mechanisms of PDX1 and SOX9 regulation in human foetal pancreas progenitors. 90

Figure 15. mRNA expression of key developmental genes in developing mouse foetal pancreas. 95

Figure 16. Whole mouse foetal pancreas culture strategy. 99

Figure 17. mRNA expression in different whole mouse foetal pancreas culture methods. 100

Figure 18. Ngn3 mRNA expression in whole mouse foetal pancreas culture in N2B27 and EF7. 103

Figure 19. mRNA expression in whole mouse foetal pancreas culture in EF7 and EF7+UC2288. 105

Figure 20. Dissociated mouse foetal pancreas culture strategy. 106

Figure 21. Mouse foetal pancreas growth in N2B27. 107

Figure 22. Mouse foetal pancreas growth in EF2. 109

Figure 23. Mouse foetal pancreas growth in EF7. 109

Figure 24. Mouse foetal pancreas growth in EF2+A83. 111

Figure 25. Mouse foetal pancreas growth in EF7+A83. 112

Figure 26. Cells expanded in EF7+A83 are $Pdx1^+/Sox9^+$ at p0. 114

Figure 27. Cells expanded in EF7+A83 are $E\text{-}cad^+$ at p0. 116

Figure 28. Mouse foetal pancreas progenitors sorted based on E-cad. 119

Figure 29. $E\text{-}cad^+$ mouse foetal pancreas cells are $Pdx1^+/Sox9^+$ progenitors. 120

Figure 30. $E\text{-}cad^+$ mouse foetal pancreas progenitors can be cultured long-term. 122

Figure 31. mRNA expression in $E\text{-}cad^+$ mouse foetal pancreas progenitors at p12. 124

Figure 32. mRNA expression in $E\text{-}cad^+$ mouse foetal pancreas progenitors in EF7+A83 vs differentiation medium. 127

Figure 33. $E\text{-}cad^+$ mouse foetal pancreas progenitors are amenable to genetic engineering. 130

Figure 34. Dissociated human foetal pancreas culture strategy. 138

Figure 35. FT3506 human foetal pancreas growth in culture. 141

Figure 36. FT3508 human foetal pancreas growth and mRNA expression in culture. 144

Figure 37. FT3509 human foetal pancreas growth and mRNA expression in culture. 148

Figure 38. FT3520 human foetal pancreas growth and mRNA expression in culture. 151

Figure 39. FT3521 human foetal pancreas growth and mRNA expression in culture. 154

Figure 40. PDX1 and SOX9 expression in FT3509 human foetal pancreas cultures. 156

Figure 41. E-cad expression in FT3509 human foetal pancreas cultures. 158

Figure 42. Isolation of $E\text{-}cad^+$ FT3509 human foetal pancreas cells by EDTA passaging. 161

Figure 43. PDX1, SOX9 and E-cad expression in EDTA-passaged FT3509 human foetal pancreas cultures. 162

Figure 44. Ki67 expression in E-cad$^+$ human foetal pancreas progenitors. 164

Figure 45. Protocol for MS7 hESC differentiation to pancreas progenitor cells. 171

Figure 46. MS7 differentiated to DE. 172

Figure 47. MS7 differentiated to foregut. 174

Figure 48. MS7 differentiated to early pancreatic progenitors. 176

Figure 49. MS7 differentiated to endocrine pancreas progenitors. 177

Figure 50. Targeting strategy for creating NGN3-GFP knock-in. 179

Figure 51. MS7 nucleofection and clonal culture strategy 181

Figure 52. PCR genotyping of nucleofected MS7 clones. 183

Figure 53. Cre-mediated excision of selection cassette in MS7 NGN-GFP. 185

Figure 54. Schematic for fluorescent readouts of proliferating NGN3-GFP/CDB-Cherry endocrine progenitors. 187

Figure 55. Generation of aatB1-CDB-Cherry-aatB2 PCR product. 188

Figure 56. Gateway cloning of CycB1-Cherry into pDEST vector. 190

Figure 57. Overnight imaging of MS7 NGN3-GFP/CDB-Cherry. 192

Figure 58. Cell cycle analysis by flow cytometry of MS7 NGN3-GFP/CDB-Cherry. 193

Figure 59. MS7 NGN3-GFP/CDB-Cherry differentiated to DE. 195

Figure 60. MS7 NGN3-GFP/CDB-Cherry differentiated to foregut. 196

Figure 61. MS7 NGN3-GFP/CycB1-Cherry differentiated to early pancreatic progenitors. 198

Figure 62. MS7 NGN3-GFP/CycB1-Cherry differentiated to endocrine pancreas progenitors. 199

Table 1. Number of fields of view (FOVs) used for image analysis of PDX1/SOX9 staining of human foetal pancreas. 79

Table 2. CT values detected by qPCR for E-cad$^+$ mouse foetal progenitors p12. . 125

Table 3. CT values detected by qPCR for E-cad$^+$ mouse foetal progenitors in differentiation media. 128

Table 4. Human foetal pancreas tissue samples used for culture 140

Table of contents

Lay summary i

Abstract ii

Acknowledgements iii

Declaration of originality iv

List of abbreviations v

List of figures and tables vii

Table of contents x

CHAPTER 1 Introduction 1

1.1 Development and function of the mammalian pancreas 1

1.1.1 Pancreas anatomy and phylogeny 1

1.1.2 Exocrine pancreas 2

1.1.3 Endocrine pancreas 4

1.1.4 Development of the pancreas 18

1.2 Diabetes 29

1.2.1 Types of diabetes 30

1.2.2 Type 1 diabetes 31

1.2.3 Type 2 diabetes 34

1.3 Cell therapies for diabetes 38

1.3.1 Regenerative medicine and diabetes 38

1.3.2 The Edmonton protocol 38

1.3.3 hESC-based therapies 40

1.4 Pancreas progenitor cells 42

1.5 Aims 47

CHAPTER 2 Materials and methods 48

2.1 Collection and processing of foetal pancreas 48

2.1.1 Collection of human foetal pancreas 48

2.1.2 Collection of mouse foetal pancreas 48
2.1.3 Fixation and embedding of foetal pancreas 49
2.1.4 Lysis of foetal pancreas and RNA extraction 49
2.2 Immunostaining 50
2.2.1 Immunocytochemistry 50
2.2.2 Immunohistochemistry 50
2.2.3 Antibodies 52
2.2.4 Image processing and analysis 52
2.3 Flow cytometry 52
2.3.1 Cell preparation and reagents 52
2.3.2 Flow cytometers and data analysis 53
2.4 Molecular biology techniques 54
2.4.1 RNA and DNA extraction 54
2.4.2 First strand cDNA synthesis 54
2.4.3 Primer design 55
2.4.4 Human RT-qPCR primers 55
2.4.5 Mouse RT-qPCR primers 56
2.4.6 PCR (polymerase chain reaction) 57
2.4.7 RT-qPCR (reverse transcription quantitative polymerase chain reaction) 57
2.4.8 Primer efficiency 58
2.4.9 Agarose gel electrophoresis 59
2.5 Mammalian cell and tissue culture 59
2.5.1 Culture of hESCs (human embryonic stem cells) 59
2.5.2 Differentiation of hESCs to pancreas progenitors 60
2.5.3 Culture of mouse foetal pancreas (whole) 60
2.5.4 Culture of mouse foetal pancreas (dissociated) 61
2.5.5 Culture of human foetal pancreas (dissociated) 62

2.5.6 Transfections and plasmid details 63

2.6 Bacterial cell culture, transformations and extracting plasmid DNA 63

2.6.1 Bacterial transformations and culture 63

2.6.2 Extracting plasmid DNA 64

2.7 Statistical analysis 64

CHAPTER 3 Characterising expression of key genes and proteins during human foetal pancreas development 65

3.1 Introduction 65

3.2 Results 67

3.2.1 Gene expression analysis of whole human foetal pancreas during early to mid-development 67

3.2.2 Histological characterisation of human foetal pancreas during early to mid-development 73

3.2.3 PDX1/SOX9 protein co-expression in human foetal pancreas during early to mid-development 76

3.2.4 Quantitative analysis of PDX1 and SOX9 cell populations in the developing human foetal pancreas 78

3.3 Discussion 85

CHAPTER 4 New methods for expansion of proliferative mouse foetal pancreas progenitors in defined monolayer conditions 91

4.1 Introduction 91

4.2 Results 94

4.2.1 Determining the spatial and temporal control of key pancreatic master regulators during mouse development 94

4.2.2 Using whole E12.5 mouse foetal pancreas to assess culture conditions for suppressing endocrine progenitor emergence 98

4.2.3 Establishing adherent monolayer culture conditions to allow expansion of E12.5 mouse foetal pancreas progenitors 106

4.2.4 Assessment of pharmacological inhibitors to improve the expansion of epithelial-like candidate progenitors 110

4.2.5 Characterising epithelial-like candidate progenitor cells expanded in monolayer 113

4.2.6 Mouse foetal pancreas progenitors can be isolated based on E-cadherin expression and cultured long-term 115

4.2.7 FACS-isolated mouse foetal pancreas progenitors remain functionally viable and are amenable to genetic engineering 126

4.3 Discussion 131

CHAPTER 5 Culture of human foetal pancreas progenitors in vitro 134

5.1 Introduction 134

5.2 Results 137

5.2.1 Human foetal pancreas progenitors from week 8–12 tissue can be cultured and expanded long-term 137

5.2.2 E-cadherin can be used to isolate cultured human foetal pancreas progenitors 157

5.2.3 Conditioned medium does not enhance proliferation of isolated E-cad^{+} human foetal pancreas progenitors 163

5.3 Discussion 165

CHAPTER 6 Generating a hESC line to identify conditions for promoting hES-derived endocrine progenitor emergence and expansion in vitro 168

6.1 Introduction 168

6.2 Results 170

6.2.1 Differentiation capacity of MasterShef7 hESCs 170

6.2.2 Generating an NGN3-GFP reporter hESC 178

6.2.3 Generating an NGN3-GFP/CDB-Cherry reporter hESC 186

6.2.4 NGN3-GFP/CDB-Cherry reporter hESCs retain the differentiation capacity of WT MasterShef7 hESCs 194

6.3 Discussion 200

CHAPTER 7 Discussion 202

References 208

CHAPTER 1
Introduction

1.1 Development and function of the mammalian pancreas

1.1.1 Pancreas anatomy and phylogeny

The pancreas is a glandular organ located behind the stomach in the abdomen of vertebrates. In humans, it has a tapered structure – a wide 'head' adjacent to the duodenum extends and narrows into the 'tail' of the organ that is situated near the spleen. The vertebrate pancreas possesses both exocrine and endocrine glands, which help to regulate the digestive system and blood glucose metabolism, respectively. Exocrine cells comprise the bulk of pancreas tissue and secrete digestive enzymes into a highly branched ductal network that feeds into a single main duct. The major pancreatic duct joins the common bile duct, and through this route supplies the duodenum with pancreatic juice to aid digestion. Several pancreatic endocrine cell types exist and are located in aggregates called pancreatic islets. Islets are highly vascularised enabling hormone secretion into the bloodstream.

The evolutionary origin of a discrete pancreatic organ can be traced back to jawless vertebrates, such as lampreys and hagfish. In these animals, aggregates of hormone-secreting endocrine cells are detectable by immunocytochemistry, and are situated adjacent to, but separate from, the gut lumen [1]. In contrast, more primitive animals such as amphioxus possess endocrine cells that are interspersed throughout the gut epithelium [1]. Interestingly, the primitive pancreas-like clusters of lampreys and hagfish do not contain exocrine cells, with zymogen-containing cells still localised to the gut epithelium [2], suggesting separate origins of exocrine and endocrine structures.

The earliest jawed vertebrates known to have a distinct pancreas integrating both endocrine and exocrine functions are the cartilaginous fish. The pancreas in this class of fish is broadly comparable to the mammalian pancreas in cellular composition and physiological function [3]. Bony fish, the other major branch of early jawed vertebrates and the ancestors of mammals, also exhibit islet structures scattered throughout exocrine tissue [2]. While various differences in pancreas anatomy and ontogeny are identifiable within vertebrates [4-6] (discussed later in this Chapter), the core functions of the vertebrate pancreas are well conserved from early tetrapod vertebrates to humans [7].

1.1.2 Exocrine pancreas

The exocrine pancreas is the larger of the two glandular compartments, making up 85% of the tissue mass in humans [8]. The exocrine pancreas includes the epithelial cells lining the ductal network of the pancreas and secretory cells clustered into acini. Acini are the basic functional units of the exocrine pancreas. They secrete digestive enzymes into a small lumen, which drains into interlobular ducts, and then onward to the main pancreatic duct.

As would be expected of secretory cells, acinar cells are structurally defined by extensive rough endoplasmic reticulum and zymogen granules that contain digestive enzymes, largely stored in inactive forms. Microvilli also line the apical surface of acinar cells to aid drainage of secretions into the ductal network. Acinar cell secretions contain an abundance of amylases, proteases, lipases and nucleases to further break down the chyme that is passed from the stomach into the duodenum, and it is here that most digestive enzymes are converted into active forms [7,8]. Zymogen release from acinar cells is regulated by neurotransmitter signals between pancreatic neural networks and acinar cells, and also through hormone signalling. Cholecystokinin

(CCK) and secretin are two prominent examples of hormones with corresponding receptors on acinar cells. CCK and secretin modulate the secretion of zymogen and other elements of pancreatic juice in response to a food stimulus [9].

Pancreatic ducts are lined with columnar or cuboidal epithelial cells that contain ample mitochondria to fuel ion transport for the ductal cell contribution to pancreatic juice. Important secretions of the ductal cells are water, to facilitate the transport of enzymes in the lumen, and sodium bicarbonate ($NaHCO_3$). The high concentrations of $NaHCO_3$ produced by ductal cells serve to neutralise the acidic chyme and provide an optimal working pH for acinar-derived digestive enzymes in the duodenum [7,8].

Centroacinar cells are specialised ductal cells that, in mammals, are found at the sites where cuboidal or columnar ductal cells meet acini [10]. Centroacinar cells are thought to share the functional properties of normal ductal cells, such as $NaHCO_3$ release. However, they can be distinguished from normal ductal cells by their morphology; centroacinar cells extend long cytoplasmic processes towards other nearby exocrine cells to form tight junctions in zebrafish pancreas [11]. The specific function of these extensions and the cell-cell contacts they create are unclear, but centroacinar cell cytoplasmic processes also reach to endocrine cells in rat and zebrafish islets [11,12]. Due to this, and also because of lineage tracing experiments, it has been suggested that they play a role in regenerating depleted cell types in the adult pancreas following injury, including endocrine cells [11]. Lineage tracing was conducted in zebrafish though, where the pancreas is known to be highly regenerative and centroacinar cells much more numerous compared to mammals [10]. Thus, the role of centroacinar cells in regenerating injured adult mammalian pancreas remains very contentious, with many contradictory studies, see reviews elsewhere [10].

Rarer cell types also support the function of the exocrine pancreas. Mucus-secreting goblet cells comprise 5-30% of cells lining the main pancreatic duct, with their proportion increasing with proximity to the bile duct [13]. Pancreatic stellate cells make up 4% of all pancreas cells in rat and can be seen adjacent to the basal side of acinar cells [14]. Stellate cells appear to have many functions in the pancreas. In adult rat and human, pancreatic stellate cells are characterised by the presence of vitamin A-storing lipid droplets [15], and there is evidence to suggest they help stimulate acinar cell secretions through acetylcholine signalling in response to CCK [16]. However, upon injury (and in culture) stellate cell functions are thought to switch to promoting fibrosis by expressing large quantities of collagen, fibronectin and laminin [15].

1.1.3 Endocrine pancreas

The endocrine cells of the pancreas are found in roughly spherical structures called islets dispersed within the exocrine tissue. The limited data on healthy adult human islets suggest that they account for approximately 4.5% of the total volume of the pancreas. Islets are mostly scattered uniformly throughout pancreas, between the head and tail, although the head of the pancreas additionally contains sizeable clusters of islets gathered around large blood vessels [17].

Mammalian islets are composed of five endocrine cell types: α-cells, β-cells, δ-cells, ε-cells and PP-cells (occasionally called γ-cells). Each cell type secretes a different hormone, and collectively these regulate processes including blood glucose homeostasis, exocrine pancreas secretions, appetite and the response of the digestive system to food [18-21]. The relative proportions of these cells within islets, and of islet architecture itself, varies even within mammals [22,23] **(Figure 1)**. In the following sections, the functions of each islet cell type in humans and rodents will be described.

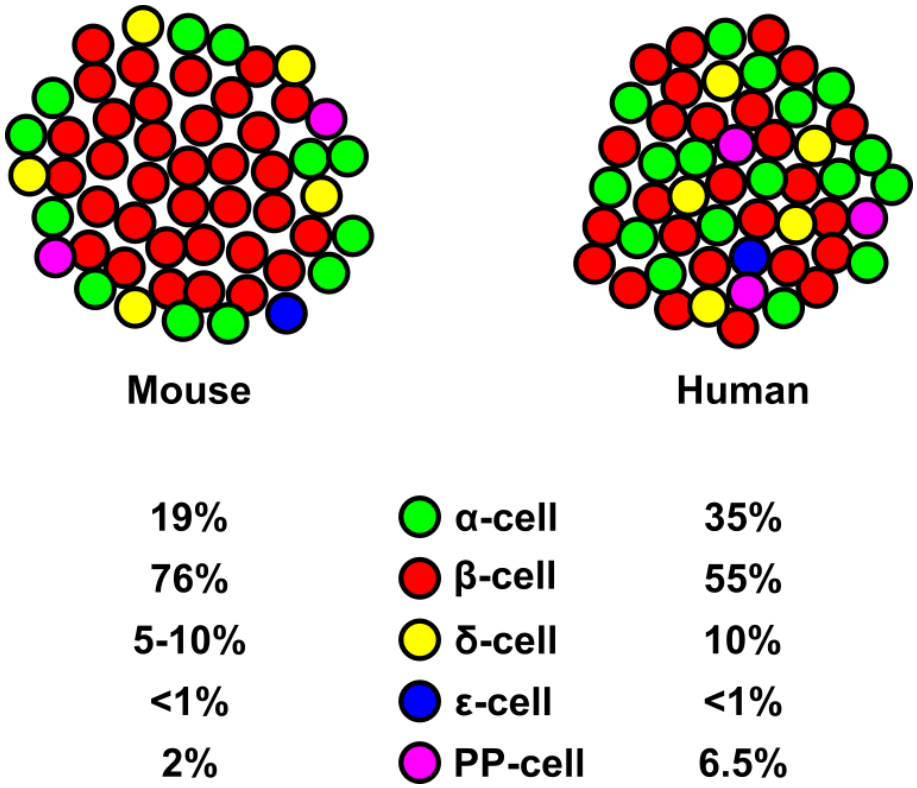

Figure 1. Mouse and human islet composition and cell distribution.

Note that cell proportions are approximate and may not total 100% due to being calculated across multiple studies.

1.1.3.1 α-cells

α-cells secrete glucagon, a hormone which stimulates increased blood glucose levels. On average, 35% of human islet cells are α-cells. In contrast, the proportion of α-cells in mouse islets is lower (19% average) [22-24]. α-cell distribution within islets also differs between mouse and human; mouse α-cells exist at the periphery of spherical islets, whereas they are distributed evenly throughout human islets [22,23]. Preliminary indications are that these species differences have functional implications. For example, cultured intact human and monkey islets were found to produce α-cell secretory responses in low glucose conditions whereas no response was detected in mouse islets [23]. Presumably the higher proportion of α-cells in primate islets is the reason for their enhanced sensitivity to low glucose concentrations.

Preproglucagon is encoded by the GCG gene which, through post-translational processing, can generate a variety of cell-type-specific hormones and peptides with varying functions [25]. In α-cells, expression of the prohormone convertase 2 (PC2) enzyme catalyses proglucagon conversion to glucagon [26]. Glucagon release from α-cells occurs passively; in vitro, α-cells fire continuous action potentials triggering hormone exocytosis [27]. Cholinergic and adrenergic stimulation of α-cells by neurons can enhance exocytosis in vivo [28,29]. Recently, expression of the G protein-coupled receptor *GPR119* was found to be enriched in mouse and human α-cells [30,31], and GPR119 agonists enhance glucagon secretion in mice in vitro and in vivo [32]. Putative endogenous ligands of GPR119 include 2-oleoylglycerol and oleoylethanolamide [33,34], both products of fat digestion. GPR119 may therefore ensure maximal glucagon secretion in the event of high-fat, low-glucose meals. Once in the circulation, glucagon's primary action is on hepatocytes. By upregulating expression of enzymes involved in the gluconeogenesis pathway glucagon stimulates glucose synthesis in

hepatocytes [35,36]. In parallel, conversion of glucose to glycogen for storage is halted by the phosphorylation and resultant inhibition of the glycogen synthase enzyme [37], thus promoting further glucose release into the blood.

Hyperglycaemia has a direct negative feedback effect on glucagon release by α-cells through a mechanism where extracellular glucose concentration is coupled to α-cell electrical activity by ATP-dependent potassium channels (K_{ATP} channels). Extracellular glucose is imported into α-cells by the membrane-bound Glut1 transporter in rats [38]. In cultured mouse and human islets, increasing glucose concentration leads to a higher rate of glucose metabolism and ATP production in α-cells. ATP blocks K_{ATP} channels, causing failure of action potentials to trigger glucagon release by exocytosis [39]. Paracrine signals from neighbouring islet cells also appears to inhibit glucagon release, although this means of regulation is at least partially dependent on blood glucose levels too [40]. In cultured rodent islets, insulin blocked glucagon secretion in a K_{ATP} channel-dependent manner [41,42]. Furthermore, somatostatin from δ-cells negatively influences glucagon release in mice [20], where somatostatin secretion is thought to be induced by electrical signal conductance between β-cell-δ-cell gap junctions [40].

An α-cell secretion specific to humans is corticotropin-releasing hormone (CRH) [43], better known for its expression in hypothalamic neurons and its role in stimulating corticotropin release from the pituitary gland [44]. β-cells in mouse and human also express a receptor for CRH, CRHR1, and CRH enhances insulin secretion by β-cells in the presence of high glucose in vitro and in vivo [45]. Thus, it seems likely that α-cells participate in paracrine regulation of β-cells, at least in human islets. Human α-cells are also known to express the peptide hormone urocortin3, another paracrine

regulator in islets [43]. However, as β-cells appear to be the primary source of urocortin3, its functions will be discussed in the next section.

1.1.3.2 β-cells

Insulin-secreting β-cells are the best known and most well-studied cell type of the pancreatic islet, primarily due to their role in diabetes. Insulin reduces blood glucose, thus acting in opposition to glucagon. β-cells are also the most abundant islet cell type, comprising 55% of human islets and 76% of mouse islets on average [22-24]. Similar to α-cells, β-cell distribution within islets also displays species-specificity. Mouse islets nearly always contain a remarkably homogeneous core of β-cells compared to the evenly distributed β-cells seen in human islets [22,23]. Once again, these differences appear to be reflective of distinct physiological functions. Mouse β-cells coordinate their insulin secretions across the whole islets, whereas human β-cells have more diversity of individual cell responses. It has been reasoned that coordination between mouse β-cells is due to a much higher degree of β-cell-β-cell contacts, and hence communication, in the mouse islet; however, it is unclear how this affects responses to glucose in vivo [23]. The issue of islet tissue architecture and β-cell microenvironments is complicated though by the observations that islet distribution in the human foetal pancreas resembles that of the adult mouse [46,47]. Also, adult islet structure and cell type composition alter in response to simple fluctuations in blood glucose [48]. Together, these studies suggest that islet architecture and cellular composition (particularly in relation to α- and β-cells) may be relatively plastic; species variations may be due to different physiological conditions and metabolic pressures [49].

The human *INS* gene encodes preproinsulin, which is cleaved to proinsulin in the endoplasmic reticulum before trafficking to the Golgi apparatus [50]. Mice and rats possess two preproinsulin-encoding genes, *Ins1* and *Ins2*, where *Ins2* is orthologous to human *INS* [51] and *Ins1* is a retrogene that arose from reverse transcription of the *Ins2* mRNA and insertion into the genome [52]. *Ins2* mRNA is more highly expressed than *Ins1* in adult mouse β-cells, although *Ins1* is expressed at higher levels early in pancreas development [53]. In humans and rodents, proinsulin is further processed in the Golgi apparatus by PC2 and PC1/3 enzymes, producing mature insulin and C-peptide [54,55]. Whether C-peptide is simply a waste product of proinsulin cleavage or an important β-cell secreted product with unique functions is currently the subject of some debate [56]. Insulin secretion from β-cells is glucose dependent – glucose sensing in β-cells is achieved by glucose shuttling through the Glut2 transporter in rodents, in contrast to Glut1 used by α-cells [38]. In humans, GLUT1 and GLUT3 may also play prominent roles in glucose sensing [57]. Thereafter, insulin secretion is regulated by many of the same mechanisms as glucagon release from α-cells, in that K_{ATP} channels direct membrane depolarisation that ultimately leads to action potential firing and exocytosis [58,59]. However, whereas high glucose concentrations cause a shutdown of action potentials in α-cells, they trigger action potential firing in β-cells.

How similar glucose-sensing mechanisms lead to opposite outcomes in these cells is not well understood, but it is proposed that expression of different subtypes of Ca^{2+} channels (that act downstream of K_{ATP} channels) between α- and β-cells may be the cause [60]. While high blood glucose is the primary mechanism inducing insulin release, several gut-derived hormones are able to potentiate β-cell insulin secretion, such as glucose-dependent insulinotropic peptide (GIP), glucagon-like peptide 1 (GLP1) and

CCK [61,62]. β-cells also express glucagon receptors [63], and insulin secretion is stimulated by α-cell glucagon signalling [64].

Circulating insulin acts to reduce hyperglycaemia by promoting glucose uptake and also glycogen synthesis, especially by cells in the liver, muscle and fat. Increased glucose uptake in these cells is largely prompted by insulin-induced translocation of the GLUT4 transporter from intracellular vesicles to the cell membrane in human and rodents [65,66]. This is controlled by the PI3K pathway. Insulin binds the insulin receptor and stimulates phosphatidylinositol-3-kinase (PI3K) to activate downstream kinases phosphoinositide-dependent kinase 1 (PDK1) and protein kinase B (PKB, or Akt), causing phosphorylation and inhibition of AS160 (Akt substrate of 160kDa) [67,68]. AS160 normally inactivates members of the Rab protein group, which are involved in vesicle fusion with the cell membrane. When insulin drives AS160 phosphorylation, Rab becomes active and GLUT4 moves to the cell membrane to enhance glucose uptake [68]. Once intracellular glucose is increased in liver, muscle and fat, it is either metabolised or insulin promotes its storage as glycogen by activating the glycogen synthase enzyme. PI3K-Akt signalling pathway is also important in this context, as Akt phosphorylates and inactivates glycogen synthase kinase 3 (GSK3), leading to dephosphorylation and activation of glycogen synthase [69]. Glycogen synthase is also activated through dephosphorylation of other residues by protein phosphatase 1 (PP1) [70], although evidence directly linking PP1 activation with insulin signalling is lacking.

Insulin-driven utilisation of blood glucose by peripheral tissues feeds back into lowering insulin release by β-cells. Several mechanisms also exist to actively inhibit β-cell insulin secretion and prevent hypoglycaemia. Paracrine somatostatin signalling from δ-cells inhibits insulin release from β-cells [20], further highlighting the importance

of the islet microenvironment for blood glucose regulation. Furthermore, neurotransmitter expressed from sympathetic neurons in the islet also decrease insulin secretion; in mice, neuropeptide Y acts through a G protein-coupled receptor to inhibit insulin release [71,72].

Although insulin is fundamentally the most important β-cell secreted product, other peptides are released by these cells that appear to be either intraislet paracrine factors or to exert physiological effects that support the action of insulin. Firstly, Urocortin3 is expressed and co-secreted with insulin by β-cells in mouse and human, and also detected in human α-cells [43]. Urocortin3, a CRH family protein, signals via CRHR2 [73] – in the islet, CRHR2 is specifically expressed on the surface of δ-cells. Urocortin3 signals from β-cells have been shown to stimulate somatostatin release from δ-cells in a paracrine-mediated negative feedback loop on insulin secretion [74].

Second, the neurotransmitters γ-aminobutyric acid (GABA) and serotonin are secreted by human β-cells in a glucose-dependent manner, with a smaller amount of glucose-independent background secretion of GABA. GABA provides an autocrine feedback loop to β-cells that increases insulin release [75], and both GABA and serotonin potentiate the glucose-driven inhibition of glucagon release from α-cells [76,77]. GABA receptors are also expressed by 91% of human δ-cells, and it is thought that GABA paracrine signalling increases somatostatin secretion [75].

Finally, amylin (also known as islet amyloid polypeptide) is co-secreted along with insulin [78], and its expression is similarly increased in response to high blood glucose levels [79]. Amylin serves to complement insulin's clearance of glucose already in circulation by preventing new sources of glucose from entering the blood. This is accomplished by slowing the rate at which stomach contents are emptied into the

intestine and inhibiting α-cell glucagon secretion, although the effect of amylin on α-cells is not paracrine [80].

1.1.3.3 δ-cells

δ-cells constitute an average of 10% of human islet cells [22-24], with studies disagreeing over whether this proportion is lower [22] or not significantly different in mice [23]. Their distribution in both species reflects that of α-cells – evenly scattered throughout human islets, but on the periphery of mouse islets [22,23]. δ-cells secrete somatostatin, one of the chief paracrine regulators of α- and β-cells in the islets. Consistent with δ-cells modulating islet secretions, they are often characterised by long cytoplasmic processes that contact many other islet cells [81]. Like the other previously described islet hormones, somatostatin is expressed in an inactive form – the SST gene encodes preprosomatostatin, which is processed to prosomatostatin in the endoplasmic reticulum [82]. Somatostatin 14 is the primary isoform found in δ-cells [83].

Somatostatin secretion by δ-cells requires many of the same stimuli as insulin from β-cells [81]. Additionally, gut-derived hormones such as GLP1 also induce somatostatin release [84,85]; indeed, the GLP1 receptor is exclusively expressed by β- and δ-cells [31,86]. While being important paracrine regulators themselves, δ-cells are also stimulated by paracrine signals from other islet cells, establishing signalling feedback loops. Glucagon perfusion is known to increase somatostatin levels in the whole pancreas [87,88] and although a direct paracrine effect has yet to be demonstrated, a subset of δ-cells do express the glucagon receptor [89]. Similarly, β-cell-derived urocortin3 and GABA both induce somatostatin release by δ-cells, as discussed earlier in this chapter. Even rare ε-cells in the islet have paracrine somatostatin-inducing effects on δ-cells [30,86].

Knockout studies have revealed that somatostatin has inhibitory effects on α- and β-cell hormone secretion [20], thus completing the paracrine negative feedback loop. In rodents, somatostatin appears to bind somatostatin receptor 2 (Sstr2) on α-cells and has variously been described to bind Sstr3 and Sstr5 on β-cells [30,86,90-92]. Once activated by somatostatin binding, the $G_{\beta\gamma}$ subunit of the SSTR interferes with β-cell Ca^{2+} trafficking, blocking exocytosis of insulin [72]. The mechanism for inhibiting glucagon release from α-cells is not known, although δ-to-α-cell paracrine signalling is likely stimulated by high glucose concentrations [20]. Somatostatin is clearly a highly important paracrine regulator within the islet, with δ-cell proximity to other islet cells also likely to be important for proper glucose homeostasis due to somatostatin's very short half-life [81].

As well as paracrine modulation, a recent study showed that δ-cells are electrically coupled to β-cells via gap junctions in mouse islets, indicating that hormone-independent mechanisms of intraislet regulation could be important for blood glucose homeostasis [40]. Furthermore, recent evidence shows that δ-cells are the only human islet cells to express the leptin receptor [31]. Leptin is released by fat cells to suppress appetite and regulate energy balance, suggesting a role for δ-cells in integrating non-pancreatic and pancreatic endocrine signals.

1.1.3.4 ε-cells

The ε-cells of the pancreas are the most recently discovered islet cell type [93] and secrete the hormone ghrelin. Prior to the discovery of a ghrelin-producing cell in the pancreas, ghrelin was more commonly associated with secretory cells in the stomach [94] and as such its effects as a stimulator of appetite and regulator of fat-store utilisation in human and rodent were the main focus of study [95,96]. ε-cells were then discovered

to be present in pancreatic islets, although only comprising <1% of all islet cells in adult humans, and probably even fewer in adult mice and rats [21,31]. ε-cells are much more abundant, however, in the developing foetal pancreas of both humans and rodents. Indeed, ε-cells make up around 10% of human foetal islet cells and are the primary source of ghrelin in the rodent foetus [21,97].

Preproghrelin is encoded by the GHRL gene and processed in ε-cells by PC1/3, and possibly also PC2, to proghrelin [98]. Proghrelin then undergoes cleavage and further modifications to purportedly produce ghrelin and obestatin [98-100], another hormone whose study is in its infancy but appears to possess physiological and islet paracrine functions [101]. The stimuli and mechanisms promoting ghrelin secretion from pancreatic ε-cells are not well known, but ghrelin cells in the gut can be stimulated to release ghrelin in response to glucagon and the neurotransmitter norepinephrine [102-104]. A recent description of the human ε-cell transcriptome indicated that expression of a receptor for neuropeptide Y, *NPY1R*, was enriched in these cells [31]; given that neuropeptide Y contributes to regulating insulin release from β-cells [71,72], it seems likely that it may also play a role in ghrelin secretion. Several other receptor types were enriched in ε-cells, such as the κ opioid receptor *OPRK1* and the prostaglandin E2 receptor *PTGER4* [31], and the function of these remains to be elucidated.

Ghrelin is a paracrine signalling peptide in the islet. While early studies variously concluded that ghrelin had either a stimulatory or inhibitory effect on insulin secretion [21,105,106], ghrelin's elevation in the circulation in a fasting state [95] would seem to favour the inhibition of insulin and the release of glucagon. Indeed, ghrelin induced glucagon expression in cultured mouse islets, although not in vivo [107]. More recently, it has been shown that ghrelin's effects on α- and β-cell secretions are almost certainly entirely mediated through the δ-cell. Expression of the ghrelin receptor *GHSR* is restricted to

δ-cells in mouse [30,86,108] and human islets [31]. In functional experiments on cultured mouse islets and perfused mouse pancreas, ghrelin promoted δ-cell somatostatin release in high glucose conditions by increasing the intracellular Ca^{2+} required for exocytosis. Ghrelin-induced somatostatin release caused a decrease in insulin and glucagon levels in mouse islets in vitro [30,86]. However, explaining an indirectly inhibitory effect of ghrelin on glucagon secretion is difficult in light of ghrelin's physiological role, and this relationship requires further research in vivo. The observation that obestatin and ghrelin independently exerted comparable effects in cultured rodent islets suggests that these two ε-cell hormones act on δ-cells in similar fashions [109].

1.1.3.5 PP-cells

The PP-cell is probably the most enigmatic islet cell, with scant recent research into this cell type. Transcriptomic analyses of islets suggest that PP-cells are rare, comprising on average only 2% and 6.5% of mouse and human islet cells, respectively [31,108]. PP-cells are located at the periphery of mouse islets, or in clusters separate from other islet cells. Furthermore, their distribution within the human pancreas is mostly restricted to a small, PP-cell-rich portion of the pancreas head [19,110].

PP-cells secrete pancreatic polypeptide (PP), a hormone that is structurally related to peptide YY and neuropeptide Y hormones that are expressed in the gut and nervous system, respectively [19]. PP is encoded by the PPY gene as prepropancreatic polypeptide, and subsequently processed to PP. The carboxyl-terminal region of the prepropancreatic polypeptide amino acid sequence is unusually poorly conserved between mammals, although the mature form of PP is highly conserved [19,111]. Background PP secretion occurs in a cyclic fashion that parallels the secretion of

gastric acid and contractions of the gut [112,113], all of which are regulated by the nervous system via cholinergic activity through the vagus nerve [114,115]. Basal PP levels are increased by eating and hyperinsulinaemia, and these increases can be attenuated by blocking muscarinic and cholinergic activity in vivo, highlighting the importance of neural activation of PP release [116,117].

The role of PP can broadly be defined as helping to integrate how the gut and pancreas deal with food intake. PP-family peptide hormones bind to a set of five related receptors – two of these, Y4 and Y6, show greatest affinity for PP compared to other PP-family hormones. Human *Y4* mRNA is expressed in gut tissues and the pancreas, while *Y6* is detectable in the gut and the brain [118-120]. By binding these receptors, exogenously administered PP has been shown to reduce appetite and food intake in mice and humans [121,122]. Additionally, gastric emptying is slowed when PP levels are high [123], and secretion of pancreatic juice by the exocrine pancreas is inhibited [124]. These findings, together with the observation that hyperinsulinaemia is a stimulus for PP secretion [117,125], suggest that PP acts to delay the absorption of nutrients following a meal, particularly if blood glucose is already high. Somatostatin can lower circulating PP levels when administered intravenously to dogs [116], although a direct regulatory or paracrine effect between δ- and PP-cells has not been shown.

In summary, there is abundant evidence that islet cells have the ability to regulate each other, often through complex paracrine means **(Figure 2)**. The importance of the islet microenvironment for efficient endocrine pancreas function is often neglected when considering potential therapies for islet cell disorders, such as diabetes. Reproducing the mixed islet cell population is an idea that will be returned to later in this Chapter.

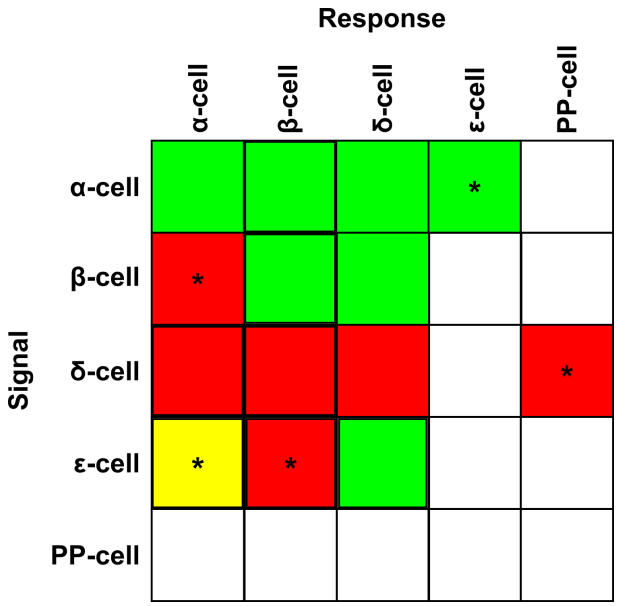

Figure 2. Inter-regulation of cells within the islet.

Islet cells are able to regulate each other through endocrine, paracrine and autocrine means, which influences the secretion of hormones. Hormone signals from islet cell types are represented on the left, while the response of islet cell types to those signals is shown along the top. Green boxes indicate where the signal response is increased secretion, red boxes indicate decreased secretion, yellow boxes indicate contradictory evidence, white boxes indicate no effect. Asterisks indicate where the signalling effect is suspected to be non-paracrine.

1.1.4 Development of the pancreas

The pancreas is derived from the definitive endoderm, one of the three germ layers formed by gastrulation in the early embryo. Definitive endoderm precursors ingress through the primitive streak. Subsequently formation of the embryonic gut begins as a sheet of squamous epithelium that extends along the anterior-posterior axis of the elongating embryo. The primitive gut undergoes morphogenesis to close into a tube first by folding at its anterior and posterior ends, followed by a curling up of the lateral walls in the midgut region. In this way, epithelial cells of the primitive gut meet along the ventral midline to close up the whole gut tube, leaving only a narrow tubular connection between the midgut and yolk sac called the yolk stalk [126]. This is all achieved by E8-8.5 in the mouse and 25-27 dpc (days post-conception) in human. The pancreas, stomach, liver and other anterior parts of the digestive system will form from the portion of the primitive gut tube anterior to the yolk stalk (termed the foregut) [127]. The pancreas therefore is generated from anterior definitive endoderm progenitors.

The first morphological evidence of pancreas organogenesis can be seen as two budding outgrowths from the foregut region – one ventral, and one dorsal. However, even prior to the development of the dorsal and ventral pancreatic buds, molecular evidence of an earlier commitment event to a pancreatic fate is indicated by expression of the pancreas lineage transcriptional master regulators, Pdx1. Pdx1 earliest expression is concomitant with the closure of the primitive gut tube in mice, in a posterior region of the ventral foregut epithelium. A dorsal foregut region begins to express Pdx1 slightly later, at about E8.75 [128,129]. In humans, PDX1 expression can first be detected at 29-31 dpc, with both dorsal and ventral posterior foregut commitment present, although the ventral region is larger and resembles the beginnings of a bud [130].

What activates Pdx1 in this region? In mouse, specification of the dorsal pancreas from the foregut is mediated by permissive ActivinβB and Fgf2 signals from the overlying notochord, causing exclusion of the morphogen sonic hedgehog (Shh) and resultant Pdx1 expression [131]. This mechanism is likely conserved in humans, where SHH is excluded from the region of foregut that gives rise to the dorsal pancreas [132]. The ventral pancreas is specified by signals from the lateral plate, or cardiac, mesoderm. Fgf signals from the cardiac mesoderm exclude Shh in the same manner as observed in the dorsal pancreas specification [133]. At this stage, most PDX1$^+$ pancreas progenitor cells co-express other key lineage determinants: GATA4, SOX17 and FOXA2; although all of these factors are also more broadly expressed across the primitive gut epithelium [130]. *Sox17* expression must be quickly excluded from the mouse ventral pancreas to block a liver fate in these cells [134]. Recent transcriptome analysis of the human dorsal pancreatic bud showed that expression of various transcription factors are able to distinguish the dorsal pancreatic bud from other primitive gut structures; these include well described pancreas regulators *PDX1*, *NKX6.1*, *MNX1*, *RBPJL* and *PTF1A*, as well as less well characterised genes like *SIM1*, *IRF6*, *CDX2*, *HOXA2* and *MEIS3P2* [135].

Pancreas-specified dorsal and ventral posterior foregut endoderm thickens into a stratified epithelium, with layers of stacked PDX1$^+$ epithelial cells **(Figure 3)**. By E9.5-10.5 in mouse (30-33 dpc in human), dorsal and ventral pancreatic buds have molecularly distinguished themselves from other endodermally-derived developing structures. These buds contain the multipotent pancreas progenitor cells that will generate every future cell type and structure in the adult pancreas; these progenitor cells are discussed in more detail later in this Chapter.

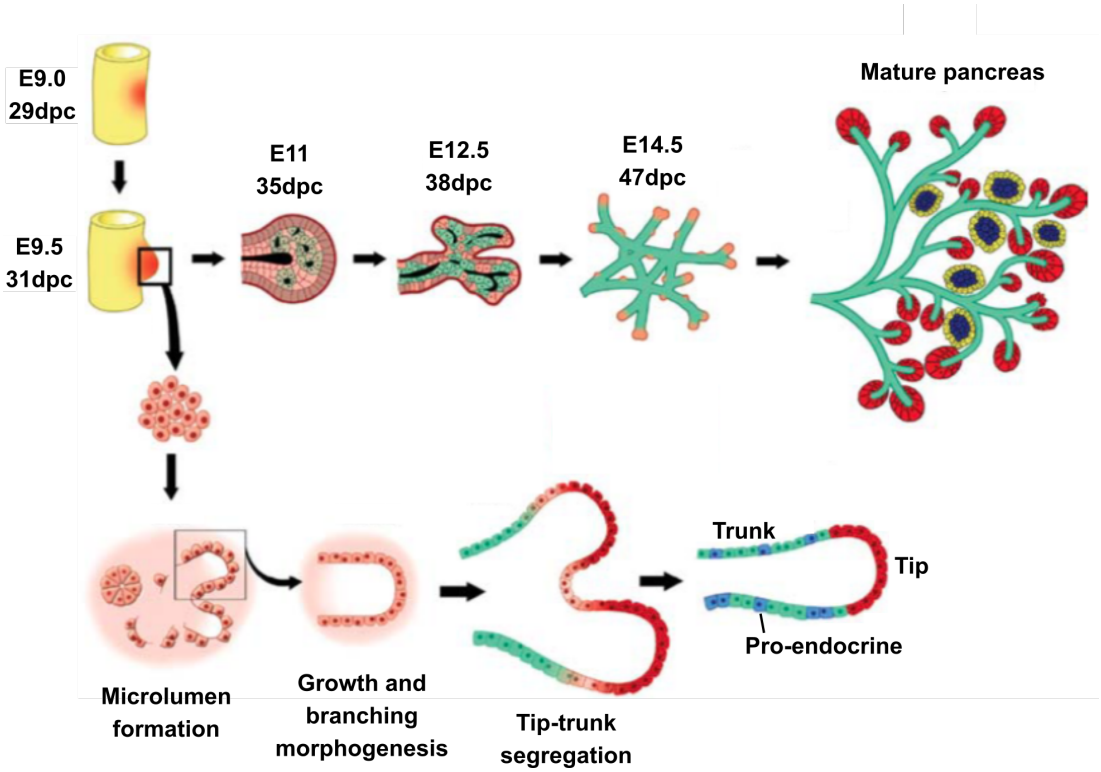

Figure 3. Overview of pancreas organogenesis.

Key events during pancreas organogenesis are depicted, along with approximate timings during development for mouse (upper) and human (lower). Ventral pancreatic bud development excluded from schematic. Figure adapted from Pan and Wright (2011) [151].3

Pancreatic buds at this stage – in both mouse and human – begin to strongly express SOX9 [130,136]. Additionally, NKX6.1 can be detected in a subset of cells in the pancreatic buds of both species [129,130]. In mice, Ptf1a is expressed in the pancreatic buds and its misexpression in non-pancreatic endodermal regions promotes pancreatic differentiation [137,138]. *PTF1A* gene expression is also enriched in the human dorsal pancreatic bud [135], where its role is presumably conserved as PTF1A enhancer mutations are associated with pancreas agenesis [139,140]. However, it is also at this stage of pancreas development that important differences between mouse and human can be detected. At E10.5, a majority of Pdx1-expressing pancreas progenitors also express Nkx2.2 [141,142], and a subset also express Ngn3 [143]. In contrast, both NKX2.2 and NGN3 are absent until much later in human pancreas development [130].

Nkx2.2 and Ngn3 are known to be important transcription factors in endocrine pancreas progenitor cells, and initiate the transcriptional program that specifies all cell types of the adult islet. Concomitantly, there is a wave of early endocrine differentiation in the developing mouse pancreas that does not occur in the human. This is called the 'primary transition', and results primarily in immature α-cells, but also immature β-, ε- and PP-cells by E10.5 [129].

Between E10.5-12.5 in mouse and 33-40 dpc in human, the progenitor cells in the pancreatic buds proliferate extensively and undergo branching morphogenesis, with the appearance of an elaborate ductal tree and associated microluminal network. Branching morphogenesis in the previously stratified epithelium is initiated and regulated by integrin-mediated signals from the extracellular matrix to progenitor cells [144]. By E12.5/37-40 dpc, the primitive gut has rotated to bring the ventral and dorsal

pancreatic buds into contact, before their fusion into a single embryonic pancreas [127,129,130].

This period of expansion and maintenance of multipotency has so far been shown to be regulated by Wnt and Notch paracrine signalling between pancreas progenitor cells, as well as Fgf signalling from the overlying mesenchyme into which the bud expands. High levels of Wnt7b appear to block differentiation of early pancreas progenitors in mice [145], while Wnt9a specifically represses expression of endocrine progenitor genes [146]. Progenitor maintenance is also controlled by Notch; ablation of Notch pathway components Dll1, RBP-Jκ and Hes1 causes pancreas hypoplasia and premature endocrine differentiation [147,148]. Proliferation is regulated by Fgf signals. Rat pancreatic mesenchyme expresses Fgf1, Fgf7 and Fgf10, and their endogenous receptor Fgfr2IIIb is expressed by multipotent pancreatic progenitors. Blocking Fgfr2IIIb signalling in embryonic pancreas explant cultures inhibited growth, and this could be rescued by exogenous application of Fgf7 or Fgf10 [149].

Pancreas progenitor cells lining the ductal epithelium of the newly branched embryonic pancreas uniformly express PDX1, SOX9, FOXA2 and NKX6.1 at approximately E12 (mouse) or 37 dpc (human) [129,130,136,150,151]. After this point, the ductal epithelium segregates into 'trunk' and 'tip' domains with more restricted lineage potential and diverging gene expression. In mouse, this lineage commitment occurs at about E12.5 – very shortly after fusion of the ventral and dorsal buds. By comparison, segregation into trunk and tip domains in the developing human pancreas can be detected at the later stage of 45-47 dpc (equivalent to E14-14.5 in mouse). This discrepancy is likely due to the need for a longer pancreas progenitor ductal tree 'expansion' phase in humans, given the requirement for larger organ size [152]. Mouse tip cells occur at the branching tips of the ductal tree, and are characterised by expression of Pdx1, Ptf1a, CpaI and high levels of cMyc; these cells retain the

multipotency and proliferative capacity of early pancreas progenitors, and continue to drive growth and branching of the pancreatic network until E14.5. At this point, cells in the tip domain commit to acinar fates and Gata4 expression becomes restricted to this population, having previously been expressed by all pancreas progenitors [153-155]. Meanwhile, trunk cells are located in the ductal epithelium and express Hnf1b, Sox9 and Nkx6.1, with new trunk cells continually laid down in the wake of early tip-driven growth of the ductal tree. Trunk cells lose the potential to generate acinar cells, becoming restricted to either a ductal or endocrine fate [156]. A key factor in deciding trunk-tip segregation is the mutually antagonistic relationship between Ptf1a and Nkx6.1, required for tip and trunk cell identity, respectively. Expression of one of these transcription factors appears to suppress expression of the other, along with its associated fate as trunk or tip [155]. This is reminiscent of the patterning in the developing spinal cord which involves cross-repressive transcription factors [157]. Suppression of Notch signalling is thought to be required for allocation to a tip cell fate, as Notch signalling components activate Nkx6.1 expression [158]. The gene expression profiles of human trunk and tip cells has been shown to be very similar to mouse. However, segregation of the expression of these markers appears to be a much more gradual process during human development, with complete separation of trunk-tip markers only apparent at approximately 14 weeks gestation [130].

Trunk-tip segregation is the beginning of large-scale differentiation commitment in the developing pancreas. Almost immediately after separation of these domains in mice – at E13 – a process called the secondary transition occurs. Defined as the onset of differentiation to all cell lineages of the mature pancreas, the secondary transition is mostly studied for being the major period of endocrine commitment in the pancreas (as opposed to the relatively small contribution of the primary transition to the endocrine cell pool) [151]. A human equivalent of the secondary transition occurs at 49-

52 dpc (roughly equivalent to mouse E15-15.5), although in contrast to mouse this is the first detectable evidence of endocrine commitment in the developing human pancreas [127,130]. Endocrine progenitor cells in both species arise from a subset of cells within the trunk domain, where the earliest marker of endocrine commitment is the transcription factor NGN3 [159-161].

NGN3 can be thought of as the gatekeeper for endocrine lineage commitment; its expression is required at a high level to activate transcription of downstream endocrine progenitor genes [162], but its expression subsequently ceases or is vastly reduced [163]. Endocrine progenitor cells will be discussed at greater length later in this Chapter.

Once NGN3 expression levels increase above a certain threshold in any particular trunk cell, evidence suggests that epithelial-to-mesenchymal transition (EMT) is triggered and cells migrate out. In mice, it is thought that endocrine progenitors delaminate from the ductal epithelium individually rather than in groups, as Ngn3 downregulates the Notch repressor Jagged1 to promote Notch signalling in adjacent trunk cells [164,165]. With high levels of Notch signalling in these trunk cells, an endocrine fate is blocked through *Ngn3* repression by the Notch target Hes1 [165,166]. The EMT is directly regulated by Ngn3, as in mouse endocrine progenitors Ngn3 is associated with increased expression of *Snail2* [167,168] and Grg3 [169]. Snail2 is a transcription factor known to be involved in inducing cell movement by repressing E-cadherin (E-cad) [170], a marker of epithelial cells. Grg3 also attenuates E-cad expression, probably by recruiting factors to make chromatin less accessible at the E-cad locus [171]. Delamination of endocrine progenitors is not well studied in human development, but staining of foetal tissue showing high levels of NGN3 expression in isolated cells of the trunk epithelium and no overlap between NGN3 and SOX9 [132,172] suggests that many of the mechanisms regulating this process are conserved from mouse.

Delaminated endocrine progenitors go on to establish foetal islets, which are initially closely associated with pancreatic ducts in cord-like structures in mouse [161]. In newly delaminated endocrine progenitors, Ngn3 directly drives transcription of pro-endocrine genes such as *NeuroD1, Insm1, Rfx6* and *Isl1*, where perturbation of any of these genes leads to a deficiency in endocrine cell development [173-176]. Together, pro-endocrine factors activate transcriptional programs required for the maturation of foetal islet cells. Key transcription factors involved in the maturation process include Nkx2.2, Pax4, Pax6 and Arx, with evidence from knockout studies suggesting that the relative expression levels of these proteins dictates which islet cell type each progenitor will produce. For example, *Nkx2.2* knockout mice completely lack β-cells, possess fewer α- and PP-cells, but have a greater number of ε-cells [141,177]. Conversely, loss of *Pax6* or *Arx* abrogates α-cell development, while promoting β- and δ-cell numbers [178,179]. *Pax4* deletion results in loss of both β- and δ-cells with a concomitant increase in α-cells [180], but simultaneous loss of both *Pax4* and *Arx* leads to islets exclusively containing δ-cells [181].

In support of the idea of a pro-endocrine regulatory network that depends on specific ratios of its key members, in both mouse and human there is evidence suggesting that each $NGN3^+$ endocrine progenitor produces only a single foetal islet cell [182,183], and that expansion of islet cells (particularly β-cells) occurs only after differentiation from an endocrine progenitor stage and continues into the period shortly after birth [184-187]. Indeed, mouse endocrine progenitors are thought to exit the cell cycle under the influence of increased Ngn3 expression and thus are not capable of a transit amplifying stage [188,189].

Although all hormone-expressing islet cell types can be detected in the mouse pancreas as early as the primary transition [129], only by approximately E18.5 have

foetal islets migrated away from the cord-like structures adjacent to pancreatic ducts and spread into the surrounding exocrine tissue, where they more closely resemble adult islets [151,161]. Islet migration and aggregation may be dependent on further inhibition of E-cad expression, which is achieved in these cells by EGF-stimulated activation of Racl Rho GTPase [190]. By contrast, all human hormone positive islet cells can be detected by 10 weeks gestation and foetal islets are evident relatively soon afterwards – from approximately 12 weeks gestation [46,132]. However, nearly 30% of early islet cells in human are polyhormonal, with the proportion of monohormonal cells increasing during development [47,191]. Regulation of endocrine cell migration and maturation may therefore be slightly different between mouse and human, though these processes are not well studied in human.

Exocrine maturation from tip and trunk cells is not so well studied as endocrine development. Mature duct cells derived from the trunk domain continue to express markers associated with pancreas progenitor cells, such as FOXA2, SOX9, HNF6 and HNF1B [127,151]. This has made it difficult to decipher the duct-specific roles of these transcription factors, as opposed to roles required for pancreas development in general, but *Hnf6* null mice fail to develop cilia in mature ductal cells [192]. One study reported that mature mouse centroacinar cells, a specialised ductal cell type, are enriched for *Sox9* and *Nestin* expression, with a subset also expressing aldehyde dehydrogenase 1 (Aldh1) [193]. Aldh1 has previously been identified as a progenitor cell marker [194], which would lend support to the theory that centroacinar cells have regenerative potential in the injured pancreas.

Acinar cell maturation depends on continued high expression of Ptf1a in mouse tip cells, as well as a switch from the Rbpj subunit to a Rbpjl isoform in the Ptf1a complex. *Rbpjl* null mice display extensive acinar maturation defects and the virtual absence of digestive enzyme production [195]. Additionally, deletion of *Ptf1a* in adult mice causes

initial loss of acinar cell function, followed by dedifferentiation and apoptosis [196]. Ptf1a drives transcription of *Mist1*, another gene whose deletion negatively affects acinar cell maturation [197]. Together, Ptf1a and Mist1 are the chief coordinators of the adult mouse acinar cell transcriptional network [198]. The expression of PTF1A and MIST1 in human acinar cells has not been investigated.

In summary, the mechanisms behind early pancreas organogenesis have been well characterised in mice using knockout and lineage tracing studies. While these techniques are obviously not possible for human development, gene and protein expression studies on fixed human foetal tissue suggest that many markers and mechanisms are conserved between species, such as the central roles for PDX1, SOX9 and NGN3 in different progenitor cells **(Figure 4)**. Induction of endocrine progenitor fate appears highly complex and dependent on gradients of expression for multiple key transcription factors and signalling pathway components. The specific requirements for endocrine induction during development remain to be convincingly established. This is especially true for human endocrine progenitors, which appear slightly divergent from mouse equivalents, illustrated by their differing *NKX2.2* expression profiles. New cell models of endocrine progenitor induction in human cells would therefore provide new opportunities for discovery and clinical application.

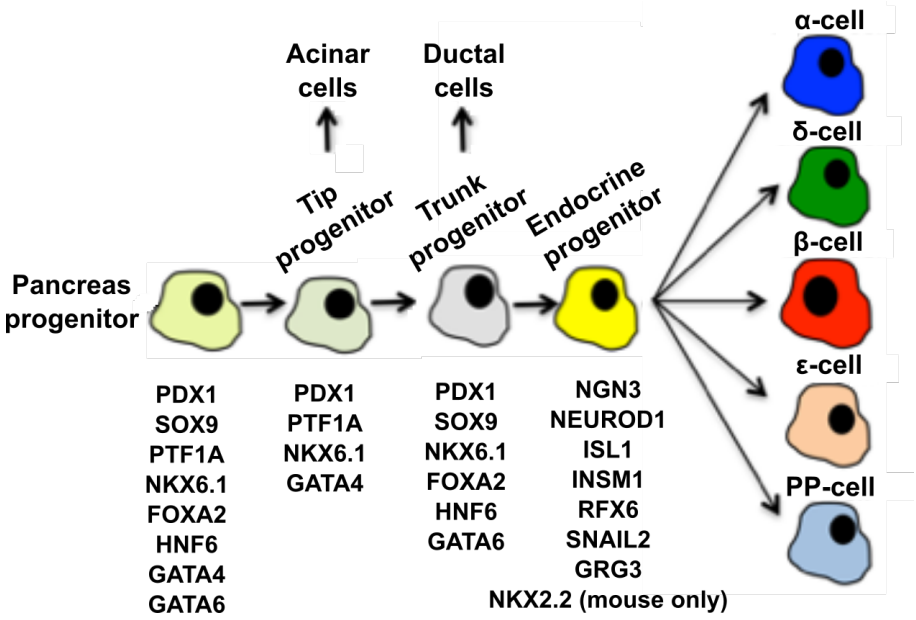

Figure 4. Markers expressed by progenitor cell types during pancreas development.

Tip and trunk progenitors of the pancreatic ductal tree have distinct lineage potentials. Note that although trunk progenitors are depicted as arising from tip progenitors, and this can occur by asymmetric division, trunk progenitors initially arise from the pool of early pancreas progenitors.

1.2 Diabetes

When development of the pancreas is perturbed, or when adult endocrine cells become depleted or dysfunctional, serious consequences arise for normal glucose homeostasis. Diseases in which blood glucose levels go unregulated are called diabetes mellitus, or more commonly simply diabetes. The word 'diabetes' is derived from the ancient Greek meaning 'to pass through', referring to the classic diabetic symptom of excessive urination (polyuria). 'Mellitus', Latin for 'honeyed', was added later to differentiate diabetes mellitus from diabetes insipidus, another metabolic disease associated with polyuria but without blood glucose dysregulation. 'Honeyed' describes a second classic symptom of diabetes mellitus, in which high blood glucose leads to glycosuria, or glucose in the urine.

Diabetes is a major public health problem; it is estimated that 4.6 million people in the UK (Public Health England, 2017), and 422 million worldwide [199], suffer from some form diabetes. Furthermore, this problem is getting worse. Global prevalence in men has increased from 4.3% to 9.0% between 1980-2014, and 5.0% to 7.9% in women [199]. Increased prevalence cannot be fully explained by an ageing population, pointing to a growing influence of environmental and lifestyle factors in contributing to the onset of diabetes.

Increasing diabetes prevalence is also having a demonstrable impact on morbidity and mortality. In 2002, diabetes was the 11th leading cause of death globally, and this is projected to rise to 7th by 2030. Furthermore, diabetes as a cause of years of life lost due to ill health is due to rise rapidly over this same period [200]. Healthcare providers must emphasise prevention of diabetes through lifestyle changes to combat the increasing prevalence of diabetes. However, even if education programs are successful in the long-term, there is an acute need for improved diabetes therapies

that tackle patient quality of life and reduce the burgeoning costs of current disease management strategies and associated complications.

1.2.1 Types of diabetes

There are three main types of diabetes mellitus, all characterised by high blood glucose, or hyperglycaemia. The prevalence and underlying causes of hyperglycaemia differ between each type as follows:

1. *Type 1 diabetes (T1D):* accounts for 10-15% of all diabetes cases. Hyperglycaemia is caused by insulin deficiency due to the complete loss of β-cells from the pancreas [201]
2. *Type 2 diabetes (T2D):* is the most common form of diabetes, accounting for 85-90% of all diabetes cases. Hyperglycaemia is caused by β-cell dysfunction leading to reduced insulin secretion and the resistance of peripheral tissues to insulin [202]
3. *Gestational diabetes mellitus (GDM):* is less common than either T1D or T2D, as it only arises during pregnancy by definition – between 2-5% of pregnant women are affected by GDM. Hyperglycaemia is caused by insulin resistance, although the contributing factors to this may be different than those in T2D. GDM will not be discussed further here, although it is noteworthy that women who have experienced GDM during pregnancy are much more likely to develop T2D later in life [203]

In addition to diabetes mellitus, relatively rare (1-2% of all diabetes) cases of heritable diabetes due to single-gene mutations exist, collectively called maturity-onset diabetes of the young (MODY). MODY typically develops during youth or young adulthood and is generally characterised by mild hyperglycaemia due to β-cell

dysfunction. MODY symptoms are usually mild enough that insulin treatment is not required, although disease prognosis is dependent on the causal mutation. Mutations in nine different genes have been described that cause MODY, all of which are important to either pancreas development, islet cell function or regulation of blood glucose. By far the most common documented mutations are in HNF1A and GCK; HNF1A is a transcription factor that participates in regulating β-cell mass, while GCK encodes the glucokinase enzyme that phosphorylates glucose, a key step in sensing intracellular glucose levels prior to insulin secretion [204,205].

T1D and T2D will now be discussed in further detail, including their causes, pathophysiology, and current treatment options.

1.2.2 Type 1 diabetes

T1D is most often caused by the autoimmune destruction of β-cells in the islet, although in rare cases there is no known reason behind β-cell loss. Little is known about how T1D is initiated, but autoantibodies to various proteins critical for β-cell function are generated, usually early in life. Presence of multiple different autoantibodies increases the risk of developing T1D, and progression from initial autoimmune response to clinical presentation of T1D can take many years [201]. Thus, incidence of T1D is highest in the 10-14 year old age group, followed closely by 5-9 year olds [206]. Once autoantibodies are present, β-cell destruction is mediated by both inflammatory and cytotoxic responses by $CD4^+$ and $CD8^+$ T cells [207,208].

Genetics are a proven risk factor in T1D. Specific alleles in the HLA system, which encodes cell surface proteins involved in antigen presentation to the immune system, are most commonly associated with T1D susceptibility. However, the associated risk

of these haplotypes is relatively small, and not necessarily predictive of certain onset of T1D [201].

T1D incidence in youths is increasing by 3.9% annually in Europe and 1.8% annually in the United States [209,210]. The reasons behind increasing incidence of a complex genetic disease such as T1D are the subject of much debate. It has recently been shown that reduced natural selection (defined as the potential loss of reproductive success by dying at a certain age) correlates with T1D prevalence, suggesting that advances in modern medicine allow for T1D incidence to increase [211]. However, environmental factors are also thought to contribute to T1D onset. For example, studies have shown that viral infections during early childhood correlate with an increased risk of developing T1D [212,213], although causal evidence has yet to be demonstrated. Supply of nutrients (particularly lipids) during gestation and infancy, as well as composition of the gut microbiome are other tentatively postulated environmental factors that may influence T1D onset [201,214-216].

Classic symptoms of T1D are hyperglycaemia, polyuria, polydipsia (excessive thirst) and ketoacidosis. Ketoacidosis stems from insulin deficiency, whereby the body breaks down fat for energy when glucose cannot be utilised properly; it is a potentially serious complication that can initially cause abdominal pain and nausea, but is fatal if untreated [201]. The long-term complications of T1D originate from the effects of chronic hyperglycaemia on peripheral tissues. When blood glucose levels are high, certain cell types are unable to reduce their glucose uptake according to their metabolic requirements. Accumulation of intracellular glucose leads to a build up of reactive oxygen species causing DNA and cellular damage, and also amassing of glycolytic intermediates that contribute to atherosclerosis. Over time in T1D patients, sustained cellular damage and development of atherosclerosis are known to cause

cardiovascular disease, vision loss, kidney disease, and a host of problems caused by peripheral and autonomic nerve damage [201,217,218].

T1D requires that patients are treated with exogenous insulin and closely monitor their diet to try and mimic normal glycaemia, while being careful to avoid the potential for hypoglycaemia introduced by improper use of insulin. Currently, insulin therapy is administered by periodic injection or, less often, by insulin pumps to control blood glucose levels; however, each necessitates regular monitoring of blood glucose levels. Insulin pumps are capable of larger doses per administration, and more advanced models are capable of continuously monitoring blood glucose. While therapies designed to dampen the autoimmune response to β-cells have been trialled, none have succeeded [201].

Overall, better disease management has been the main focus for improving T1D outcomes for many decades. A study that assessed risk of death among T1D patients found that risk of death from any cause increased steadily as glycaemic control worsened. Therefore, maintaining tight control over blood glucose can improve disease prognosis [219]. However, even the group of patients who best managed their T1D were at least twice as likely to die from any cause as the non-diabetic control group. Increased risk of death in the diabetic group was mostly attributable cardiovascular and diabetes-related causes [219]. Another study showed that amongst T1D patients with preserved kidney function (an indicator of good disease management), life expectancy from the age of 20 was reduced by approximately 8 years compared to non-diabetic individuals [220].

Treatments for T1D need to be improved, as insulin injections only crudely mimic the normal homeostatic control of blood glucose levels. Consequently, risk of health

complications and death remain high, which significantly impacts patient quality of life and presents an ongoing cost burden for healthcare providers.

1.2.3 Type 2 diabetes

In T2D, β-cells are still present in the pancreas, though their number may be reduced compared to the healthy pancreas [221]. Reduction in β-cell mass is thought to occur by β-cell apoptosis caused by defective autophagy [222]. Dysfunctional autophagy is also known to cause an inflammatory response, and macrophage infiltration in T2D islets has been shown [223]. Interestingly, α-cell mass is unaffected by T2D, showing that this is a specific pathology of β-cells [224]. The altered proportion of α- and β-cells and resulting hyperglucagonaemia likely contributes to failure to lower blood glucose. However, β-cell death is not thought to be the primary driver of T2D onset. Almost certainly more impactful to the development of T2D is β-cell dysfunction combined with reduced sensitivity of peripheral tissues to insulin, called insulin resistance. The rate of insulin secretion in response to hyperglycaemia is reduced in T2D, indicating impaired glucose sensing [202]. Even when insulin secretion does eventually peak in T2D, tissues in the body fail to respond to this signal properly. Insulin resistance has been documented in muscle, liver, fat, kidney, gut, vascular, brain and pancreas tissues, showing that fundamental elements of the insulin signalling pathway are perturbed in T2D.

The incidence rate of T2D is highest in the 30-39 age group, much later than T1D [225]. Worryingly, T2D incidence among children has seen an even sharper rise than T1D, with a 4.8% annual increase in the United States [210]. This surge correlates well with the rise in prevalence of obesity and adiposity in modern times [226]. The environmental factors contributing to T2D onset are much better defined than T1D; a high percentage of body fat, especially abdominally, increases risk even in the absence of

obesity. Diet and exercise habits are obviously closely linked to adiposity, but can be contributing factors to T2D onset even in non-obese individuals. A healthy diet including lots of green vegetables and unsaturated fats, complemented by regular aerobic and strength training lowers T2D risk. In contrast, consuming red meat, processed meat and sugary drinks, or an excessively sedentary lifestyle are associated with increased risk. Smoking also increases T2D risk [227-229]. All of the above environmental risk factors directly feed in to promoting insulin resistance, which in turn elevates fasting blood glucose levels. Worsening control over blood glucose can be incremental and last many years before proceeding to T2D – this stage is known as prediabetes. Conversion from prediabetes to T2D can be prevented by lifestyle and medical interventions. However, lifestyle changes are often only maintained temporarily and annual conversion rates from prediabetes to T2D are generally between 5-10% [230].

The mechanisms of insulin resistance are complex and multifactorial, but ultimately all negatively affect the insulin signalling pathway. As described in Chapter 1.1.3.2, cells in peripheral tissues respond to insulin by activating the PI3K pathway. Insulin resistance causes phosphorylation of insulin receptor components at residues which block the normal insulin signalling response. Consequently, glucose uptake and storage as glycogen is impaired. Inappropriate insulin receptor phosphorylation is associated with increased expression or activation of serine kinases [231], which can be caused by high tissue lipid content [232,233], mitochondrial dysfunction [234], endoplasmic reticulum stress [235] and cytokine signalling during the inflammatory response [236,237]. The vast topic of mechanisms of insulin resistance will not be tackled further here.

Genetic predisposition also increases T2D risk, but this component is not as significant a contributing factor as lifestyle [238]. Single nucleotide polymorphisms (SNPs) at hundreds of genetic loci have been associated with T2D, with mechanisms

of increased risk defined for only a handful of these that occur within exons [202]. For example, a variant in the gene TCF7L2, a transcription factor and Wnt signalling effector, appears to impair the response of β-cells to gut hormones GIP and GLP1 (see Chapter 1.1.3.2) [239].

Short-term symptoms of T2D are generally milder than T1D and, indeed, many patients are asymptomatic at the time of diagnosis. However, hyperglycaemia and ketoacidosis are also common symptoms associated with T2D. In the long-term, chronic hyperglycaemia leads to all the same health complications previously described for T1D [202]. Furthermore, the fact that T2D is so often associated with general poor health and obesity can exacerbate these complications, as is well documented for hypertension [240].

Exogenous insulin treatment is not usually required for T2D, but can be effective if administered as a long-acting insulin analogue or with meals, and in conjunction with various medications [241]. T2D medications encompass several classes. Metformin is the most common antidiabetic medication, and works by reducing glucose production in the liver. Other examples of antidiabetic medication include those designed to increase insulin secretion (such as sulfonylureas and meglitinides), to improve insulin sensitivity in peripheral tissues (thiazolidinediones), to increase sensitivity of β-cells to insulin-stimulating gut hormones (such as DPP4 inhibitor saxagliptin and GLP1 agonist exenatide), and to reduce the rate at which carbohydrates are absorbed after meals (such as α-glucosidase inhibitor acarbose and SGLT2 inhibitor dapagliflozin). Combinations treatments between these classes of drugs are common [202]. Of course, in tandem with any pharmacological treatment, lifestyle changes are a key component in managing T2D.

In summary, it has been estimated that up to 90% of T2D cases are preventable simply by making lifestyle changes [202,242], making education the key to reducing prevalence in the long-term. For now though, T2D patients are up to 4 times more likely to die of any cause compared to healthy individuals, although this can be improved with good disease management [243]. The cost associated with medicating and treating associated complications of T2D is huge [226], with a definite decrease in patient quality of life. Health-adjusted life expectancy estimates for men and women with T2D predict a loss of 5.3 and 5.8 years, respectively, from the age of 55 [244].

1.3 Cell therapies for diabetes

1.3.1 Regenerative medicine and diabetes

In the context of regenerative medicine, diabetes makes for an attractive disease to research. Chiefly, this is due to the increasing prevalence of both types of diabetes mellitus, and the urgent need for improved treatment options. However, T1D is an especially good target for therapeutic research due to its relatively simple pathophysiology and well understood disease mechanisms. β-cells alone are absent from the diabetic pancreas and, furthermore, treatment with insulin injections overcomes the acute symptoms associated with β-cell loss. Replacing β-cells and thereby reinstating an endogenous source of insulin should theoretically resolve T1D symptoms, and provide a much tighter level of blood glucose control comparable to the healthy pancreas. β-cell replacement therapy could even be of use in certain T2D cases, especially in those patients with an underlying genetic predisposition affecting their own β-cells.

This section will describe the progress behind cell-based diabetes therapies so far, and discuss whether this represents an improvement on current diabetes therapies.

1.3.2 The Edmonton protocol

Clinical cell therapies for diabetes in humans have existed for some time now. Transplanting pancreatic islets from donor cadavers to diabetic recipients provides a means of cell replacement with authentic islet cells. Islet cell transplant in humans was first documented in 1990, although the success rate was very poor; of 9 patients in the study, 3 died and the rest either had a persistent exogenous insulin requirement or had sub-optimal responses to a glucose challenge [245]. Of all transplants performed over the next decade, only 8.2% of recipients remained insulin-free one year after the

procedure. A breakthrough in islet cell transplants occurred in 2000. Improvements to islet cell isolation and subsequent patient immunosuppressive regime resulted in significant improvements to transplant outcome. All 7 patients in the initial study became free of their dependence on exogenous insulin, with follow-up periods ranging from 4.5-15 months. This required 2 or 3 separate transplant procedures per patient, and response to glycaemic control was normal after this [246]. This procedure quickly became the standard islet cell transplantation technique and became known as the Edmonton protocol.

Briefly, the Edmonton protocol involves perfusion of the donor pancreas with collagenase, followed by an automated method of tissue breakdown involving both enzymatic and mechanical digestion in a device called the Ricordi chamber. Islets are purified from digested tissue by centrifugation and cultured for 1-3 days to enhance purification of viable islet cells, before injection into the recipient's hepatic portal vein. In successful transplants, donor islets establish themselves within the portal vein [247].

At present, islet cell transplants are available for the treatment of severe cases of T1D in many developed countries across the world. However, a recent update stated that only 864 allogeneic islet transplants had been performed worldwide in the period since 1990. While patient outcomes after transplant are now good – 50-70% of patients remain insulin-free by 5 years post-transplantation – the limited availability of this procedure is a reflection of the insufficient number of donor organs and the cost associated with a chronic immunosuppressive regime [247].

While immunosuppressive drugs may become cheaper over time, a lack of donor pancreases is going to be a permanent barrier to widespread transplant, particularly as diabetes prevalence increases. To make cell therapies for diabetes more widely available, there is a need to look beyond traditional cell sources.

1.3.3 hESC-based therapies

Differentiating human embryonic stem cells (hESCs) and induced pluripotent stem cells (iPSCs) towards islet cells in the laboratory could provide an unlimited supply of cells for transplantation. Much focus has been placed on producing pancreatic β-cells by attempting to mirror the pancreas development process described earlier in this Chapter in vitro.

Until recently pancreatic β-cells generated by this process more closely resembled foetal β-cells than their adult counterparts; crucially, these β-cells were often polyhormonal and functionally immature [248], where they did not release appropriate amounts of insulin in response to glucose in animal models [249,250].

Progress has been made in refining the β-cell differentiation process, which has improved functionality [251,252]. These cells showed their functional potential by rapidly and sustainably reversing diabetes in mouse models. However, both studies also noted key differences in gene expression and functionality between their hES-derived β-cells and those from adult human islets. For example, generation of polyhormonal cells and the lack of NKX6.1 expression in β-cells, a transcription factor important for adult β-cell function [253]. Subsequent research has attempted to further improve these protocols by refining earlier stages of the differentiation process. By improving the specification of hESC-derived pancreas progenitors, β-cells were produced that appear to express more of the markers commonly associated with mature β-cells than has been reported previously, as well as reducing (but not eliminating) the amount of polyhormonal cells generated [254,255]. However, global gene expression analysis in hES-derived β-cells was not performed for either of these recent studies. Given the deficiencies in prior differentiation protocols, this seems like a notable caveat. Furthermore, it was found that the amount of insulin secreted from hES-derived β-

cells in vitro was about half that of human islets [255], while in vivo this was reduced to one third [254].

Therefore, while progress has been made in improving β-cell differentiation protocols, cell functionality remains sub-optimal and the efficiency of generation is poor. Insulin^{+}/NKX6.1^{+} cells arise at frequencies of 20-31% [254,255], although it was recently shown that a purification step at the pancreas progenitor stage of differentiation may be able to improve this yield [256]. However, obtaining sufficient quantities of cells for transplant would require scale up of cultures at the hESC stage. Even if these yield requirements could be met, evidence shows that authentic islet cells cultured ex vivo undergo a process of dedifferentiation and exhibit unstable gene expression signatures [257]. This suggests that current culture conditions are fundamentally inadequate for maintaining or producing mature islet cells.

An alternative cell therapy approach is to utilise pancreas progenitor cells, rather than mature β-cells. Pancreas progenitors reflect transitory cell types during pancreas development, which ultimately give rise to all adult pancreatic cell types. hESC-derived pancreas progenitors engrafted into adult mice are able to mature into insulin-producing cells in vivo that prevent hyperglycaemia in streptozotocin-induced diabetes [258]. The following section will address the use of pancreas progenitor cells for cell therapy in diabetes, and potential future directions for this research.

1.4 Pancreas progenitor cells

Generating pancreas progenitors in vitro for the purpose of cell therapy offers a number of significant practical advantages over β-cells – they can be generated more quickly and with higher efficiency. Differentiation to pancreas progenitors can be achieved in 9-11 days with reported efficiencies between 75-95%, although it should be noted that different studies are not consistent with markers used to identify progenitor cells. While all use PDX1 as the primary marker, NKX6.1 and FOXA2 have variously been used as secondary markers of trunk progenitor cells [254,255,259]. Recent transcriptome data from the developing human pancreas suggests that while FOXA2 is expressed in pancreas progenitors, SOX9 would be a more relevant marker to assess hESC-derived progenitors due to its role in regulating many pancreas-associated genes. The same study reaffirmed the validity of using NKX6.1 as a pancreas progenitor marker [135]. Pancreas progenitors are also innately proliferative and expand their numbers in a relatively short time period during development to produce the bulk of the foetal pancreas, as described in Chapter 1.1.4. This is in stark contrast to β-cells in vivo, where only 1-3% of the population are in cycle even at their proliferative peak shortly after birth [260]. hESC-derived pancreas progenitors retain this potential if supplied with the right signals; these cells can be stably cultured and serially passaged when grown on feeder cells in the presence of growth factors and small molecules to repress differentiation [261], or in suspension culture systems [262]. An expandable progenitor population allows scale up of cells at a point immediately prior to transplantation, which is more convenient and may aid purification of the progenitor population.

The promise of pancreas progenitor-based cell therapy has been explored in recent research. Macrodevices that encapsulate hESC-derived pancreas progenitors have been developed, which can then be implanted subcutaneously. Progenitors are able

to differentiate and mature in vivo within the device, producing α-, β-, and δ-cell aggregates which can rescue diabetic mice [263]. This could be a highly important step in transferring hESC-based therapies to the clinic and reducing the dependence on immunosuppressive drug regimes – while pancreas progenitors themselves enjoy a certain amount of immune privilege due to low HLA expression, in vivo differentiated cells require protection from the host immune response [264]. Macrodevices provide a suitable environment for progenitor maturation, as their cell-impermeable inner membranes suggest that implanted progenitors would benefit from some amount of protection from host immune cells while retaining proximity to host vasculature [263]. Furthermore, macrodevices are easily retrievable from recipients, which would be an important step in safe clinical trials of progenitor cell therapy.

During development, pancreas progenitors also produce exocrine cells, which would be of no clear benefit to diabetes cell therapies. Follow up studies examining the composition of encapsulated pancreas progenitor grafts have shown that up to 90% of transplanted cells can generate non-endocrine cells types, with ductal cells predominating. In grafts containing the fewest endocrine cells, basal circulating insulin levels were lower, while blood glucose levels were higher both during fasting and immediately after a glucose challenge [265,266]. Consistent conversion of progenitor cells to endocrine cells appears to be vital for ideal graft function.

The pancreatic endocrine progenitor is a more restricted progenitor cell that generates only the endocrine islet cells of the pancreas. Endocrine progenitors arise from trunk progenitor cells in the developing pancreas, where Pdx1, Hnf6, Sox9, and an intermediate level of Notch signalling are all cooperatively required to induce expression of the endocrine progenitor marker Ngn3 in mice [166,267,268]. Using endocrine progenitors as a cell source for transplant would theoretically preclude any non-endocrine differentiation in vivo and ensure that all transplanted cells contribute

to ameliorating diabetes. The high level of paracrine and gap junction signalling between islet cell types required for effective regulation of secretion also advocates for a pure population of endocrine cells for effective graft function.

Several barriers exist preventing the use of endocrine progenitors for cell therapy. Generation of $NGN3^+$ endocrine progenitors from hESCs is generally less efficient than the preceding $PDX1^+$ pancreas progenitor stage. Efficiency at this stage was not quantified in one differentiation study, but showed NGN3 protein expression in only a subset of cells [254]. In the other, more robust induction was reported, with 72% of cells $NGN3^+/NKX6.1^+$; an encouraging result that will require further testing in different hESC lines [255]. Even so, further refinement of the differentiation to endocrine progenitor cells will certainly benefit the proportion of cells that convert to mature endocrine cells in transplant. Another issue is that endocrine progenitor cells in development appear to exit the cell cycle. In mouse, Ngn3 protein expression is associated with G1, but not other stages, of the cell cycle [189]. Ngn3 is initially phosphorylated at a single serine residue by cyclin-dependent kinases Cdk2 and Cdk4/6 during G1, which triggers its transcriptional activity in the presence of binding partner E47 [269]. Phospho-Ngn3 is able to bind the regulatory region of the cell cycle controller Cdkn1a (p21), promoting its transcription and subsequent cell cycle arrest [188,270]. Hyperphosphorylation at up to 5 further serine residues promotes Ngn3 degradation in cells that do not commit to the endocrine lineage [269,270].

Endocrine progenitor cell cycle exit means that, under normal circumstances, these cells may resist expansion in vitro prior to transplantation. Only one previous study has reported the ability to expand hESC-derived $NGN3^+$ endocrine progenitors in vitro, and this required co-culture on organ-matched mesenchymal cells [271]. The signals provided by mesenchymal feeder cells to promote expansion of endocrine progenitors remains to be elucidated. In optimal defined culture conditions, a balance

is likely to be required between allowing NGN3 hyperphosphorylation to continue proliferation, while preventing differentiation to non-endocrine lineages permitted by low NGN3 protein expression.

Foetal pancreas has been used to study the process of differentiation from a multipotent pancreas progenitor cell to the endocrine progenitor, although foetal tissue has been under-utilised in recent years compared to hESC-derived pancreatic cells. This is arguably something of an oversight, as embryonic and foetal pancreas are the only endogenous sources of pancreas progenitor and endocrine progenitor cells under physiological conditions [272] **(Figure 5)**, and therefore represent the 'gold standard' in research of progenitor cell gene expression and phenotype. For example, rat foetal pancreas was used a source of authentic pancreas progenitor cells to show that histone deacetylases (HDACs) are downregulated during pancreas development and differentiation; whole foetal pancreas tissue was then cultured in explants to show that HDAC inhibitors could be used to induce endocrine progenitor differentiation and Ngn3 expression [273]. This shows that foetal pancreas progenitor cells can be useful research tools. However, the requirement for freshly isolated foetal tissue is a limiting factor to building upon experiments such as this one, and almost certainly contributes to the under-utilisation of foetal pancreas progenitor cells. There have been few efforts to culture expandable pancreas progenitor cell lines, and methods that have been published suffer from various drawbacks which will be described in later Chapters.

In conclusion, using pancreas progenitor cells for cell therapies for diabetes is a promising alternative with advantages over transplanting pure β-cells. Endocrine progenitors in particular seem to be the ideal cell type for transplant due to their restricted differentiation potential that may eliminate generation of non-endocrine pancreas cell types while retaining the ability to mimic the heterogeneous nature of the adult pancreatic islet where, as detailed earlier in this Chapter, the complex

interplay of multiple paracrine and gap junction signals appears integral to maintaining homeostatic signalling. In contrast, the utility of β-cell-only transplant strategies may be limited as they do not reflect the microenvironment of normal islets. However, advances must first be made in identifying the correct conditions to specify and expand these cells in vitro. The ease, scale, and reliability of future experiments would benefit greatly from having a source of expandable pancreas progenitor cells on which to work.

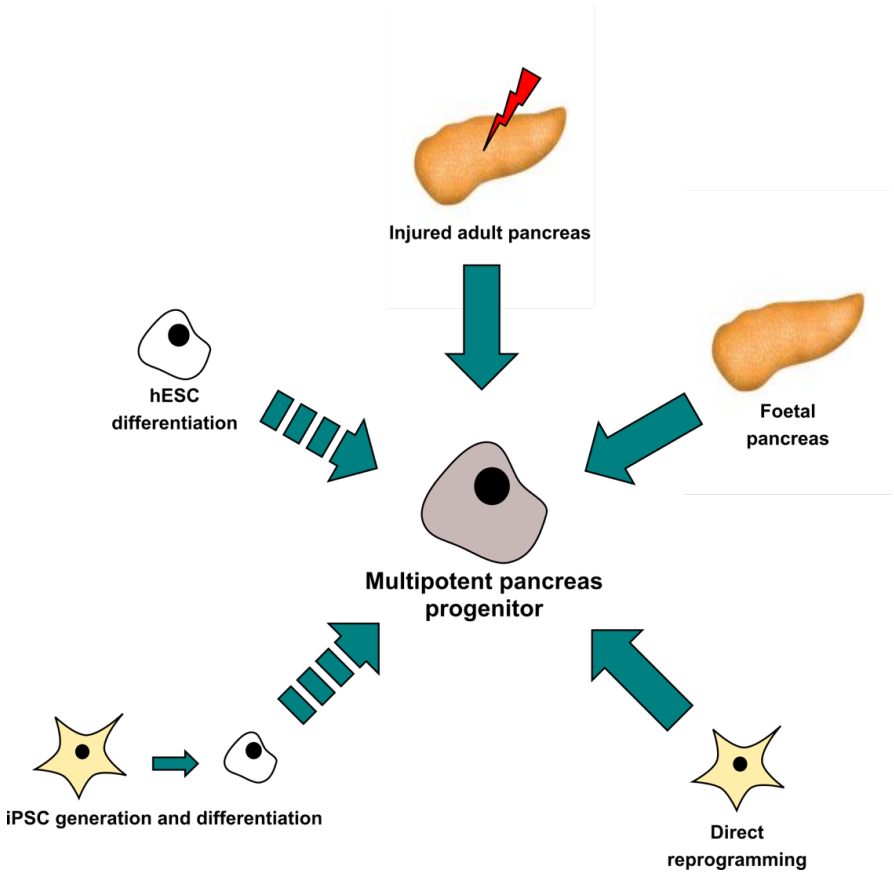

Figure 5. Documented sources of multipotent pancreatic progenitor cells.

Pancreatic progenitor cells do not reside in the healthy adult pancreas – they are a transient amplifying cell type present only during pancreas development, with islet β-cell turnover in the adult occurring by a slow rate of self-replication[297]. However, injury to the adult pancreas (by pancreatic duct ligation, for example) is thought to induce dedifferentiation of exocrine cells to a foetal progenitor-like state as a means of limited tissue regeneration. Pancreatic progenitor cells can also be generated in vitro by reprogramming, differentiation, or a combination of both techniques[315,360-362]. However, results from in vitro progenitor generation can be variable and often require significant investments of time or reagents.

1.5 Aims

All current evidence suggests that we still lack the ideal conditions to stimulate proper endocrine progenitor differentiation in vitro, with most focus being placed on generating mature β-cells. We suggest that effort should instead be placed on uncovering the signals required to stimulating endocrine progenitor emergence in vitro, and potentially allow endocrine progenitor expansion as well.

In light of this, the aims of this project are as follows:

1. To improve our knowledge of human pancreas development by better characterising expression of key progenitor genes and proteins in human foetal pancreas, in order that this may lead to knowledge that can improve selection of in vitro conditions (Chapter 3)
2. To establish simple, defined conditions for the stable culture of authentic pancreas progenitor populations from mouse foetal pancreas – these can then be used to more easily investigate conditions for improving endocrine differentiation (Chapter 4)
3. To investigate whether pancreas progenitors from human foetal pancreas behave in the same way as those from mouse (Chapter 5)
4. To produce a reporter hESC tool for simultaneously tracking endocrine progenitor emergence and proliferation in vitro (Chapter 6)

CHAPTER 2
Materials and methods

2.1 Collection and processing of foetal pancreas

2.1.1 Collection of human foetal pancreas

Human foetal samples were collected and used with ethical approval from Lothian Research Ethics Committee in connection with Professor Richard Anderson (study code LREC 08/S1101/1), and women gave informed written consent. Fixed human foetal pancreas tissue was additionally received from the Human Developmental Biology Resource (HDBR), for which ethical approval was obtained by the Institute of Human Genetics, Newcastle and the Institute of Child Health, London.

Human foetuses (8-19 weeks gestation) were obtained after medical termination of pregnancy by Mifepristone. Gestational age was determined by ultrasound scan, and later confirmed for second trimester foetuses by foot length measurement. Foetal age was described in the format 'weeks+days' (e.g. 8+5). Foetuses were stored at 4°C and dissection of the pancreas was performed as soon as possible. Dissection was performed using scissors and forceps under a stereomicroscope or by eye, with extra-pancreatic tissue removed manually. Dissected tissue was briefly kept in PBS at 4°C until use.

2.1.2 Collection of mouse foetal pancreas

All mouse foetal samples were the product of timed matings between C57BL/6 mice. Matings were set up overnight and females were checked for the presence of a vaginal plug the following morning by trained staff. If a plug was present, midday of that day was described as embryonic day 0.5 (E0.5). Pregnant mice were culled by trained staff using cervical dislocation, and foetal pancreas dissection was performed

using scissors and forceps under a stereomicroscope in PBS. Extra-pancreatic tissue, particularly the overlying mesenchyme, was manually removed as much as possible. Embryos were kept at 4°C whenever possible during dissection. Embryos between E12.5-15.5 were used. Remaining tissues were passed to other users wherever possible.

2.1.3 Fixation and embedding of foetal pancreas

Human and mouse foetal pancreas was fixed by immersion in 4% paraformaldehyde (PFA) for 1 hour at room temperature, or overnight at 4°C. Once fixed, tissue was washed in 70% ethanol for 3x5 minutes, and then used immediately or stored in 70% ethanol at 4°C.

Fixed foetal pancreas was embedded in paraffin wax for sectioning. Tissue was first dehydrated by successive immersion in 70% ethanol, 80% ethanol, 95% ethanol, 100% ethanol (x2) and xylene (x2), each for 30 minutes. Tissue was then transferred to molten paraffin wax for 1 hour, before being placed into a mould filled with molten wax and allowed to set at room temperature. Completed paraffin blocks were stored at room temperature until sectioning.

2.1.4 Lysis of foetal pancreas and RNA extraction

Work benches and dissection equipment were cleaned with RNaseZap® prior to RNA extraction, and RNAse-free filter tips were used during processing. Foetal tissue lysis and RNA extraction differed depending on tissue size as judged by eye. For large tissue samples, the pancreas was mechanically disrupted using dissection equipment or a tissue grinder, followed by homogenisation using the Qiagen QIAshredder® Kit (Qiagen, 79654). RNA was extracted from QIAshredder lysates using the Qiagen RNeasy® Mini Kit (Qiagen, 74104). For small tissue samples, the pancreas was lysed

directly without mechanical disruption using the MasterPure™ Complete DNA/RNA Purification Kit (Cambio, MC85200), a non-column based extraction kit that allowed recovery of a higher yield of nucleic acid. Purified RNA was resuspended in nuclease-free water (ThermoFisher, AM9937) and RNA quality and quantity were assessed using the NanoDrop™ Spectrophotometer or the Qubit™ Fluorometer. RNA was kept on ice during use, and stored at -80°C.

2.2 Immunostaining

2.2.1 Immunocytochemistry

Cells were fixed in 4% PFA for 10 minutes, then washed in PBS three times quickly. Cells were then either stored in PBS at 4°C or the staining process continued. For staining, cells were first permeabilised in 0.5% Triton™X-100 (Sigma, T8787) in PBS (PBST) for 15 minutes, then blocked in solution containing 5% donkey (Sigma, D9663) or goat serum (Sigma, G9023) and 1% bovine serum albumin (BSA) (Sigma, A9647) in PBST for 1 hour at room temperature on a plate rocker. Cells were incubated with primary antibodies (see Chapter 2.2.3) diluted in blocking solution overnight at 4°C on a plate rocker, followed by three brief washes in PBST and incubation with appropriate secondary antibodies diluted in PBST for 2 hours at room temperature in the dark. Finally, cells were incubated with 4',6-diamidino-2-phenylindole dihydrochloride (DAPI) (AppliChem, A4099) diluted 1:7,500 in PBS for 10 minutes at room temperature in the dark before imaging. Cells were imaged using a Zeiss Observer or Nikon Eclipse Ti-E microscope.

2.2.2 Immunohistochemistry

Sections were either pre-prepared by the Lothian NRS BioResource (for adult pancreas) or self-prepared from paraffin blocks. Paraffin blocks were sectioned using

a Leica Manual Microtome, where sections were cut at 5μm thickness and affixed to polysine slides by placing slides on a heated rack overnight.

Slides for immunohistochemistry were de-waxed in xylene (2x5 minutes), then rehydrated in 100% ethanol (2x3 minutes) followed by 95% ethanol and 70% ethanol (1 minute each) before immersion in tap water. Antigen retrieval was routinely performed in TE buffer pH9.0 (10mM Tris (Sigma, T1503), 1mM EDTA (Sigma, E4884), 0.05% Tween 20 (Sigma, P9416) in Milli-Q® water). TE buffer was pre-heated in the microwave for 10 minutes at full power in a sealed container, before slides were placed in the buffer and heated for a further 2x10 minutes at full power. Buffer volume was topped up with Milli-Q® water between heating steps. After heating, slides were allowed to sit in retrieval before until cool, then transferred to tap water. Sections were then permeabilised, blocked and stained using the same methods as described in Chapter 2.2.1, except that secondary antibody incubation was extended to overnight. After staining, sections were briefly dried using an aspirator and VECTASHIELD® Antifade Mounting Medium (Vector Laboratories, H1400) immediately applied with a glass cover slip. Mounting medium was allowed to set for 10 minutes at 4°C in the dark, then cover slips were sealed by painting with clear nail varnish around the edges. Stained slides were stored at -20°C. Slides were imaged using Olympus BX61 or Nikon Eclipse Ti-E microscopes, or the Operetta High-Content Imaging System.

2.2.3 Antibodies

Antibody	Dilution	Catalogue number
PDX1	1:100 (IHC) 1:200 (ICC)	R&D, AF2419
SOX9	1:200 (IHC) 1:500 (ICC)	EMD Millipore, AB5535
Ki67	1:50	Dako, M7240
NKX2.2	1:100	Atlas, HPA003468
SOX17	1:200	R&D, AF1924
FOXA2	6.66μg/ml	Abnova, H00003170-M10
HNF1B	10μg/ml	Santa Cruz, sc7411
E-cad (ICC)	1:200	Sigma, U3254
E-cad (FACS)	1:300	ThermoFisher, 50-3249-82

2.2.4 Image processing and analysis

Microscope images were processed using Fiji software. Processing typically entailed improving image brightness and contrast by utilising the image histogram feature to display only the optimal distribution of pixel intensities, as well as adding colour to images. Image data were analysed using either CellProfiler (for microscope images) or Columbus software (for Operetta images).

2.3 Flow cytometry

2.3.1 Cell preparation and reagents

Live cells were washed in PBS and detached by incubating in accutase for 5-10 minutes, depending on the cells. Accutase was neutralised in culture medium before

cells were counted on a haemocytometer. The desired cell number was pelleted by centrifugation at 1,300 rpm for 3 min, then resuspended in fluorescence-activated cell sorting (FACS) buffer (2% foetal calf serum (APS, S-001B-BR) and 2mM EDTA (Life Technologies, 15575020) in PBS) including antibody if applicable.

If antibody was being used, cells were resuspended at a concentration of 500,000 cells/100μl antibody solution and cells were incubated at 4°C for 15 minutes. 10ml FACS buffer was subsequently added and cells were pelleted as above. The cell pellet was washed by resuspending in 5ml FACS buffer followed by pelleting, and this process repeated twice more. After the final wash, cells were resuspended in at least 200μl FACS buffer and passed through a cell strainer for flow cytometry or FACS. DAPI was added to cells as a live/dead stain.

For cell cycle analysis by flow cytometry, live cells were detached as above and resuspended in 1ml normal culture medium before adding 1μl Hoescht 33342 nucleic acid dye (5mg/ml) and incubating cells at 37°C for 1 hour. Cells were then pelleted as above, resuspended in at least 200μl FACS buffer and passed through a cell strainer for flow cytometry.

2.3.2 Flow cytometers and data analysis

Flow cytometry was performed on a BD LSR Fortessa machine, while FACS was performed on a BD FACSAria II machine. FACSDiva software was used for initial data collection and analysis, with further analysis performed and figures generated using FlowJo software.

2.4 Molecular biology techniques

2.4.1 RNA and DNA extraction

RNA and DNA extraction from cells and subsequent purification was performed using the MasterPure™ Complete DNA/RNA Purification Kit (Cambio, MC85200). For hESC clone genotyping, genomic DNA (gDNA) was obtained by lysing cells in lysis buffer (0.45% NP40 (Sigma, I8896), 0.45% Tween 20 (Sigma, P9416), 0.2μg/ml Proteinase K (ThermoFisher, EO04921), 1X GC PCR buffer (ThermoFisher, supplied with F530S) in water), with lysates then incubated in a thermal cycler at 55°C for 2 hours and 95°C for 10 mins before direct use in PCR or short-term storage at 4°C. Purified RNA and DNA was resuspended in nuclease-free water (ThermoFisher, AM9937) and quality and quantity were assessed using the NanoDrop™ Spectrophotometer or the Qubit™ Fluorometer. RNA was kept on ice during use, and stored at -80°C. DNA was stored at -20°C.

2.4.2 First strand cDNA synthesis

cDNA was synthesised from RNA by first transferring the desired quantity of RNA (between 200-1000ng depending on the experiment) to a 0.2ml PCR tube and making up the total volume to 12μl with nuclease-free water if required (ThermoFisher, AM9937). PCR tubes were transferred to ice before adding 1μl each of Oligo dT18 (ThermoFisher, SO132) and 10mM dNTP mix (ThermoFisher, R0192). Samples were mixed and briefly centrifuged before incubation in a thermal cycler at 65°C for 5 minutes, then immediately placed on ice for 1 minute. To each sample 4μl 5X FS buffer, 1μl 0.1M DTT and 0.5μl RNaseOUT (Life Technologies, all supplied with 18080044) was added. 0.5μl SuperScript™III Reverse Transcriptase (Life Technologies, 18080044) was further added to samples, except in the case of -RT

controls. Samples were mixed and briefly centrifuged again, then placed in a thermocycler at 25°C for 5 minutes, 50°C for 50 minutes, then 70°C for 15 minutes. cDNA was stored at -20°C.

2.4.3 Primer design

Primers for routine PCR were designed using Primer3 web software. Primers for RT-qPCR were designed using Universal ProbeLibrary Assay Design Center web software. Wherever possible, RT-qPCR primers were designed to be intron spanning. Primers were ordered as dry pellets from Sigma.

2.4.4 Human RT-qPCR primers

Gene	UPL probe	Left primer	Right primer
GAPDH	60	agccacatcgctcagacac	gcccaatacgaccaaatcc
B-ACTIN	64	ccaaccgcgagaagatga	ccagaggcgtacagggatag
OCT4	3	gagtgagaggcaacctggag	gccggttacagaaccacact
SOX17	61	acgccgagttgagcaaga	tctgcctcctccacgaag
HNF1B	9	caccaacatgtcttcaagtaaacag	ttgttgcgcacgaagtaagt
HNF4A	68	gagatccatggtgttcaagga	gtgccgagggacaatgtagt
PDX1	78	aagctcacgcgtggaaag	gccgtgagatgtacttgttgaa
SOX9	61	gtacccgcacttgcacaac	tctcgctctcgttcagaagtc
NGN3	60	ttttgcgccggtagaaag	gggcaggtcacttcgtctt

NEUROD1	30	ctgctcaggacctactaacaacaa	gtccagcttggaggacctt

2.4.5 Mouse RT-qPCR primers

Gene	UPL probe	Left primer	Right primer
Gapdh	29	ttcaccaccatggagaagg	cacacccatcacaaacatgg
B-actin	64	ctaaggccaaccgtgaaaag	accagaggcatacagggaca
Pdx1	67	aagctcacgcgtggaaag	ggccgggagatgtatttgt
Sox9	66	gtacccgcatctgcacaac	ctcctccacgaagggtctct
Krt19	97	agtcccagctcagcatgaa	taacgggcctccgtctct
Hes1	99	acaccggacaaaccaaagac	cgcctcttctccatgatagg
Ngn3	25	tccagtgttgcgtcttacctc	agacgacgaacatcatctatgg
NeuroD1	1	cgcagaaggcaaggtgtc	tttggtcatgtttccacttcc
Nkx2.2	20	tctacgacagcagcgacaac	cgtgcagggagtattggag
Amy2a	7	gtggaatggcgagaagatgt	ctctgtcagaaggcaccaaa
p19	22	ggtcagcttcctagctcctg	aactccaggggagtgagacc
p21	21	tccacagcgatatccagaca	ggacatcaccaggattggac

p27	10	tggagggcagatacgagtg	cgggggcctgtagtagaact
p57	17	caggacgagaatcaagagca	gcttggcgaagaagtcgt
Ins2	32	gaagtggaggacccacaagt	agtgccaaggtctgaaggtc
Glu	33	cacgcccttcaagacacag	gtcctcatgcgcttctgtc
Vim	79	tgcgccagcagtatgaaa	gcctcagagaggtcagcaaa
Cpa1	25	agcagtcttcggcaatgag	cagaagtccaacttcaagtgctc
Nkx3.2	29	aggtgctgaggccacctt	ccgggagacagtagtaagggta

2.4.6 PCR (polymerase chain reaction)

Routine PCR was performed using Phusion® High-Fidelity DNA Polymerase (ThermoFisher, F530S) as described in the product manual with HF buffer for 30 cycles. For amplification from gDNA templates, GC buffer was used and 3% DMSO added. PCR extension times were altered according to amplicon size (30 seconds/kb) and specific primer pair annealing temperatures were calculated using NEB Tm Calculator web software, with annealing temperature reduced by -1.8°C if DMSO present.

2.4.7 RT-qPCR (reverse transcription quantitative polymerase chain reaction)

Work benches and dissection equipment were cleaned with RNaseZap® prior to RT-qPCR, and RNAse-free filter tips were used during setup. cDNA templates were initially prepared as described in Chapter 2.4.2, then stock cDNA was diluted 1:10 in

nuclease-free water (ThermoFisher, AM9937). 2μl of diluted cDNA was pipetted into wells of a MicroAmp® Fast Optical 96-Well Plate (ThermoFisher, 4346907). 8μl RT-qPCR mastermix comprised of 5μl TaqMan® Gene Expression Master Mix (ThermoFisher, 4369016), 2.5μl nuclease-free water, 0.4μl 10μM primer pair mix and 0.1μl Universal ProbeLibrary probe was added to each well. The plate was sealed, before being vortexed and centrifuged briefly. RT-qPCR was performed in a QuantStudio™7 Flex Real-Time PCR machine on the preset cycling conditions for 40 cycles.

Cycle threshold (CT) values were obtained and fold change data calculated in Microsoft Excel. Technical replicate CT values were first averaged, then normalised to housekeeping gene CT values. The resulting data were then normalised to a reference or control sample, before fold change and standard deviation calculated. For certain experiments where more stringent analysis was required, the geometric mean of CTs for two housekeeping genes was calculated and used for normalisation.

2.4.8 Primer efficiency

A selection of RT-qPCR primer pairs were evaluated for primer amplification efficiency to validate the Universal ProbeLibrary Assay Design Center primer design software. Serial dilutions of positive control cDNA (1X, 0.1X, 0.01X, 0.001X, 0.0001X, where undiluted cDNA is considered to be 10X) or gBlock DNA (0.1ng, 0.01ng, 0.001ng, 0.0001ng, 0.00001ng) were made. 2μl of each cDNA dilution was used in triplicate for RT-qPCR as described in Chapter 2.4.5. CT values were obtained and, in Microsoft Excel, plotted against Log_{10} values template dilutions. Primer efficiency was calculated using the following formula:

$$10^{(-1/\text{slope value of regression line})}$$

Primer efficiency was converted to a percentage, and all primer pairs tested achieved efficiencies between 90-110%, validating the Universal ProbeLibrary Assay Design Center primer design software.

2.4.9 Agarose gel electrophoresis

Agarose gels were prepared at concentrations between 0.8-2%, depending on the size of the DNA sample, by adding the required mass of UltraPure™ agarose powder (ThermoFisher, 16500500) to 100ml 1X TAE buffer (40mM Tris (Sigma, T1503), 20mM acetic acid (Sigma, A6283), 1mM EDTA (Life Technologies, 15575020)). The solution was heated in a microwave for 2x1 minutes on full power or until agarose had fully dissolved. Molten agarose was cooled briefly before 4μl 10mg/ml ethidium bromide (Sigma, E1510) was added and mixed. Agarose was poured into a clean gel tray with comb and allowed to set. Set gels were placed in a gel tank and enough 1X TAE buffer was added to cover the gel. The required amount of DNA to be run was mixed with water and loading dye in the appropriate proportions, alongside GeneRuler 1kb Plus DNA Ladder (ThermoFisher, SM1333). Gels were typically run at 135V for 20 minutes before being visualised.

2.5 Mammalian cell and tissue culture

2.5.1 Culture of hESCs (human embryonic stem cells)

MasterShef7 (MS7) hESCs were derived by the University of Sheffield, and were a kind gift to us from Dr Tilo Kunath. MS7 hESCs were routinely cultured on Human Recombinant Laminin 521 (LN521) (BioLamina, LN521). Cell culture plates were pre-coated with 5μg/ml LN521 diluted in PBS calcium/magnesium (Life Technologies, 14040083). Coated plates were incubated at 37°C for 2 hours prior to use or stored overnight (or for up to 1 month) at 4°C. MS7 hESCs were cultured in Essential 8™

Medium (Gibco™, A1517001) (E8) and routinely passaged by incubating in 0.5mM EDTA (Life Technologies, 15575020) in PBS at 37°C for 5 minutes. For flow cytometry or nucleofection, hESCs were detached using accutase at 37°C for 10 minutes. For cryopreservation, MS7 hESCs were detached as usual and resuspended in STEM-CELLBANKER® (AMSBIO, 11897), transferred to a cryovial and stored overnight at -80°C before transferring to liquid nitrogen for long-term storage.

2.5.2 Differentiation of hESCs to pancreas progenitors

Differentiation of MS7 hESCs was performed exactly as described in the literature [259], with the exception that cells were cultured on LN521 rather than Matrigel®, and A83-01 was used instead of Alk5iII during Stage 5. In this protocol, multiple previously published protocols for pancreas differentiation were aggregated for optimal efficiency. Briefly, Stage 1 of differentiation (3 days) yields definitive endoderm [274], Stage 2 (2 days) yields posterior foregut [252], Stage 3+4 (5 days) yields pancreas progenitors [252], and Stage 5 (3 days) yields endocrine progenitors [252].

2.5.3 Culture of mouse foetal pancreas (whole)

Mouse foetal pancreatic buds were dissected at E12.5 as described in Chapter 2.1.2. Overall dissection time for all buds procured for a single experiment was kept to under 2 hours wherever possible to maximise cell viability. Dissected buds were transferred to the relevant basal culture medium on ice. For experiments where whole pancreatic buds were cultured without extracellular matrix, buds were transferred from basal medium to a tube containing relevant complete culture medium by pipetting. From here, buds were transferred to a culture well plate containing complete culture medium by pipetting. For experiments where whole pancreatic buds were embedded in collagen on a transwell, dissected buds were transferred to Hank's Balanced Salt

Solution (HBSS) (Gibco™, 14025092) on ice. 2.5mg/ml Collagen V (Sigma, C3657) was prepared on ice by dissolving 5mg collagen powder in 1.5ml 0.1% glacial acetic acid (Sigma, A6283). 200μl 10X RPMI culture medium (Sigma, R1145) and 300μl 1M $NaHCO_3$ (Sigma, S5761) were then added, followed by dropwise addition of 1M NaOH (Sigma, S5881) until the solution turned pink/purple. Transwell filters (Millicell, PICM03050) were floated on 1ml culture medium in cell culture wells. Cold collagen solution was transferred to a small dish on ice and dissected buds were added. 10-20μl of cold collagen solution containing pancreatic buds was pipetted onto the filter in a droplet, and the plate was incubated at 37°C. The small molecule inhibitor of p21, UC2288, was a kind gift from Prof. Robert Weiss.

2.5.4 Culture of mouse foetal pancreas (dissociated)

Mouse foetal pancreatic buds were dissected at E12.5 as described in Chapter 2.1.2. Overall dissection time for all buds procured for a single experiment was kept to under 2 hours wherever possible to maximise cell viability. Dissected buds were transferred to the relevant basal culture medium on ice, with the desired number of buds for each well pooled into separate tubes. Tubes were centrifuged at 1,300 rpm for 3 minutes and supernatant removed. 500μl 0.05%/0.02% trypsin/EDTA solution (Sigma, 59417C) was added to the pelleted buds, and the tube was incubated in a thermomixer heated to 37°C at 1,400 rpm for 5 minutes. The solution was then mixed by pipetting with a P1000 pipette set to 400μl to further mechanically dissociate buds. Thermomixer incubation was repeated, followed by subsequent pipetting with a P200 set to 200μl. Thermomixer incubation was repeated once more, then trypsin/EDTA was neutralised by adding 500μl culture medium. Tubes were centrifuged at 1,300 rpm for 3 minutes and supernatant removed, then cells resuspended in complete culture medium before adding to culture wells. Wells were pre-coated with Matrigel®

Growth Factor Reduced Basement Membrane Matrix (Corning, 354230), which had been diluted 1:10 in Advanced DMEM/F12 (Gibco™, 12634010). Enough diluted Matrigel® was added to coat the well, and plated were incubated at 37°C for 30 minutes before Matrigel® was aspirated and culture medium added.

Basal culture medium for dissociated mouse pancreas progenitors was a variation on N2B27. This included Advanced DMEM/F12, 1:100 GlutaMAX™ (Gibco™, 35050061), 1:100 Penicillin/Streptomycin (ThermoFisher, 15140-122), 1:100 B27 minus vitamin A (Life Technologies, 12587-010), 1:200 N2 (Life Technologies, 17502-048) and 10μM Y-27632 (Cambridge Bioscience, SM02). As required, this was further supplemented with 50ng/ml EGF (Peprotech, 315-09), 50ng/ml FGF7 (Biolegend, 752206), 50ng/ml FGF2 (Peprotech, 100-18B) and/or 0.5μM A83-01 (Sigma, SML0788).

2.5.5 Culture of human foetal pancreas (dissociated)

Human foetal pancreas was dissected as described in Chapter 2.1.1. For small samples, foetal pancreas was dissociated exactly as described for mouse foetal pancreas in Chapter 2.5.4. For large samples where more mechanical dissociation was required, foetal pancreas was first disrupted in a glass tissue grinder (ThermoFisher, 11522443), before also proceeding exactly as described for mouse foetal pancreas.

Culture medium for human foetal pancreas was as described for mouse foetal pancreas.

2.5.6 Transfections and plasmid details

Lipofection was performed using Lipofectamine® LTX with Plus™ Reagent (ThermoFisher, 15338100) as specified in the product manual. hESC nucleofection was performed using the Human Stem Cell Nucleofector Kit 2 (Lonza, VAPH-5022) as specified in the product manual. Roughly $1x10^6$ cells were used for nucleofection of 4μg NGN3 targeting vector plasmid and 2μg of each zinc finger nuclease (ZFN). Cells were nucleofected on programme A13 of a Nucleofector™ IIb. For CycB1-Cherry random insertion, plasmid was linearised with ScaI-HF® (NEB, R3122) and purified by ethanol precipitation, then 4μg was used for nucleofection on programme B16. Selection of NGN3-targeted cells was performed using 25μg/ml Hygromycin B (Sigma, 10843555001) and 4μM Ganciclovir (Sigma, G2536) after selection cassette removal, and CycB1-Cherry-inserted cells using 2μg/ml Blasticidin S hydrochloride (VWR, A3784).

NGN3 targeting vector and ZFN plasmids were a kind gift from Prof. Catherine Verfaillie. CycB1-Cherry lentiviral vector plasmid was a kind gift from Prof. Yuval Dor, which was cloned to a Gateway vector plasmid as described in the main text.

2.6 Bacterial cell culture, transformations and extracting plasmid DNA

2.6.1 Bacterial transformations and culture

Routine bacterial transformations were performed using DH5α Competent Cells (ThermoFisher, 18265-017). For Gateway cloning, One Shot™ TOP10 Competent Cells (ThermoFisher, C404010) were used. Agar plates were prepared in a sterile hood and made with either 1:1,000 Kanamycin (ThermoFisher, 11815024) or 1:1,000 Ampicillin (Sigma, 10835242001). 50μl aliquots of bacteria were retrieved from -80°C

storage and thawed on ice prior to use. For transformation, plasmid DNA was added to cells, stirred with a pipette tip and incubated on ice for 30 minutes. Heat shock was performed in a thermomixer at 42°C for 45 seconds, followed by rest on ice for 2 minutes. 950µl pre-warmed SOC medium (Sigma, S1797) was added, then cells were incubated in a thermomixer at 37°C at 500 rpm for 1 hour before spreading on agar plates. Plates were incubated at 37°C overnight and subsequently stored at 4°C if required.

Bacterial colonies were picked using a sterile P1000 tip, which was incubated in 5ml lysogeny broth (LB) containing 1:1,000 antibiotic at 37°C at 500 rpm over the course of a working day. These cultures were used to seed 100ml LB cultures incubated at 37°C at 500 rpm overnight.

2.6.2 Extracting plasmid DNA

DNA was extracted from overnight bacterial cultures and purified using QIAprep Spin Miniprep Kit (Qiagen, 27104), Qiagen Plasmid Midi Kit (Qiagen, 12143) or Qiagen Plasmid Maxi Kit (Qiagen, 12162) as specified in the product manual. DNA was eluted in water.

2.7 Statistical analysis

All statistical analysis was performed in GraphPad Prism 7 software. Where significant p values are indicated in Figures as asterisks, * = $p \leq 0.05$, ** = $p \leq 0.01$, *** = $p \leq 0.001$, **** = $p \leq 0.0001$.

CHAPTER 3

Characterising expression of key genes and proteins during human foetal pancreas development

3.1 Introduction

Studying tissue and organ development in model organisms has provided valuable insights into candidate pathways that can be used to direct differentiation of stem cells in vitro. It also reveals cell lineage markers that can be explored in human tissues, helping to better classify the cellular composition in the development human embryo and foetus. Several comprehensive reviews are available in the literature that cover the topic of pancreas development, but these invariably focus on mouse development [7,151,275,276] or other vertebrate models, such as xenopus or zebrafish [277]. There is clearly a need to elucidate the molecular and cellular regulation of human pancreatic development. Inevitably, due to issues of accessing human foetal tissues, this has lagged behind. Current views suggest there are enough differences between mouse and human pancreas structure and cellular composition in the adult to suggest that developmental mechanisms and timings may well differ between the species – the disparity between mouse and human islets was discussed in Chapter 1.1.3, but other differences exist too. The mouse pancreas is also more diffuse than the human pancreas both macroscopically and microscopically [6]. Such knowledge will help developing stem cell-based approaches to new therapies or disease modelling.

Mouse studies in particular have been an important reference point for pancreas research in the context of diabetes [278]. Murine models offer the possibility of knockout and lineage tracing studies, which cannot be performed in human foetal stages. These have proved very valuable in elucidating pancreas-specific gene function and

provide candidate key functional regulators which are explored in this thesis (see Chapter 1.4).

The limited number of studies that have explored human foetal pancreas development have focused on determining the expression of a few key genes and proteins during only the early developmental stages [46,130,172]. There is a paucity of data documenting co-expression patterns of progenitor markers in the human foetal pancreas in the post-Carnegie stages of development, with most co-expression studies opting for describing single progenitor markers alongside mature cell markers [279].

There is a clear need to build on the existing body of evidence describing human pancreas development by examining co-expression of protein markers of pancreas progenitor cells. This will give us a more reliable expectation of the transcriptional profile of authentic human pancreas progenitors in culture and at what stages/regions we are likely to be able to derive successful cultures.

The aim of this Chapter therefore, was to characterise human foetal pancreas progenitors during a window of development spanning from 10 weeks to 19 weeks gestation – a hitherto unexplored stage of human development. Specifically, our goal was to determine the dynamics of the expression of PDX1 and SOX9 – markers of multipotent pancreas progenitors – to compare and contrast our results with mouse development and improve our understanding of human pancreas development.

3.2 Results

3.2.1 Gene expression analysis of whole human foetal pancreas during early to mid-development

To examine how expression of pancreas progenitor marker genes changes over the course of early to mid-development in the human pancreas, we first assessed mRNA expression of *PDX1* and *SOX9* in whole foetal pancreas by RT-qPCR. Due to the small size of the foetal pancreas early in development, relatively small quantities of RNA could be recovered and used for synthesise cDNA for gene expression analysis. To ensure gene expression data were as robust and reliable as possible, two housekeeping genes were used for normalisation during data analysis (see Chapter 2.4.5). Fold change in expression of both *PDX1* and *SOX9* was significantly different from both *GAPDH* and *B-ACTIN* ($p<0.001$) housekeeping genes at 16 and 19 weeks gestation, indicating changes in progenitor gene expression at these developmental stages. However, neither *PDX1* or *SOX9* showed a fold change in expression significantly different from both housekeeping genes at earlier weeks analysed ($p>0.05$), suggesting that no meaningful changes in progenitor gene expression occurred at these timepoints **(Figure 6A)**.

PDX1 mRNA levels were relatively consistently expressed between weeks 11 to 15 of pancreas development, but rose significantly at week 16 (1.83-fold) and again at week 19 (3.470-fold) **(Figure 6A)**. While *PDX1* expression at week 12 was found to be significantly higher than weeks 11, 14 and 15, these differences were discounted due to no statistical difference between housekeeping gene and *PDX1* expression at this stage.

Expression of *SOX9* closely matched the pattern observed for *PDX1* and increases in expression were detected at week 16 (2.17-fold) and week 19 (3.48-fold) **(Figure 6B)**.

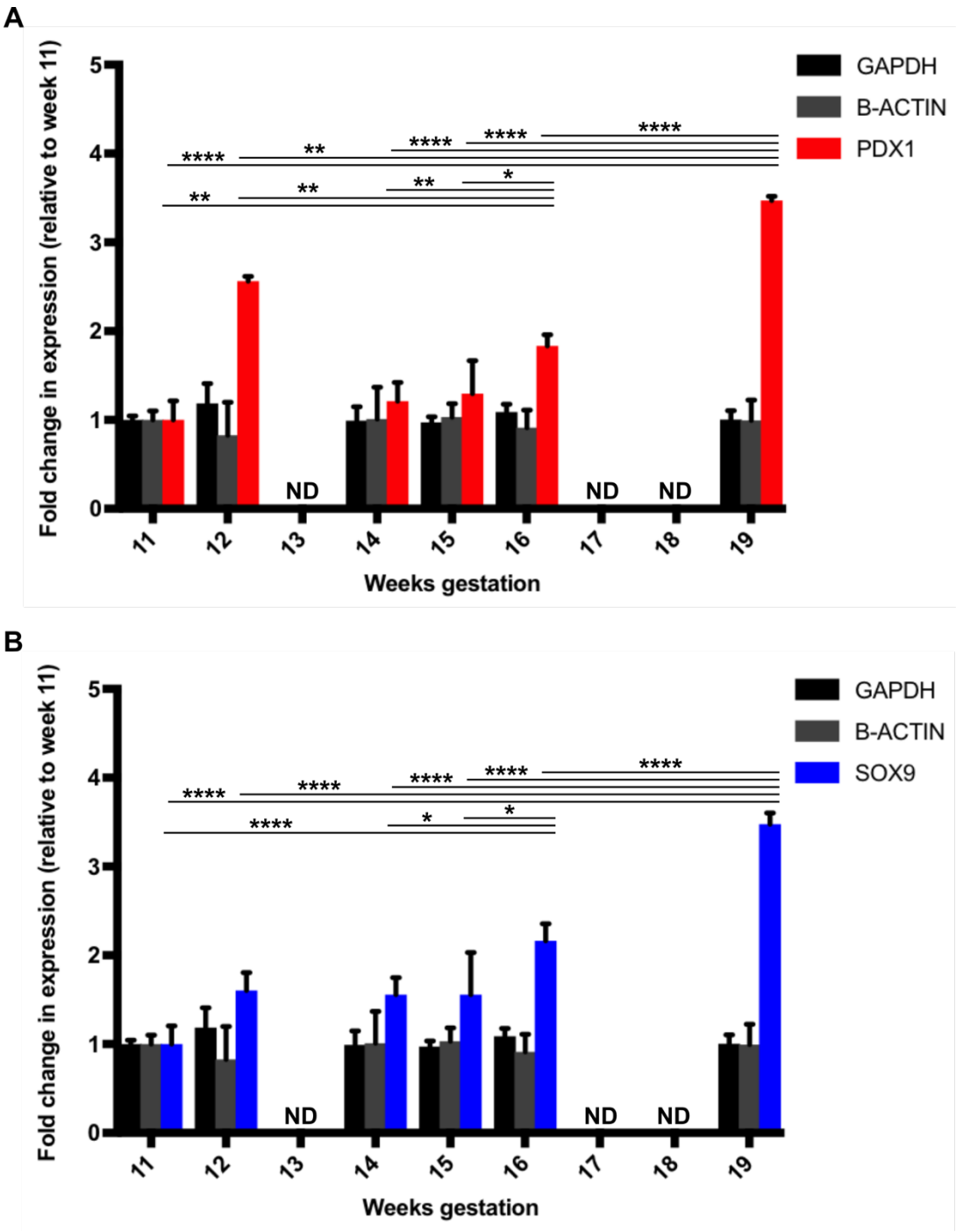

Figure 6. mRNA expression of *PDX1* and *SOX9* in whole human foetal pancreas.

200ng of RNA was used to make cDNA. Relative expression of *PDX1* and *SOX9* was calculated by first normalising CT values of the gene of interest to the geometric mean value of both *GAPDH* and *B-ACTIN* CTs from the same sample. The resultant ΔCT value was subsequently normalised to the ΔCT for week 11, the earliest timepoint available. Fold change was then calculated from ΔΔCTs. **(A)** Weeks 11, 12, 19 n=2, weeks 14, 15 n=3, week 16 n=4. **(B)** Weeks 11, 12, 19 n=2, weeks 14, 15 n=3, week 16 n=4. Error bars show standard deviation. Significance between housekeeping genes and genes of interest tested using multiple unpaired t-tests with Holm-Sidak correction (not shown). Significance between foetal stages tested using two-way ANOVA with Tukey's test (shown on graphs, * = p≤0.05, ** = p≤0.01, *** = p≤0.001, **** = p≤0.0001). ND=not determined.

Commitment to the endocrine pancreas progenitor lineage is thought to between 8-21 weeks gestation [47,172,279]. We therefore wanted to assess expression of endocrine pancreas progenitor markers to see if this period of endocrine commitment is reflected in changes to mRNA levels over the course of development. *NGN3* expression progressively increased across the duration of human pancreas development **(Figure 7A)**. While *NGN3* expression only differed significantly from expression of both *GAPDH* and *B-ACTIN* in weeks 16 ($p<0.01$ for both housekeeping genes) and 19 ($p<0.05$ for both housekeeping genes) of gestation, there appears to be a trend for increasing *NGN3* transcript expression with each week of gestation. Relative *NGN3* expression between weeks was significantly higher at week 19 compared to previous weeks, with a 27.9-fold increase over week 11. Expression at week 16 was also significantly higher than week 11 (10-fold). The lack of statistical significance in *NGN3* expression levels between early weeks of gestation (week 11, 14 and 15) may reflect a modest rise in transcript levels early in development, or simply a lack of statistical power caused by sample size.

To further explore the observed trend for increased endocrine progenitor marker expression from early to mid-development, We examined expression of *NEUROD1*. This is an endocrine progenitor marker expressed downstream of NGN3.

NEUROD1 mRNAs were only detectable from week 11 onwards **(Figure 7B)**, consistent with the idea that *NEUROD1* expression in endocrine progenitors occurs subsequent to *NGN3*, which is reportedly expressed from week 8 [172]. *NEUROD1* expression was significantly different from *GAPDH* (weeks 15 and 19 $p<0.05$, weeks 12 and 14 $p<0.01$, week 16 $p<0.001$) and *B-ACTIN* (weeks 12, 14, 15 and 19 $p<0.05$, week 16 $p<0.001$) in all weeks tested. Relative expression of *NEUROD1* steadily rose between weeks 11 and 19, with significant increases detected at most successive weeks tested, rising to a 26.6 fold increase over week 11 at week 19. We conclude

that both *NGN3* and *NEUROD1* progressively increase in expression between weeks 9 and 19 of gestation. The data suggest that endocrine progenitors are specified in significant numbers around weeks 15-16.

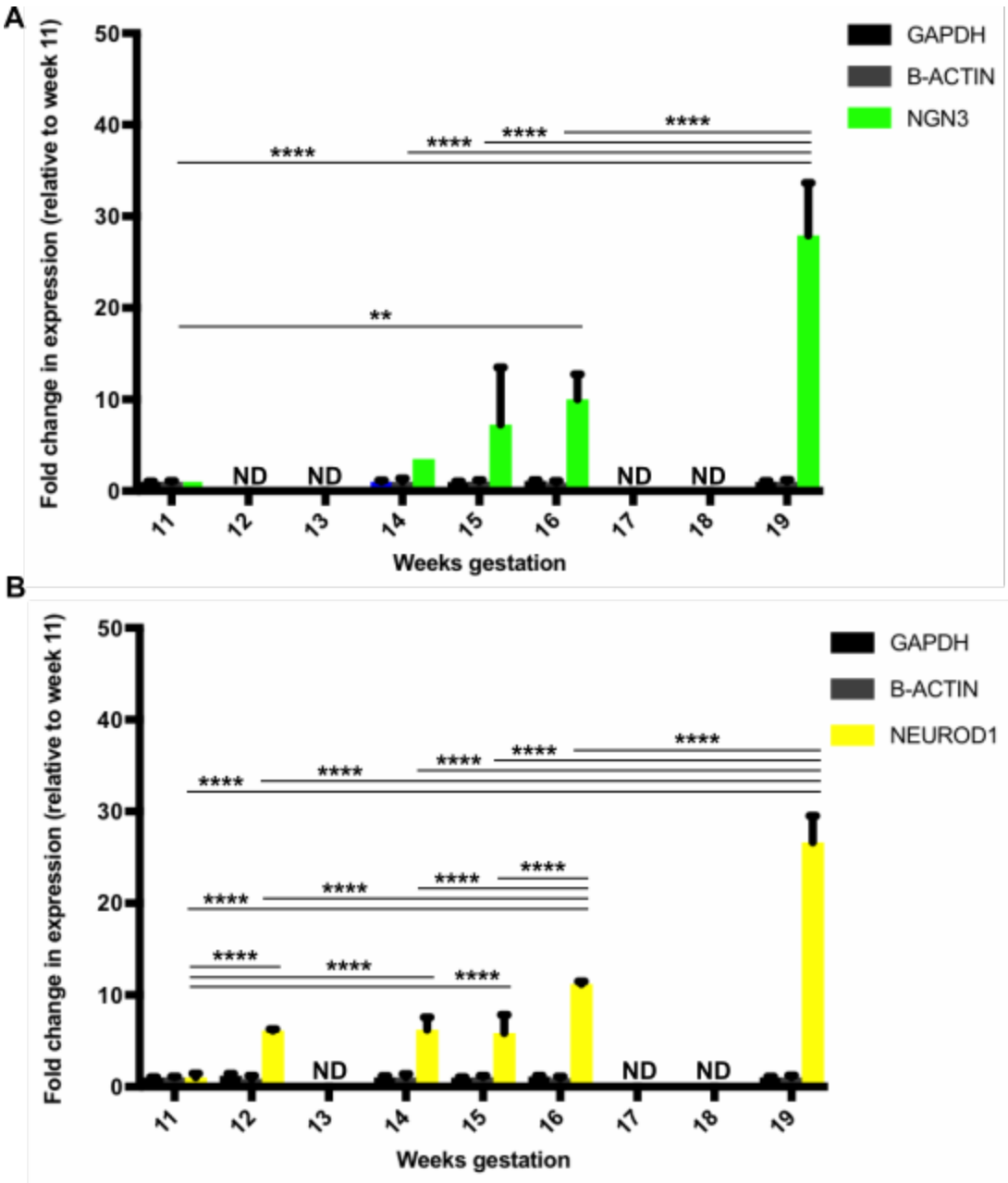

Figure 7. mRNA expression of *NGN3* and *NEUROD1* in whole human foetal pancreas.

200ng RNA was used to make cDNA. Relative expression of *NGN3* and *NEUROD1* was calculated by first normalising CT values of the gene of interest to the geometric mean value of both *GAPDH* and *B-ACTIN* CTs from the same sample. The resultant ΔCT value was subsequently normalised to the ΔCT for week 11, the earliest timepoint available. Fold change was then calculated from ΔΔCTs. **(A)** Weeks 11, 14 n=1, weeks 15, 19 n=2, week 16 n=3 **(B)** Weeks 11, 12, 19 n=2, weeks 14, 15 n=3, week 16 n=4. Error bars show standard deviation. Significance between housekeeping genes and genes of interest tested using multiple unpaired t-tests with Holm-Sidak correction (not shown). Significance between foetal stages tested using two-way ANOVA with Tukey's test (shown on graphs, * = $p \leq 0.05$, ** = $p \leq 0.01$, *** = $p \leq 0.001$, **** = $p \leq 0.0001$). ND=not determined.

3.2.2 Histological characterisation of human foetal pancreas during early to mid-development

As the pancreas grows in size it becomes more heterogeneous as the varied cell types are specified. The changes in gene expression are accompanied by gross structural and morphological changes (see Introduction Figure 3) . We therefore next performed histological staining and immunohistochemistry of key markers: PDX1 and SOX9. Unfortunately, despite many attempts, we were unable to achieve good IHC staining using available antibodies for NGN3, including those utilised in previous studies by other groups. The staining results observed with common NGN3 antibodies (AB5684, F25A1B3, AF3444 and TA500090) were not reproducible in our hands.

Haematoxylin and eosin (H&E) staining on sections of paraffin-embedded human foetal pancreas tissue from different stages was performed **(Figure 8)**. Gestational weeks 10-12 are characterised by a ductal epithelium (known to contain early pancreas progenitors) that is stained almost exclusively blue by haematoxylin, indicating a large nucleus and very little cytoplasm. Ductal epithelium is present across the whole tissue section at early stages. However, ducts only undergo branching at later stages via branching morphogenesis.

From week 12, pink eosin staining of cytoplasm becomes more evident, allowing for distinguishable apical and basal sides of ductal epithelial cells. This is presumably because ductal cells undergo morphogenesis to form the lumens on the apical side in preparation for channelling digestive enzymes through pancreatic ducts in later life. At weeks 17 and 19, the ductal epithelial network becomes noticeably more compacted and ducts coalesce into discreet groups. Eosin staining is strongest in these sections, where foetal pancreatic tissue begins to resemble the architecture of the adult pancreas. Additionally, later sections contain recognisable islet-like structures (Figure 8; red arrows). These are characterised by small nuclei and pale

cytoplasm, confirming that commitment to endocrine lineages is occurring by the later stages of human development examined here.

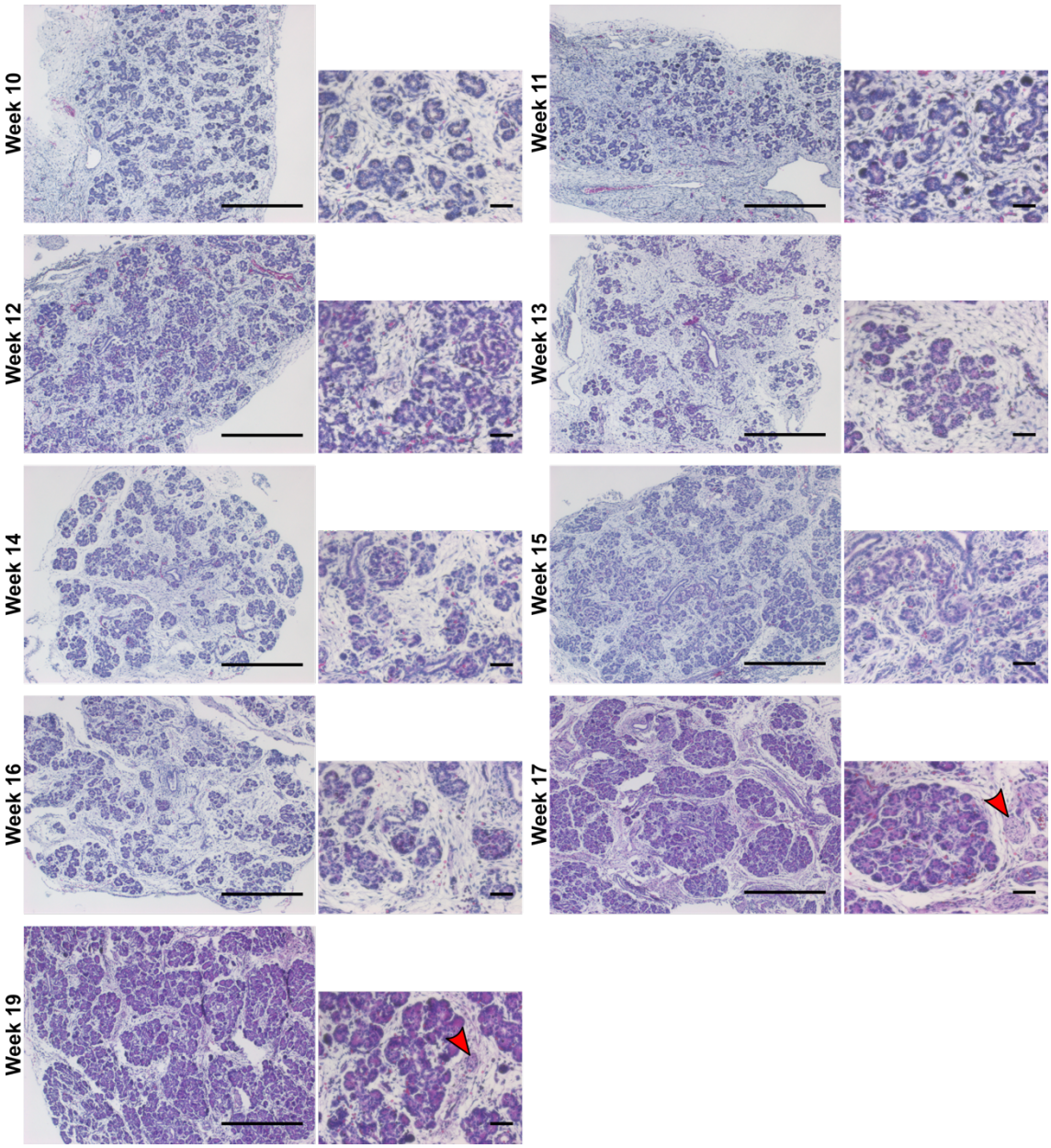

Figure 8. H&E staining of human foetal pancreas.

Whole human foetal pancreas was embedded in paraffin wax and 5μm sections cut for H&E staining. Bright field images were taken under the 5X and 20X objectives (scale bars represent 500μm and 50μm, respectively). Red arrows in weeks 17 and 19 images indicate presumptive foetal islets.

3.2.3 PDX1/SOX9 protein co-expression in human foetal pancreas during early to mid-development

Histology and mRNA expression of key markers within the whole foetal pancreas provided an initial indication of the transitions from progenitor to differentiation. However, we next wished to determine levels of PDX1 and SOX9 protein using immunohistochemistry; this provides single cell resolution of candidate progenitor compartments within the developing tissue. Also, changes to mRNA transcript levels do not necessarily directly reflect changes at the protein level [280] and so we wished to confirm the timing when progenitors emerge.

Fluorescence immunohistochemistry (IHC) was performed on sections of paraffin-embedded human foetal pancreas to determine the expression levels and localisation of the putative PDX1 and SOX9 co-expressing pancreas progenitor cells during early to mid-development.

An example field of view (FOV) for PDX1 and SOX9 staining for each foetal pancreas stage is shown in **Figure 9**. Double positive cells were localised to the same ductal epithelial cells identified in earlier H&E stains. Consistent with the qPCR data for mRNA expression, we found that both proteins were detectable at similar levels across the week 10 to week 19 series of tissue.

Initial observations of IHC suggested that PDX1 and SOX9 co-expression is seen in nearly all cells between weeks 10-13 of gestation. After these stages their expression becomes more divergent, with SOX9 especially extinguished from many ductal cells (see Figure 9, small panels). The loss of SOX9 expression would fit with progenitor cell differentiation to acinar or endocrine lineages as development proceeds.

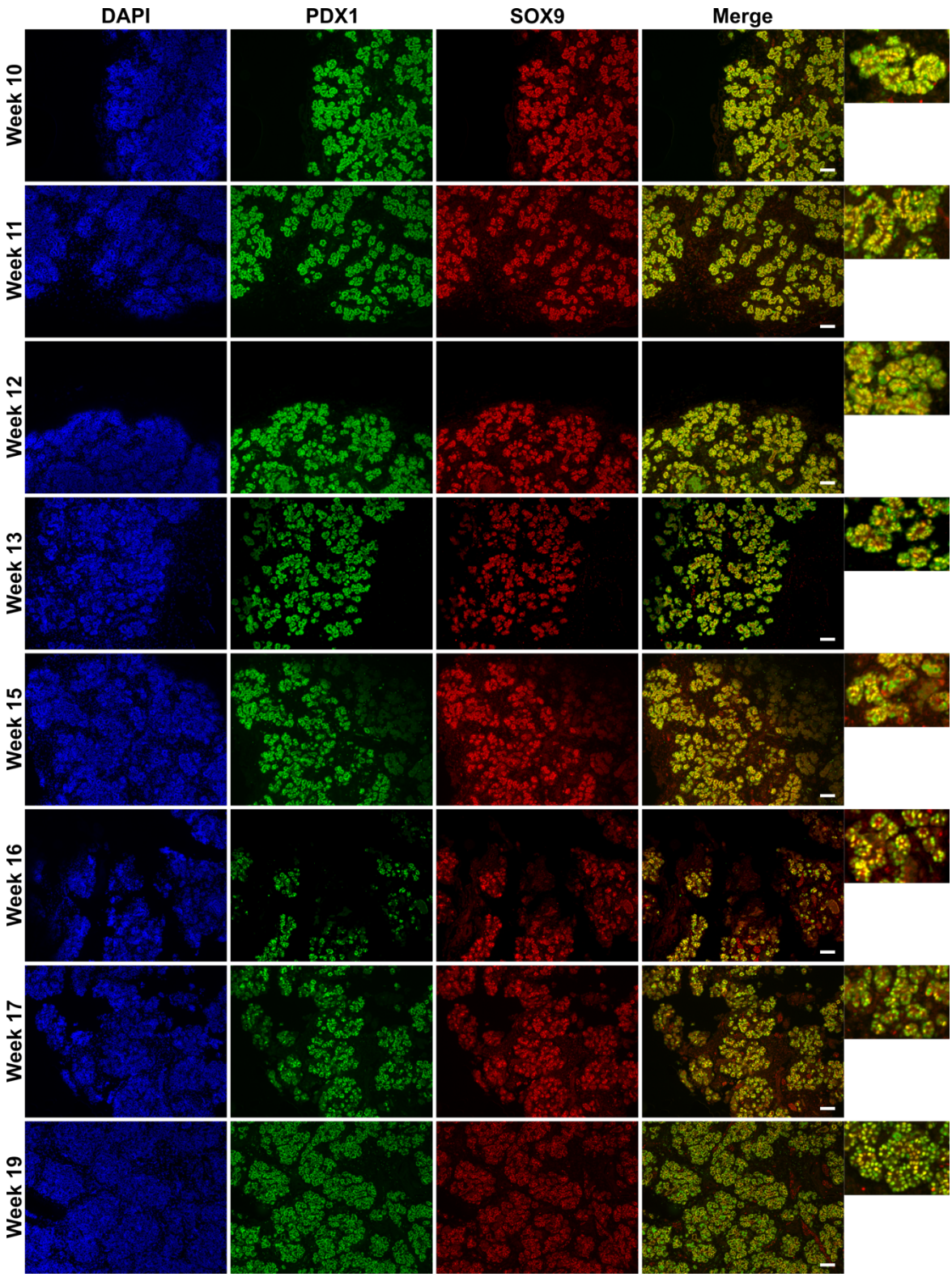

Figure 9. PDX1 and SOX9 expression in human foetal pancreas.

Whole human foetal pancreas was embedded in paraffin wax and 5μm sections cut for IHC. All FOVs shown are were included in the image analysis, along with other suitable FOVs (not shown). Images were taken using 10X objective (scale bar represents 100μm). Small panels (right) show zoomed merged images.

3.2.4 Quantitative analysis of PDX1 and SOX9 cell populations in the developing human foetal pancreas

To provide quantitative readouts of developing cell populations, stained sections of human foetal pancreas were pre-scanned using the PerkinElmer® Operetta High-Content Imaging System. We selected as many appropriate fields of view (FOVs) as possible for each section for final scanning through the 10X objective. FOV selection was occasionally limited by small tissue size **(Table 1)**.

All FOVs were subject to the same analysis parameters on Columbus™ Image Analysis software. First, nuclear segmentation was performed by initially applying a predefined algorithm 'M' to images, and subsequently fine-tuning segmentation parameters (12μm diameter, 0.45μm splitting coefficient, 0.40μm common threshold). Quality control was performed on segmented presumptive nuclei by checking DAPI staining intensity histograms for all FOVs of every scanned tissue section – cut-offs to staining intensity were applied that suitably captured the majority of nuclei on all FOVs, while excluding artefacts (DAPI staining intensity >50 and <6,000). Total nuclei were counted **(Figure 10A)** and each nucleus assigned positive or negative for PDX1 and SOX9 expression based on mean staining intensity. Once again, this was performed by checking staining intensity histograms to determine cut-offs that could be suitably applied to all tissue sections. As the PDX1 and SOX9 antibodies used were reliable with minimal background, histograms displayed clear positive and negative populations between which cut-offs were placed ($PDX1^+$=staining intensity >800, $SOX9^+$=staining intensity >650) **(Figure 10B and 10C)**, enabling good quantitation.

Table 1. Number of fields of view (FOVs) used for image analysis of PDX1/SOX9 staining of human foetal pancreas.

Suitable FOVs were manually selected from whole section scans.

Tissue sample (weeks gestation)	FOVs for analysis
10	4
11	2
12	2
13	2
15	7
16	3
17	8
19	9

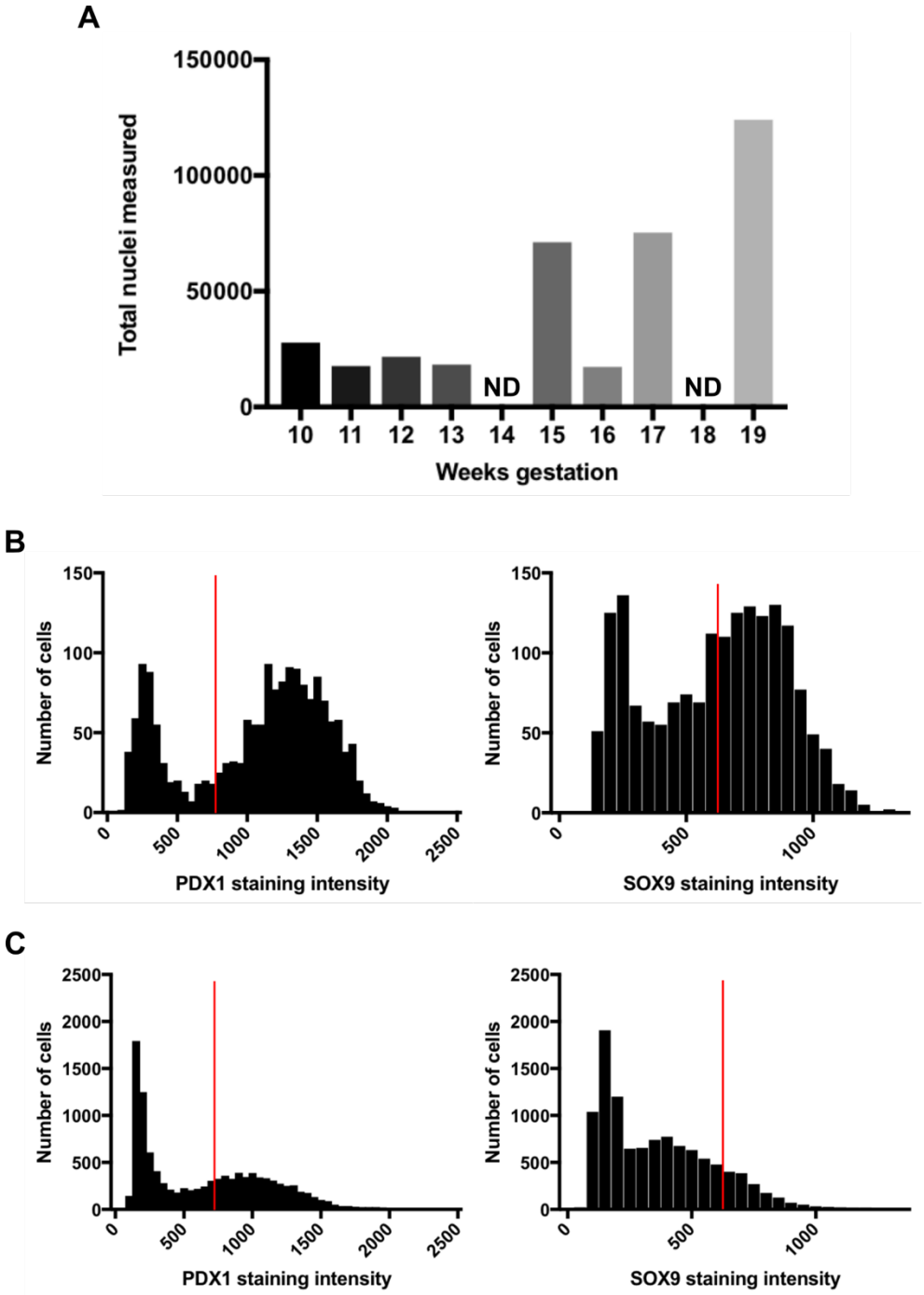

Figure 10. Total nuclei measured and example staining intensity cut-offs.

Image analysis was carried out using PerkinElmer® Columbus™ Image Data Storage and Analysis system. **(A)** Total nuclei measured at each stage. Nuclei were detected automatically using the software, with manual quality control steps to ensure detection accuracy. ND=not determined. **(B)** PDX1 and SOX9 staining intensity histograms for week 10, with cut-offs indicated (red line). **(C)** PDX1 and SOX9 staining intensity histograms for week 19, with cut-offs indicated (red line).

At week 10, 49.89% and 36.51% of all nuclei were positive for PDX1 and SOX9, respectively, compared to 35.98% and 11.66% at week 19 **(Figure 11A)**. Thus, the proportion of all cells positive for either PDX1 or SOX9 tended to decrease during the course of weeks 9 to 19 of gestation, consistent with more differentiated progeny emerging. The lowest proportion of progenitor marker expression was detected at week 16, where 18.83% and 5.72% of nuclei were positive for PDX1 and SOX9, respectively. At each developmental stage examined, PDX1 protein was more widely expressed than SOX9 protein. Furthermore, SOX9 expression was nearly always restricted to a subset of cells also expressing PDX1 **(Figure 11B)**.

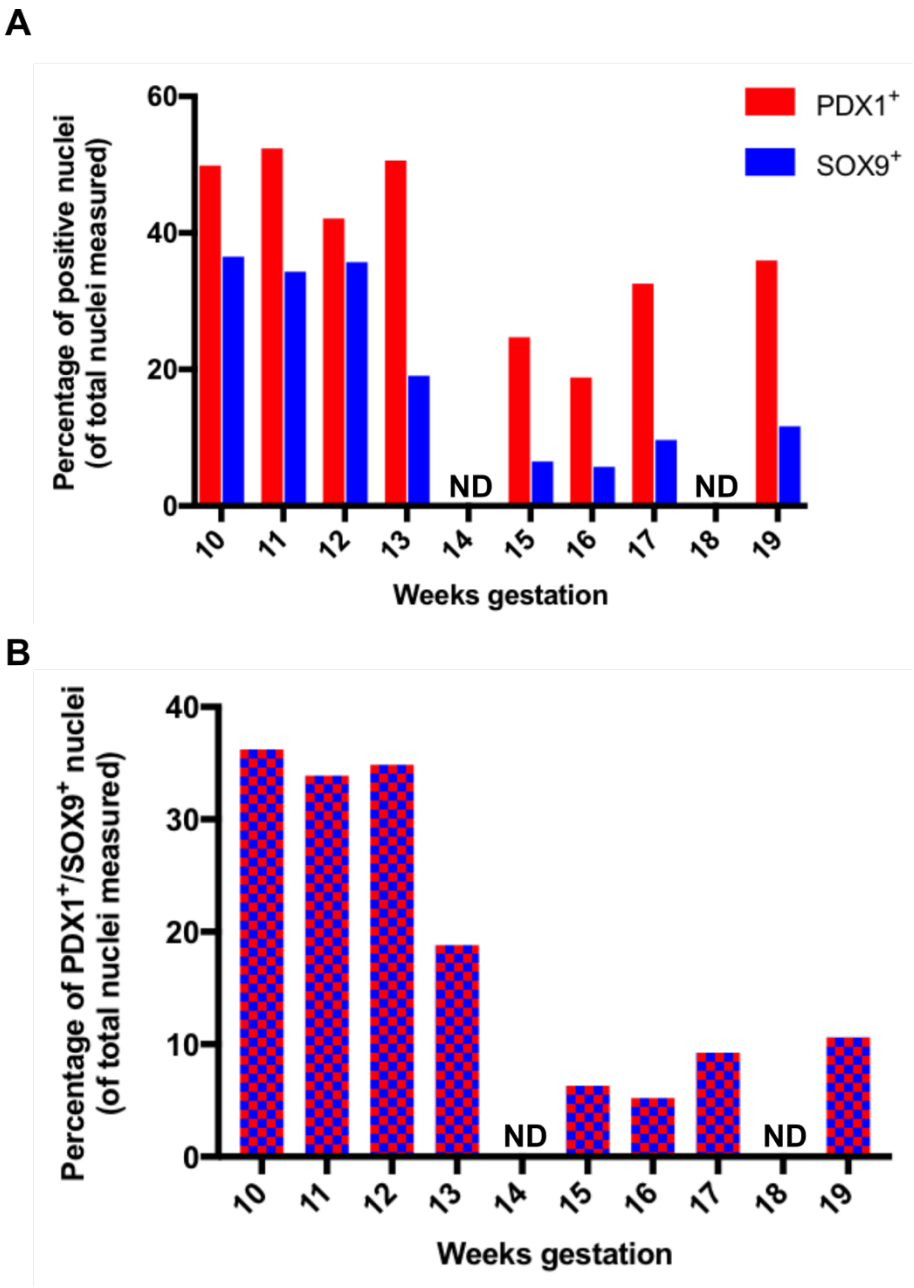

Figure 11. PDX1 and SOX9 positivity at the cellular level in human foetal pancreas at different stages of development.

(A) Proportion of PDX1$^+$ and SOX9$^+$ cells. Positivity in nuclei was determined based on staining intensity measurements from clearly positive and negative cells, with thresholds for set accordingly, and positive cells calculated as a proportion of total nuclei. **(B)** Proportion of PDX1$^+$/SOX9$^+$ cells. The same thresholds were used as for single positive cells, and calculated as a proportion of total nuclei. ND=not determined.

The proportion of total cells that were $PDX1^+/SOX9^+$ was very similar to the proportion of $SOX9^+$ only cells; for instance, $PDX1^-/SOX9^+$ nuclei compromised only 1.03% of all cells at week 19, and the proportion was even lower at other stages. $PDX1^+/SOX9^-$ cells were relatively abundant in contrast, ranging from 7.28% of the total at week 12 to 25.35% at week 19. $PDX1^+/SOX9^+$ progenitors tended to be more common at earlier stages of development, particularly prior to week 13 of gestation.

To explore more deeply the double positive presumptive endocrine progenitors we compared levels of signal to single positive cells. While it may be misleading to compare staining intensity between different sections due to possible variations in tissue processing between samples, comparing staining intensity in single and double positive cells within each section can give an indication of the relative levels of protein in distinct progenitor populations. At each stage of development, the average PDX1 staining intensity in double positive cells exceeded that of the overall average staining intensity for PDX1 **(Figure 12A)**. Interestingly, this suggests that PDX1 protein expression is increased in double positive cells compared to single positive, perhaps identifying a distinct progenitor state. SOX9 staining intensity did not appear to differ between single and double positive cells **(Figure 12B)**, concomitant with the earlier finding that very few $PDX1^-/SOX9^+$ cells exist at any of the developmental stages analysed here.

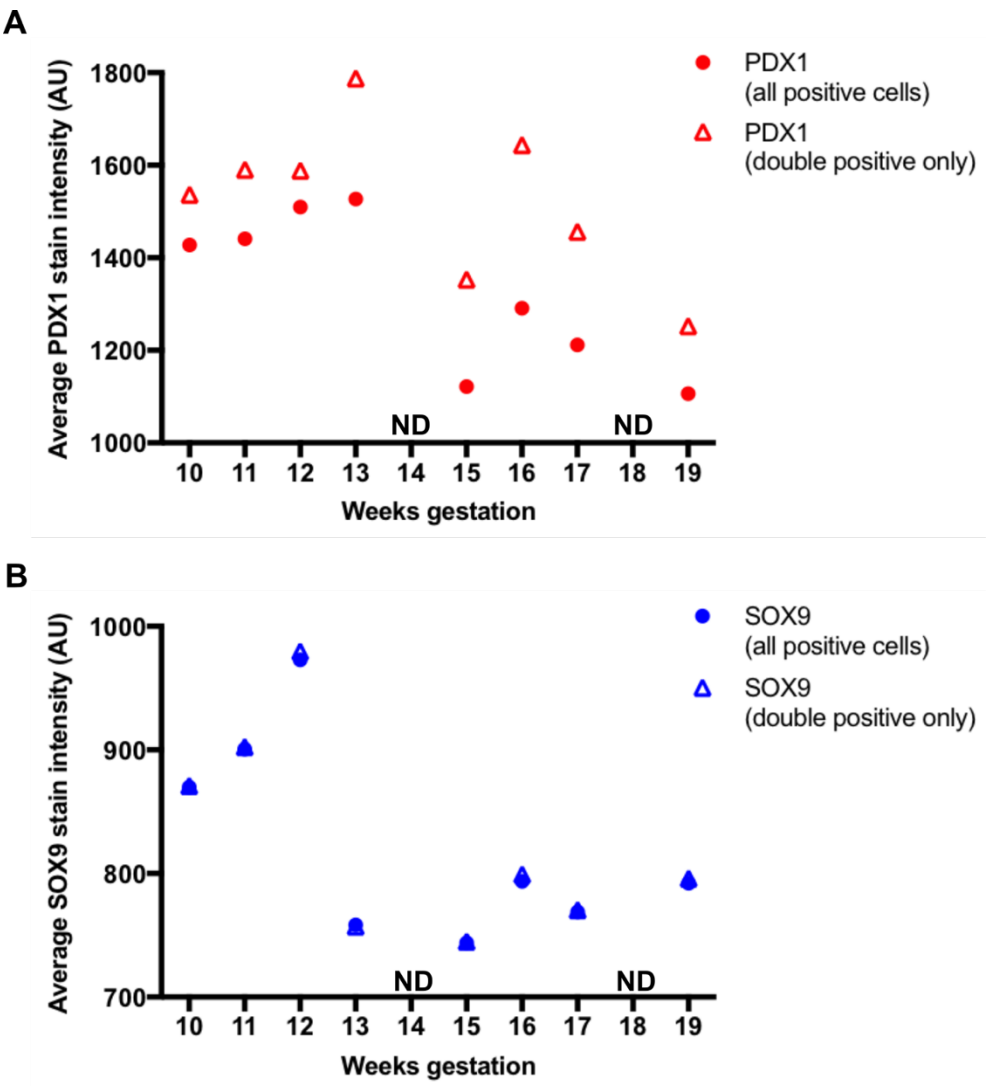

Figure 12. PDX1 and SOX9 staining intensity in sections of human foetal pancreas at different stages of development.

Image analysis was carried out using PerkinElmer® Columbus™ Image Data Storage and Analysis system. **(A)** Average PDX1 staining intensity in single positive cells and double positive cells **(B)** Average SOX9 staining intensity in single positive cells and double positive cells. ND=not determined.

3.3 Discussion

In this chapter, we have been able to utilise an available series of human foetal pancreatic specimens and characterise for the first time expression of PDX1 and SOX9 expression levels during early to mid-development of the human pancreas.

We observed that mRNA expression of early progenitor markers *PDX1* and *SOX9* increased at week 16, and persists at week 19, although the relative increases were modest. Fluctuations in *PDX1* transcript expression during a similar period of human pancreas development have been reported before, although these appeared stochastic with no clear pattern discernible [47]. Our data appear to indicate a trend of increasing *PDX1* and *SOX9* expression, but analysis of their expression after week 19 is required to strengthen this observation. Meanwhile, increased mRNA expression of endocrine progenitor markers *NGN3* and *NEUROD1* was much more robust and demonstrated a similar trend. Expression of both markers steadily increased to peak at week 19, which was the latest stage analysed in this work.

A previously published study documenting the period of NGN3 expression during human development found that the number of $NGN3^+$ cells peaked between weeks 12-14, with the count being significantly lower between weeks 18-21 [172]. Our data does not necessarily contradict these findings, as both datasets would fit with a model in which NGN3 dosage is an important factor for promoting endocrine commitment in individual cells, as is known to be the case in the developing mouse pancreas [162]. In this scenario, many $NGN3^+$ cells may be detectable at early stages of development, but express only relatively low levels of *NGN3* mRNA. If NGN3 protein ultimately only persists in highly expressing cells, later stages of pancreas development may exhibit a smaller $NGN3^+$ cell population by IHC, but still contain a greater total level of transcript. This hypothesis is supported by another study that looked at *NGN3*

transcript expression over a similar time period of human pancreas development to our work, and found that mRNA expression peaked at week 17 [47] – slightly earlier than our results indicate, but later than may have been assumed from the protein expression data shown by Salisbury and colleagues (2014).

The qPCR data clearly shows increasing *NGN3* mRNA expression closely matches that of *NEUROD1*, another endocrine pancreas progenitor marker. We detected *NEUROD1* expression later in development than *NGN3*, and mRNA levels continued to rise throughout the period of development examined, in agreement with other studies [47,279]. This suggests that *NEUROD1* expression can be used a surrogate readout for endocrine commitment, or as further evidence that a cell has reached the required NGN3 dosage for endocrine commitment. Unfortunately, several attempts to validate commercial antibodies for both NGN3 and NEUROD1 were unsuccessful, so characterisation of human endocrine progenitor cells could not be performed. Additional attempts were made to develop a new anti-human NGN3 antibody in collaboration with Atlas Antibodies, but these too were unsuccessful. While RNA in situ hybridisation (ISH) was considered as an alternative strategy, it was ultimately rejected due to *NGN3* transcriptional activity reportedly being an unreliable indicator of NGN3 protein expression [281].

We also analysed *NKX2.2* expression during human pancreas development, but mRNA was barely detectable, and did not display any clear trend over this time period (data not shown). Nkx2.2 plays an important role in mouse endocrine progenitor commitment, but its role in human pancreas development is thought to be more limited [130]. In agreement with this idea and our own qPCR data, IHC of human foetal pancreas for NKX2.2 did not produce clear nuclear staining, although cytoplasmic staining was increasingly evident as development progressed and appeared to be localised to cells outside of the ductal epithelium. The same antibody did stain islet

cell nuclei of adult pancreas, as expected **(Figure 13)**. Cytoplasmic expression of NKX2.2 has not been reported previously to the best of our knowledge, and is a finding warranting further investigation. However, as pancreas progenitors were the focus of this research and NKX2.2 was absent from these cells we did not pursue this factor further.

Our analysis of PDX1 and SOX9 expression at the cellular level has revealed that, while transcript levels of these genes increase modestly and in tandem at the population level, protein expression is highly dynamic. The observation that a large proportion of $PDX1^+$ cells do not express SOX9 highlights how crucial it is to use more than one marker for characterising pancreatic cell types. PDX1 is the most commonly used gene for describing early multipotent pancreas progenitor cells, probably due its expression being so clearly restricted to the primitive pancreas and duodenum [282], and its mutation resulting in pancreas agenesis in mouse and human [283,284]. However, we know that PDX1 is not only detectable in ductal progenitor cells, but also differentiated cell types of the pancreas such as foetal β-cells [130,279].

PDX1 and SOX9 together mark early pancreas progenitor cells of the human ductal epithelium, and we show that these double positive cells are proportionally more common in the developing human pancreas prior to week 13. It is known that Sox9 expression maintains proliferative pancreas progenitors in mice, likely through modulation of Notch/Hes1 signalling pathway [136]. Interestingly, Sox9 is also thought to be essential for initial activation of endocrine commitment in mice, but must then be lost for Ngn3 expression to reach high levels. In Sox9 haploinsufficient mice, fewer endocrine progenitors arise and islet size is reduced. Furthermore, Sox9 binding can be detected at the Ngn3 promoter, giving more evidence for its role in initiating endocrine commitment [285]. However, observations in both mouse and human developing pancreas suggests that robust Ngn3 expression can only be detected in

cells with low Sox9, or where Sox9 is absent [130,286]. Sox9 expression is also absent from acinar cells in mice [136]. Meanwhile, Pdx1 continues to be expressed in certain differentiating cells of the mouse pancreas, such as foetal β-cells and acinar cells [282,287]. Therefore, it is likely that the $PDX1^{+}/SOX9^{-}$ cells identified in our analysis are progenitors that are beginning to differentiate, either committing to endocrine or acinar lineages.

In mouse foetal pancreas, Pdx1 and Sox9 directly reinforce each other's expression to coordinate a pancreas-specific gene network [288]. Our novel finding that, in human foetal pancreas, PDX1 expression is higher in double positive cells compared to single positive cells represents the first evidence that PDX1 and SOX9 elevate each other's expression to promote pancreas identity **(Figure 14)**.

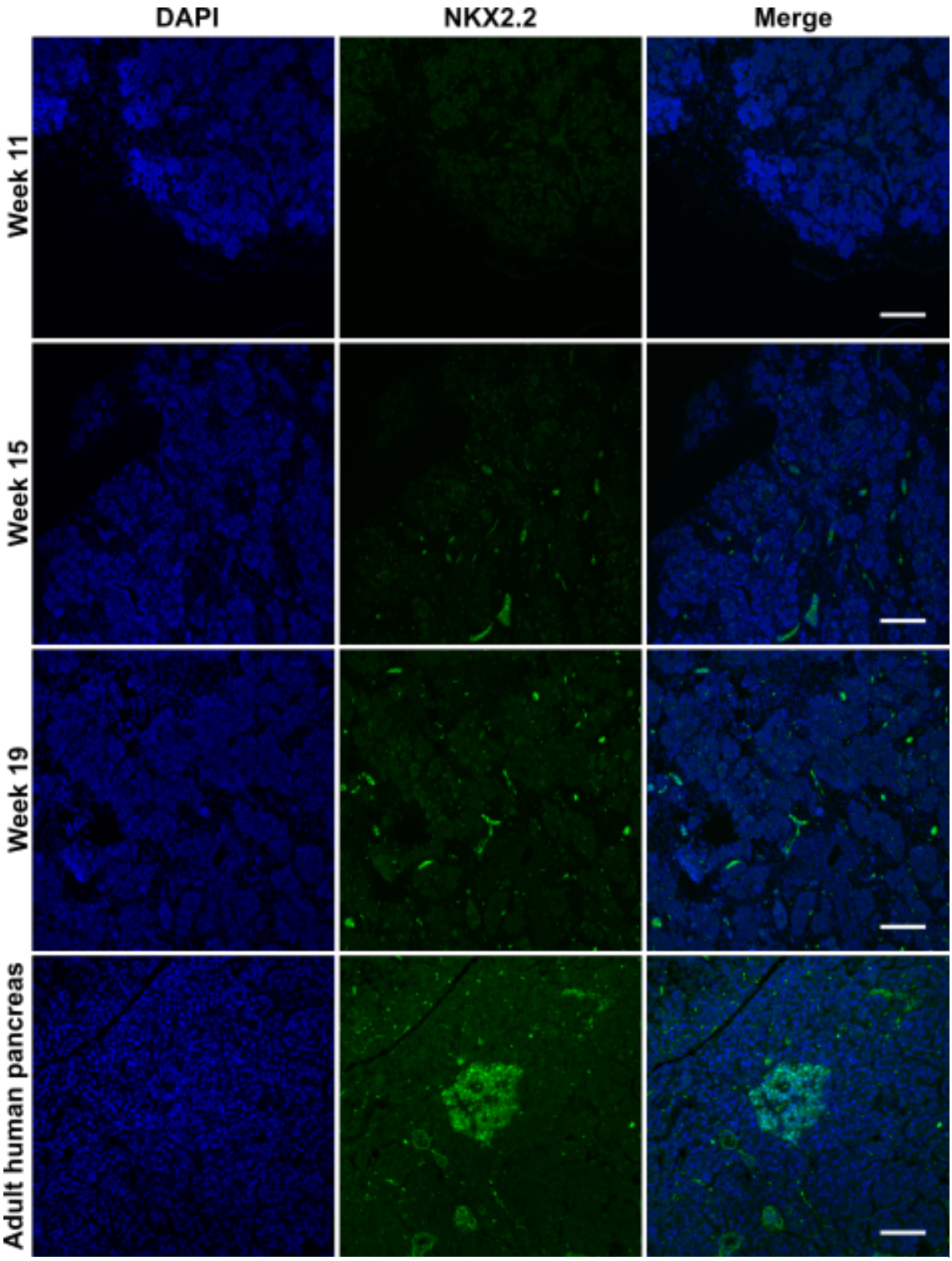

Figure 13. NKX2.2 expression in foetal and adult human pancreas.

Paraffin wax sections of foetal or healthy adult human pancreas at 5μm thick were obtained for IHC. Images were taken using 20X objective (scale bar represents 100μm).

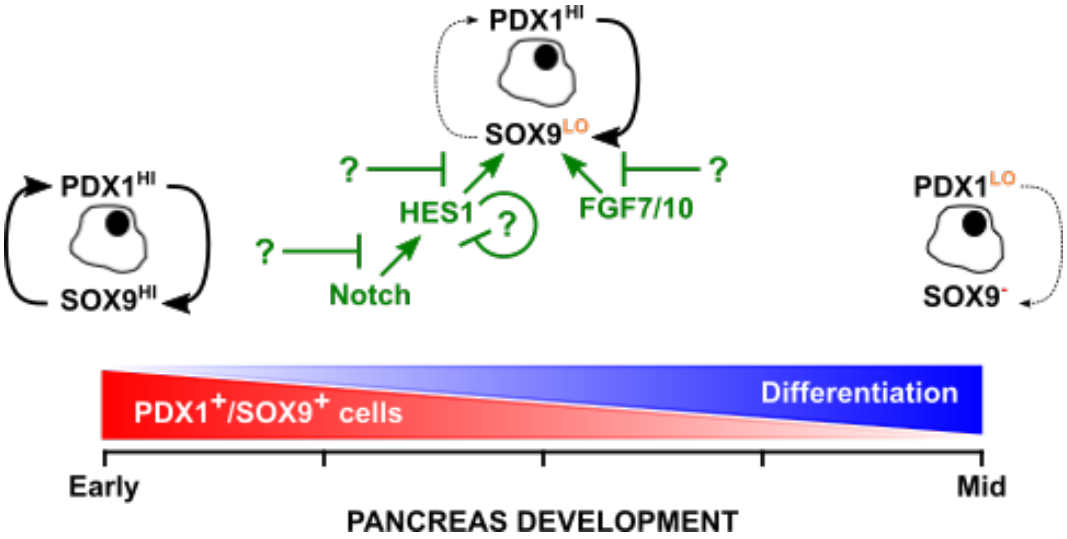

Figure 14. Proposed mechanisms of PDX1 and SOX9 regulation in human foetal pancreas progenitors.

Pdx1 and Sox9 are thought to directly reinforce each other's' expression in mouse (schematic left). I have shown that in PDX1 expression is reduced in PDX1^{+}/SOX9^{-} cells (schematic right), and that the number of SOX9^{+} cells in the developing human foetal pancreas begins to decrease prior to the reduction in PDX1^{+} cells (schematic middle). Notch and Fgf7/10 signalling (depicted in green) are known to maintain Sox9 expression in mice[166,358], and likely also play a role in human development. Decreased SOX9 expression may therefore be due to inhibition of these signalling pathways by unknown mechanisms, or built in negative feedback on pro-SOX9 signalling, as has been proposed in models of foetal pancreatic duct development[289,290].

CHAPTER 4

New methods for expansion of proliferative mouse foetal pancreas progenitors in defined monolayer conditions

4.1 Introduction

In vitro cellular models are a valuable tool in disease research. Manipulation of signalling pathways and gene expression can be carried out relatively easily in cultured cells using both genetic and chemical perturbations (candidate or unbiased screens). Transformed cancer cell lines have been widely used as their rapid growth and simple culture requirements means they are easy to work with and experimentally tractable [291]. These have been widely deployed in genetic and chemical screening, including phenotypic screening. However, while they have proven valuable, they have inherent limitations as genetic and epigenetic changes accumulated in culture leads to a drift away from their original disease state. [292].

Certain types of stem cell can be propagated continuously without genetic transformation using specialised culture conditions. The harnessing of stem cells in culture has led to new opportunities for modelling biology and disease. Often the stem cells can be expanded easily in culture (e.g. embryonic stem cells, intestinal stem cells [293] and neural stem cells [294]) while maintaining the genomic integrity that is lacking from cancer cell lines. Furthermore, stem cells have the added benefit of being able to generate multiple lineages and cell types, thus potentially expanding the number of tissue- and cell-specific models available. Mesenchymal stem cells (MSCs) are a good example. MSCs exist in adult tissues and are thus readily accessible, with isolation of endogenous MSCs possible from various tissues including bone marrow, fat and epidermis. These cells exhibit a capacity for long-term culture in monolayer

and multi-lineage differentiation potential [295]. MSCs have been used as cellular models to identify mechanisms behind chondrogenesis and osteogenesis, and to improve directed differentiation towards bone-forming cells [296-298].

In both mouse and human adult pancreas, the evidence for existence of a stem cell population under normal physiological conditions has been controversial, with pancreas progenitors only thought to be active transiently during development [299-301]. This makes the isolation of a multipotent cellular model system more difficult than for MSCs.

Embryonic or foetal tissues have been used to isolate stem cell populations from several lineages; e.g. foetal brain tissue is a common source of neural stem (NS) cells for culture [294], while foetal liver is used to isolate hepatoblasts that can be maintained in vitro [302]. Similarly, pancreas progenitors have been taken from the developing mouse pancreas and successfully cultured; however, there are major limitations of available culture methods developed to date.

3D culture 'organoid' culture systems are increasingly popular, and this has led to mouse foetal pancreas cell organoid cultures; however, these more often model pancreas development rather than promoting expansion of pure progenitors. In one study, mixed populations of E11.5 mouse foetal pancreas progenitor cells and foetal pancreatic mesenchymal cells were suspended in Matrigel, yielding growth of $Sox9^+$ cells in sphere structures; however, a high proportion of $Ngn3^+$ cells and hormone-expressing islet-like cells were also present, indicating poor progenitor cell maintenance [303]. Another group used E10.5 mouse foetal pancreas to produce single cell suspensions of pancreatic epithelial cells, subsequently suspending 40-50 cells in Matrigel droplets. Once again, resulting organoids were mixed populations of multipotent progenitor and islet-like cells. Furthermore, when the authors attempted

to culture foetal pancreas progenitors in 2D, Pdx1 expression was extinguished in vitro [304]. This spontaneous differentiation can be partly improved by using higher concentrations of EGF in E12-13 foetal pancreas cell culture medium [305]. However, the organoids reported in this study had to be individually transferred to 2D culture format to be fixed and stained for analysis of cellular composition, an impractical and unreliable solution for readouts of large-scale experiments. While the aforementioned studies have limitations, they benefited from use of defined culture medium to attempt to expand foetal pancreas cells. The very few studies that have focused exclusively on 2D mouse foetal pancreas progenitor cell culture have relied on feeder cells [306] and serum-containing conditions [307] to promote progenitor cell expansion. In both of these studies, Pdx1 was expressed at the population level while endocrine-associated genes were not detectable. However, such an ill-defined culture environment is often unreliable and hard to reproduce between labs. It would not be suitable for us in experiments designed to investigate isolated pro-endocrine regulatory pathways under controlled conditions.

In this chapter, we aim to develop new defined and reliable methods to isolate and expand in adherent monolayer pancreas progenitor isolated from the developing mouse pancreas. We aimed to identify serum-free conditions that would enable for the first time routine large-scale expansion of foetal pancreas progenitor cells. Such cultures would be useful in future chemical and genetic screening. They also simplify imaging-based studies to explore differentiation to therapeutically useful endocrine pancreas cells. Additionally, mouse culture conditions might be transferrable to human foetal tissue.

4.2 Results

4.2.1 Determining the spatial and temporal control of key pancreatic master regulators during mouse development

Endocrine commitment in the developing mouse pancreas is known to occur in two distinct phases, or 'transitions'. The secondary transition initiates at around E12.5 and is accompanied by large scale changes in pancreas structure and cellular composition. At this stage the majority of commitment to endocrine cell fates occurs [143]. To facilitate successful culture of early proliferative multipotent pancreas progenitors from mouse, we reasoned that it would be beneficial to use foetal pancreas tissue at early developmental stages.

To confirm that the majority of differentiation to endocrine and exocrine lineages occurs in mouse foetal pancreas during the secondary transition, we collected tissue from E12.5-E15.5 mice and analysed gene expression during this period by qPCR. Due to the small size of the mouse foetal pancreatic bud, each biological replicate within an age group consisted of a pool of multiple individual buds to ensure a good yield of RNA. Pancreatic bud dissection at developmental stages earlier than E12.5 was more complex and time-consuming due to their significantly smaller size. To prevent a negative impact of longer dissection times on cell viability, stages earlier than E12.5 were not included in these experiments.

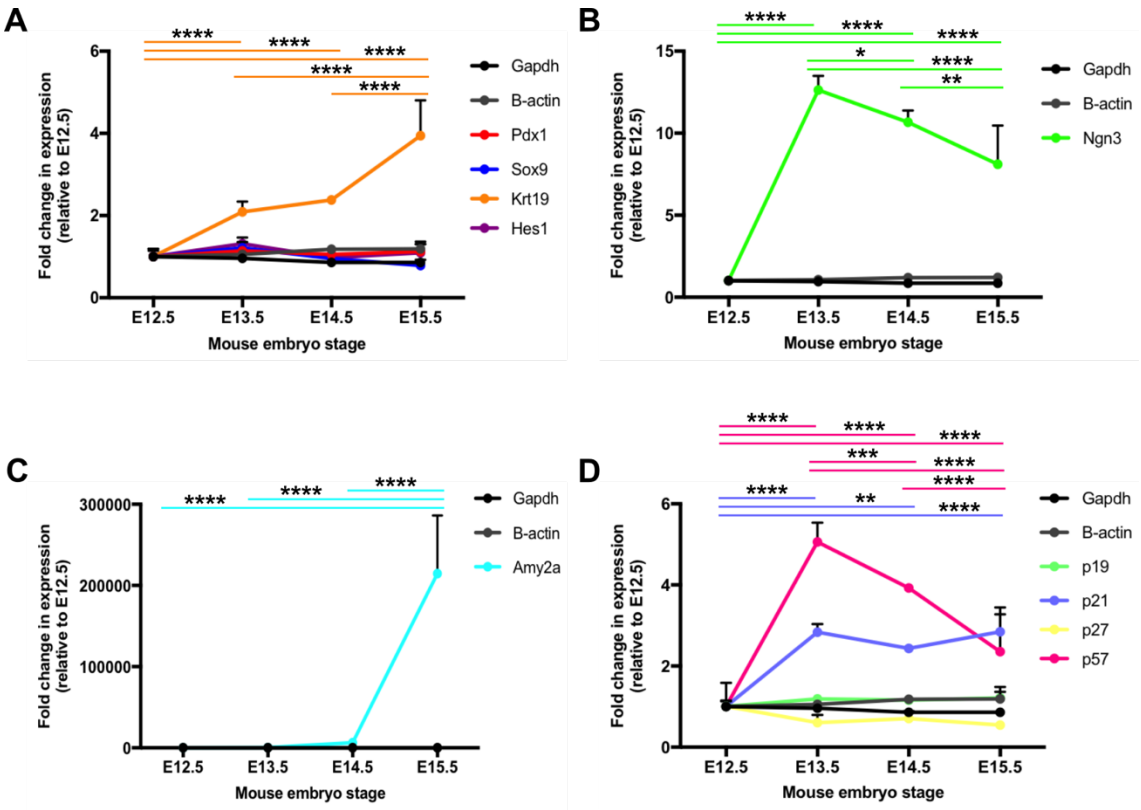

Figure 15. mRNA expression of key developmental genes in developing mouse foetal pancreas.

(A) Pancreas progenitor markers *Pdx1*, *Sox9*, *Krt19* and *Hes1* **(B)** Endocrine progenitor marker *Ngn3* **(C)** Acinar marker *Amy2a* **(D)** Cell cycle-related genes *p19*, *p21*, *p27* and *p57*. 200ng of RNA was used to make cDNA. Relative expression of all genes normalised to the geometric mean of *Gapdh* and *B-actin*. E12.5 n=2, E13.5 n=5, E14.5 n=3, E15.5 n=5. Error bars show standard deviation. Each pool of buds was deemed one biological replicate, and the number of biological replicates for each developmental stage is indicated here as n. Significance between fold change of housekeeping genes and genes of interest tested using multiple unpaired t-tests with Holm-Sidak correction (not shown). Significance between embryo stages tested using two-way ANOVA with Tukey's test (shown on graphs, * = p≤0.05, ** = p≤0.01, *** = p≤0.001, **** = p≤0.0001).

Similar to human development, mRNA expression of *Pdx1* and *Sox9* did not vary significantly at any stage analysed ($p>0.05$) **(Figure 15A)**. We also assessed expression of *Hes1*, a Notch signalling effector. Notch and Hes1 are understood to be crucial for maintaining early pancreas progenitor cells by repressing endocrine-associated transcription factors [148]. While *Hes1* expression was significantly higher than both *Gapdh* and *B-actin* at E13.5 only, the effect was very modest. Furthermore, when comparing *Hes1* means between age groups by two-way ANOVA, *Hes1* was not significantly different between any stage ($p>0.05$). *Krt19*, a marker of the ductal epithelium where multipotent progenitor cells reside, showed a steady and significant increase over time ($p<0.0001$). Our expression data of Krt19 therefore fits with the extensive growth and branching of the pancreatic ductal network during the secondary transition, with *Krt19*-expressing cells making up a greater proportion of the pancreas with each successive stage of development.

The fact that *Pdx1*, *Sox9* and *Hes1* expression is relatively constant between E12.5-E15.5 appears to indicate that the pool of multipotent early progenitor cells is maintained at a steady proportion throughout this window, and that tissue from any of these stages might be suitable for isolating progenitor cells for culture. However, as demonstrated in the previous chapter, differentiation may be occurring at the cellular level in spite of unchanged transcript levels at the population level. *Ngn3* expression rose sharply to peak at E13.5, with a 12.6-fold increase over E12.5 **(Figure 15B)**. After E13.5, *Ngn3* declined slowly with each stage of development (E13.5 vs E14.5 $p=0.0255$, E14.5 vs E15.5 $p=0.0025$). Exocrine commitment could also be detected during this window of development, with *Amy2a* expression increasing suddenly and significantly at E15.5 (E13.5 vs E14.5 $p=0.9877$, E14.5 vs E15.5 $p<0.0001$) **(Figure 15C)**. These data confirm that while early progenitor marker expression is unchanged

when assessed by RT-qPCR at the population level, endocrine and exocrine differentiation is occurring during the secondary transition.

We next explored cell cycle and proliferation markers within the cell populations of the developing pancreas. Cdkn1c (p57), in coordination with decreased Hes1 levels, regulates cell cycle exit in early pancreas progenitor cells [308], while Cdkn1a (p21) and to a lesser extent Cdkn1b (p27) are upregulated in non-cycling mouse endocrine progenitor cells from E14.5 onwards [188]. We reasoned that identifying the developmental stage at which *p21*, *p27* and *p57* are expressed at relatively low levels might maximise our potential for capturing proliferative pancreas progenitor cells.

p21 expression increases significantly at E13.5 by 2.83-fold (E12.5 vs E13.5 $p<0.0001$), but does not alter further **(Figure 15D)**. This increase coincides with activation of *Ngn3* expression, corroborating previous publications on the role of p21 in endocrine progenitor cell cycle exit [188]. In contrast, *p27* did not significantly different between any stage of development ($p>0.05$), in agreement with a more limited role compared to p21. *p57* expression peaked at E13.5 at 5.06-fold over E12.5 (E12.5 vs E13.5 $p<0.0001$), subsequently declining significantly at latter stages (E13.5 vs E14.5 $p=0.0001$, E14.5 vs E15.5 $p<0.0001$). The early increase in *p57* expression suggests a wave of multipotent progenitor cell cycle exit shortly after the start of the secondary transition, and is then followed by increased expression of markers of differentiated cells later in the transition. *Cdkn2a* (*p16*), which was undetectable by qPCR at all stages, whereas C*dkn2d* (*p19*), was expressed, but remained unchanged throughout development ($p>0.05$).

We conclude that E12.5 mouse foetal pancreas would be the best stage to attempt the ‘capture’ of pancreatic progenitors in culture, as the bulk of the tissue would be comprised of undifferentiated proliferative progenitors.

4.2.2 Using whole E12.5 mouse foetal pancreas to assess culture conditions for suppressing endocrine progenitor emergence

At the E12.5-E13.5 transition, there is a peak in expression of both *Ngn3* and *p57*, with a concurrent rise in *p21*, indicating cell cycle exit and onset of endocrine differentiation in a subset of early pancreas progenitors. Therefore, when considering how to maintain early multipotent pancreas progenitors in culture, the challenge would be to find ways in culture to suppress endocrine differentiation but sustain self-renewal.

To investigate the optimal culture conditions, we started by using a simple approach of culturing whole E12.5 mouse foetal pancreatic buds (without dissociation), where buds were placed in culture medium without the use of any extracellular matrix and incubated for three days **(Figure 16)**. As well as being an effective method for testing culture media, we wanted to assess the viability of whole bud culture as a potential screening platform in itself. As this culture method retains normal tissue architecture and associated ongoing endocrine differentiation, it served as an ideal platform to assess our efforts to suppress endocrine differentiation and capture pancreatic progenitors.

In parallel to testing buds free-floating in media without no surrounding supportive matrix, we also tested a previously reported culture method for rat pancreatic bud culture; this involves embedding whole pancreatic buds in collagen on a transwell filter floated on culture media to allow growth at the air-liquid interface [309,310]. This culture system was shown to closely model pancreas development ex vivo, where rat pancreatic buds demonstrated a loss of $Pdx1^+$ progenitors and an increasing number of $Ngn3^+$ endocrine progenitors over time in culture.

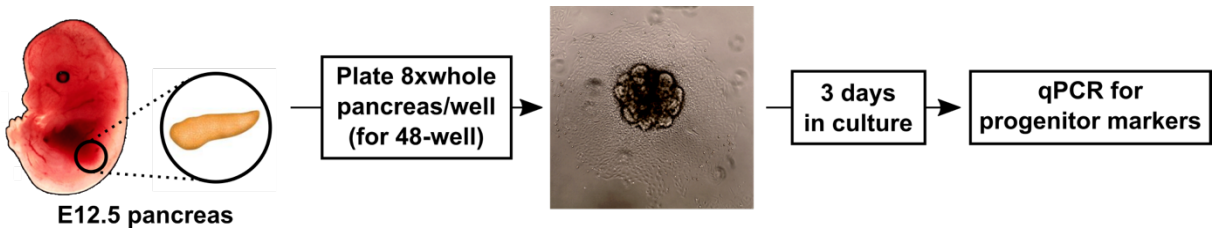

Figure 16. Whole mouse foetal pancreas culture strategy.

Multiple foetal pancreases were microdissected and cultured in each well to allow enough RNA to be recovered for eventual analysis by qPCR. Mouse embryo image adapted from Li et al. (1999) [307].

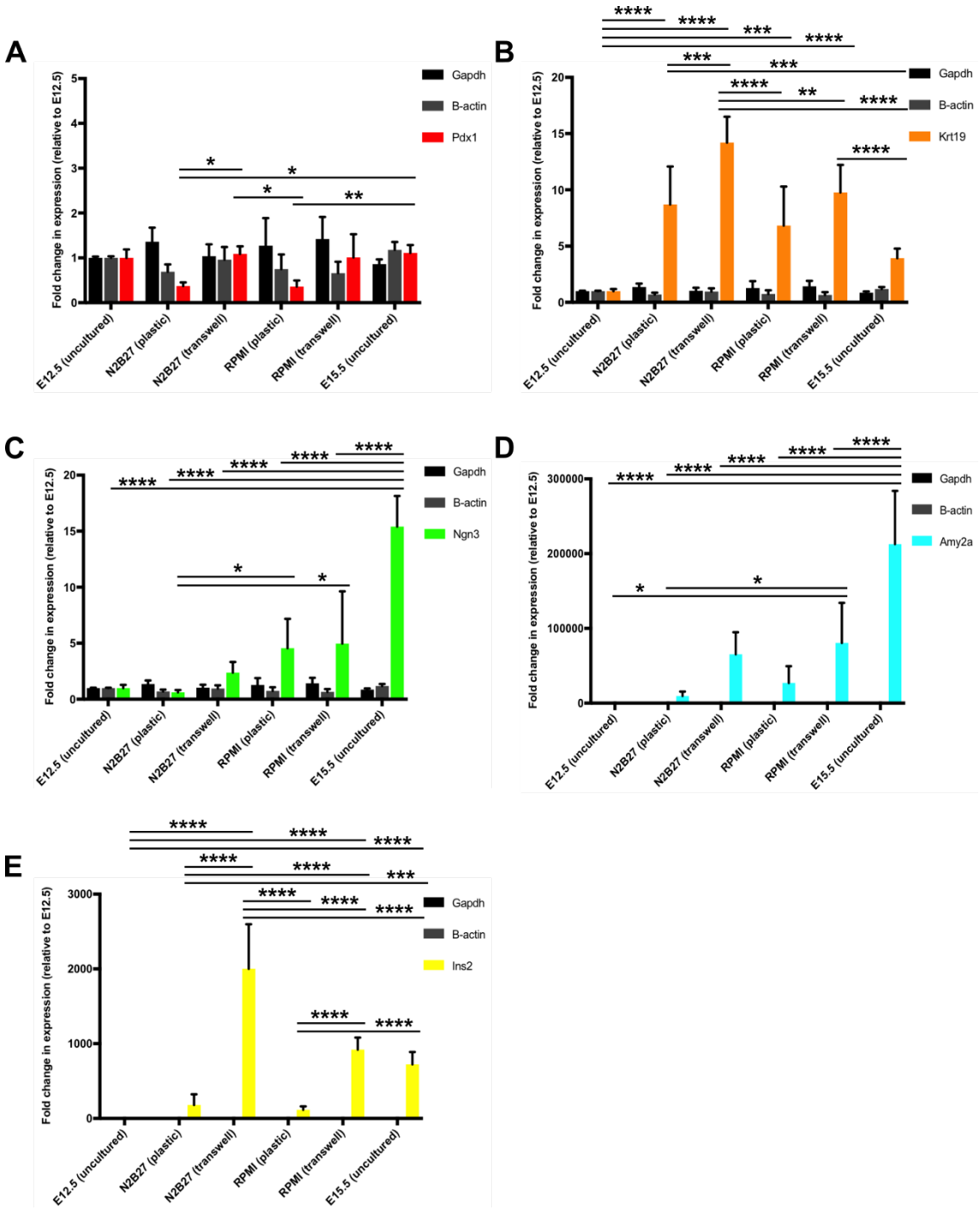

Figure 17. mRNA expression in different whole mouse foetal pancreas culture methods.

(A) qPCR for pancreas progenitor marker *Pdx1* **(B)** Ductal marker *Krt19* **(C)** Endocrine progenitor marker *Ngn3* **(D)** Acinar marker *Amy2a* **(E)** β-cell marker *Ins2*. 200ng of RNA was used to make cDNA. Relative expression of all genes normalised to the geometric mean of *Gapdh* and *B-actin*. E12.5 n=2, bud culture experiments n=3, E15.5 n=5. Error bars show standard deviation. Significance between treatments tested using two-way ANOVA with Tukey's test (shown on graphs, * = p≤0.05, ** = p≤0.01, *** = p≤0.001, **** = p≤0.0001).

We explored a variety of distinct basal culture media, as these often have a significant impact on progenitor expansion. N2B27 media has been used for defined progenitor cell expansion in other tissue contexts [294], while RPMI-based medium was used for previous transwell culture experiments [310]. These were tested and compared head-to-head with either transwell or plastic, to which buds loosely attached.

E12.5 pancreatic buds cultured for 3 days on plastic had a significantly lower *Pdx1* expression level than controls uncultured fresh E12.5 or E15.5 buds. *Pdx1* expression decreased 3-fold from E12.5 levels in both N2B27 and RPMI-based media **(Figure 17A)**. Buds grown on transwells maintained *Pdx1* expression compared to those grown on untreated plastic. *Krt19* expression in all treatments was increased compared to E15.5, although the difference was not significant for RPMI (plastic) ($p>0.05$) **(Figure 17B)**. Buds grown on transwells showed a trend towards higher *Krt19* than for plastic, suggesting that ductal branching morphogenesis is promoted in these conditions (N2B27 plastic vs N2B27 transwell $p=0.0003$, RPMI plastic vs N2B27 transwell $p<0.0001$). Altogether these data indicate that culturing whole buds promotes ductal growth, and pancreas progenitor identity may be better preserved in a transwell format compared to plastic.

We then examined how these conditions influence the expression of differentiation markers. Firstly, we assessed the endocrine progenitor marker *Ngn3* **(Figure 17C)**. *Ngn3* never reached its E15.5 levels in any of the conditions ($p<0.0001$ for all). However, RPMI-based media appeared to favour endocrine commitment compared to N2B27 (N2B27 plastic vs RPMI plastic $p=0.0348$). Transwells had higher *Ngn3* expression relative to plastic, but this difference was not significant ($p>0.05$). Similar results were obtained for exocrine differentiation; *Amy2a* expression was greater in transwells, although not significantly ($p>0.05$) **(Figure 17D)**. Finally, we looked at *Ins2* expression as a marker of β-cell emergence **(Figure 17E)**. Here, transwells showed

a large effect for promoting differentiation to β-cells compared to plastic (N2B27 plastic vs N2B27 transwell $p<0.0001$, RPMI plastic vs RPMI transwell $p<0.0001$).

Altogether, these data suggest that transwells and collagen promotes a more heterogeneous cell population in culture, with expected ongoing differentiation. A key finding was that on plastic, N2B27 suppressed *Ngn3* expression better than RPMI-based medium, with *Ngn3* actually 0.62-fold lower than its original E12.5 levels in N2B27. This suggested that N2B27 may be an improved basal medium to use for efforts to capture and maintain early pancreas progenitors in culture. However, *Pdx1* expression was slightly reduced in N2B27 on plastic compared to uncultured buds, so it is clear that additional culture supplements might be needed.

EGF is known to stimulate the proliferation of epithelial pancreas progenitors, while simultaneously decreasing endocrine progenitor number in cultured rat pancreas [311]. FGF7 (and also the related FGF10) has also been used to increase epithelial pancreas progenitor proliferation in rat by signalling through FGFR2IIIb [312,313], a pathway normally stimulated in vivo in development by the pancreatic mesenchyme. These are two candidate growth factors that might aid in the capture and expansion of multipotent pancreatic progenitors.

To build upon our findings with N2B27, we therefore compared N2B27 (no growth factors) to N2B27 supplemented with 50ng/ml EGF and 50ng/ml FGF7 (EF7). Culture of buds in EF7 significantly reduced *Ngn3* expression compared to N2B27 alone **(Figure 18)** after 1 day of culture ($p=0.0003$). This suggests EF7 are indeed helpful to block the transition to Ngn3-expressing endocrine progenitor cells.

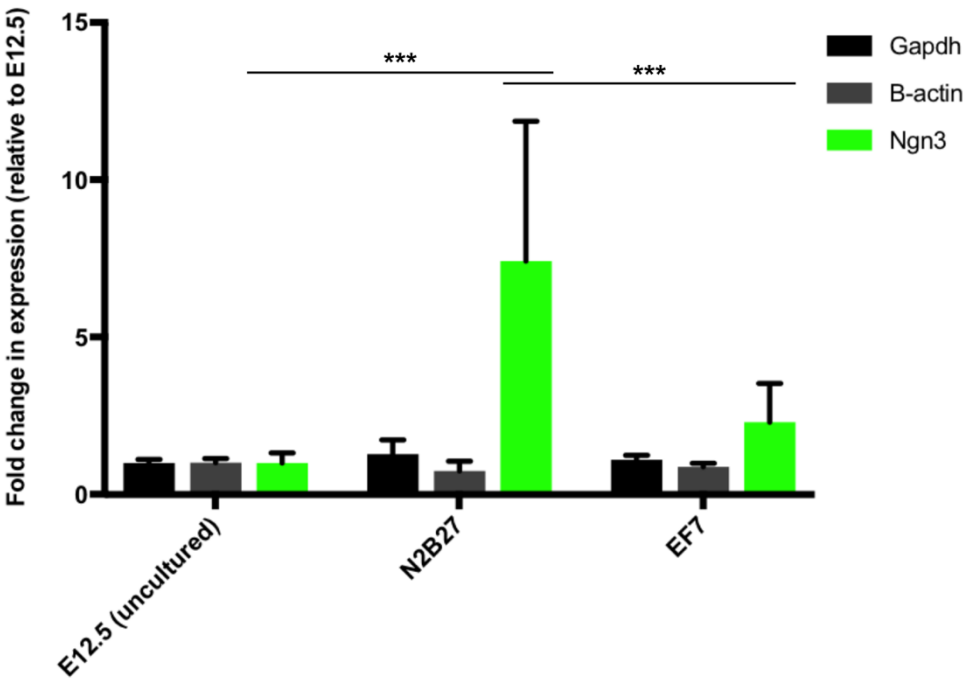

Figure 18. Ngn3 mRNA expression in whole mouse foetal pancreas culture in N2B27 and EF7.

Endocrine progenitor marker *Ngn3*. Relative expression of all genes normalised to the geometric mean of *Gapdh* and *B-actin*. E12.5 n=2, bud culture experiments n=5. Error bars show standard deviation. Significance between treatments tested using two-way ANOVA with Tukey's test (shown on graphs, * = $p \leq 0.05$, ** = $p \leq 0.01$, *** = $p \leq 0.001$, **** = $p \leq 0.0001$). Although significant, we believe the variability is likely due to variations in RNA yield and quality between whole bud culture experiments.

To characterise tissue grown in EF7 culture conditions further, we explored a larger set of markers. *Pdx1* was reduced by 0.4-fold compared to E12.5, while *Sox9* reduction was less dramatic at 0.8-fold **(Figure 19)**. We observed very modest increases in pro-endocrine factors *Ngn3* and *NeuroD1* (1.5-fold and 1.9-fold, respectively), while *Nkx2.2* was relatively stable at 0.9-fold. *Ins2* expression was increased to similar levels seen for N2B27 in earlier experiments (230-fold), while *Glu*, a marker of α-cells and immature polyhormonal cells, was much reduced from E12.5 (0.06-fold).

In addition to culturing early pancreas progenitor cells, we were also interested in developing methods to capture and expand $Ngn3^{+}$ endocrine pancreas progenitors. *p21* expression is increased in these cells [188], leading to an extended G1 phase of the cell cycle, which in turn is linked to maturation and differentiation of endocrine progenitor cells [269,270]. In parallel to EF7 alone, we also added the p21 inhibitor UC2288 (1μM) to EF7 to test whether endocrine progenitor proliferation could be induced in a controlled manner, consequently preventing endocrine progenitor maturation. However, UC2288 did not significantly reduce expression of any genes associated with mature endocrine progenitors (*NeuroD1*, *Nkx2.2*) or islet cells (*Ins2*, *Glu*) compared to EF7 alone ($p>0.05$).

It therefore appears that whole mouse foetal pancreatic bud cultures still differentiate towards an insulin-expressing cell even in the presence of EGF and FGF7. In addition, we uncovered many problems with the whole bud culture system including the quality and amount of RNA recovered being inconsistent and high levels of cell death within the buds during culture (data not shown). However, our observation that N2B27 plus EGF and FGF reduced expression of Ngn3 encouraged us to investigate the potential of this media to expand pancreatic progenitors using alternative culture techniques.

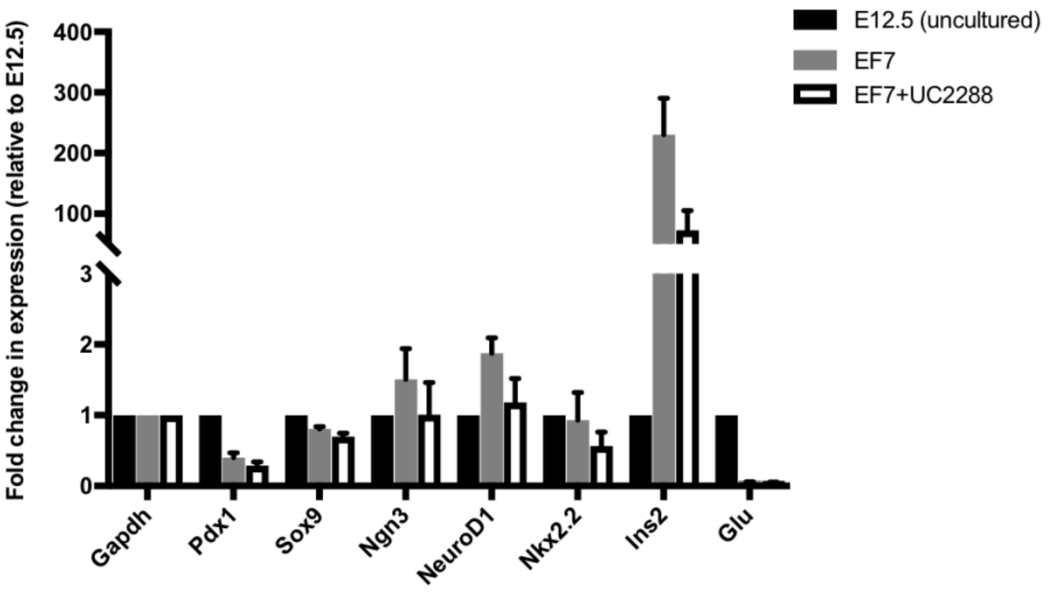

Figure 19. mRNA expression in whole mouse foetal pancreas culture in EF7 and EF7+UC2288.

Pancreas progenitor markers *Pdx1* and *Sox9*, endocrine progenitor markers *Ngn3*, *NeuroD1* and *Nkx2.2*, mature endocrine markers *Ins2* and *Glu*. 200ng of RNA was used to make cDNA. Relative expression of all genes normalised to *Gapdh*. E12.5 n=1, bud culture experiments n=3. Error bars show standard deviation. Significance between treatments tested using multiple unpaired t-tests with Holm-Sidak correction.

4.2.3 Establishing adherent monolayer culture conditions to allow expansion of E12.5 mouse foetal pancreas progenitors

Monolayer culture conditions provide an alternative to 3D whole bud culture that might enable capture of the progenitors and has certain experimental advantages.

E12.5 mouse pancreas was dissected and as much of the overlying mesenchyme as possible was removed manually by microdissection. A combination of low concentration trypsin/EDTA and trituration with a Gilson pipette was used to dissociate the tissue **(Figure 20)**. The resulting cell suspension was then plated in wells coated with thin-gel Matrigel® (Growth Factor Reduced), so that cells had a basement matrix on which to attach. As an initial assessment of optimal culture conditions for expanding pancreas progenitors in monolayer, we tested N2B27-based media with various different supplements included. Pancreas progenitors form the early pancreatic budding outgrowth from the foregut during development, and subsequently organise to form lumens lined by epithelial progenitor cells. Our hypothesis was that the ideal conditions would result in growth of progenitor cells with an epithelial morphology.

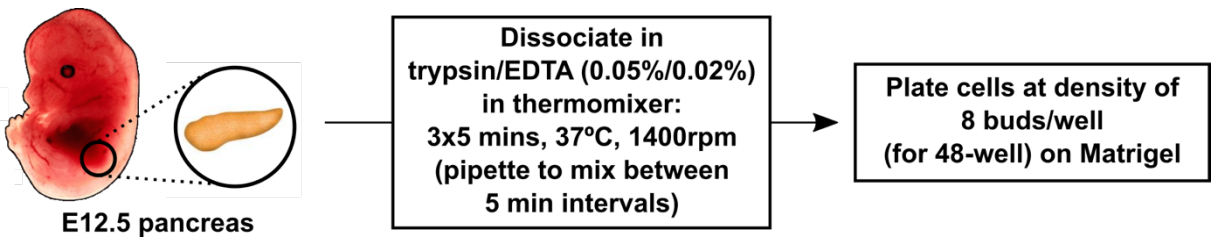

Figure 20. Dissociated mouse foetal pancreas culture strategy.

Multiple foetal pancreases were pooled for each well to increase cell density. Mouse embryo image adapted from Li et al. (1999) [307].

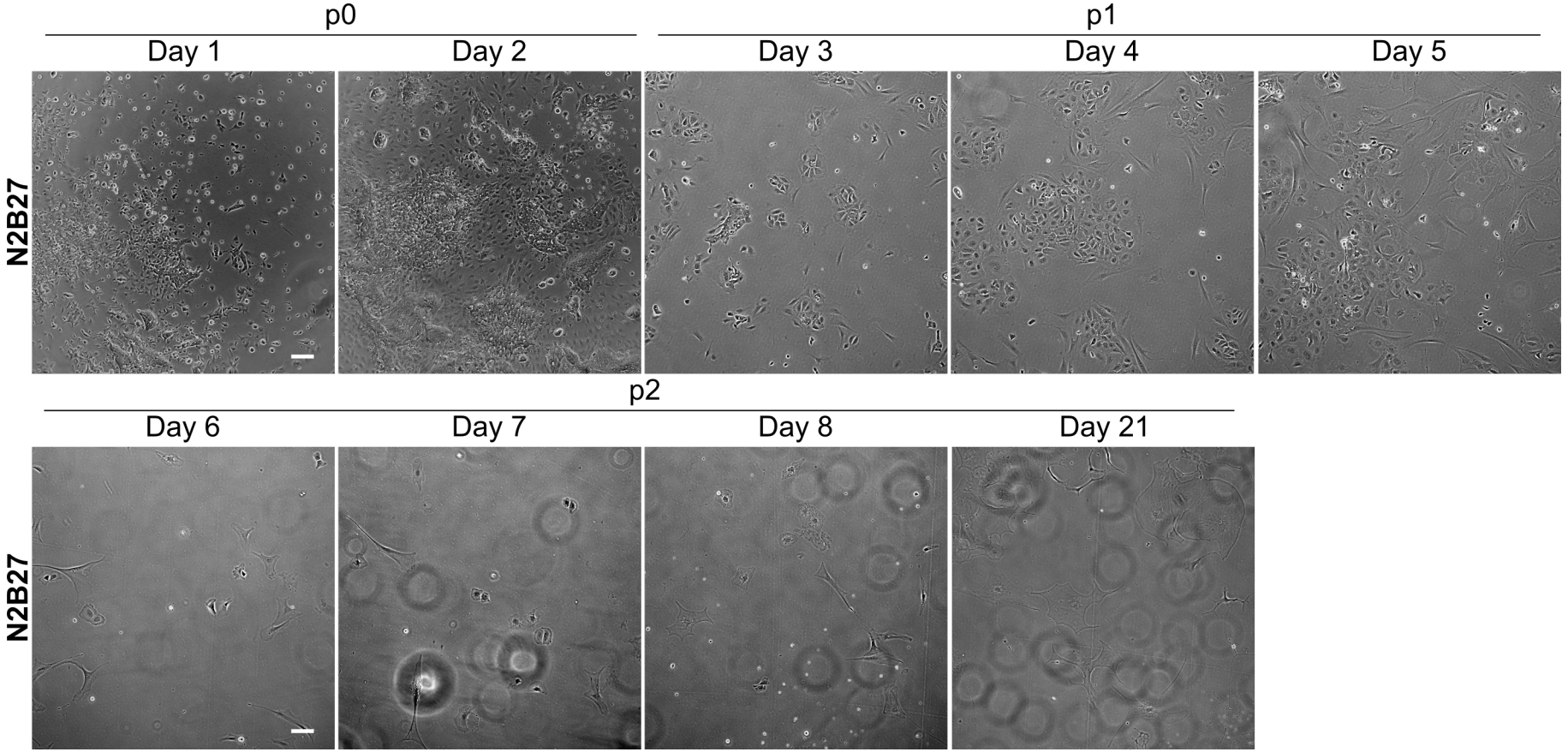

Figure 21. Mouse foetal pancreas growth in N2B27.

Phase images were taken using the 10X objective (scale bar represents 100μm). Day of culture since initial dissection and passage number indicated above images.

Cells cultured in this way in N2B27 alone initially supported growth of epithelial-like cells at p0. These were characterised by many small, tightly packed cells growing in slightly raised colonies **(Figure 21)**. These epithelial-like colonies were surrounded by cells of much flatter, larger morphology, which we reasoned would be pancreatic stromal or mesenchymal cells. However, disappointingly these epithelial-like cells were lost on passaging, either due to cell death or differentiation. By the second passage very few cells remained.

We next compared the morphologies of cells grown in N2B27 media supplemented with 50ng/ml EGF and either FGF2 (termed EF2) or FGF7 (termed EF7) (both at 50ng/ml). By using FGF2 in parallel, we wanted to see whether the effects of FGF7 could be mimicked by an FGF from a separate subfamily, but one which activates a broad spectrum of FGFRs [314] and has been used for progenitor cell expansion in other contexts, such as neural stem cells [294].

Both EF2 **(Figure 22)** and EF7 conditions **(Figure 23)** supported initial growth of epithelial cells – the putative progenitors. After the initial replating both EF2 and EF7 appeared to preserve epithelial cell morphology better than N2B27 alone, with tightly packed colonies of small cells being retained for longer. However, epithelial colonies appeared in higher numbers in EF7 compared to EF2. Disappointingly, upon further expansion at passage 2 , most of these epithelial-like cells were lost in both conditions. Nevertheless, following growth of the culture over the following 3 weeks we did notice epithelial-like morphology colonies in EF7 – but not in EF2.

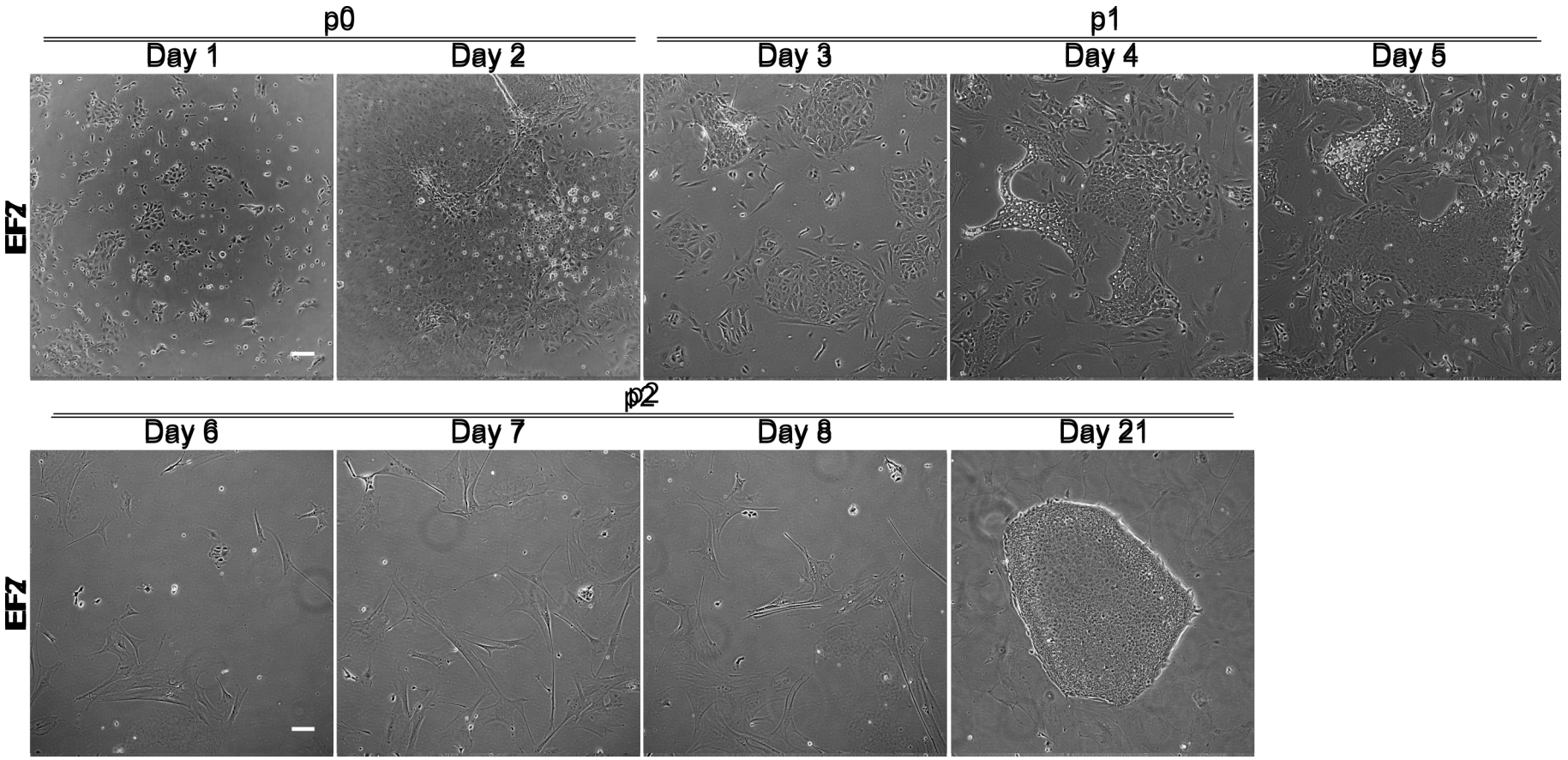

Figure 23. Mouse foetal pancreas growth in EF7.

Phase images were taken using the 10X objective (scale bar represents 100μm). Day of culture since initial dissection and passage number indicated above images.

4.2.4 Assessment of pharmacological inhibitors to improve the expansion of epithelial-like candidate progenitors

While EF7 appeared to be permissive to supporting growth of foetal pancreatic epithelial cells, these cells had limited proliferation. Epithelial cell loss was due to both cell death post-passaging, and in part due to differentiation in culture. To attempt to limit the loss of epithelial-like cells in culture, we tested another culture supplement: the small molecule A83-01 (A83) (0.5μM). A83 was first characterised with respect to its ability to potently block epithelial-to-mesenchymal transition through inhibition of Alk5-mediated TGFβ signalling and how this could be beneficial in halting cancer progression [315]. More recently, A83 was used to help expand induced pancreatic progenitor cells converted from human fibroblasts in vitro [316].

Our data indicated that both EF2 and EF7 in combination with A83 **(Figure 24) (Figure 25)** supported an increased proliferation of epithelial-like cells, even by p1. Strikingly ,three days after initial passaging in both conditions, cells with epithelial morphology had formed a confluent sheet across the well. After a second passage, epithelial expansion was slower but noticeable in both conditions, with colonies of tightly packed cells forming the vast majority of surviving cells. Thus, A83 greatly supports the growth of putative foetal pancreatic epithelial cells in monolayer, possibly by blocking epithelial-to-mesenchymal transition. The observation that A83 can support epithelial expansion even when FGF2 is used rather than FGF7, suggests the latter is better able to modulate TGFβ signaling and block EMT (although we did not test this directly).

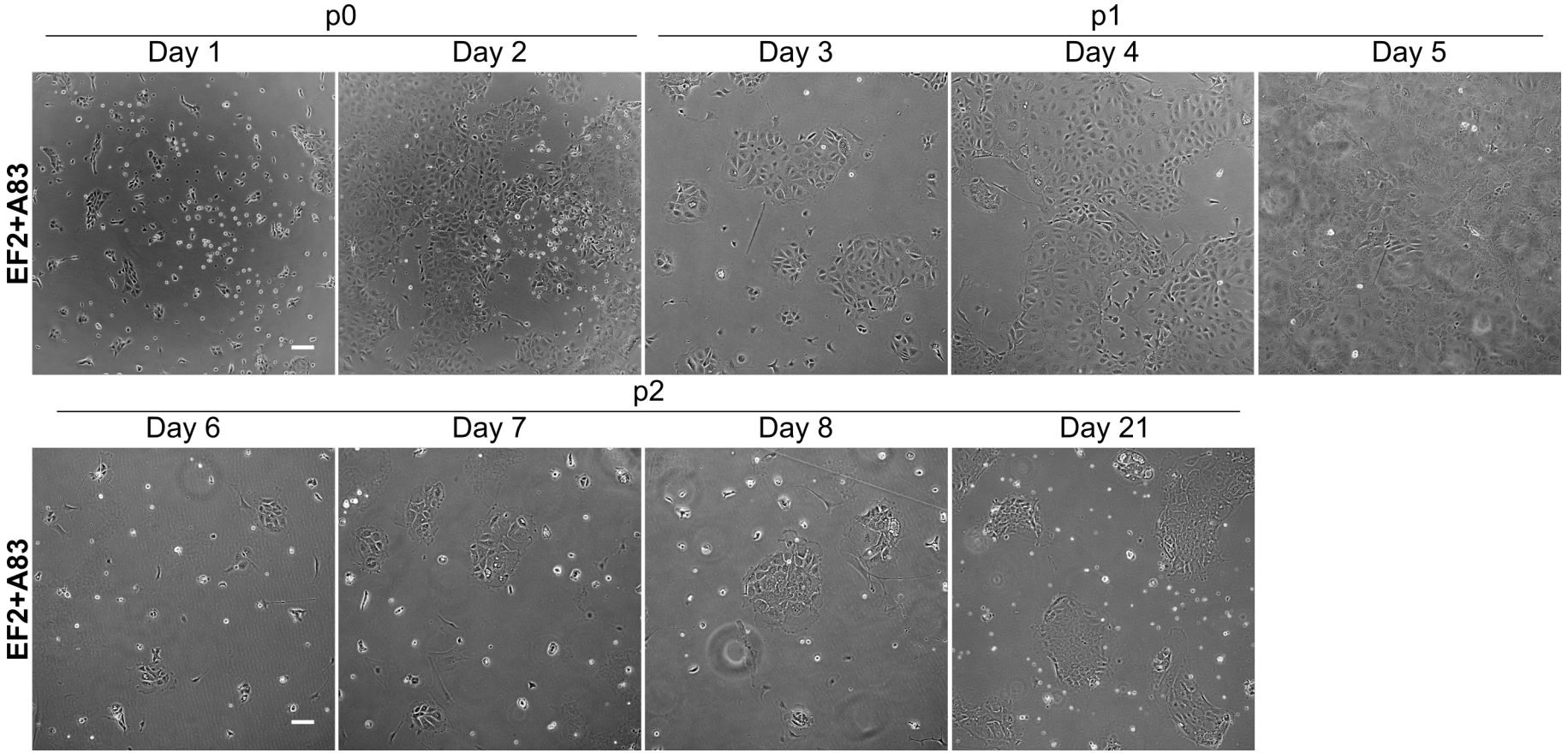

Figure 24. Mouse foetal pancreas growth in EF2+A83.

Phase images were taken using the 10X objective (scale bar represents 100μm). Day of culture since initial dissection and passage number indicated above images.

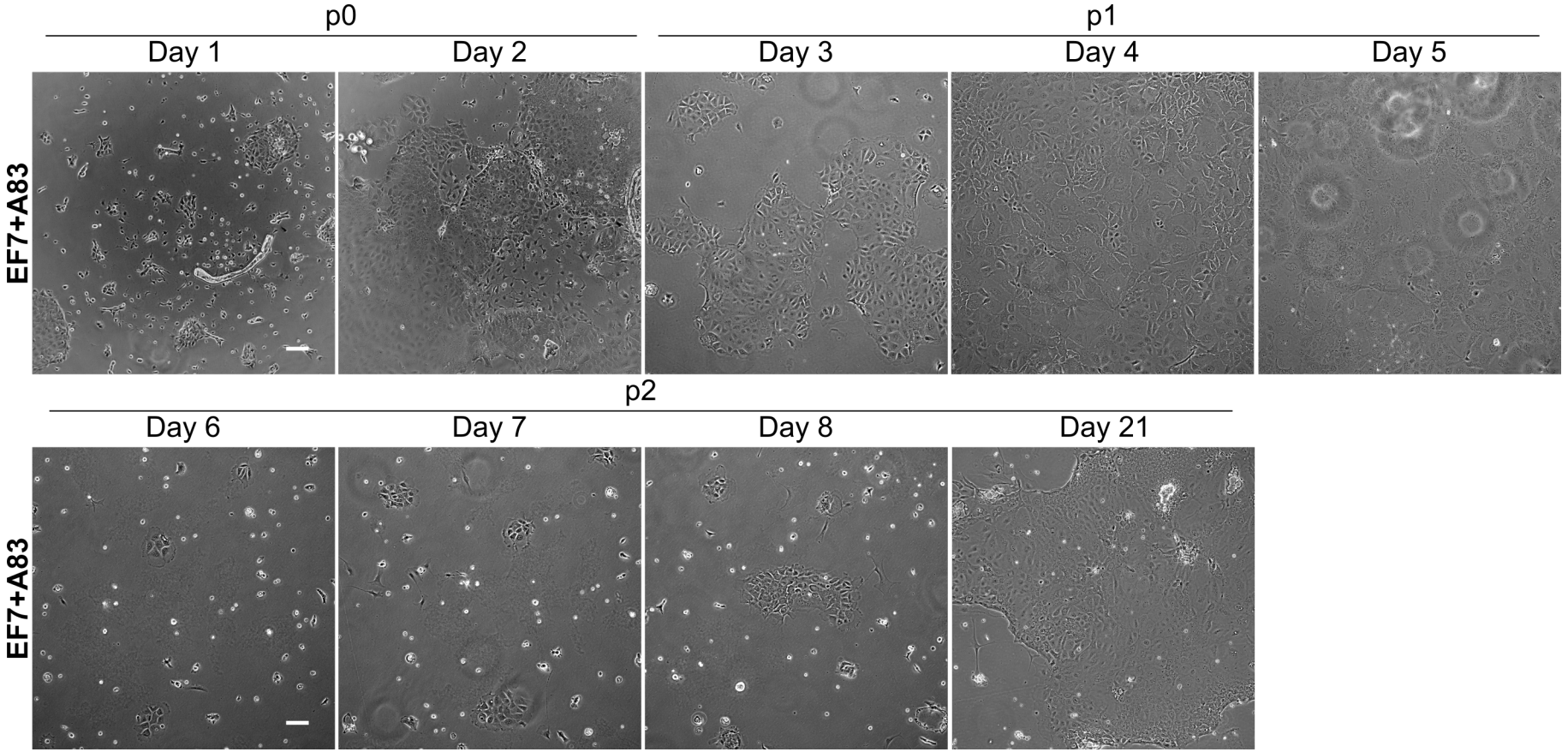

Figure 25. Mouse foetal pancreas growth in EF7+A83.

Phase images were taken using the 10X objective (scale bar represents 100μm). Day of culture since initial dissection and passage number indicated above images.

4.2.5 Characterising epithelial-like candidate progenitor cells expanded in monolayer

To support our initial observations that EF7+A83 can support a striking expansion of epithelial-like cells, we wanted to confirm that the resulting cells were early pancreas progenitors. Mouse foetal pancreas cells were cultured in EF7+A83 to form a sheet of epithelial cells and immunostaining was performed **(Figure 26A)**. All cells were $Pdx1^{+}/Sox9^{+}$ **(Figure 26B)**, indicating that the cells are pancreas progenitor cells.

While epithelial-like cells appeared to comprise the majority of $Pdx1^{+}/Sox9^{+}$ mouse foetal pancreas cells in EF7+A83, cells of non-epithelial morphology were still evident especially at lower cell densities. Therefore, while EF7+A83 conditions induced robust expansion of epithelial-like pancreas progenitor cells, they did not appear to eliminate other foetal pancreatic cell types from the culture.

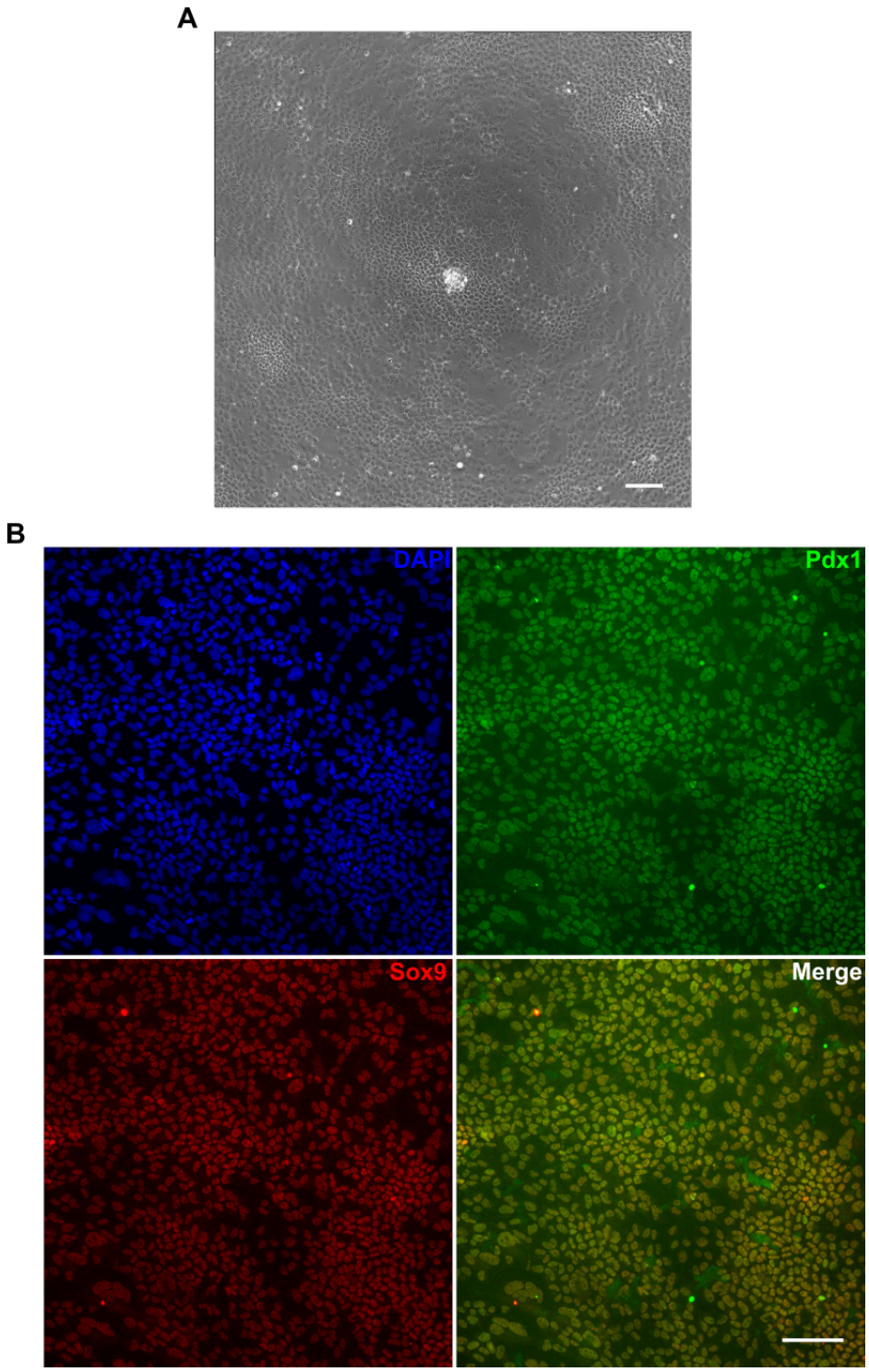

Figure 26. Cells expanded in EF7+A83 are Pdx1^{+}/Sox9^{+} at p0.

(A) Stitched 2x2 phase image taken using the 20X objective (scale bar represents 100μm) **(B)** ICC of mouse foetal pancreas cultures showing staining for Pdx1 (green) and Sox9 (red). Images taken using the 20X objective (scale bar represents 100μm).

4.2.6 Mouse foetal pancreas progenitors can be isolated based on E-cadherin expression and cultured long-term

In the previous section we identified culture conditions permissive to expanding mouse foetal pancreas progenitors, but these cultures appeared to contain non-epithelial $Pdx1^{+}/Sox9^{+}$ cells that presumably did not originate from the ductal epithelium of the pancreatic bud. As pancreas progenitors during development are known to reside in the ductal epithelium, we aimed to purify pancreas progenitors based on their expression of epithelial cell markers.

To confirm that p0 mouse foetal progenitors enable growth of a confluent sheet of epithelial cells and are E-cadherin (E-cad)-positive we performed ICC **(Figure 27)**. Most cells appeared positive for E-cad at the cell membrane, although E-cad-negative cells were evident in between clusters of epithelial cells, confirming the heterogeneous nature of the cell population at p0.

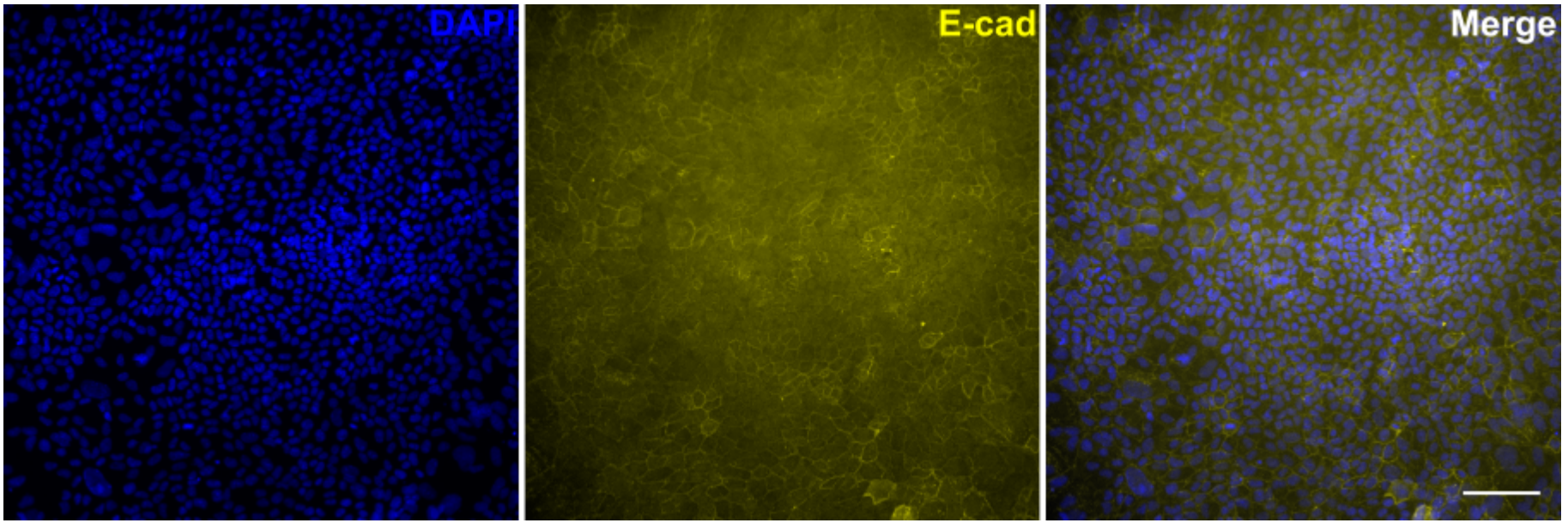

Figure 27. Cells expanded in EF7+A83 are E-cad^{+} at p0.

ICC of mouse foetal pancreas cells showing staining for E-cad (yellow). Images taken using the 20X objective (scale bar represents 100μm).

Next, p0 cells isolated from E12.5 mouse foetal pancreas and allowed to grow to confluence in EF7+A83 were purified by fluorescence-activated cell sorting (FACS) based on E-cad expression **(Figure 28A)**. The heterogeneous nature of p0 cultures was further confirmed by the finding that 27.8% of cells in the sorted population were E-cad^{-}. Both E-cad^{+} and E-cad^{-} cell fractions were collected after sorting for culture. E-cad^{+} cells were re-plated at a density of 10,000 cells per well in a 96-well plate in EF7+A83. A portion of E-cad^{+} cells were retained and mixed with the E-cad^{-} cell population at a ratio of approximately 7:3 to reflect the makeup of p0 cultures, and the resulting E-cad^{mixed} cell population was also re-plated in the same conditions **(Figure 28B)**. E-cad^{+} cultures at p1 contained cells that appeared epithelial in morphology and grew as colonies. Cells continued to grow in this fashion after multiple passages into increasing well sizes. E-cad^{mixed} cultures also contained epithelial colonies of cells, but in addition possessed cells that were flattened, elongated in appearance and presumably not of epithelial origin. Epithelial colonies grew well in E-cad^{mixed} cultures, and interestingly cells within these colonies often appeared smaller and more compact than E-cad^{+} equivalents. At p3, nearly all of the flattened non-epithelial-like cells had been lost in E-cad^{mixed} cultures, leaving only epithelial-like colonies. This may have been a delayed stress response from sorting, or due to culture conditions unsuitable for the growth and/or survival of the non-epithelial like cells.

E-cad^{+} and E-cad^{mixed} cultures were assessed for continued expression of pancreas progenitor markers post-sorting. All cells at p1, including the flat non-epithelial-like cells in the E-cad^{mixed} population, still expressed both Pdx1 and Sox9, in agreement with the result we obtained at p0 **(Figure 29A)**. Cell colonies in E-cad^{+} cultures were clearly positive for E-cad expression **(Figure 29B)**. Taken together, this shows that

epithelial pancreas progenitors can be successfully sorted by FACS based on E-cad expression and suggest that they remain unchanged by the process.

A significant portion of mouse foetal $Pdx1^{+}/Sox9^{+}$ cells were E-cad^{-} when sorted by FACS. There are two potential explanations for this finding. First, a subset of $Pdx1^{+}/Sox9^{+}$ cells derived from the ductal epithelium may have lost E-cad expression as a result of an initial period in culture. Or second, these cells could represent a $Pdx1^{+}/Sox9^{+}$ cell population in the developing pancreas that resides outside of the ductal epithelium. This second explanation cannot be ruled out, although would be contrary to what is known about pancreas progenitors in the developing mouse pancreas and also contrary to our own observations of human foetal development, where PDX1 and SOX9 appeared restricted to ductal structures.

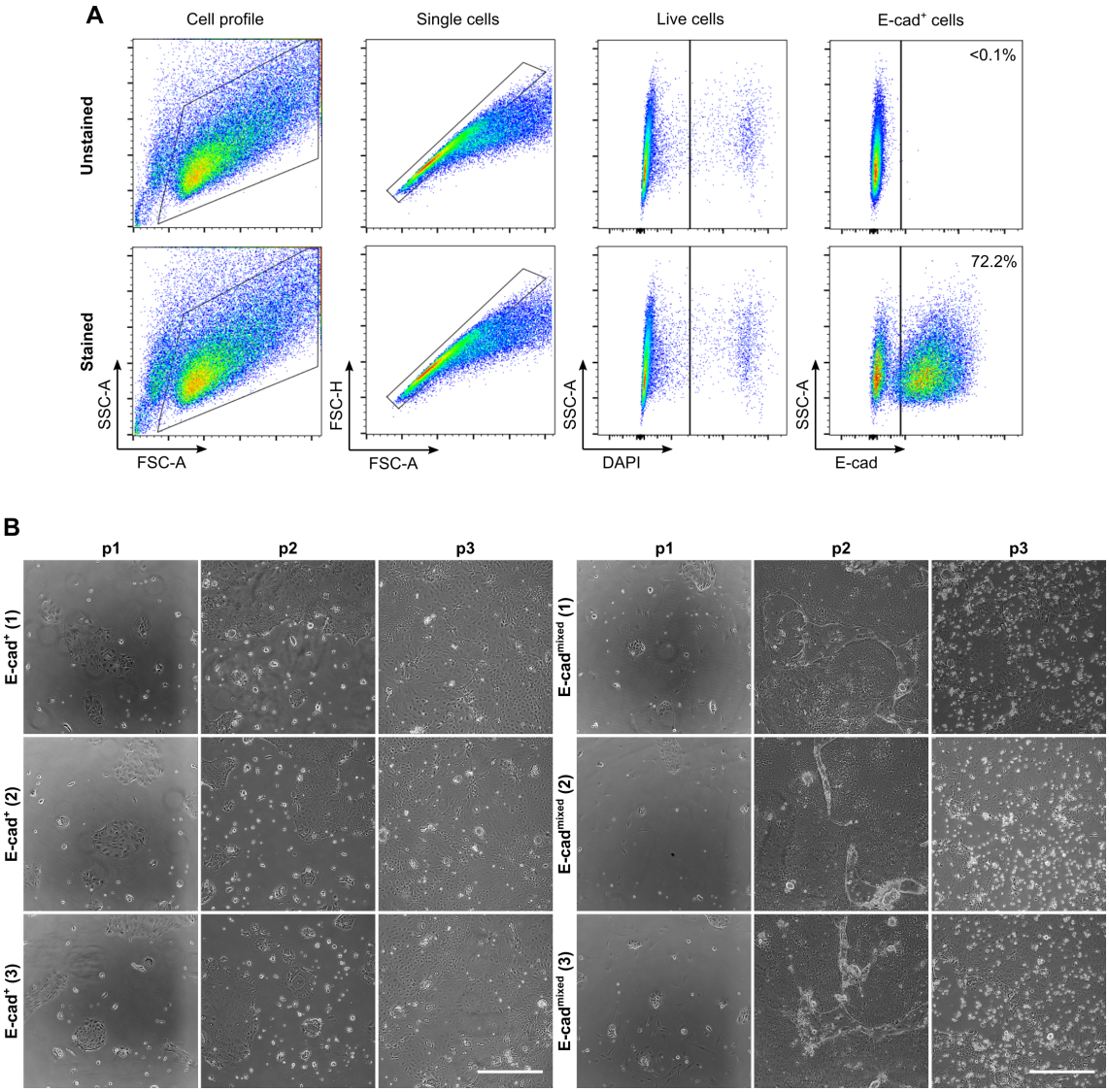

Figure 28. Mouse foetal pancreas progenitors sorted based on E-cad.

(A) Sorted cells were gated on cell profile, single cells, and live cells (DAPI), before sorting based on E-cad staining (far right plots, proportion of E-cad$^+$ cells indicated). Unstained cells used as controls. **(B)** Phase images of three replicates of sorted mouse foetal pancreas E-cad$^+$ and E-cad^{mixed} populations over three passages. Images taken using the 5X objective where whole wells were scanned and stitched, then 10X regions were cropped out to be shown here (scale bar represents 500μm).

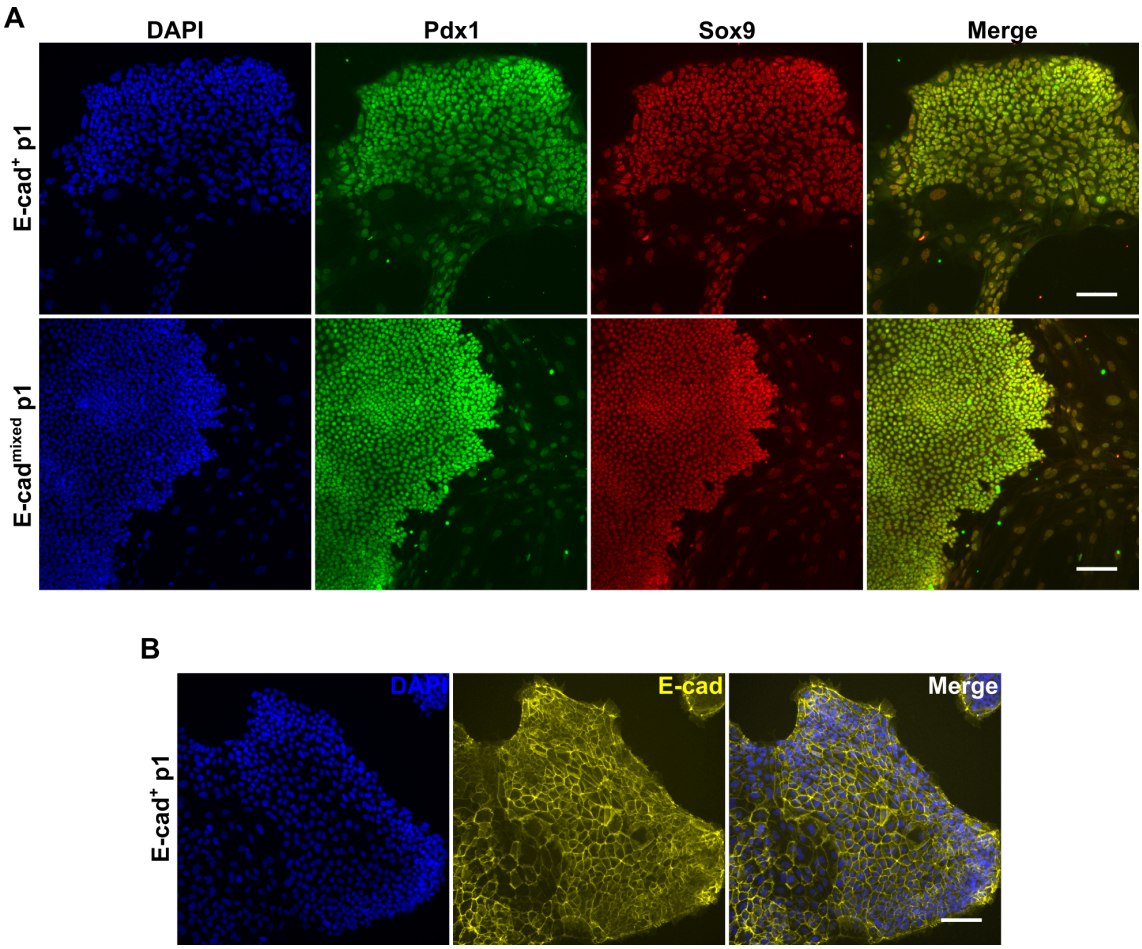

Figure 29. E-cad^{+} mouse foetal pancreas cells are Pdx1^{+}/Sox9^{+} progenitors.

(A) ICC of mouse foetal E-cad^{+} and E-cad^{mixed} populations at p1 post-sort stained for Pdx1 (green) and Sox9 (red). Images taken using the 20X objective (scale bar represents 100μm) **(B)** ICC of E-cad^{+} mouse foetal pancreas progenitors showing staining for E-cad (yellow). Images taken using the 20X objective (scale bar represents 100μm).

Importantly, we found that purified E-cad^{+} mouse foetal pancreas progenitors can be cultured long-term, passaged, and tolerate freeze-thawing well. Cultures were checked at regular intervals for progenitor marker expression **(Figure 30A)**, and continued to express Pdx1 and Sox9. While Pdx1 appeared to be stably expressed in the nucleus of cultured cells, Sox9 expression was more heterogeneous. Sox9 can be observed in the cytoplasm of some cultured cells at each passage tested, and staining intensity varies widely between cells.

Sox9 protein is known to contain a nuclear export signal (NES), and its translocation between cytoplasm and nucleus is thought to be an important mechanism in sex determination during development [317,318]. As such, cytoplasmic Sox9 in these pancreas progenitors cannot immediately be attributed to an artefact of culture. E-cad expression was still noted in the mouse foetal pancreas progenitors at late passages (p15) **(Figure 30B)**.

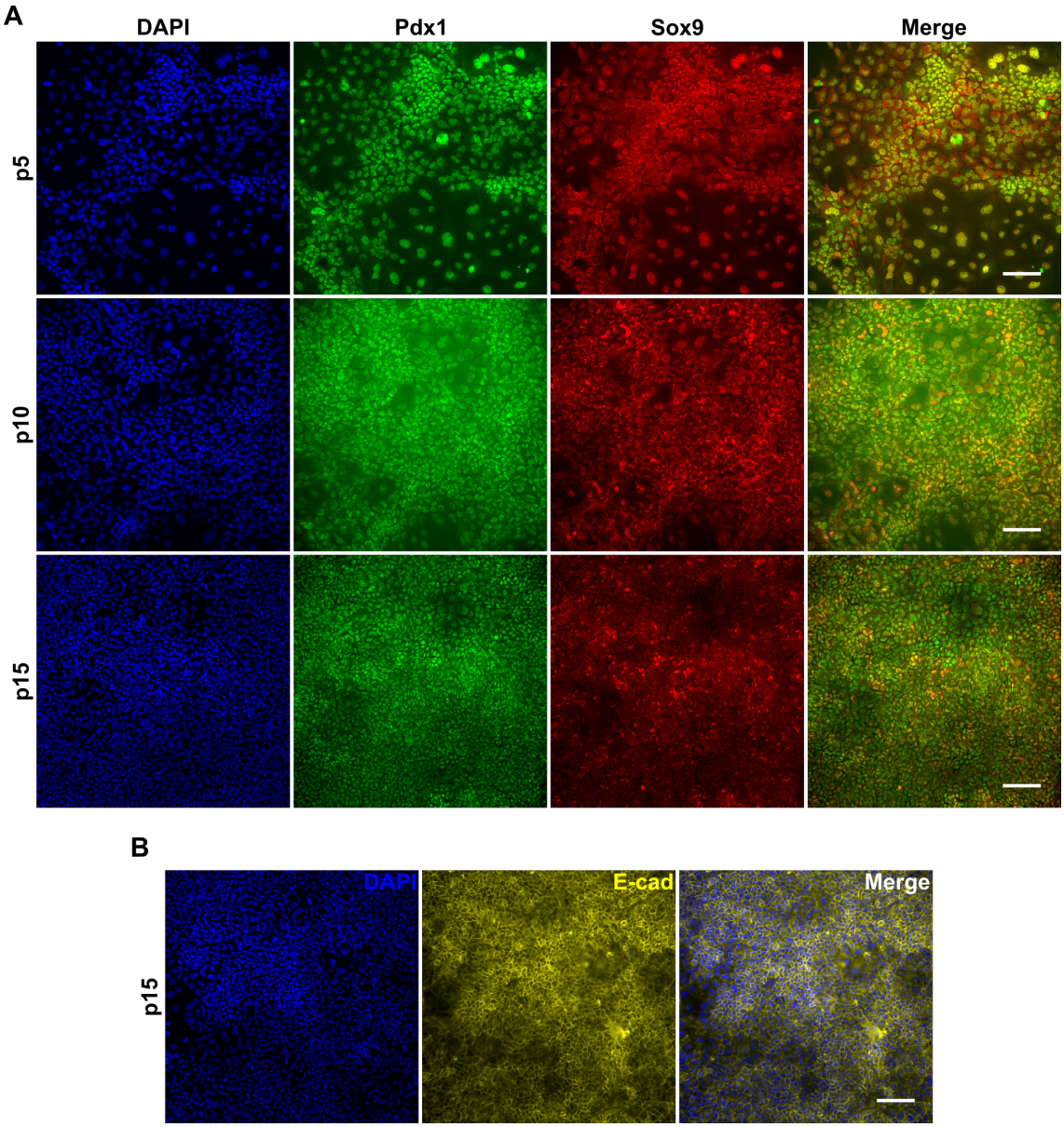

Figure 30. E-cad^{+} mouse foetal pancreas progenitors can be cultured long-term.

(A) ICC of E-cad^{+} mouse foetal pancreas progenitors at p5, p10 and p15 stained for Pdx1 (green) and Sox9 (red). Images taken using the 20X objective (scale bar represents 100μm) **(B)** ICC of E-cad^{+} mouse foetal pancreas progenitors at p15 showing staining for E-cad (yellow). Images taken using the 20X objective (scale bar represents 100μm).

To more fully characterise cultured mouse foetal pancreas progenitors, gene expression of a panel of markers was performed **(Figure 31)**. *Pdx1* and *Sox9* were among the genes that could be detected at mRNA level, although expression was much reduced from E12.5. *Pdx1* was reduced 10-fold, while *Sox9* was reduced 5-fold from its original levels. *Krt19* was upregulated in cultured progenitors by 17.26-fold, reflecting the ductal epithelial origin of expanded cells. Surprisingly, both *NeuroD1* and *Vim* were detectable in cultured progenitors. Weak *NeuroD1* expression was detected, but other endocrine progenitor markers *Ngn3* and *Nkx2.2* were not detected. *Vim* expression is traditionally associated with mesenchymal cells, but many cell types are reported to acquire *Vim* expression in vitro, including epithelial cells [319]. That is likely to be the case here, given the strong E-cad expression in these cells and that *Nkx3.2*, a marker of pancreatic mesenchyme [320], could not be detected. Furthermore, markers of mature endocrine cells *Ins2* and *Glu*, as well as exocrine markers *Amy2a* and *Cpa1* were also undetectable **(Table 2)**.

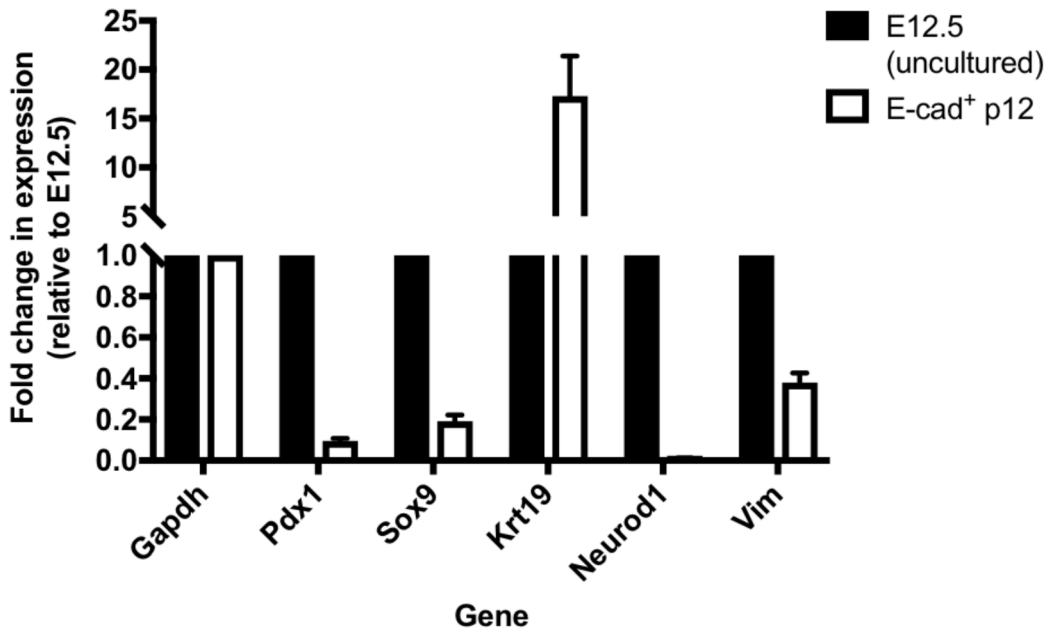

Figure 31. mRNA expression in E-cad$^+$ mouse foetal pancreas progenitors at p12.

Pancreas progenitor markers *Pdx1* and *Sox9*, ductal marker *Krt19*, endocrine progenitor marker *NeuroD1*, mesenchymal marker *Vim*. 1μg of RNA was used to make cDNA. Relative expression of all genes normalised to *Gapdh*. E12.5 n=1, E-cad$^+$ progenitors n=3. Error bars show standard deviation.

Table 2. CT values detected by qPCR for E-cad$^+$ mouse foetal progenitors p12.

Average CT values after 40 cycles for all genes analysed shown. -RT indicates cDNA controls where reverse transcriptase was excluded. ND=not detectable.

	Gapdh	Pdx1	Sox9	Ngn3	NeuroD1	Nkx2.2	Ins2	Glu	Krt19	Amy	Cpa1	Vim	Nkx3.2
E12.5 (uncultured)	23.809	29.671	26.226	26.910	29.244	28.533	30.389	27.927	26.919	ND	24.915	22.458	27.077
E12.5 (uncultured)-RT	33.231	ND	ND	36.037	ND	ND	ND	ND	ND	ND	ND	ND	ND
E-cad$^+$ p12	21.435	30.715	26.249	ND	33.520	ND	ND	ND	20.435	ND	ND	21.489	ND
E-cad$^+$ p12-RT	32.798	ND	ND	ND	ND	ND	ND	ND	ND	ND	ND	ND	ND

4.2.7 FACS-isolated mouse foetal pancreas progenitors remain functionally viable and are amenable to genetic engineering

To be useful as a cellular model for research, pancreas progenitor cells must be able to differentiate in vitro. To investigate the differentiation potential of E-cad$^+$ mouse foetal pancreas progenitors, we attempted to force their differentiation in culture. Pancreas progenitors were re-plated at low density and allowed to recover for 1 day in EF7+A83. After recovery, cells were exposed to culture medium reported to induce differentiation from pancreas progenitors to endocrine progenitors in hESC differentiation protocols (Stage 5 medium) [259]. After 6 days, *Sox9* and *NeuroD1* were both significantly reduced in differentiated cells (0.51- and 0.03-fold, p=0.01 and p=0.0001, respectively) **(Figure 32)**. Meanwhile, *Ngn3* became detectable at mRNA level where it had been undetectable previously **(Table 3)**. This data suggests that E-cad$^+$ mouse foetal pancreas progenitors retain the capacity to further differentiate to Ngn3 expressing endocrine pancreas progenitors in vitro.

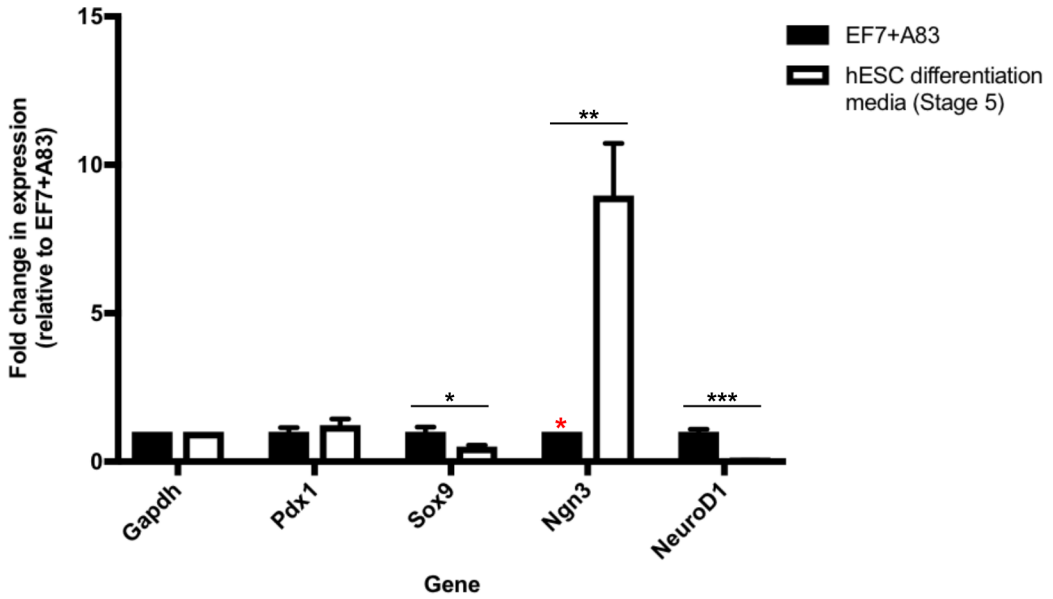

Figure 32. mRNA expression in E-cad^{+} mouse foetal pancreas progenitors in EF7+A83 vs differentiation medium.

Pancreas progenitor markers *Pdx1* and *Sox9*, endocrine progenitor markers *Ngn3* and *NeuroD1*. 1μg of RNA was used to make cDNA. Relative expression of all genes normalised to *Gapdh*. EF7+A83 n=3, differentiation medium n=3. Error bars show standard deviation. Significance tested using multiple unpaired t-tests with Holm-Sidak correction (shown on graph, * = p≤0.05, ** = p≤0.01, *** = p≤0.001, **** = p≤0.0001). Red asterisk indicates where an arbitrary CT value had to be assigned to an undetectable gene to enable fold change calculation.

Table 3. CT values detected by qPCR for E-cad^{+} mouse foetal progenitors in differentiation media.

Average CT values after 40 cycles for all genes analysed shown. -RT indicates cDNA controls where reverse transcriptase was excluded. ND=not detectable.

	Gapdh	Pdx1	Sox9	Ngn3	NeuroD1	Nkx2.2
EF7+A83	21.435	30.715	26.249	ND	33.520	ND
EF7+A83-RT	33.231	ND	ND	36.037	ND	ND
Differentiation media	19.143	28.134	24.941	35.187	36.265	ND
Differentiation media-RT	31.531	ND	ND	ND	ND	ND

Future research uses of E-cad$^+$ mouse foetal pancreas progenitors may be facilitated by genetic engineering of these cells, for example in the case where reporter gene knock-in may be desired. To demonstrate that E-cad$^+$ mouse foetal pancreas progenitors are amenable to simple genetic engineering, we created a line bearing a stable integration cassette designed to constitutively express eGFP. Cells were lipofected with a plasmid encoding PiggyBac (PB) transposase and a second 9.8kb plasmid including eGFP under the CAG promoter, as well as an antibiotic resistance gene, flanked by PB transposable elements **(Figure 33A)**. One day after lipofection, GFP-expressing cells were evident **(Figure 33B)**. At day 16 after Blasticidin selection was applied to cells, GFP-expressing colonies could be seen. The variable GFP intensity between colonies is typical of transposase-based integration strategies where the location and frequencies of PB integration varies between clones. After passaging and continued selection, nearly all cells were GFP$^+$ at day 21. Thus, E-cad$^+$ mouse foetal pancreas progenitors are amenable to genetic manipulation. We tested our GFP-expressing E-cad$^+$ mouse foetal progenitors in pancreatic bud engraftment experiments, where progenitor cells were incubated with whole mouse foetal pancreatic buds to allow their migration into the tissue. Buds were then cultured in transwell format as before, with the intention of assessing GFP-expressing E-cad$^+$ progenitor cell differentiation. However, cell migration into buds was low and survival poor. This is an area for future development when assessing cultured progenitor differentiation capacity, which could benefit from more advanced techniques such as microinjection.

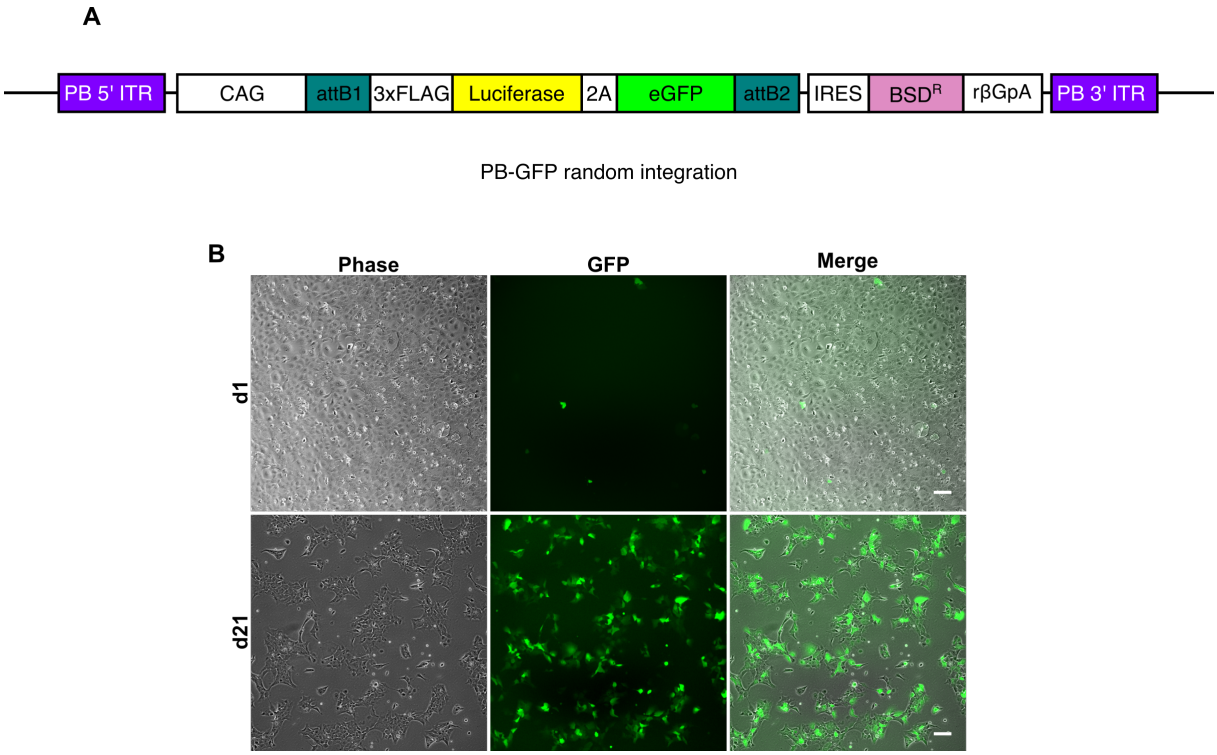

Figure 33. E-cad^{+} mouse foetal pancreas progenitors are amenable to genetic engineering.

(A) Schematic of the PB-GFP integration induced by PB transposase **(B)** Phase images and GFP expression at days 1, 16 and 21 post-lipofection and during blasticidin selection. Images taken using the 10X objective (scale bar represents 100μm).

4.3 Discussion

Here we have shown that mouse foetal pancreas can be dissected prior to the secondary transition, at which point the bulk of differentiation towards endocrine and exocrine lineages during development occurs. Dissected mouse foetal pancreas can be dissociated, expanded in simple monolayer culture conditions, and $Pdx1^{+}/Sox9^{+}$ epithelial progenitors then isolated based on E-cad expression. Homogeneous mouse foetal epithelial pancreatic progenitors can be serially passaged and retain expression of progenitor markers. Furthermore, mouse foetal epithelial pancreas progenitors have the potential to differentiate into *Ngn3*-expressing endocrine pancreas progenitors in vitro, a key requirement for the use of these cells as a model for improving in vitro directed differentiation to endocrine cell types.

Past protocols for culturing endogenous pancreas progenitor cells from mouse foetal tissue have often relied on 3D culture systems. In these systems, dissociated ductal progenitor cells were demonstrated to expand exponentially [303-305]. However, the 3D culture environment often recapitulated pancreas development in that ongoing differentiation continued and progenitors were not specifically captured and expanded, a finding that we also found in whole pancreatic bud culture experiments. Amylase, insulin and glucagon could all be detected in pancreas organoids [304], while pancreatic spheres also contained subsets of C-peptide and glucagon-expressing cells [303]. While the sphere culture method was subsequently improved upon to reduce onward differentiation [305], assessing the protein expression in these cultures involved the lengthy process of fixation, embedding and sectioning for each sample. This type of assay is clearly not compatible with scaling up for experiments ending in, for example, high-content imaging screens, where 2D culture models are highly advantageous. Our goal was to identify improved conditions for capture and proliferation of pure populations of Pdx1 and Sox9 expressing progenitors.

We identified conditions that support long-term 2D culture and expansion of epithelial $Pdx1^{+}/Sox9^{+}$ mouse foetal pancreas progenitors, thereby enabling future experiments that could test hundreds of conditions in parallel to improve endocrine specification from early progenitor cells. There have been previous reports of mouse foetal pancreas progenitors being captured and grown in 2D cultures, but only in culture medium with a high serum content [307] and on feeder fibroblasts [306]. In such undefined conditions, it would be impossible to reliably elucidate signalling pathways and regulatory mechanisms governing the switch from early progenitor to endocrine progenitor. By contrast, the serum-free, feeder-free conditions we detail here are conducive to such studies.

The finding that the TGFβ inhibitor A83 is an important component in foetal progenitor expansion, possibly through inhibition of epithelial-to-mesenchymal transition, is of particular interest. As reported earlier in this chapter, A83 was also key to maintaining induced human pancreas progenitors [316]. Paradoxically however, TGFβ inhibitors have more typically been used to actually induce endocrine cell formation in the hESC-to-pancreas differentiation field [251,252,321]. The role of TGFβ signalling during development is similarly unclear, with reports suggesting that TGFβ signalling both induces [322,323] and inhibits [324] endocrine cell specification. More research should be conducted to tease apart the effects of different TGFβ ligands and receptors, or whether TGFβ signalling dosage and interplay with other pathways is important, as is known to be the case for mesendoderm and DE specification [325,326]. Our monolayer culture system is an ideal platform to perform such studies on molecular mechanism.

Our cultured mouse foetal pancreas progenitors can be forced to differentiate in vitro, although it must be noted that induction of endocrine progenitor markers was weak. This could be a reflection of the inadequacy of hESC differentiation medium to induce

endocrine lineages, and may actually prove to be a benefit to identifying subtle effects in pro-endocrine culture conditions in the future. However, repeated observations of our forced differentiation culture experiments suggested that high progenitor cell density and increasing cell-cell contact as cultures grew confluent was a significant barrier to differentiation. Indeed, forced differentiation cultures that yielded detectable endocrine markers had to be started at very low density (1:40) to allow for differentiation to occur without the cultures becoming too confluent. In light of this, forced differentiation efficiency could probably be improved with minor adjustments to seeding density to enable longer forced differentiation time, limit progenitor cell-cell contacts, and reduce the concentration of signalling factors released into the media by early progenitor cells. Time constraints limited the further assessment of differentiation conditions. Further studies are therefore needed to deeply probe the differentiation potential of these cells in vivo; the GFP derivatives we generated could be useful for this purpose.

We have therefore identified methods for isolating and culturing homogeneous populations of expandable epithelial pancreas progenitor cells that retain their capacity to differentiate in vitro. These cells represent a convenient and useful cellular model for future studies to improve methods for inducing endocrine differentiation in vitro, and potentially probing the mechanisms involved in this induction.

CHAPTER 5
Culture of human foetal pancreas progenitors in vitro

5.1 Introduction

Mouse tissue provides a useful model system to explore mechanisms of development and emergence of pancreas progenitors. However, if we are to understand and characterise human pancreas progenitor cells more fully, extrapolation of data from mouse cells may only take us so far and characterisation of human development might reveal important differences.

Culture of human foetal pancreas progenitors directly from dissociated tissue has been attempted previously. Indeed, the potential for using human foetal pancreas cells directly for cell therapy in diabetic patients was recognised in early studies whose aims leaned more towards sustaining foetal β-cells in vitro, rather than progenitor cells. These early protocols gave rise to apparently mixed cell populations in culture, amongst which were islet-like cell clusters (ICCs). Either due to an inherent property of the foetal cells or because of the culture conditions, ICCs differentiated to insulin-producing cells that could be sustained in culture for only short periods [327] [328]. Still, it was recognised that cultured human foetal pancreas cells could be used as a tool for identifying conditions to promote endocrine differentiation and insulin production; both growth hormone [329] and nicotinamide [330] were found to be culture additives that improved ICC formation and insulin production in vitro.

It was only recently that the first reports of the successful in vitro capture of a putative human foetal pancreas progenitor cell was reported [331]. It was reported that 'Nestin-positive islet-derived progenitors' (NIPs) could be continously expanded in serum- and FGF2-containing medium in monolayer, and could be forcibly differentiated to

insulin-expressing cells. Paradoxically, NIPs under these self-renewal conditions did not express traditional markers of developmental pancreatic ductal progenitors such as PDX1 and KRT19, but did express the exocrine marker AMY [331]. Thus, it seems likely that NIPs represent artefacts of culture, or unusual injury response type states, rather than bone fide pancreas progenitor cells.

Both Zhang et al. (2013) [332] and Lopez et al. (2014) [333] described methods for isolating human pancreas progenitors from foetal pancreas. Using tissue from between 10 to 12 weeks gestation, Zhang et al. (2013) [332] cultured progenitors that expressed both PDX1 and KRT19, as well as other stem cell markers including OCT4 and SCF. Lopez et al. (2014) [333] showed that proliferative PDX1$^+$ pancreas cells from 12 to 23 weeks gestation could be cultured in suspension. Finally, long-term expansion of PDX1$^+$/SOX9$^+$/E-cadherin$^+$ human foetal pancreas progenitors in a 3D culture system has been demonstrated [305]. In all studies, when these cells were forced to differentiate, insulin and glucagon expression could be detected by immunostaining.

While the aforementioned studies may mark significant progress in techniques to isolate and culture genuine human pancreas progenitors there are caveats. Both Zhang et al. (2013) [332] and Lopez et al. (2014) [333] relied on ill-defined culture medium that included serum. Furthermore, in characterising their cell cultures, both these studies appeared to describe heterogeneous cells populations. For instance, mRNA of the exocrine marker AMY was expressed at a much higher level than either PDX1 or NGN3 in cultured progenitors in the first study [332], and 15% of all cultured cells in basal conditions reportedly expressed endocrine markers [333]. Progenitors expanded by Bonfanti et al. (2015) [305] appear to express authentic pancreas progenitor markers much more uniformly than either prior study, and are able to propagate cells in serum-free media including EGF, FGF10 and R-spondin. However, they did not describe a method for expanding these cells in monolayer, and such 3D culture systems are

more suited to modelling development rather than high throughput screening and high-content imaging that could be used to interrogate progenitor cell biology and identify culture conditions to optimise cell production for therapy.

In this chapter, we present the results of our efforts to improve on existing human foetal pancreas culture methods. To do this, we built on the knowledge gained from the literature on this topic. We also apply approaches and conditions that were identified in our work with the mouse foetal pancreas, described in the previous chapter.

5.2 Results

5.2.1 Human foetal pancreas progenitors from week 8–12 tissue can be cultured and expanded long-term

After finding that EF7+A83 culture medium permits expansion of mouse foetal pancreas progenitors on Matrigel in 2D culture, we aimed to determine whether these conditions were also conducive to human foetal pancreas progenitor culture. Human foetal pancreas was dissected and dissociated in the same way as mouse foetal pancreas **(Figure 34)**. For relatively large foetal pancreas samples, additional mechanical dissociation in a tissue grinder prior to enzymatic/chemical dissociation was necessary to fully break down the tissue. All samples were dissociated and plated into EF7+A83 media. Any proliferating cultures that arose were passaged into successively larger wells. At p2, the culture was split into three wells and continued cell expansion in three different medias was compared– neural stem cell (NS) medium, EF7 and EF7+A83. The NS medium, containing EGF and FGF2, was that routinely used in the Pollard lab for the growth of neural stem cell lines.

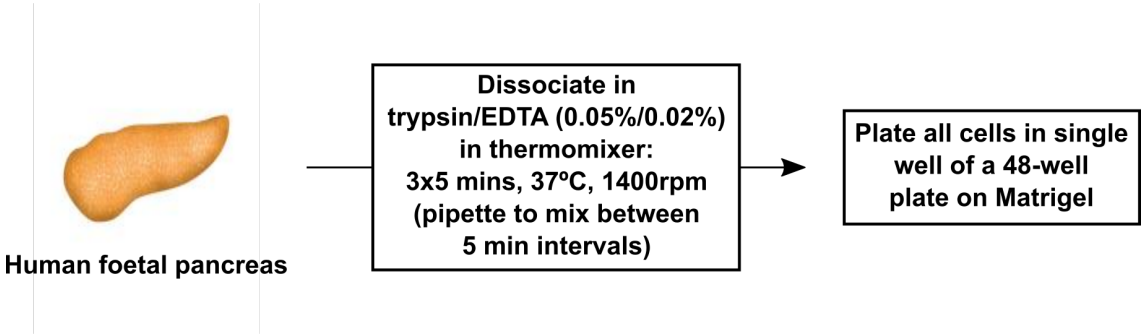

Figure 34. Dissociated human foetal pancreas culture strategy.

Human foetal pancreases were dissected and overlying mesenchyme removed manually.

In vitro culture was attempted for 12 independent human foetal pancreas specimens **(Table 4)**. Initial culture outcomes were variable, with foetal pancreas from weeks 8 and 9 of development being the most amenable to expansion in EF7+A83. Week 12 pancreas occasionally produced expandable cell populations, but all samples from later than week 12 either failed to survive and/or did not proliferate sufficiently in culture. Images were taken of successful cultures at each passage and RNA was collected to be used for RT-qPCR to assess pancreas progenitor gene expression in cultured cells (where sufficient RNA could be purified).

Five of the 12 human foetal pancreas samples resulted in cultures that could be passaged at least three times. At p0, FT3506 (week 12+6) appeared to consist of a morphologically heterogeneous cell population **(Figure 35)**. Colonies that were epithelial in appearance could not be maintained beyond the first passage. Upon splitting the culture to different media, cells in EF7 ceased to grow beyond p3. NS medium supported cell growth to p5, but cells were elongated and non-epithelial in appearance. At p2 in EF7+A83, the culture consisted of cuboidal-like cells surrounded by cells of non-epithelial morphology. By p5, cuboidal-like cells were no longer apparent and the EF7+A83 cell cultures ceased growing at p7. Unfortunately, RNA could not be isolated from any of the FT3506 cell cultures due to the low cell numbers.

Table 4. Human foetal pancreas tissue samples used for culture.

Gestational stage, tissue grinder use and success in culture indicated.

Human foetal pancreas sample	Gestational stage (weeks+days)	Tissue grinder used in dissociation?	Cultured beyond p3?
FT3502	12+4	No	No
FT3503	13+3	No	No
FT3504	12+6	No	No
FT3506	12+6	Yes	Yes
FT3508	9+6	No	Yes
FT3509	8+1	No	Yes
FT3513	12+5	Yes	No
FT3514	13+1	Yes	No
FT3518A	18+4	Yes	No
FT3518B	18+4	Yes	No
FT3520	8+1	No	Yes
FT3521	12+4	Yes	Yes

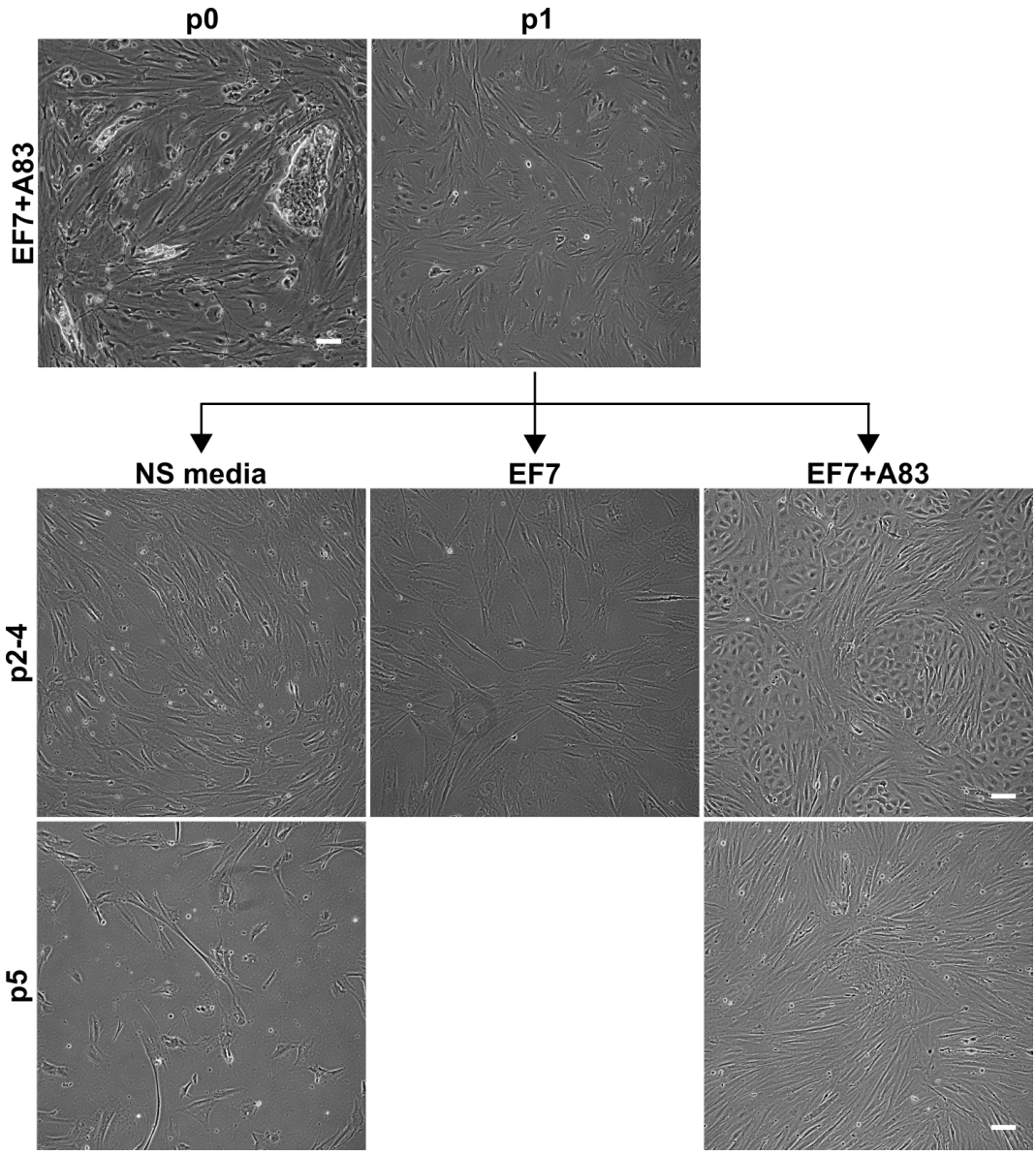

Figure 35. FT3506 human foetal pancreas growth in culture.

Phase contrast images were taken using the 10X objective (scale bar represents 100μm). Passage numbers and culture media indicated.

FT3508 cells, derived from week 9 foetal pancreas, appeared to have a greater capacity for growth in culture than FT3506. Similarly to FT3506, FT3508 cultures initially consisted of cells of both epithelial-like and fibroblast-like morphologies **(Figure 36A)**. Unlike FT3506 cultures, epithelial-like cells remained evident by microscopy even after the first passage and persisted in EF7 and EF7+A83 at p2. However, most cells in NS medium at p2 possessed a flattened, elongated appearance and epithelial-like colonies were absent. These flat cells could be grown in NS medium up to at least p9, at which point they were frozen. In contrast, cells in EF7 could not be grown past p4. Finally, cells in EF7+A83 retained a more cuboidal morphology compared to cells in NS medium, and could also be cultured to at least p10 before cryopreservation. In gene expression analysis of FT3508 cultures, *PDX1* mRNA was never detectable in NS media cell populations, but was detectable by qPCR in EF7+A83 at p2, and also at p5 where expression was reduced 50-fold compared to p2 **(Figure 36B)**. Robust *SOX9* mRNA expression was detected at the earliest passage analysed in both NS and EF7+A83 media (NS p4 CT=25.614, EF7+A83 p2 CT=25.269) and *SOX9* continued to be detectable at every subsequent passage analysed. However, the levels of *SOX9* decreased significantly over time in EF7+A83 media – expression was reduced 100-fold by p4 and 333-fold at p10 compared to p2. *SOX9* expression was maintained better in NS media, where expression was reduced 3.6-fold at p9 compared to its NS p2 level.

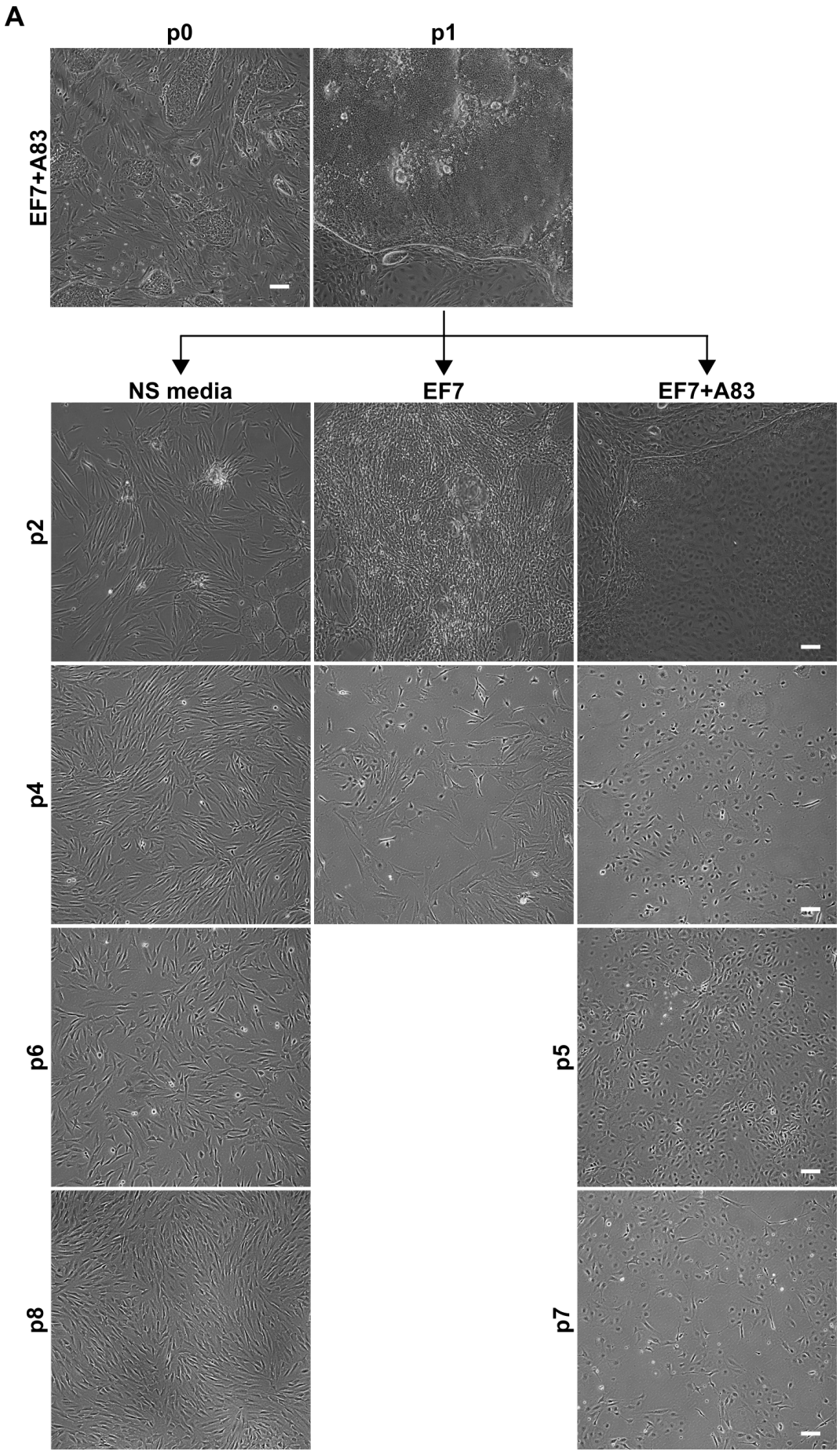

Figure continued on next page

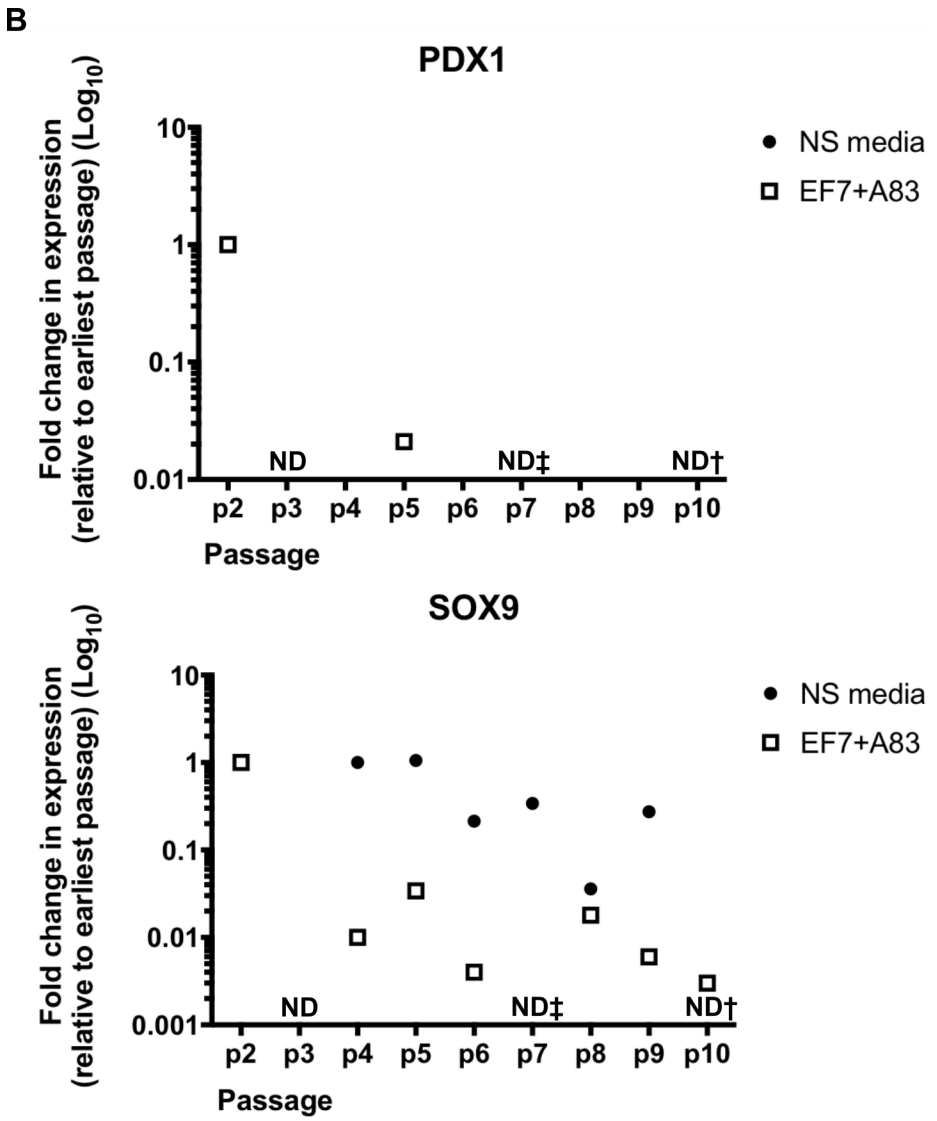

Figure 36. FT3508 human foetal pancreas growth and mRNA expression in culture.

(A) Phase contrast images were taken using the 10X objective (scale bar represents 100μm). Passage numbers and culture media indicated. **(B)** qRT-PCR for pancreas progenitor markers *PDX1* and *SOX9* at different passages. 500ng of RNA was used to make cDNA. Relative expression of all genes normalised to *GAPDH*. ND=not determined, where RNA could not be collected (no symbol=ND for all media, †=ND for NS, ‡=ND for EF7+A83).

The next foetal pancreas sample to be used for attempted culture – FT3509 – was from week 8 of gestation. Unlike previous cultures, FT3509 cells at p0 and p1 were homogeneous in their morphology, where cells appeared cuboidal with large nuclei **(Figure 37A)**. After splitting the culture to different media at p2, EF7+A83 maintained many of these cuboidal cells. Additionally, rare epithelial-like colonies could also be seen consisting of numerous small, tightly-packed cells. These structures were not seen in EF7 or NS media at p2 or beyond. By p4, cells in NS medium had the same fibroblast-like morphology seen in other samples. EF7 and EF7+A83 cells exhibited similar morphologies up to p6, but cell growth ceased in EF7 at p8.

EF7+A83 cultured cells continued to grow well and by p9 epithelial-like colonies once again began to emerge in the culture, more numerous than at p2. The apparent absence of epithelial-like cells between p2-p9 could potentially be explained by a high background of differentiated cells out-competing low numbers of slowly dividing epithelial progenitor cells at early passages. Differentiated cells may then have been lost over time in culture, allowing epithelial progenitors to expand. By phase contrast microscopy, many of these colonies appeared to be raised above the surrounding flattened cells. Epithelial-like cells persisted in EF7+A83 culture, even after serial passaging and freeze-thawing. FT3509 cell populations could be expanded quickly – cells were routinely grown in 6-well plate format and split 1:6 every 3-4 days, by which point wells were completely confluent.

EF7+A83 was the only condition in which *PDX1* mRNA expression could be detected, although not at p5 or p7 **(Figure 37B)**. In EF7+A83, there was a general trend for increasing *PDX1* expression with each passage, and by p15 when epithelial-like colonies comprised most of the cell population, *PDX1* expression had increased 68.522-fold over its original level. However, absolute expression of *PDX1* remained relatively low throughout culture (EF7+A83 p4 CT=37.169, EF7+A83 p15

CT=34.364). *SOX9* mRNA was once again more abundantly expressed and detectable in all conditions (NS p4 CT=23.807, EF7 p4 CT=32.404, EF7+A83 p4 CT=26.819). While *SOX9* levels did tend to decrease over time in culture, the decrease was not as pronounced as had been detected in FT3508, particularly in EF7+A83. The average reduction in *SOX9* expression in EF7+A83 across all passages tested (excluding the earliest passage, which had a fold change of 1 by definition) in FT3509 was 1.9-fold, compared to 76.9-fold for FT3508. Indeed, at p15 *SOX9* expression had increased to 1.937-fold of its original level.

In summary, although absolute *PDX1* expression was low in these cultures, this can likely be explained by the low percentage of epithelial cells present in the total population. Indeed, as epithelial cell proportion increased, large increases in *PDX1* expression were detected. Changes in *SOX9* expression were more modest by comparison, which highlights the importance of using multiple markers for identifying pancreas progenitor cells that was introduced in Chapter 3.

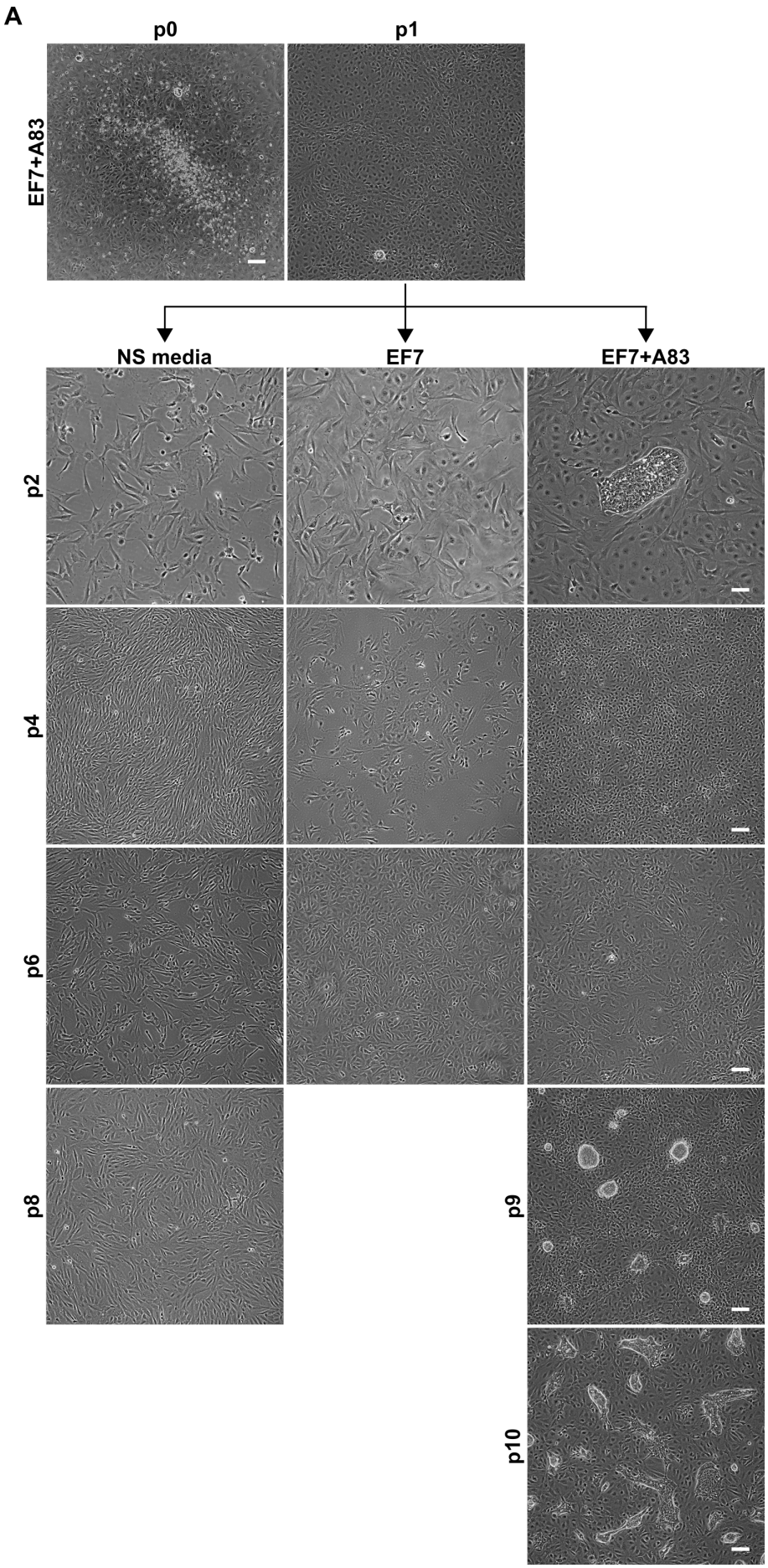

Figure continued on next page

B

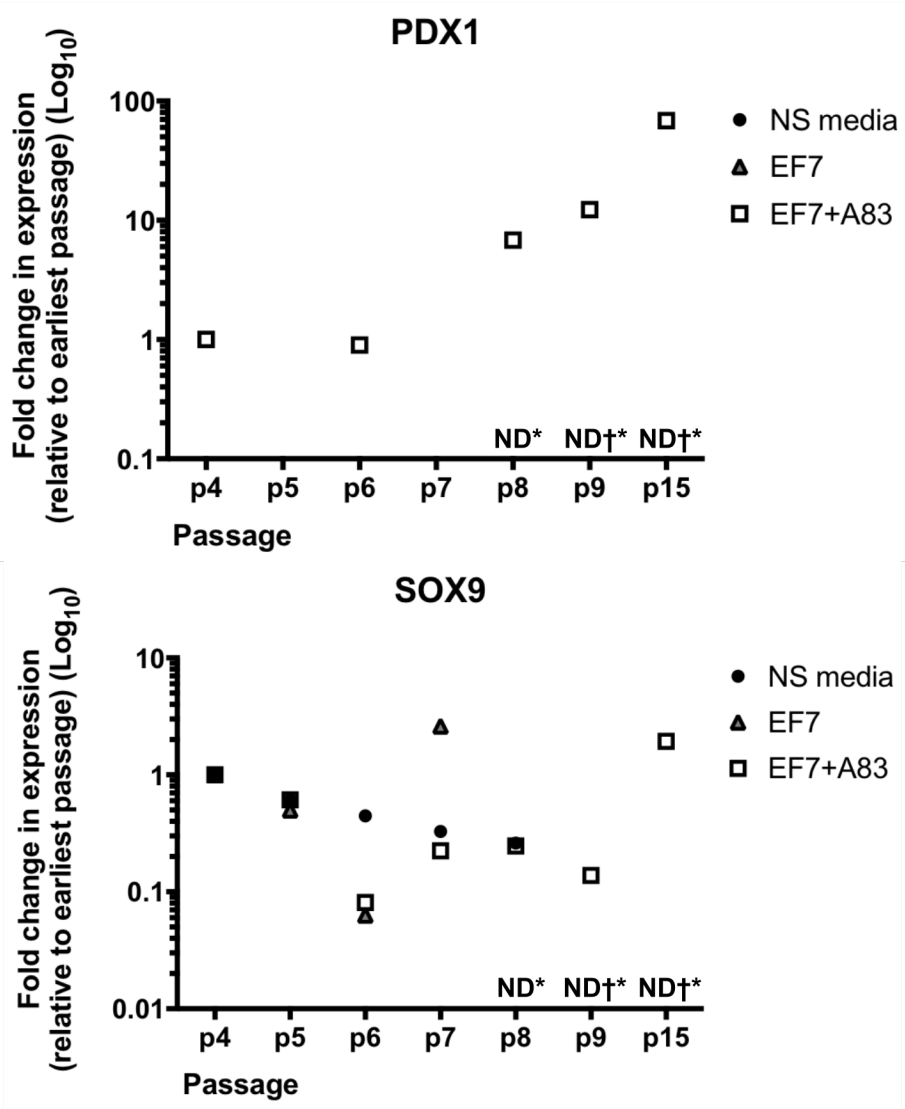

Figure 37. FT3509 human foetal pancreas growth and mRNA expression in culture.

(A) Phase contrast images were taken using the 10X objective (scale bar represents 100μm). Passage numbers and culture media indicated. **(B)** qRT-PCR for pancreas progenitor markers *PDX1* and *SOX9* at different passages. 500ng of RNA was used to make cDNA. Relative expression of all genes normalised to *GAPDH*. ND=not determined, where RNA could not be collected (no symbol=ND for all media, †=ND for NS, *=ND for EF7).

A second human foetal pancreas from week 8 of gestation – FT3520 – was obtained. While epithelial-like colonies were apparent by p2 in EF7+A83, but not other conditions, these colonies did not re-emerge in later passages of EF7+A83 as for FT3509 **(Figure 38A)**. However, the cells that were present had a cuboidal morphology that resembled FT3509 cells at early passages. Due to time constraints, FT3520 cultures had to cryopreserved while cells were still growing well, so the possibility that epithelial-like colonies may have arisen at later passages cannot be ruled out. As in FT3509, cells in NS medium acquired a fibroblast-like morphology, while cells in EF7 ceased growth by p3. *PDX1* mRNA could not be detected in NS medium or EF7+A83 at any stage **(Figure 38B)**. *SOX9* was consistently detectable and maintained relatively high levels of expression over time, with an average fold change (excluding the earliest passage) of 0.619-fold in NS medium and 1.062-fold in EF7+A83.

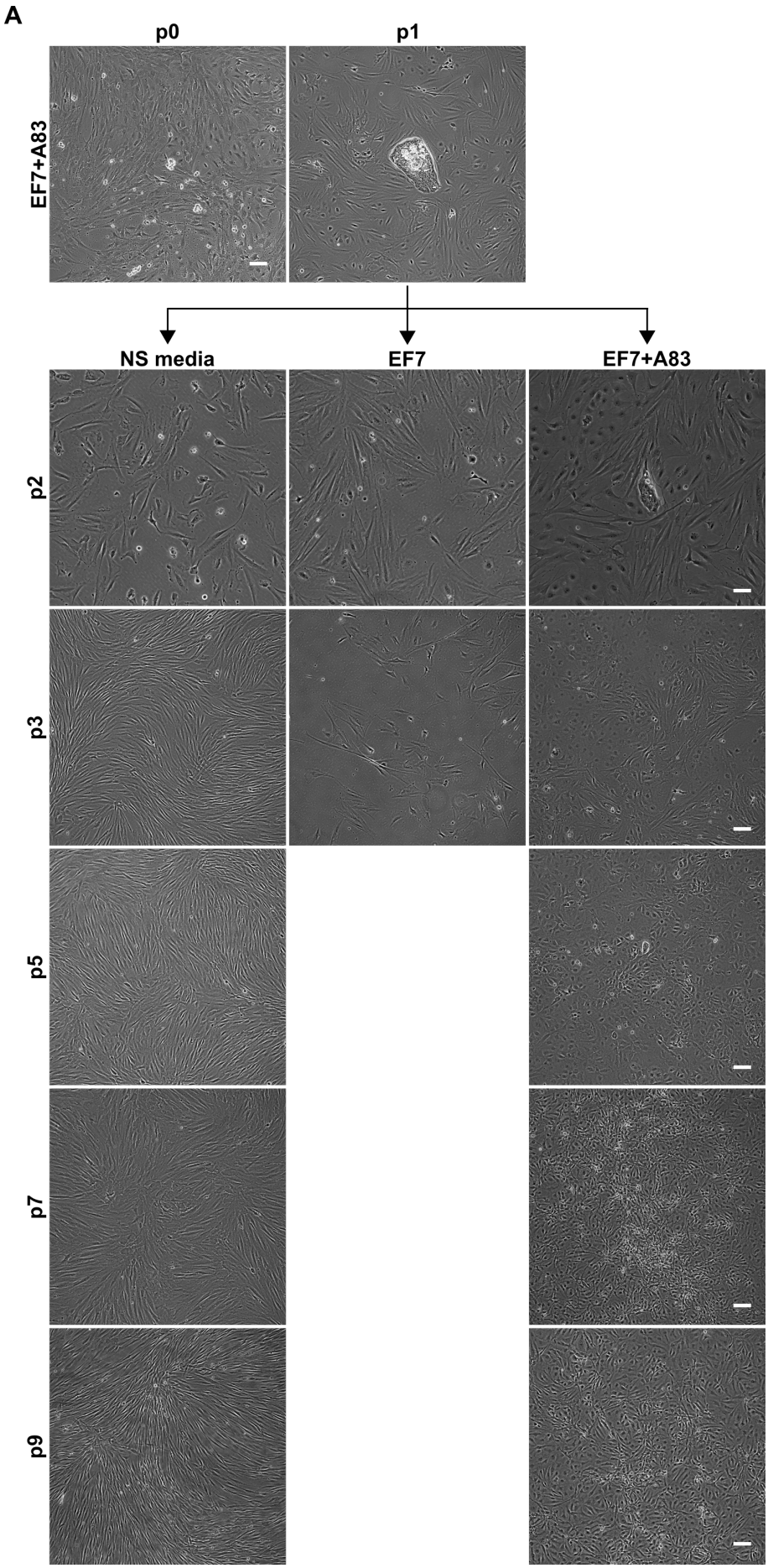

Figure continued on next page

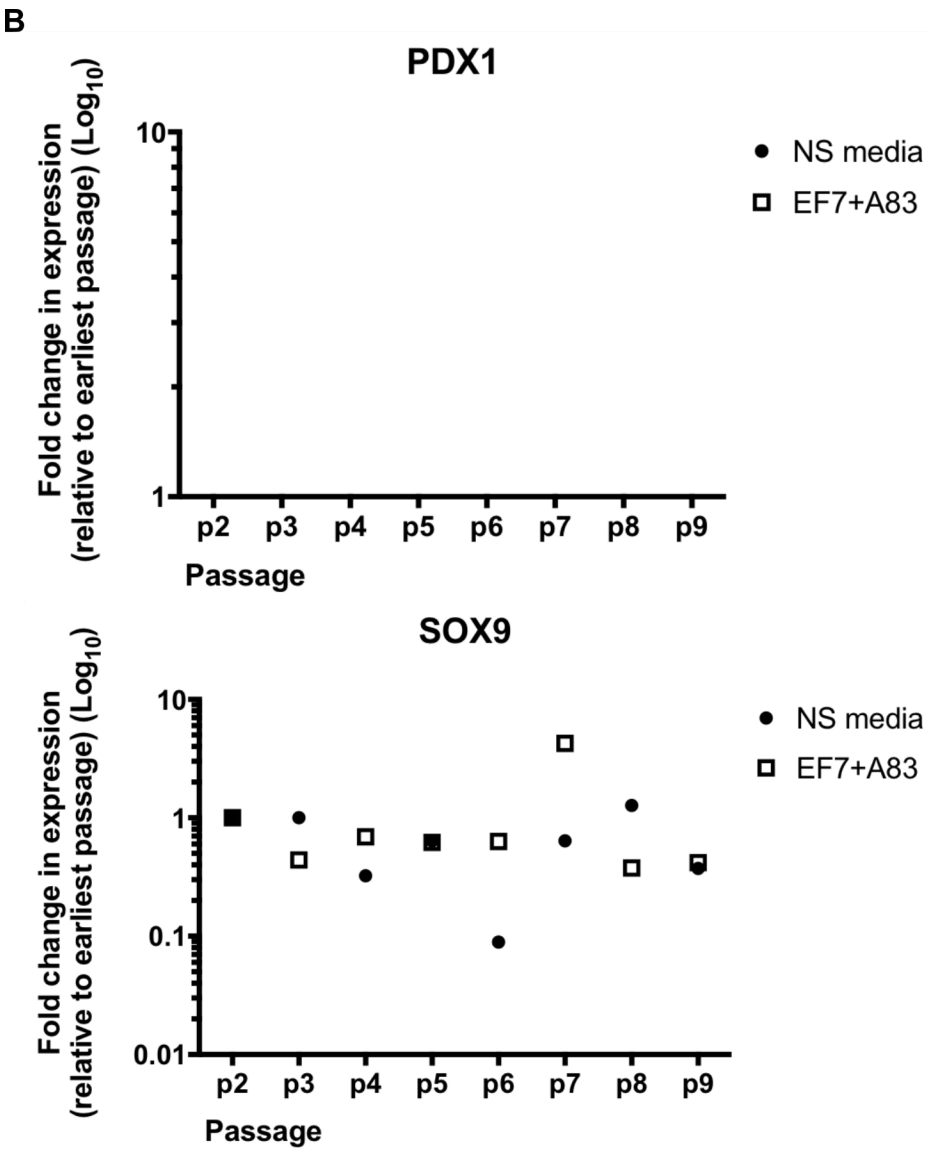

Figure 38. FT3520 human foetal pancreas growth and mRNA expression in culture.

(A) Phase contrast images were taken using the 10X objective (scale bar represents 100μm). Passage numbers and culture media indicated. **(B)** qRT-PCR for pancreas progenitor markers *PDX1* and *SOX9* at different passages. 500ng of RNA was used to make cDNA. Relative expression of all genes normalised to *GAPDH*.

FT3521, the final human foetal pancreas sample to be cultured, was from week 12 of development. FT3521 cells at p1 were morphologically heterogeneous, with epithelial-like colonies present **(Figure 39A)**. At p2 in EF7+A83, FT3521 cells resembled those from FT3506 at p2, which was also a week 12 sample. Cells of cuboidal morphology were surrounded by fibroblast-like cells. Rare epithelial-like colonies could also be seen. Subsequent passages in EF7+A83 appeared to contain progressively fewer cuboidal cells, until the culture was cryopreserved at p6. As in all previous samples, NS medium supported the growth of fibroblast-like cells, and EF7 was not conducive to long-term growth. *PDX1* mRNA was never detected in EF7+A83 or NS media **(Figure 39B)**, whereas *SOX9* could be detected in all RNA samples except EF7+A83 p5. *SOX9* expression showed a trend towards increasing in NS medium, with a 1.644-fold increase by p6 compared to p2 levels. In contrast, *SOX9* mRNA levels decreased in EF7+A83, with a 1.6-fold reduction by p6 compared to p2.

In conclusion – and with the caveat of a limited sample numbers – these human foetal pancreas cell culture experiments suggest that using tissue from developmental week 8 is more likely to result in expandable cell populations than even tissue from 3 weeks later in development. Furthermore, EF7+A83 was the only culture medium that ever supported detectable *PDX1* mRNA expression and long-term culture of apparently epithelial cells. EF7 alone was not enough to allow continued cell expansion, while cells in NS medium eventually uniformly acquired a fibroblastic morphology, which would be unexpected for epithelial pancreatic progenitor cells.

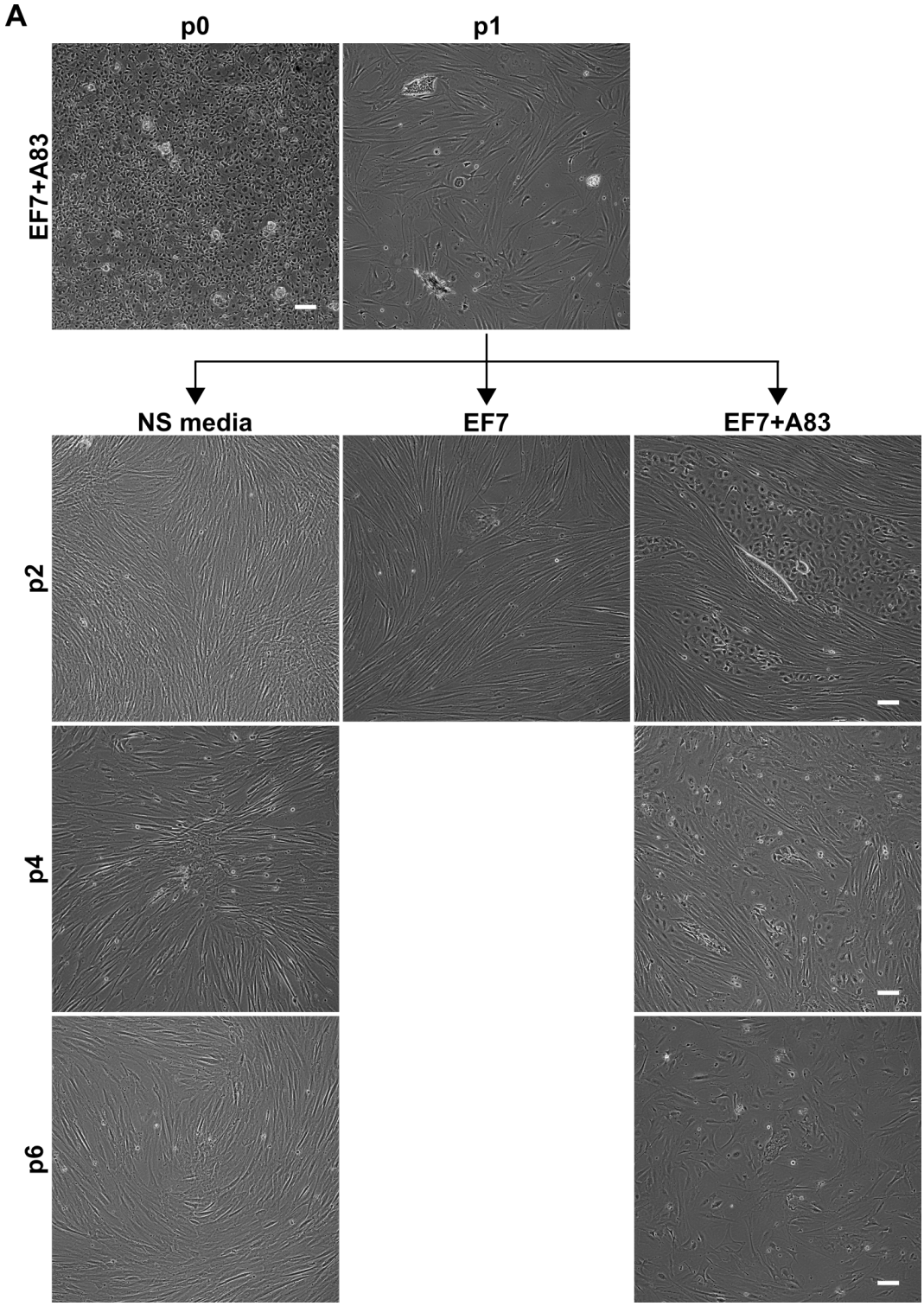

Figure continued on next page

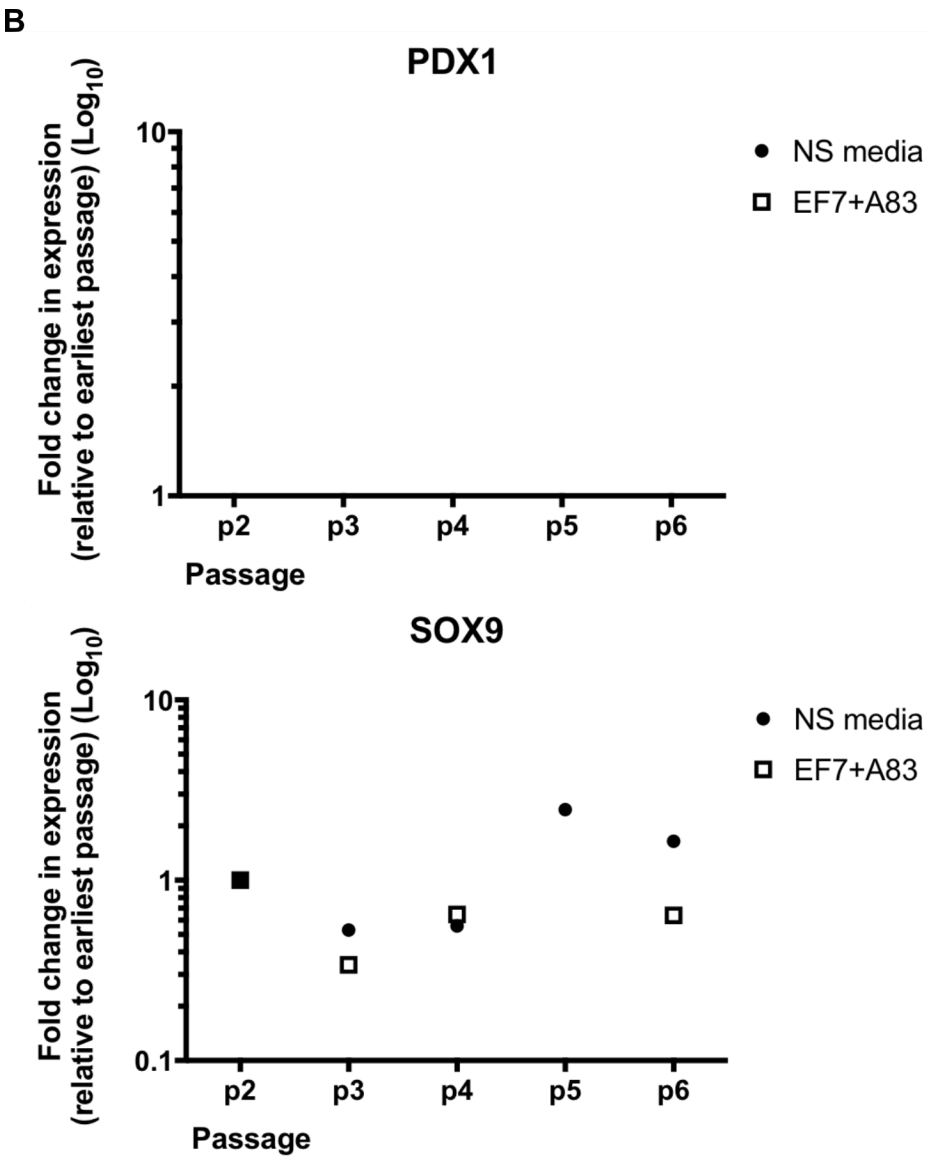

Figure 39. FT3521 human foetal pancreas growth and mRNA expression in culture.

(A) Phase contrast images were taken using the 10X objective (scale bar represents 100μm). Passage numbers and culture media indicated. **(B)** qRT-PCR for pancreas progenitor markers *PDX1* and *SOX9* at different passages. 500ng of RNA was used to make cDNA. Relative expression of all genes normalised to *GAPDH*.

In light of these observations, FT3509 human foetal pancreas cells cultured in EF7+A83 appeared to be the best candidates for further characterisation of the cells. Cultured FT3509 human foetal pancreas cells were fixed and ICC performed for PDX1 and SOX9 **(Figure 40)**. At p13, once epithelial-like colonies were common in the culture, pancreas progenitor markers PDX1 and SOX9 appeared strongly expressed in the cells within colonies. Cells surrounding epithelial-like colonies exhibited comparatively weak or absent PDX1 and SOX9 staining, indicating that surrounding cells are unlikely to be pancreas progenitors. PDX1 was similarly weak in other culture media tested – while it cannot be ruled out that differences in staining intensity between wells may be artefactual, the increase over culture time in *PDX1* mRNA expression described above for EF7+A83 suggests that the difference in intensity is likely to reflect a real difference in protein expression. Given that *PDX1* mRNA could not be detected in EF7 or NS media, the weak protein staining signal in these conditions may actually represent background staining.

In summary, we were able to culture epithelial human foetal pancreas progenitors that express pancreatic master transcription factors PDX1 and SOX9 after multiple passages. Maintenance and expansion of these cells was achieved in defined monolayer conditions, which is novel and valuable for downstream applications of these cell as cellular models of endocrine cell differentiation.

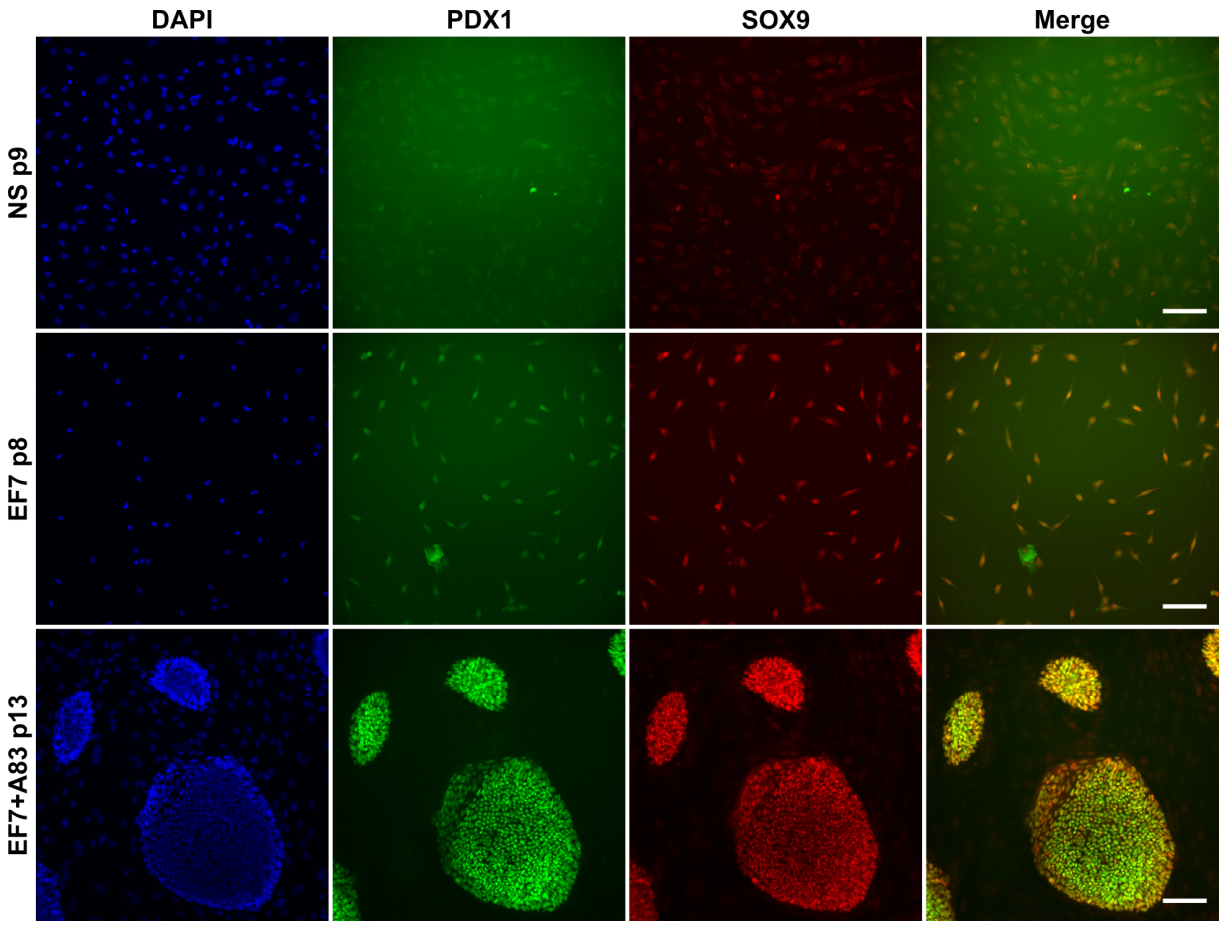

Figure 40. PDX1 and SOX9 expression in FT3509 human foetal pancreas cultures.

ICC of human foetal pancreas cultures in different culture media stained for PDX1 (green) and SOX9 (red). Images taken using the 20X objective (scale bar represents 100μm). Culture media and passage number indicated.

5.2.2 E-cadherin can be used to isolate cultured human foetal pancreas progenitors

PDX1 and SOX9 protein staining in epithelial-like colonies, combined with increased *PDX1* and *SOX9* mRNA expression coinciding with the increase in epithelial-like cells, suggested that the epithelial–like cells were human foetal pancreas progenitors. An epithelial morphology was expected for these cells given their developmental origin and earlier results from mouse foetal pancreas progenitor cultures. To confirm that these cells were epithelial, ICC was performed for E-cad **(Figure 41)**. E-cad staining was clearly visible and localised to the membranes of cells within epithelial colonies at EF7+A83 p15. The surrounding flatter fibroblast-like cells did not express E-cad. In contrast, in NS media p9 E-cad staining could only very weakly be seen in cell nuclei, consistent with background expression. This confirmed that, as for cultured mouse foetal pancreas progenitors, E-cad marked epithelial colonies that co-expressed PDX1 and SOX9 in FT3509 EF7+A83 cultures. Surrounding $PDX1^-/SOX9^-$ cells were also $E\text{-}cad^-$.

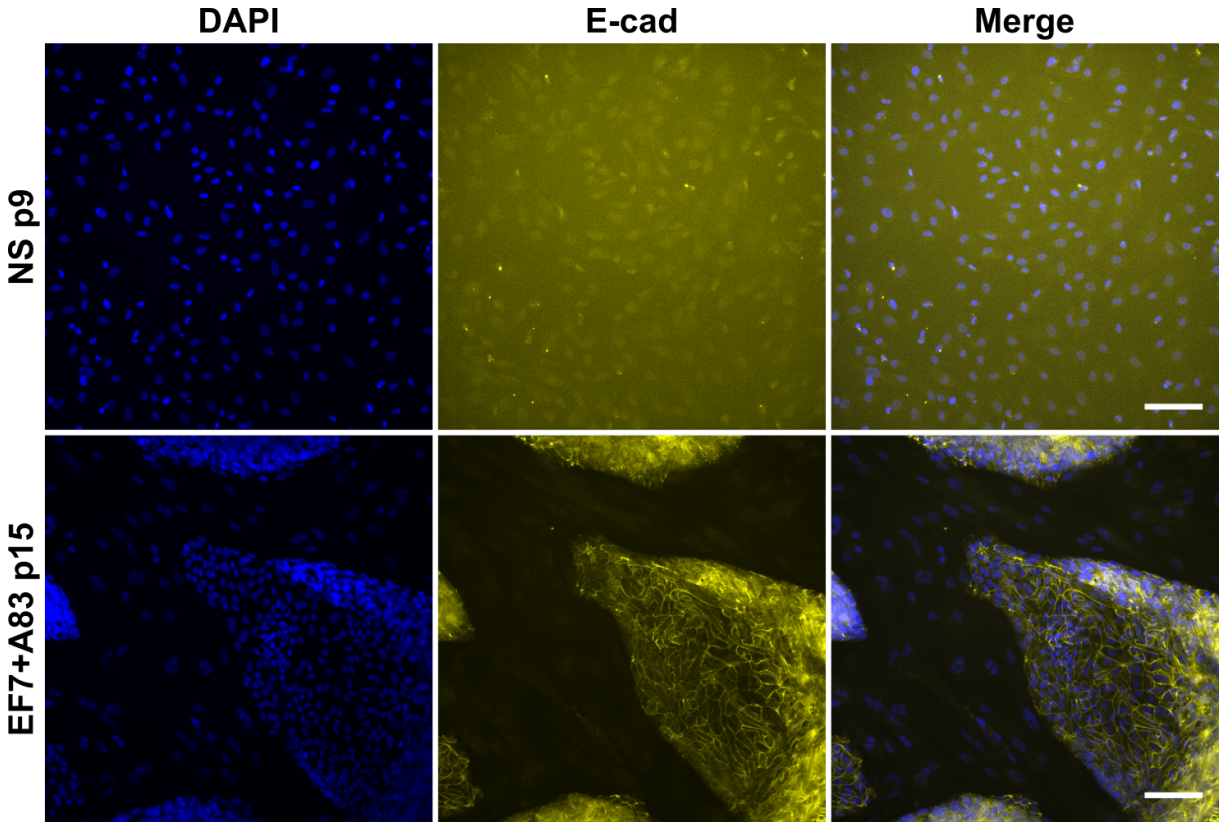

Figure 41. E-cad expression in FT3509 human foetal pancreas cultures.

ICC of human foetal pancreas cultures in different culture media stained for E-cad (yellow). Images taken using the 20X objective (scale bar represents 100μm). Culture media and passage number indicated.

If human foetal pancreas progenitors are to be utilised for experiments in vitro, it would be beneficial to isolate the epithelial progenitor cells in FT3509 cultures from surrounding non-progenitor cells. This would provide a pure population of cells and simplify conclusions regarding signalling pathways and cell regulatory mechanisms behind initiation of the endocrine progenitor cell differentiation programme. To obtain pure populations of human foetal pancreas progenitors, we performed cell sorting cells based on E-cad staining, similar to the mouse strategy.

Unfortunately, E-cad$^+$ cells were consistently absent from cell populations analysed by flow cytometry following several attempts (not shown). Since the antibody used for FACS was the same that produced positive E-cad staining by ICC in FT3509 cultures, the absence of E-cad$^+$ cells by flow cytometry was almost certainly a technical issue caused by E-cad$^+$ colony loss during cell processing.

To overcome this issue, an alternative strategy for isolating epithelial cell colonies was pursued. Routine passaging of cultured FT3509 human foetal pancreas cells was performed using accutase. While accutase is commonly perceived as a gentle cell dissociation reagent, particularly in comparison to trypsin, it still utilises proteolytic and collagenolytic enzymes that mimic trypsin cleavage of peptide bonds involved in cell adhesion. These methods of passaging lead to detachment of all cells in a well, usually to clonal density. To preferentially detach epithelial colonies in FT3509 cultures, EDTA was used tested as a passaging reagent. EDTA can induce enzyme-free cell detachment through its action as a calcium chelator. Cell-cell and cell-matrix adhesion molecules such as integrins and cadherins work in a calcium-dependent manner [334,335], and indirect inhibition of their activity by EDTA alone has been used to passage epithelial cells previously [336]. Treating FT3509 human pancreas cells with 0.5mM EDTA for approximately 8 minutes led to detachment of epithelial colonies from the culture substrate, particularly smaller colonies **(Figure 42A)**. Many non-

epithelial cells appeared to remain attached to the matrix during EDTA treatment. In the same time period, accutase treatment appeared to detach many of the non-epithelial cells that were present pre-passaging, while leaving many epithelial colonies only partially detached. Following plating and 8 days of growth, EDTA-passaged cells appeared to consist exclusively of epithelial colonies **(Figure 42B)**. Accutase-passaged cells appeared the same as for previous passages, with epithelial colonies surrounded by non-epithelial cells. After a further 8 days of growth, EDTA-passaged cells had continued to proliferate into colonies of various sizes in the absence of surrounding cells. This differential sensitivity to EDTA provides a means to separate the distinct populations.

To confirm that isolated FT3509 human foetal pancreas cells continued to express progenitor markers, ICC for PDX1 and SOX9 was performed **(Figure 43A)**. PDX1 and SOX9 staining in EDTA-passaged and accutase-passaged cells was equally robust. even after multiple further rounds of EDTA passaging to p20. Epithelial colonies also continued to express E-cad at the cell-membrane and Ki67, a marker of proliferation, in the nucleus after EDTA passaging **(Figure 43B)**. This shows that isolated epithelial human foetal pancreas progenitor cells do not depend on non-epithelial surrounding cells to maintain progenitor marker expression or proliferation.

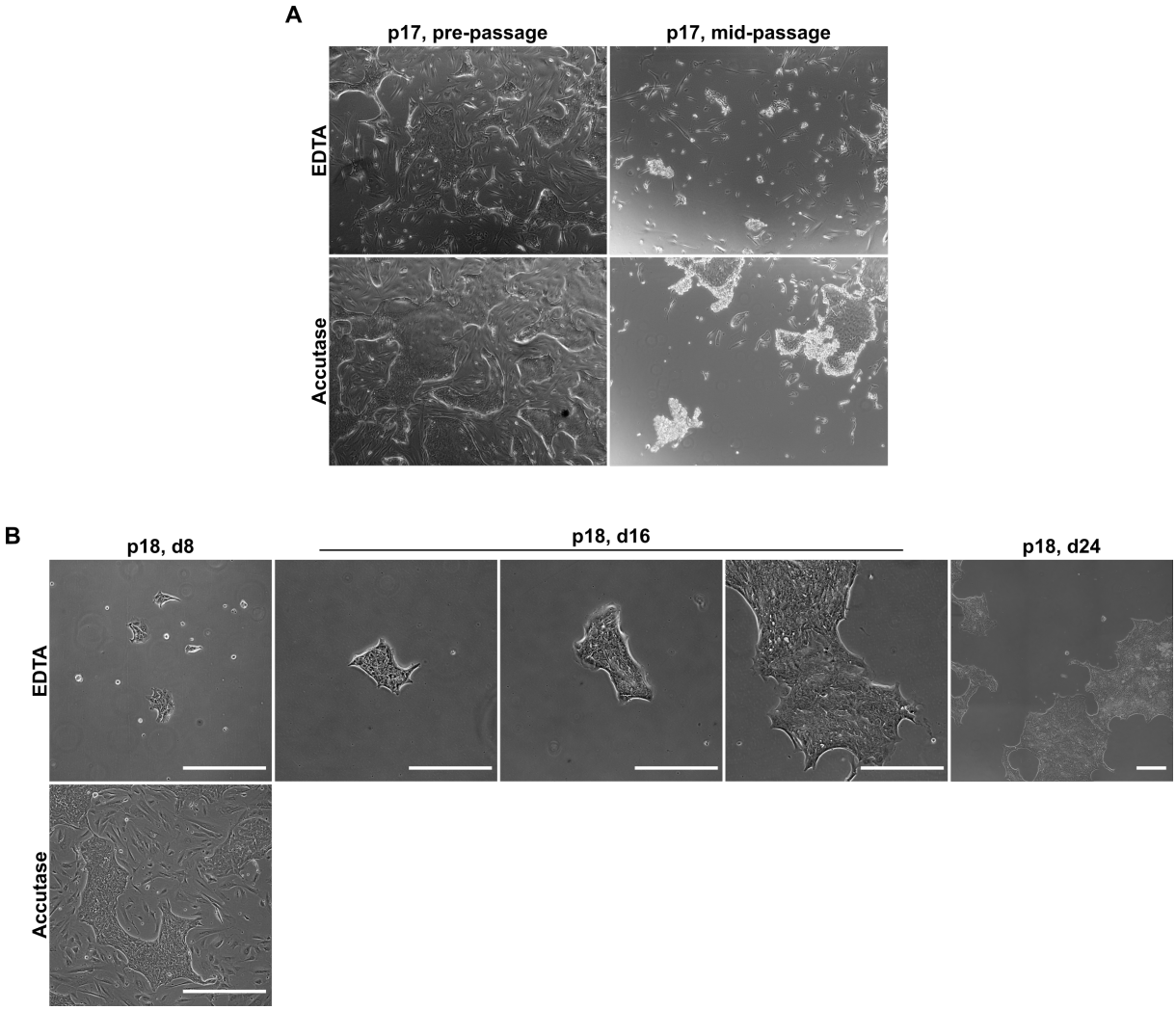

Figure 42. Isolation of E-cad^{+} FT3509 human foetal pancreas cells by EDTA passaging.

(A) FT3509 human foetal pancreas cells before and during passaging. Phase contrast images were taken using the 4X objective. Passage number and passage method indicated. **(B)** FT3509 human foetal pancreas cells after passaging. Phase contrast images were taken using the 10X objective (scale bar represents 500μm). Passage number, day of culture since plating and passage method indicated.

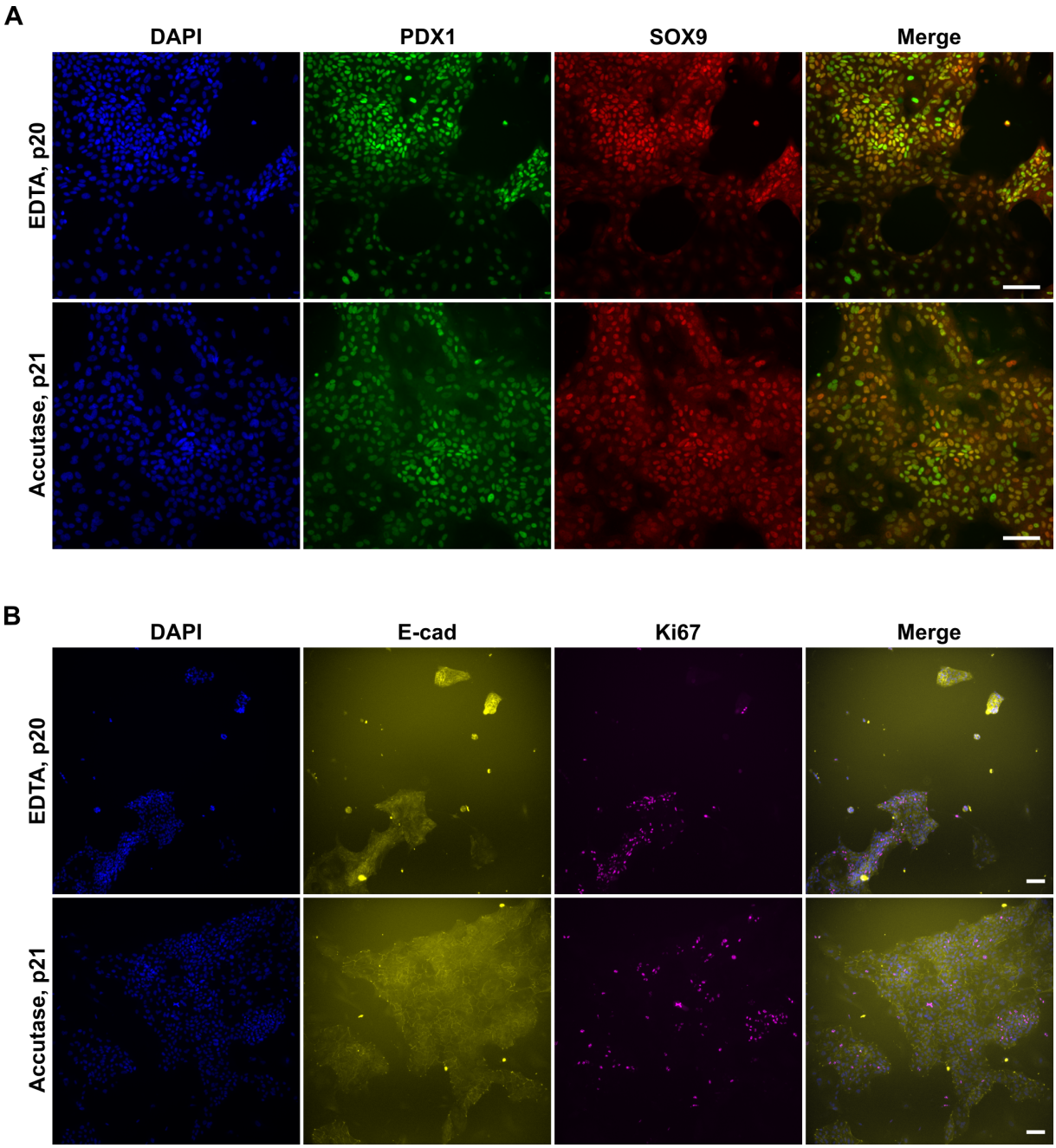

Figure 43. PDX1, SOX9 and E-cad expression in EDTA-passaged FT3509 human foetal pancreas cultures.

(A) ICC of human foetal pancreas cultures in EF7+A83 stained for PDX1 (green) and SOX9 (red). Images taken using the 20X objective (scale bar represents 100μm). Passage method and passage number indicated. **(B)** ICC of human foetal pancreas cultures in EF7+A83 stained for E-cad (yellow) and Ki67 (magenta). Images taken using the 10X objective (scale bar represents 100μm). Passage method and passage number indicated.

5.2.3 Conditioned medium does not enhance proliferation of isolated E-cad^{+} human foetal pancreas progenitors

Although E-cad^{+} progenitor colonies proliferated in culture, slower growth was observed in these cells compared to E-cad^{mixed} progenitor cultures. We wanted to test whether non-epithelial supporting cells in E-cad^{mixed} pancreas progenitor populations were providing secreted factors that enhance E-cad^{+} cell proliferation. EF7+A83 culture medium that had been applied to E-cad^{mixed} FT3509 human foetal pancreas cultures, or to highly proliferative E-cad^{+} mouse foetal pancreas cultures, was collected after 1 day of culture. This conditioned medium was collected and then applied to E-cad^{+} FT3509 human foetal pancreas cultures, with fresh conditioned medium added every 2 days. Cultures were allowed to grow until approximately 50% confluent, then number of proliferative cells ascertained by Ki67 expression.

No significant difference in Ki67 expression was observed when E-cad^{+} human foetal pancreas cells were cultured in conditioned medium from when E-cad^{mixed} human foetal cultures compared to EF7+A83 (p=0.09) **(Figure 44A)**. Similarly, conditioned medium from E-cad^{+} mouse foetal cultures had no significant effect (p=0.16) **(Figure 44B)**. This suggests that secreted factors from non-epithelial foetal pancreas cells play a minimal role in supporting E-cad^{+} cell proliferation when culture medium is already supplied with exogenous EGF and FGF7. However, it cannot be ruled out that non-epithelial cells may produce extracellular matrix factors that aid proliferation. Additionally, it should be noted that the proportion of proliferative cells in EF7+A83 conditions was highly variable between experiments, which indicates that cell handling plays an important part in the growth of cultures. While passaging conditions were kept identical between experiments as much as possible, it is likely that seeding density and the extent of dissociation had a large effect on cell proliferation.

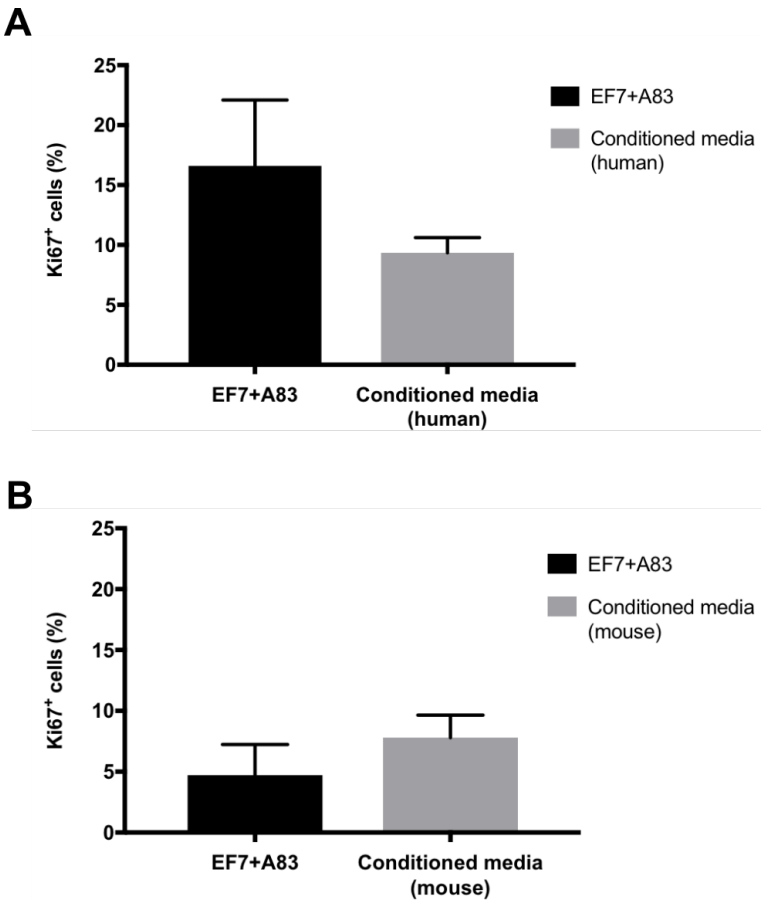

Figure 44. Ki67 expression in E-cad^{+} human foetal pancreas progenitors.

Cell cultures were fixed and immunocytochemistry performed for Ki67. For each replicate well, a 3x3 10X stitched image was taken, from which proportion of Ki67^{+} cells was calculated using CellProfiler. **(A)** FT3509 E-cad^{+} human foetal pancreas progenitors from the same split were cultured in EF7+A83 (n=3) or conditioned medium from FT3509 E-cad^{mixed} human foetal pancreas cultures (n=3). **(B)** FT3509 E-cad^{+} human foetal pancreas progenitors from the same split were cultured in EF7+A83 (n=3) or conditioned medium from E-cad^{+} mouse foetal pancreas cultures (n=3). Error bars show standard deviation. Significance between treatments tested using unpaired, two-tailed t-tests.

5.3 Discussion

In this chapter, we have demonstrated for the first time that human foetal pancreas progenitors can be maintained and expanded long-term in defined culture medium in 2D format. Cultured progenitors sustained expression of PDX1 and SOX9 following long term expansion. These cells were identifiable from other cultured cell types by their epithelial morphology and E-cad expression, reminiscent of the mouse cultures. Epithelial progenitor cells could be purified from heterogeneous cell cultures using simple alternative passaging methods with differential attachment in EDTA to enrich the epithelial progenitors.

An encouraging observation from the work presented in this chapter is that culture conditions used to successfully expand mouse foetal pancreas progenitors were successfully transferred to human cells. Therefore, the signalling requirements and other external factors needed to maintain pancreas progenitor cells between mouse and human are likely to be shared. This has an impact on the design of future experiments that aim to improve methods of endocrine progenitor induction in vitro; conserved regulatory mechanisms between species means that the use of a mouse cellular model is justifiable as a first line of investigation.

Successful derivation of expandable human pancreas progenitors could only be achieved here from a single foetal tissue sample at 8 weeks of development. There is a criticism to be made that the methods described here for culturing human foetal pancreas are therefore not be reproducible. Indeed, further independent verification will be needed but was not possible in the time of this PhD (week 8 embryos were not frequently available). While lack of reproducibility is a valid concern, it could be argued that the success in long-term culture of human foetal pancreas tissue samples may be heavily dependent on gestational age. While we have demonstrated reproducible

derivation of mouse foetal pancreas progenitors could be achieved from E12.5 tissue, to find a developmentally equivalent source of cells in human would require access to foetal tissue of approximately 37 days (5 weeks) gestation [337]. Such access was not possible here. Furthermore, it was only possible to test two week 8 samples in culture experiments, with culture time limited for the second sample due to time constraints.

We speculate that several reasons behind potential age-dependent success of human foetal pancreas progenitor culture. Firstly, technical differences may play a part – foetal pancreases from later stages of development were larger and much more fibrous, presumably due to the presence of more connective tissue. As such, greater mechanical force was required to dissociate these samples, which may have negatively impacted the culture outcome. Also, the failure in culture of later stage samples could be linked to the proportion of $PDX1^{+}/SOX9^{+}$ cells in the pancreas during human development being reduced as gestation proceeds, as described in Chapter 3. A low proportion of double positive progenitors in cultured cell populations may have negatively impacted the ability of these cells to maintain their progenitor identity. Notch paracrine signalling between pancreas progenitors is known to be important for maintaining cell identity during mouse development [147,148], and Notch signal transduction is thought to be dependent on continued Sox9 expression [136]. Our data suggest an increasing proportion of $PDX1^{+}/SOX9^{-}$ cells concurrent with human pancreas development progression, consistent with a model where a high proportion of double-positive, Notch-responsive pancreas progenitors are required for human foetal cell culture to succeed long-term.

Expandable human foetal pancreas progenitors cells were localised to E-cad-expressing colonies in culture, while surrounding non-epithelial cells had low or absent PDX1/SOX9 protein expression. A recent study that characterised gene

expression in sorted human foetal pancreas cell populations also showed that pancreatic mesenchymal cells can be separated from progenitor cells based on the expression of epithelial markers, and that the transcriptomes of these populations are significantly different [338]. The same study also determined that endocrine progenitor cells arise as progeny of cells within the epithelial fraction; *NGN3* mRNA expression was first detected during week 8, and only after *NGN3* expression arose did E-cad levels decrease in the endocrine progenitor population. This study provides evidence that the expandable epithelial pancreas progenitor isolated here is the correct cell type for modelling endocrine commitment in vitro. It also suggests further reasons why utilising human foetal tissue for culture after developmental week 8 may have been unsuccessful, and that foetal tissue from earlier stages should be tried in culture in the future.

Future experiments with the purified human foetal pancreas progenitors described here still need to address the question of whether these cells retain the capacity to differentiate in vitro in monolayer. Various simple protocols were attempted (e.g. serum treatment and growth factor withdrawal, not shown). However, time constraints meant we were not able to probe this deeply. This will be important in future studies and might be best addressed through in vivo transplantation.

If human foetal pancreas progenitors can generate endocrine progenitors in vitro, they will provide the ideal human cellular model system for screening conditions to improve in vitro differentiation to pancreatic endocrine progenitors.

CHAPTER 6

Generating a hESC line to identify conditions for promoting hES-derived endocrine progenitor emergence and expansion in vitro

6.1 Introduction

While foetal pancreas tissue provides a hugely valuable model and reference point for characterising true pancreas progenitor cells, future cell therapies for diabetes will almost certainly benefit from using hESCs as a cell source. hESCs boast the advantages of fewer ethical concerns regarding their use and limitless supply compared to foetal tissue, and many well characterised clinical-grade hESC lines are now available [339]. Our studies of hESCs were performed in parallel to the foetal work.

In addition, considerable effort has already been invested into devising protocols for directed differentiation of hESCs to insulin-secreting β-cells. While we give a detailed description of this research area in Chapter 1.3.3, it is pertinent to this section to highlight that none of the published methods so far have focussed specifically on generating the pancreatic endocrine progenitor cell marked by NGN3 expression. Early research in the hESC-to-pancreas differentiation field focussed on producing stem and progenitor cells from incremental stages of the differentiation process, from definitive endoderm [340], to foregut [341,342], to early pancreas progenitor [258,343]. Soon after was the important demonstration that β-cell generation was possible in vitro [251,252]. However, these methods were inefficient and highly variable. By skipping the step where we focus on the generation of endocrine pancreas progenitors, which represent the next logical incremental step along the differentiation process, it is likely that we have missed important factors for efficiently specifying endocrine cells in vitro.

Since originally demonstrating in vitro production of $PDX1^{+}/SOX9^{+}$ early pancreas progenitor cells from ES cells, protocols that refined and improved the process have been published [259]. Having methods for efficiently generating early pancreas progenitors is the first vital component of a strategy for investigating how to correctly specify endocrine progenitor cells. A highly beneficial second component would be a system to allow for easy, reliable identification of endocrine progenitor emergence in vitro, coupled with a means of evaluating whether these progenitors are able to be expanded in culture, similarly to previous progenitor cell stages of pancreas differentiation. In this chapter, we developed a novel NGN3-GFP/CyclinB1DestructionBox-Cherry reporter hESC that addresses both of these challenges. While the hESC line that we have developed will not directly be used for clinical applications due to its exposure to a research environment and genetic alterations, these cells were originally derived from a clinical-grade line and thus serve as a useful proof of concept for what could be achieved in a clinical laboratory. Our cell line therefore has the potential to be an important tool in future efforts to capture hESC-derived endocrine pancreas progenitors in culture.

6.2 Results

6.2.1 Differentiation capacity of MasterShef7 hESCs

Given that hES-derived pancreas cells are eventually intended for use in cell therapy applications, it will be important to show that clinical-grade hESCs are capable of producing pancreatic lineages in vitro. Previous studies interested in demonstrating hES to pancreas differentiation utilised popular research-grade hESC lines such as HUES8 [251], H1 [252] and H9 [259]. Furthermore, before investing time and resources on inducing targeted genetic modifications in these cells, it was vital to know if they held the potential to produce our cell types of interest.

We tested the clinical-grade MasterShef7 (MS7) hESC line for its capacity to differentiate to pancreatic lineages. MS7 hESCs have been subject to molecular karyotyping and while two significant copy number variations were detected in its genome, they were accounted for as either being naturally occurring in the general population or not associated with acquired cell culture adaptations [339].

MS7 hESCs were grown on recombinant human laminin isoform 521 (LN521), a defined cell culture substrate with versions suitable for clinical applications commercially available. The media used for differentiation towards pancreatic progenitors was similar to that used by Rostovskaya et al. (2015) [259]. Differentiating MS7 cells were analysed at key stages of the process to determine their suitability for pancreas cell generation **(Figure 45)**.

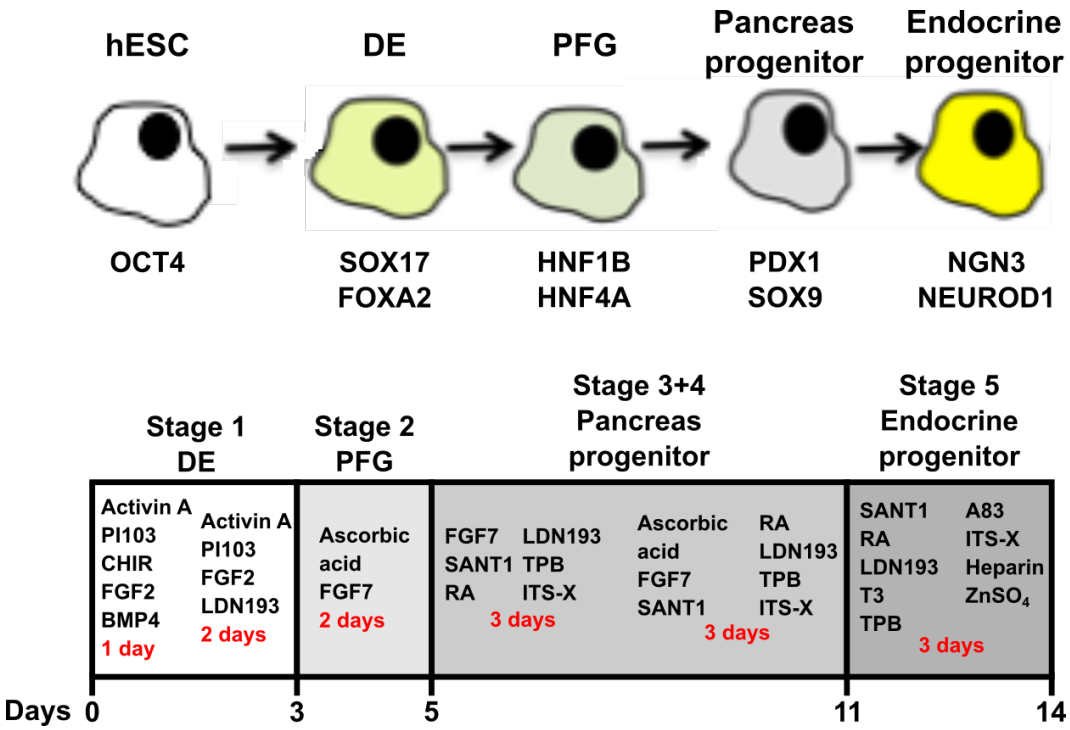

Figure 45. Protocol for MS7 hESC differentiation to pancreas progenitor cells.

MS7 hESCs were differentiated using a protocol adapted from Rostovskaya et al. (2015) [259] , which utilised growth factors, small molecules, and other culture additives. Key developmental stages were analysed during the differentiation process.

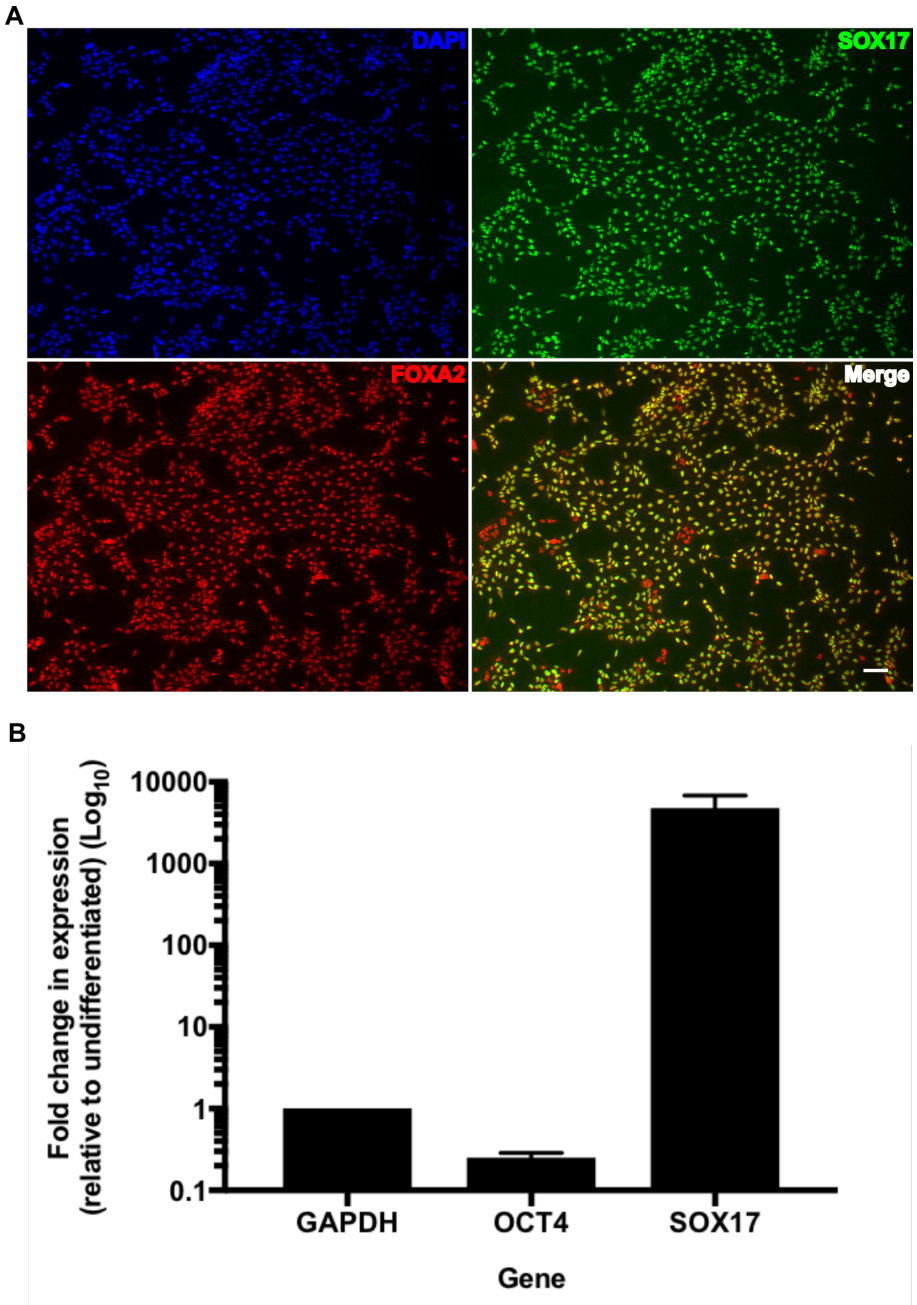

Figure 46. MS7 differentiated to DE.

(A) ICC of differentiated cells showing staining for SOX17 (green) and FOXA2 (red). Images taken using 5X objective (scale bar represents 100μm). **(B)** mRNA expression of *OCT4* and *SOX17* in differentiated cells. 1μg RNA was used to make cDNA. Expression of all genes normalised to *GAPDH* (shown in Figure at 1-fold) and relative to undifferentiated MS7 hESCs. n=3. Error bars show standard deviation.

MS7 cells differentiated to definitive endoderm (DE) exhibited robust induction of DE markers SOX17 and FOXA2 **(Figure 46A)**. All cells appeared FOXA2^{+}, with the majority also SOX17^{+}. Efficient differentiation to DE was confirmed at the transcript level, with a roughly 4-fold average reduction in *OCT4* mRNA levels and an average 4761-fold increase in *SOX17* at day 3 of differentiation **(Figure 46B)**.

MS7 differentiation to the foregut lineage was equally robust. HNF1B, a foregut marker known to be critical to both liver and pancreas development where patients with HNF1B mutations can suffer severe hepatic and pancreatic phenotypes [344,345], was uniformly detectable by immunocytochemistry (ICC) **(Figure 47A)**. *HNF1B* was upregulated by an average 119-fold, and *HNF4A*, a second foregut marker, was increased by an average 1855-fold by differentiation day 5. *OCT4* was further reduced by this stage to around 10-fold below its level in undifferentiated cells **(Figure 47B)**.

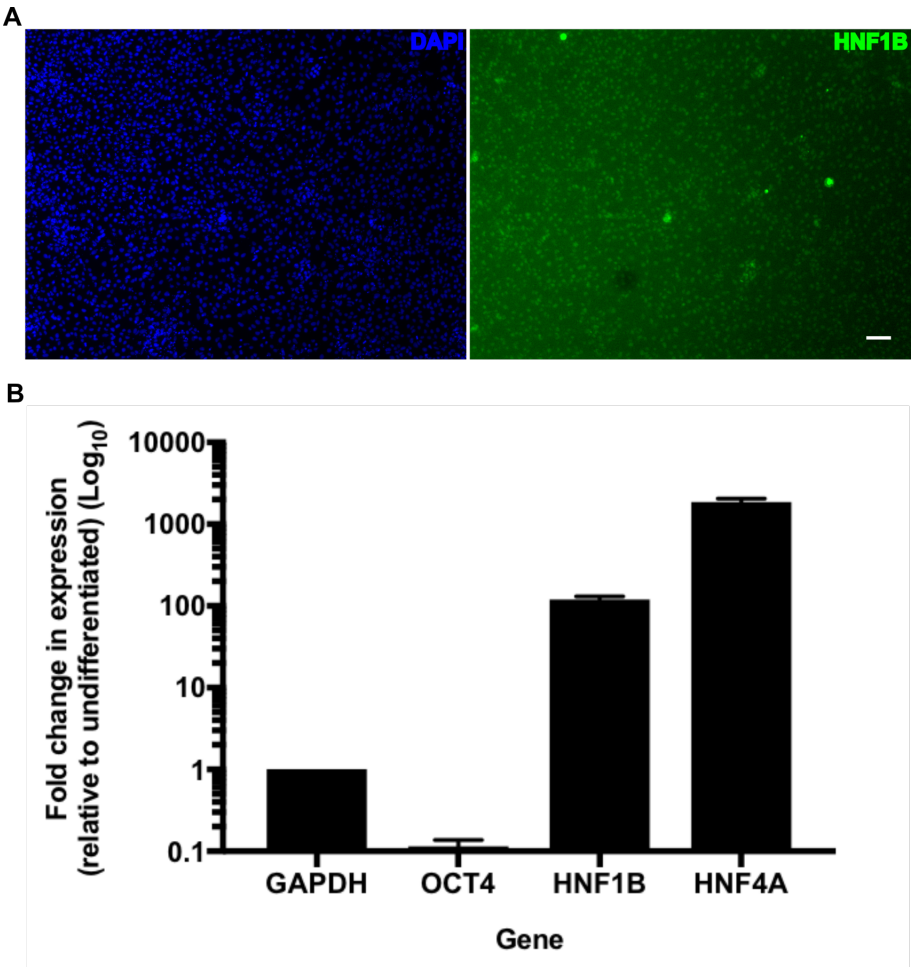

Figure 47. MS7 differentiated to foregut.

(A) ICC of differentiated cells showing staining for HNF1B (green). Images taken using 5X objective (scale bar represents 100μm). **(B)** mRNA expression of *OCT4, HNF1B* and *HNF4A* in differentiated cells. 1μg RNA was used to make cDNA. Expression of all genes normalised to *GAPDH* (shown in Figure at 1-fold) and relative to undifferentiated MS7 hESCs. n=3. Error bars show standard deviation.

By the end of the early pancreas progenitor stage of differentiation, MS7 cells were very confluent and a high proportion expressed both PDX1 and SOX9, with a high degree of overlap in their expression **(Figure 48A)**. Both transcription factors saw increased expression at the mRNA level too, with 1152-fold and 59-fold increases in *PDX1* and *SOX9*, respectively, by day 11 of differentiation **(Figure 48B)**.

MS7 hESCs cultures also expressed markers of endocrine pancreas progenitors, *NGN3* and *NEUROD1*, following the final stage of differentiation at day 14. *NGN3* expression was increased 37-fold over undifferentiated cells, while *NEUROD1* increased by 918-fold **(Figure 49)**. Reliable antibodies could not be found for these markers, and it was therefore not possible to determine protein expression at the cellular level.

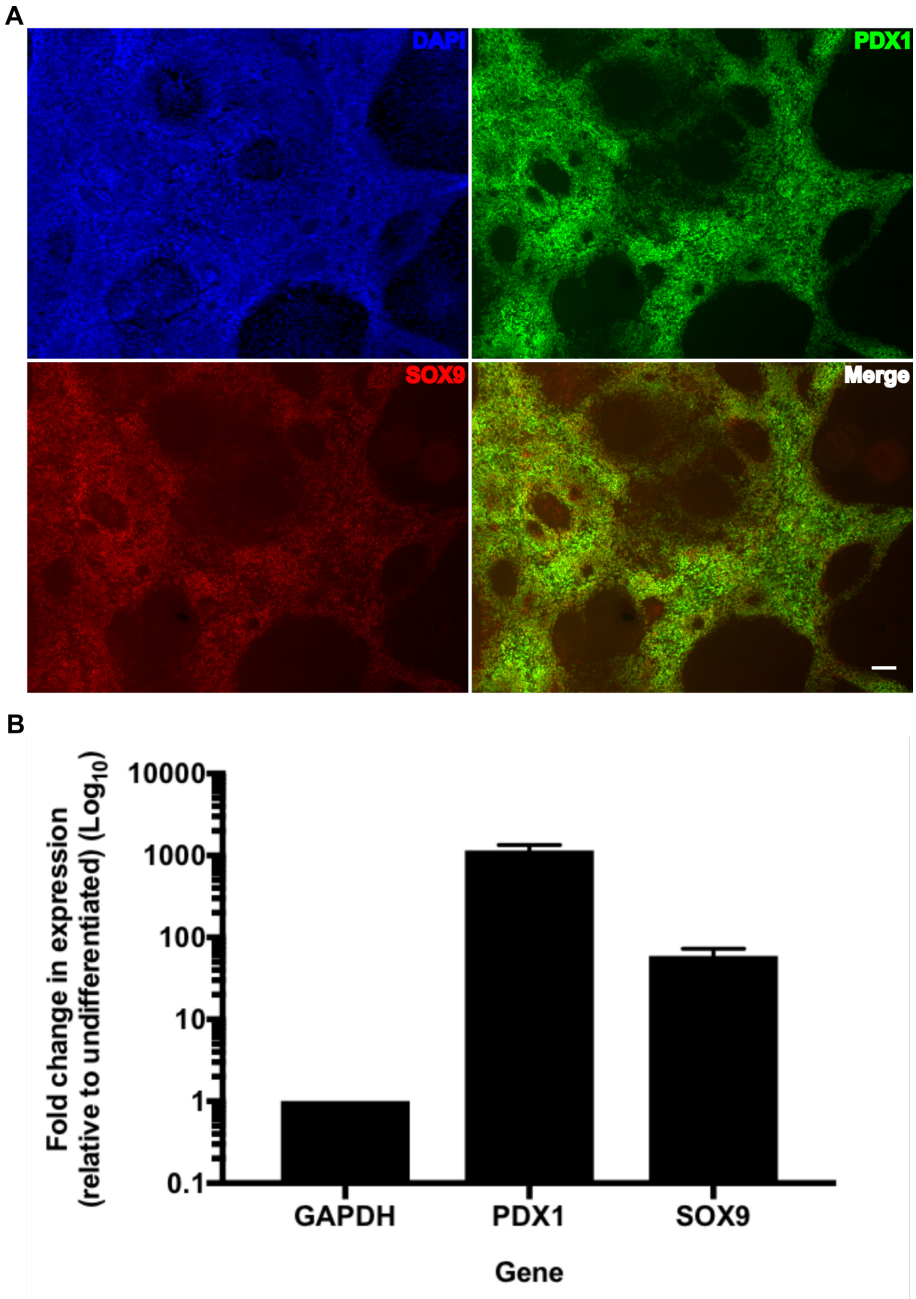

Figure 48. MS7 differentiated to early pancreatic progenitors.

(A) ICC of differentiated cells showing staining for PDX1 (green) and SOX9 (red). Images taken using 5X objective (scale bar represents 100μm). **(B)** mRNA expression of *PDX1* and *SOX9* in differentiated cells. 1μg RNA was used to make cDNA. Expression of all genes normalised to *GAPDH* (shown in Figure at 1-fold) and relative to undifferentiated MS7 hESCs. n=3. Error bars show standard deviation.

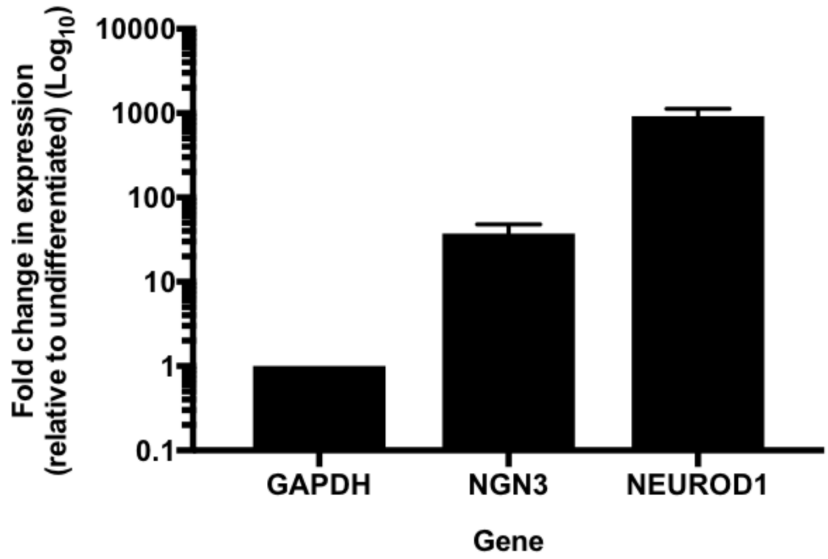

Figure 49. MS7 differentiated to endocrine pancreas progenitors.

mRNA expression of *NGN3* and *NEUROD1* in differentiated cells. 1μg RNA was used to make cDNA. Expression of all genes normalised to *GAPDH* (shown in Figure at 1-fold) and relative to undifferentiated MS7 hESCs. n=3. Error bars show standard deviation.

6.2.2 Generating an NGN3-GFP reporter hESC

Having shown that MS7 hESCs are capable of producing endocrine pancreas progenitors, we deemed that they were well suited to engineering a knock in reporter system for tracking endocrine pancreas progenitor specification in live cells.

We obtained previously described tools for creating an NGN3-GFP knock-in reporter cell line [346], in which the authors had used the reporter system to isolate hES-derived endocrine progenitors for characterisation and functional analysis. We wanted to utilise these tools for creating NGN3-GFP reporter cell line in the clinically applicable, well characterised MS7 hESC line [339]. The tools comprised plasmids encoding paired zinc-finger nucleases (ZFNs) and an NGN3-targeting vector plasmid. ZFNs were designed to induce a double strand break (DSB) adjacent to the stop codon of NGN3 **(Figure 50A)**. The NGN3-targeting vector would then act as a repair template for homology-directed repair (HDR) **(Figure 50B)**; the targeting vector plasmid contained homology arms to the genomic NGN3 locus of roughly 800bp each. Homology arms flanked the desired insert, including a 2A peptide sequence followed by eGFP, so that eGFP would be cleaved from NGN3 during translation. Avoiding an NGN3-eGFP fusion protein prevents any negative effects on NGN3 function, while also overcoming potential experimental design problems caused by the very short half-life of NGN3 protein [347]. The insert also contained elements designed to be used for selection of targeted cells.

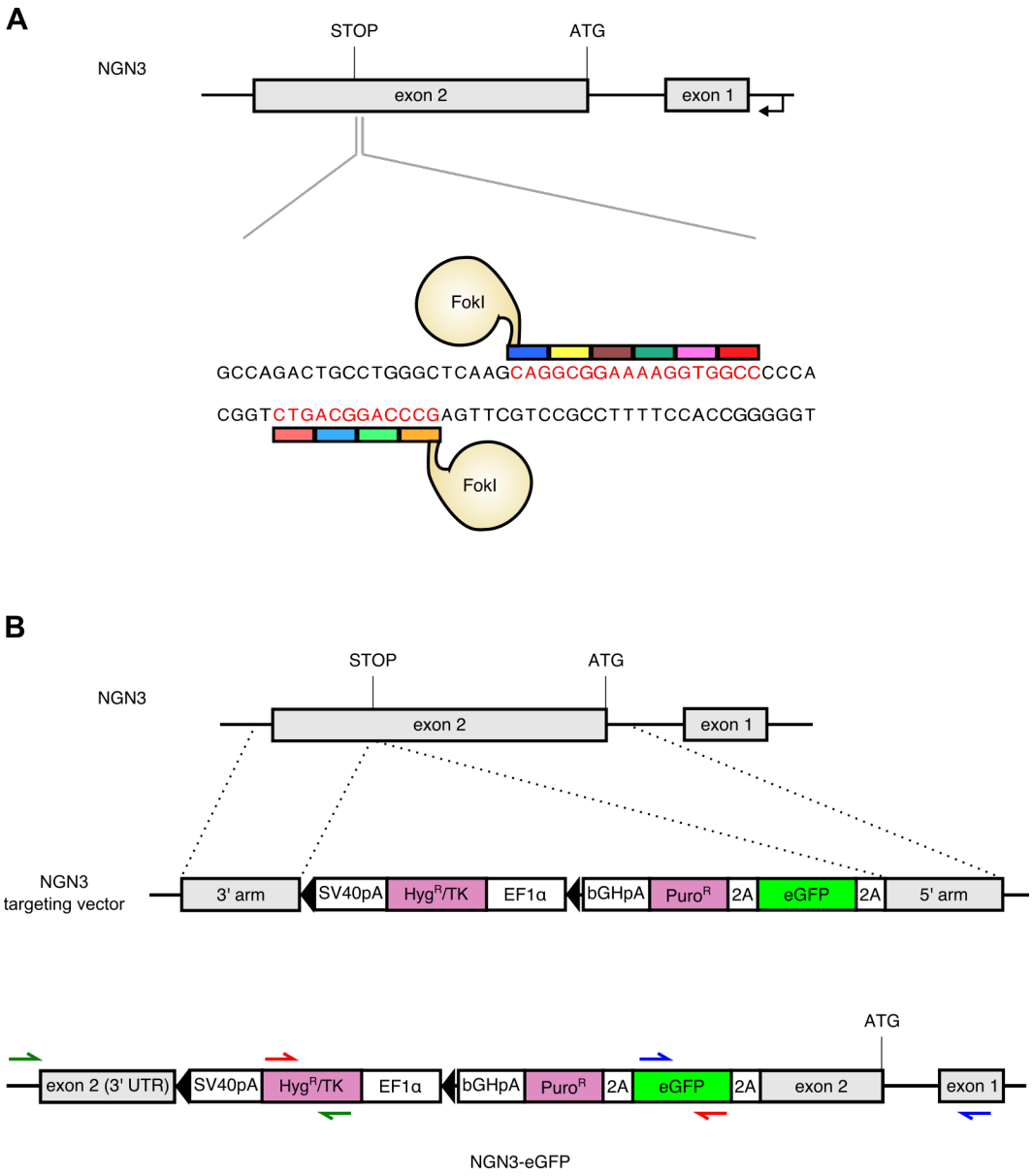

Figure 50. Targeting strategy for creating NGN3-GFP knock-in.

(A) Paired ZFNs induce a DSB at the NGN3 stop codon through FokI nuclease domains. Nucleotides in red indicate ZFN recognition sites, with coloured blocks representing each module recognising 3bp subsites. **(B)** DSB repair using a targeting vector template. Repair leads to deletion of the endogenous stop codon and inserts 2A-eGFP followed by regulatory and selection elements. Black triangles indicate LoxP sites. Red arrows indicate internal genotyping PCR primers, blue arrows indicate junction 1 genotyping PCR primers, green arrows indicate junction 2 genotyping PCR primers.

MS7 hESCs were dissociated to single cells, nucleofected with plasmids encoding ZFNs and the NGN3-targeting vector, and re-plated in normal medium including Y-27632 (ROCKi) to limit cell death **(Figure 51A)**. After a brief recovery period, ROCKi was removed from the medium and cells were allowed to grow. Selection for targeted cells was then performed by adding Hygromycin B to the medium **(Figure 51B)**. Once surviving cells had formed colonies of reasonable size, 96 colonies were picked by visualising through an EVOS Cell Imaging System and manually removing colonies from the dish to be transferred to separate wells of a 96-well plate for clonal culture, again in the presence of ROCKi until recovery **(Figure 51C)**. 30 surviving clones were grown and passaged into wells of increasing size, until enough cells were available to obtain genomic DNA (gDNA) from clonal lines to confirm correct targeting.

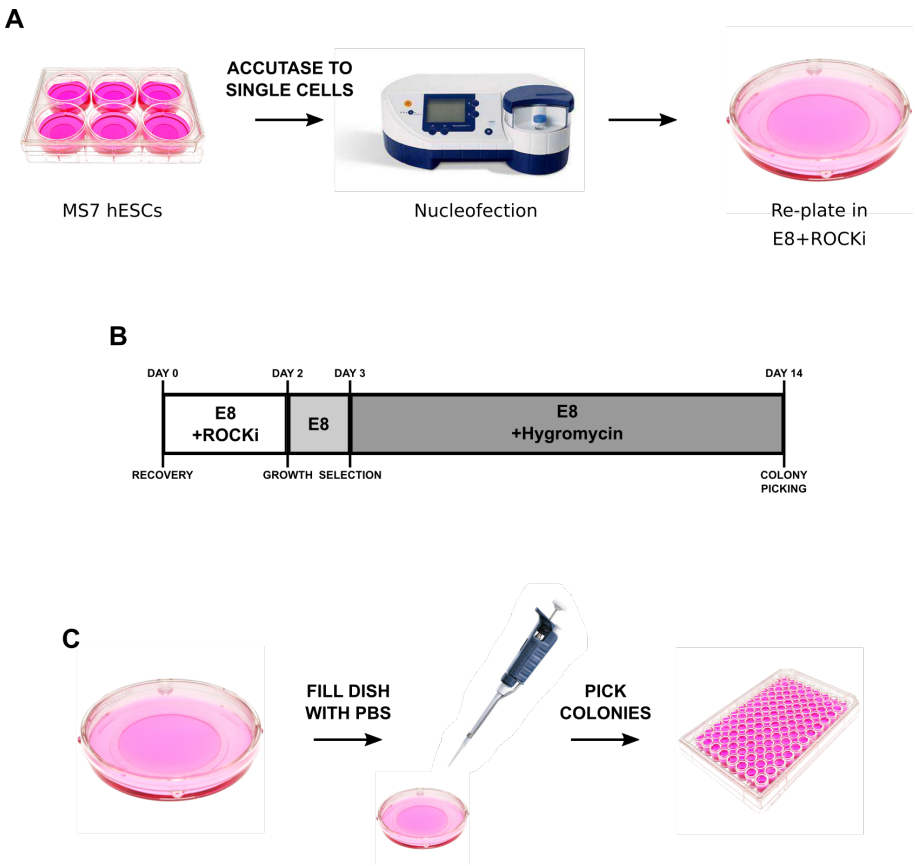

Figure 51. MS7 nucleofection and clonal culture strategy.

(A) One well of a confluent 6-well plate was dissociated to single cells, nucleofected with ZFNs and targeting vector plasmids, and re-plated in a 10cm dish. **(B)** Culture conditions for nucleofected cells in 10cm dish. **(C)** Surviving colonies were picked in PBS and transferred to separate wells of a 96-well plate.

Confirmation of successful GFP knock-in was carried out by PCR genotyping of clone gDNA using three sets of primer pairs **(Figure 52A)** designed to assess the presence or absence of the insert, as well as its insertion at the desired locus by using primers that spanned the junction between inserted and genomic DNA on both sides of the insert. 23 of 30 genotyped clones were positive for the insert **(Figure 52B)**. 20 of 30 clones produced PCR products for one end of the insert-genomic junction assay **(Figure 52C)**, while 29 of 30 clones were positive at the other junction **(Figure 52D)**. 19 of 30 clonal lines gave a positive result in all 3 genotyping assays, indicating a 63.3% targeting efficiency. Clone 1 was selected for the next step due to correct targeting and displaying good hESC morphology.

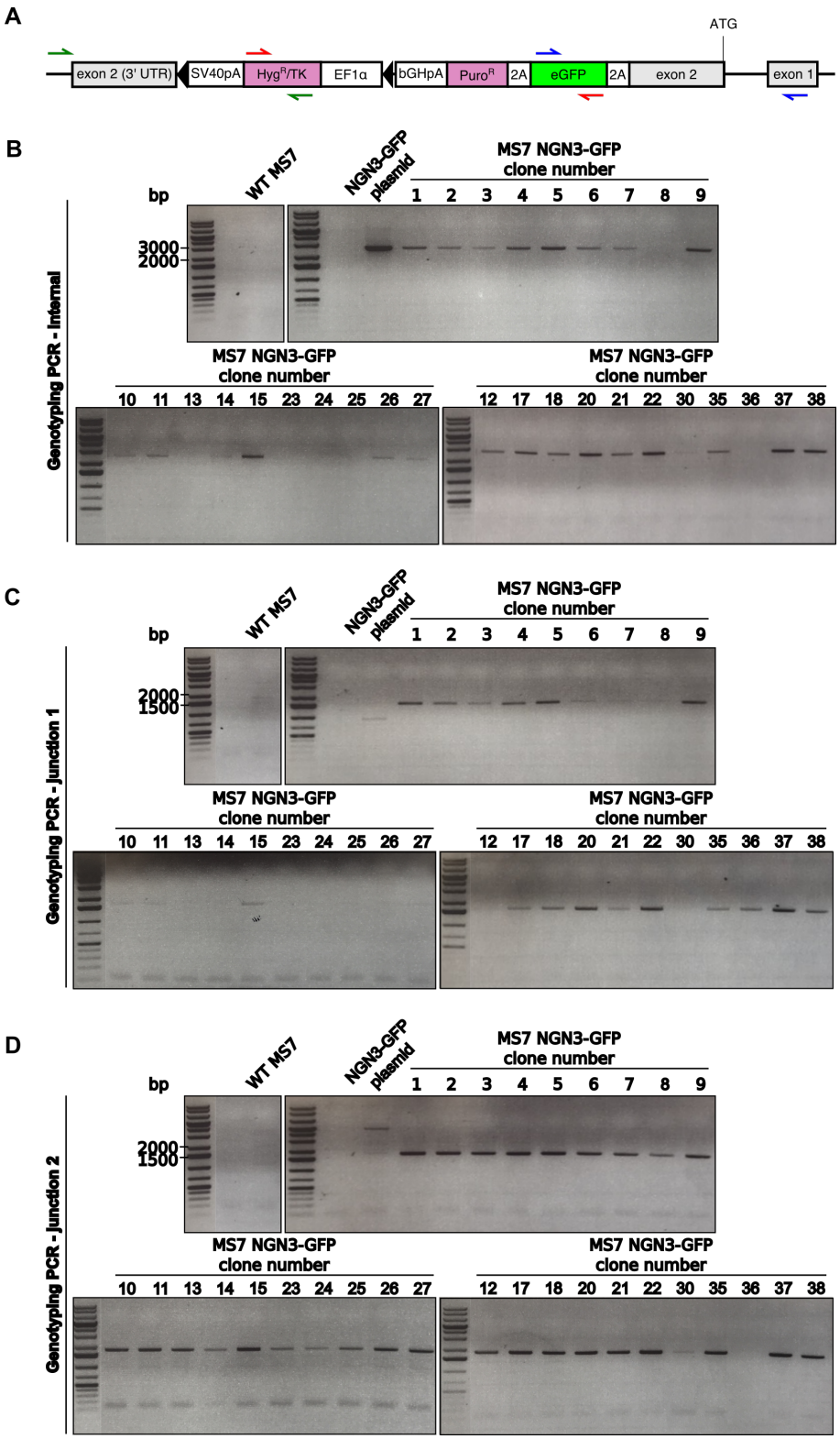

Figure 52. PCR genotyping of nucleofected MS7 clones.

(A) Schematic of NGN3-targeted locus with genotyping primer sites. Red arrows indicate internal genotyping PCR primers, blue arrows indicate junction 1 genotyping PCR primers, green arrows indicate junction 2 genotyping PCR primers. **(B)** Internal PCR primers, expected product=2477bp. **(C)** Junction 1 PCR primers, expected product=1550bp. **(D)** Junction 2 PCR primers, expected product=1713bp. WT MS7 and targeting vector (NGN3-GFP plasmid) used as controls.

To minimise disruption to any 3' regulatory regions at the NGN3 locus potentially caused by inserting large pieces of DNA, we wanted to remove the extraneous selection cassette from the targeted locus. The LoxP-flanked EF1α-Hygro^R/TK-SV40pA cassette was excised by nucleofecting NGN3-GFP clone 1 with a plasmid designed to transiently express Cre recombinase **(Figure 53A)**. The nucleofection and subsequent culture strategy depicted in Figure 50 was repeated again, with Ganciclovir replacing Hygromycin B at the selection stage, where the absence of thymidine kinase (TK) in clones with successful cassette excision prevents the conversion of Ganciclovir into a toxic product. 33 clones were picked and, of these, 9 were genotyped for successful excision in anticipation of a high efficiency. Genotyping was carried out on gDNA by PCR using primers designed to produce a product only in clones still containing the selection cassette **(Figure 53B)**. A PCR strategy involving primers flanking the selection cassette to produce bands of different sizes in excised compared to non-excised clones was also attempted, but this PCR could not be sufficiently optimised for the results to be conclusive (data not shown). Genotyping PCR indicated that selection cassette excision was successful in 3 of 9 clones (33.3% efficiency) **(Figure 53C)**. NGN3-GFP Cre clone 9 was chosen to pursue further experiments.

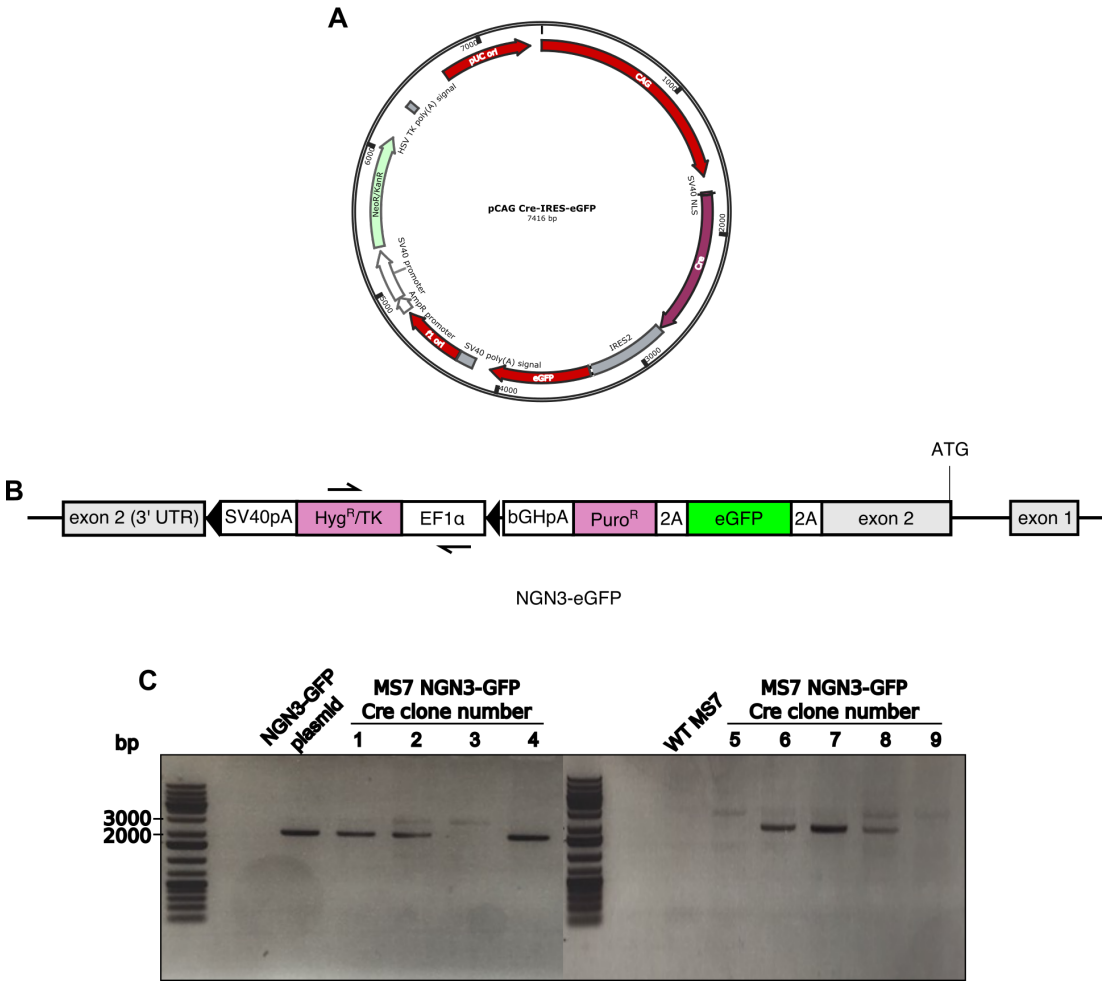

Figure 53. Cre-mediated excision of selection cassette in MS7 NGN-GFP.

(A) Plasmid encoding Cre recombinase. **(B)** Diagram showing NGN3-GFP locus, with black arrows indicating Cre excision genotyping PCR primers. **(C)** PCR genotyping, expected product=2089bp, or no product if successful. WT MS7 and targeting vector (NGN3-GFP plasmid) used as controls.

6.2.3 Generating an NGN3-GFP/CDB-Cherry reporter hESC

Next, we wanted to create a reporter system for proliferation in our NGN3-GFP MS7 hESC line, allowing determination of whether endocrine pancreas progenitor cells are proliferative in test conditions in vitro. A proliferative endocrine pancreas progenitor would permit expansion at this stage of differentiation, which would be beneficial for scaling up relevant cells for cell therapy.

A lentiviral vector encoding a domain of the mouse CyclinB1 (CycB1) protein called the destruction box (D-box) fused to Cherry by a linker peptide was generously given to us by collaborators, based on a similar construct published by their group [348]. Prior to mitosis CycB1 is almost exclusively localised to the cytoplasm, but at late prophase enters the nucleus, where it plays a role in regulating events governing cell division [349]. At the end of mitosis it is rapidly degraded [350]. The CyclinB1 destruction box (CDB) can be tagged onto fluorescent proteins such as Cherry to regulate their localisation and destruction in the same manner as CyclinB1. Thus CDB-Cherry may be used to assess whether cells are in cycle (proliferating). Combined with NGN3-GFP this will give a readout of whether NGN3 positive cells are proliferating **(Figure 54)**.

Mouse CycB1 bears 82% sequence identity to human CYCB1 protein, and the pathway controlling ubiquitination of the CDB domain in these proteins is also highly conserved [351], indicating that mouse CDB protein function would be conserved in human cells.

To utilise techniques optimised for earlier genetic modifications of the MS7 NGN3-GFP hESC line, we wanted to clone CDB-Cherry from the lentiviral plasmid into a vector suitable for delivery into cells by nucleofection, with a method for selection of successfully modified cells. To do this, we decided to pursue Gateway cloning; PCR primers were designed to amplify CDB-Cherry from the lentiviral plasmid and flank

the sequence with attB sequences required for recombination during Gateway cloning **(Figure 55)**.

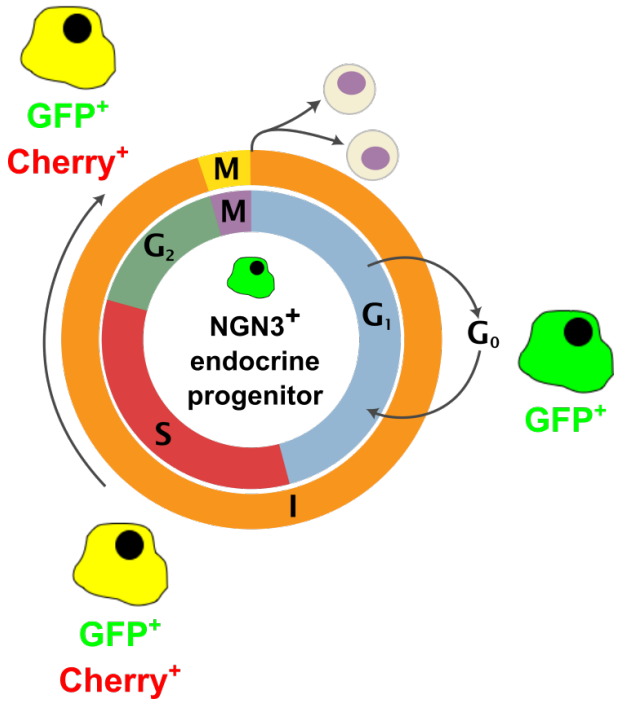

Figure 54. Schematic for fluorescent readouts of proliferating NGN3-GFP/CDB-Cherry endocrine progenitors.

Quiescent or non-proliferative endocrine progenitor cells differentiated from NGN3-GFP/CDB-Cherry MS7 hESCs would fluoresce green, while proliferating endocrine progenitors would appear yellow-orange due to simultaneous green and red fluorescence.

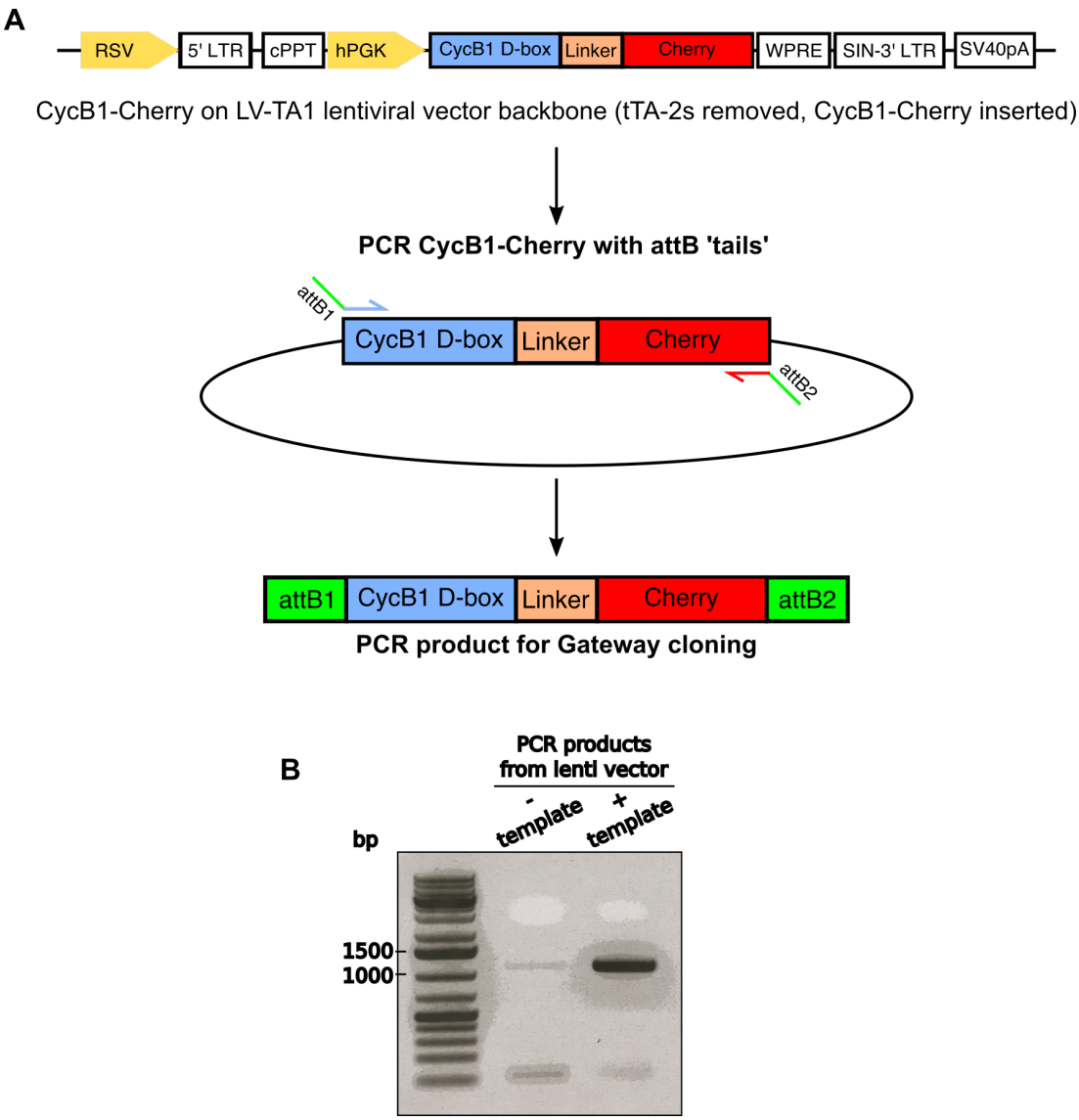

Figure 55. Generation of aatB1-CDB-Cherry-aatB2 PCR product.

(A) Diagram of original lentiviral vector and strategy for amplifying CDB-Cherry with attB adapters. **(B)** PCR products from amplifying CDB-Cherry flanked by attB sites from lentiviral vector, expected product=1114bp.

The purified PCR product was recombined with pDONR™221 using BP clonase, and the products were used to transform bacteria. Once large quantities of resultant plasmid DNA were isolated, diagnostic digests were performed to confirm its identity as pDONR-CDB-Cherry **(Figure 56A)**. CDB-Cherry was then cloned into a pDEST vector in a recombination reaction between pDONR-CDB-Cherry and pDEST using LR clonase. Plasmid quantity scale up was repeated and new diagnostic digests were performed to confirm the identity of pDEST-CDB-Cherry **(Figure 56B)**. pDEST-CDB-Cherry was linearised **(Figure 56C)** and nucleofected into MS7 NGN3-GFP hESCs and cells plated using the same methods as described previously. Cells harbouring a random integration of the CDB-Cherry construct were selected for using Blasticidin and 96 colonies were picked using established methods.

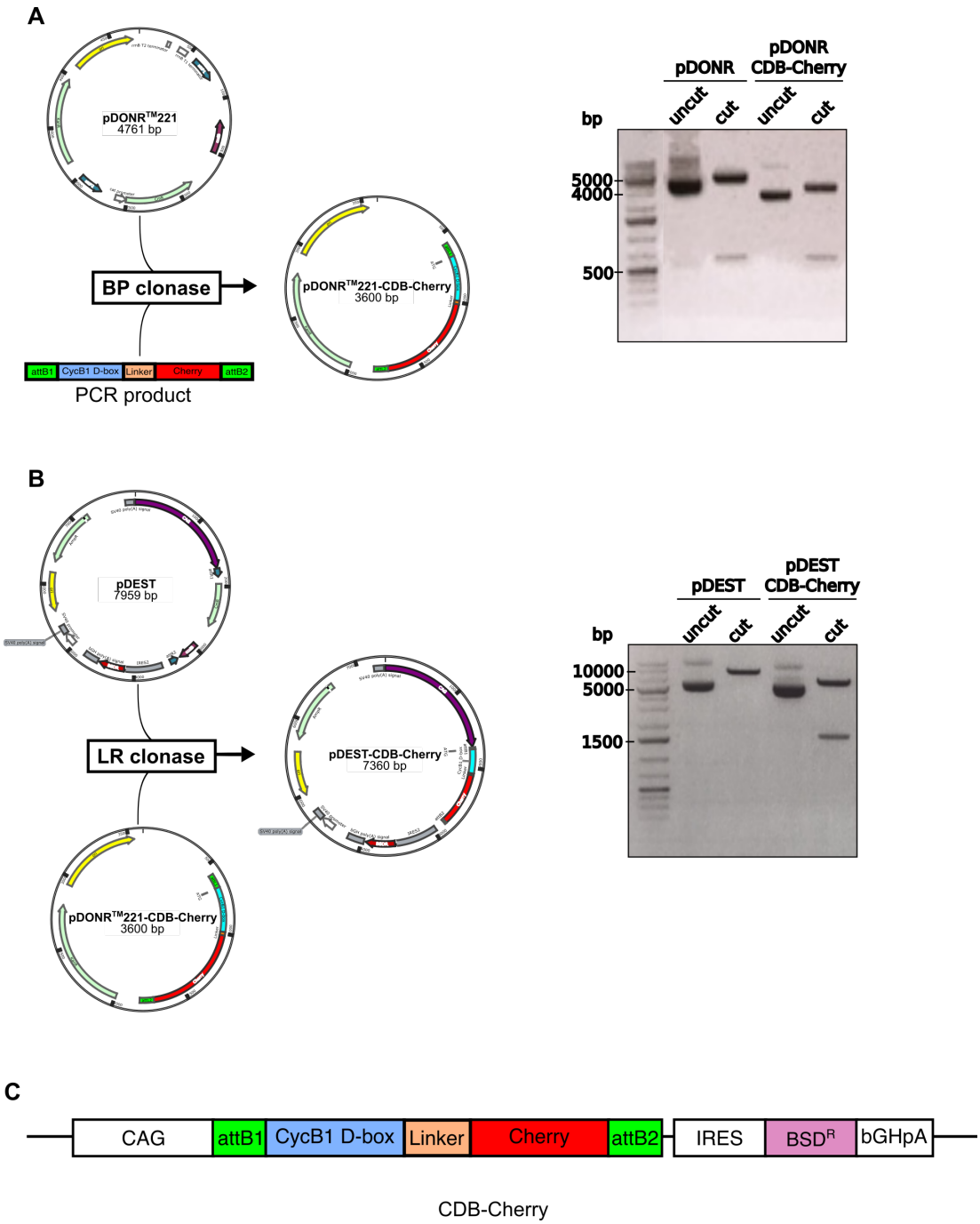

Figure 56. Gateway cloning of CycB1-Cherry into pDEST vector.

(A) Production of pDONR-CycB1-Cherry. Digested by EcoRV+PvuI, expected product pDONR cut=582bp+4179bp, expected product pDONR-CycB1-Cherry cut=582bp+3018bp. **(B)** Production of pDEST-CycB1-Cherry. Digested by SbfI-HF+HpaI, expected product pDEST cut=7959bp, expected product pDEST-CycB1-Cherry cut=5869bp+1494bp. **(C)** Linearised pDEST-CycB1-Cherry plasmid for nucleofection.

A NGN3-GFP/CDB-Cherry clone that clearly included Cherry^{+} cells when viewed by microscopy was selected for further testing. To assess the functionality of the CDB-Cherry reporter and how faithfully its expression reflects the cell cycle, this clonal line was imaged overnight. Cherry expression was observed in cells during mitosis and then rapidly extinguished from the cells at cytokinesis just prior to G1, as expected of proteins under the control of CDB. **(Figure 57)**. To confirm this result quantitatively, flow cytometry was performed on NGN3-GFP/CDB-Cherry hESCs using Hoescht 33342, a cell-permeable DNA-labelling dye with low cytotoxicity, as an indicator of cell cycle stage. As cells replicate their DNA during S phase to an eventual doubling of genetic material at G2/M, Hoescht incorporation increases proportionally. Cherry^{+} NGN3-GFP/CBD-Cherry hESCs were all in S/G2/M phases, while Cherry^{-} cells were predominantly in G0/G1 **(Figure 58)**, showing that the CDB-Cherry fusion protein faithfully reports cell cycle stage in hESCs.

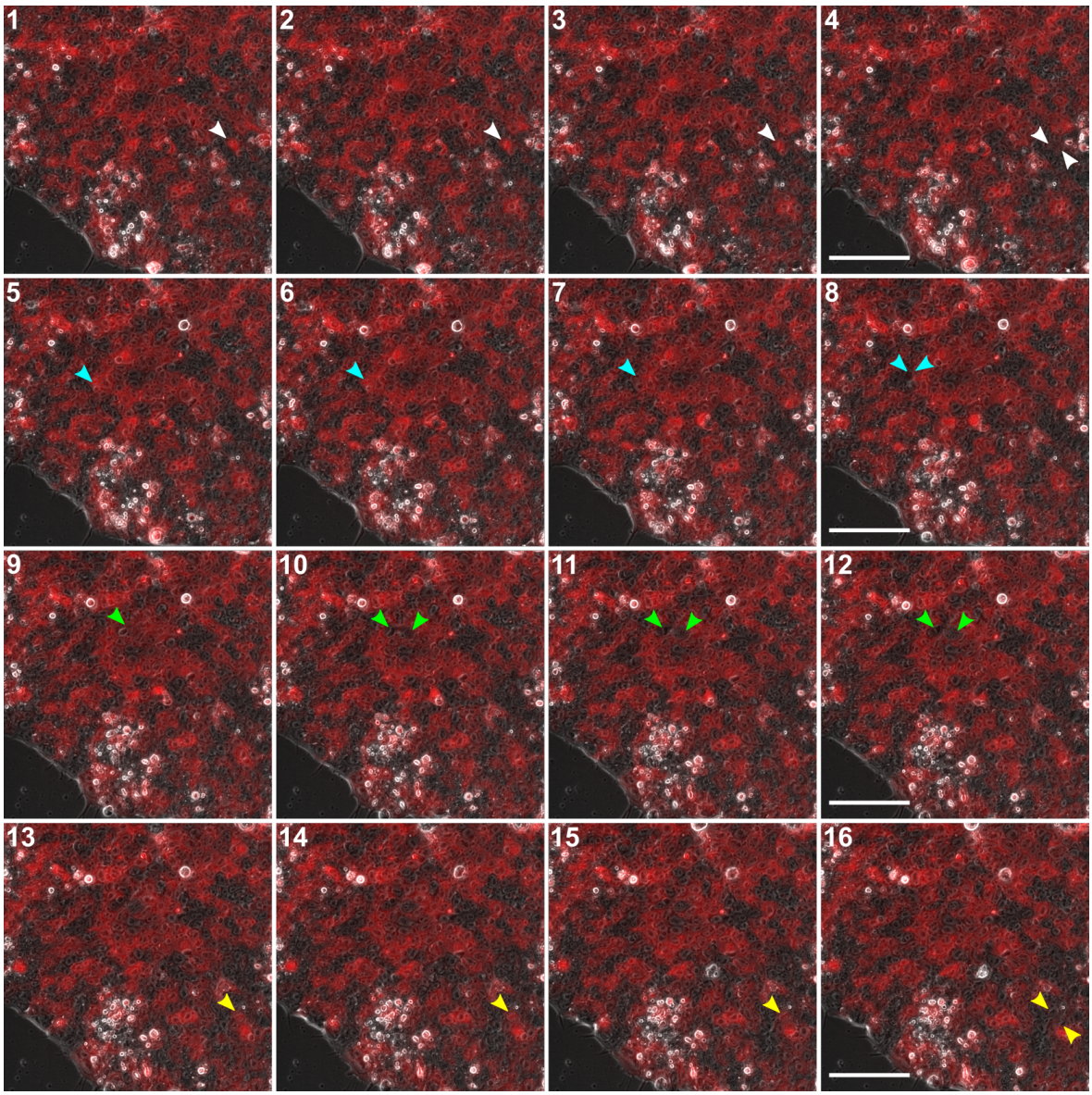

Figure 57. Overnight imaging of MS7 NGN3-GFP/CDB-Cherry.

Images were taken at 10 minute intervals using the 40X objective (scale bar represents 100μm). Phase and fluorescent images merged. Numbers indicate place in the image series. Single arrows indicate Cherry^{+} cells before division, double arrows indicate Cherry^{-} daughter cells.

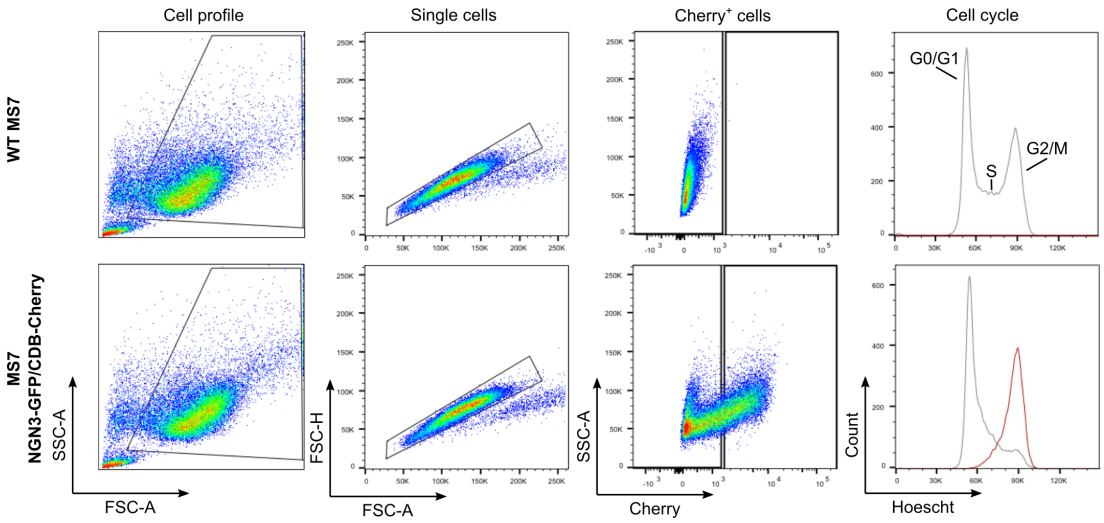

Figure 58. Cell cycle analysis by flow cytometry of MS7 NGN3-GFP/CDB-Cherry.

Cells were dissociated in accutase and incubated in normal medium with Hoescht 33342 for 60 minutes at 37°C, before being transferred to buffer. Analysed cells were gated on cell profile, single cells, and Cherry expression, before plotting based on Hoescht incorporation (far right plots, cell cycle stages indicated, Cherry$^-$ cells in grey, Cherry$^+$ cells in red). WT MS7 cells used as controls.

6.2.4 NGN3-GFP/CDB-Cherry reporter hESCs retain the differentiation capacity of WT MasterShef7 hESCs

Owing to the extent of genetic modifications and handling undergone by NGN3-GFP/CDB-Cherry hESCs, it was important to test if they had retained their capacity to differentiate towards pancreatic lineages. Reporter hESCs were subjected to the same differentiation protocol used previously in parallel with WT MS7, and these two lines were compared in their potential to generate definitive endoderm, foregut and pancreatic progenitors.

MS7 NGN3-GFP/CDB-Cherry differentiated to DE exhibited a very similar pattern of staining, where all cells appeared $FOXA2^+$ and the majority were also $SOX17^+$ **(Figure 59A)**. *SOX17* increased 10057-fold compared to undifferentiated cells and *OCT4* expression was reduced by greater than 5-fold **(Figure 59B)**. Neither change was significantly different to WT MS7.

Foregut differentiation was also found to be as efficient as the parental cell line. HNF1B protein was detected in differentiated reporter cells **(Figure 60A)**, and *HNF1B* mRNA increased 86-fold, with an average increase of 1395-fold for *HNF4A* mRNA. *OCT4* was also reduced to similar levels as WT **(Figure 60B)**.

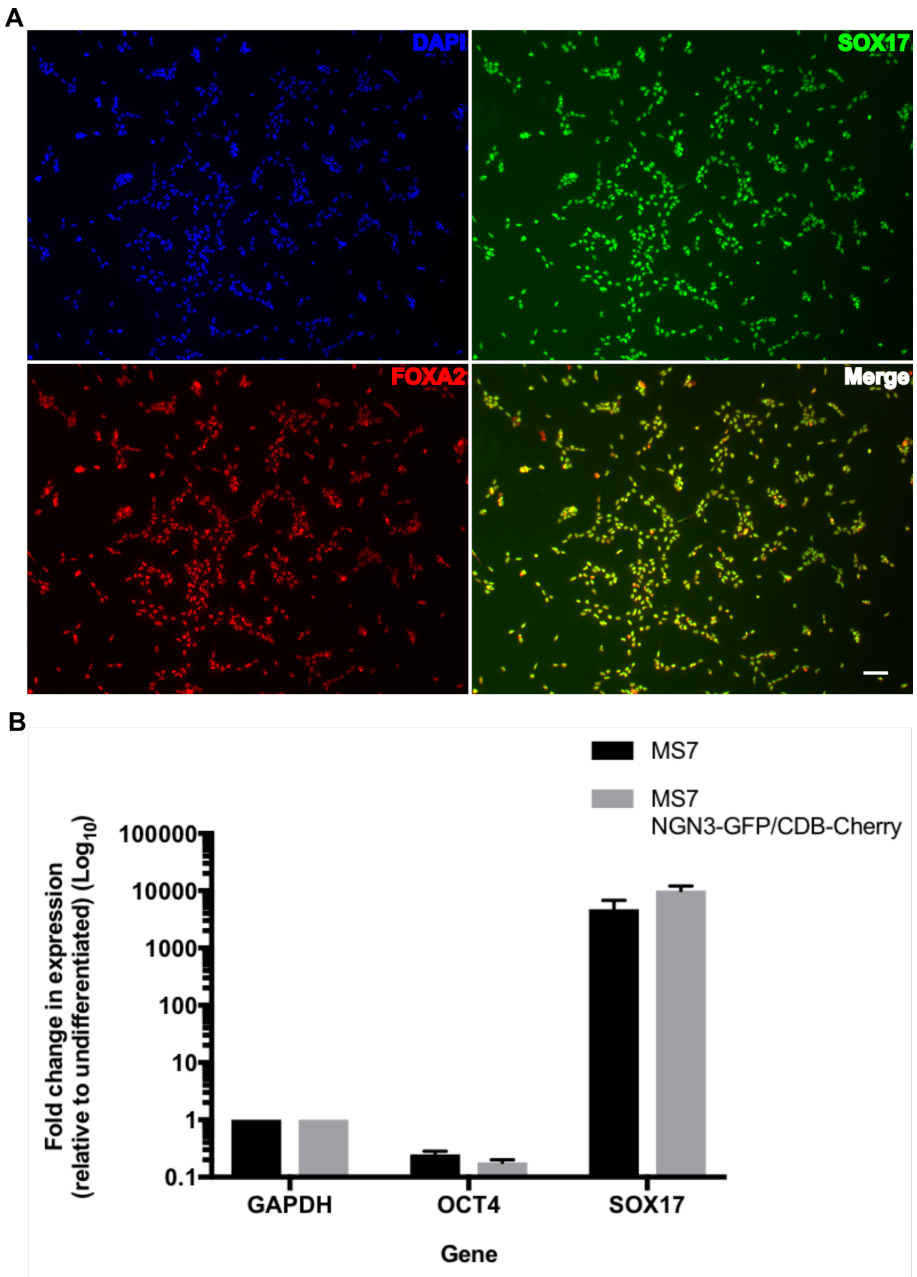

Figure 59. MS7 NGN3-GFP/CDB-Cherry differentiated to DE.

(A) ICC of differentiated cells showing staining for SOX17 (green) and FOXA2 (red). Images taken using 5X objective (scale bar represents 100μm). **(B)** mRNA expression of *OCT4* and *SOX17* in differentiated cells. 1μg RNA was used to make cDNA. Expression of all genes normalised to *GAPDH* (shown in Figure at 1-fold) and relative to undifferentiated MS7 hESCs. n=3. Error bars show standard deviation. Significance tested using multiple unpaired t-tests with Holm-Sidak correction.

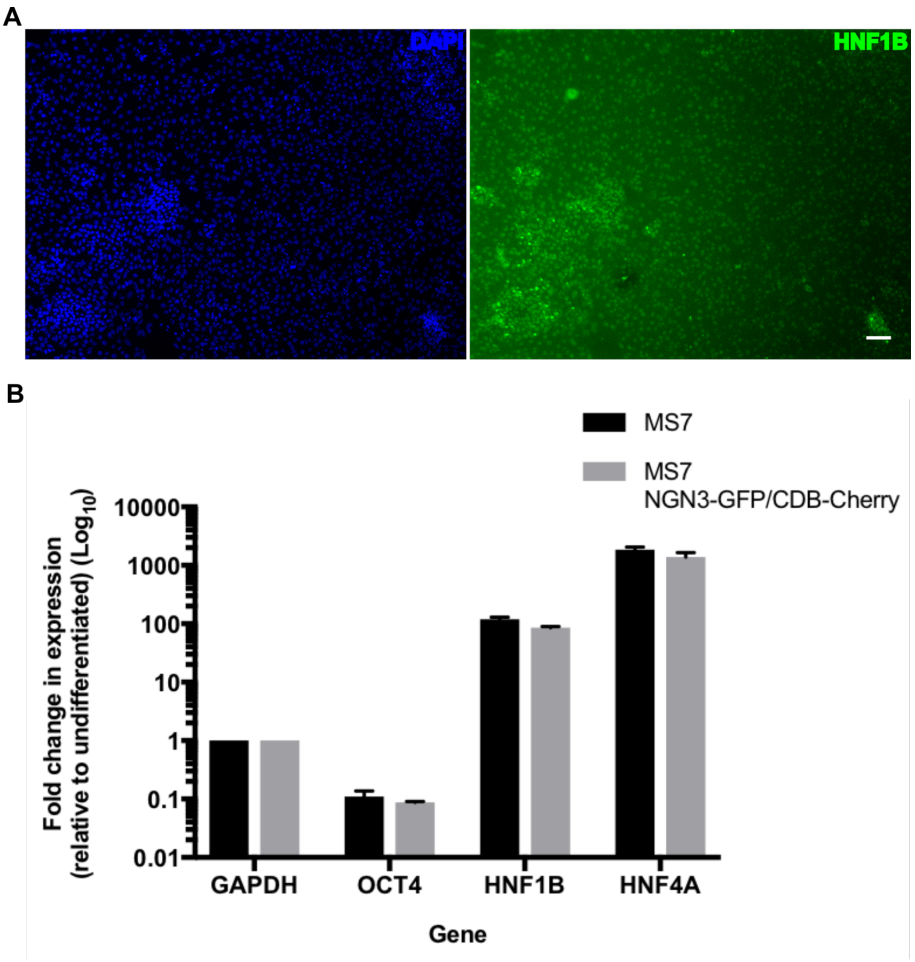

Figure 60. MS7 NGN3-GFP/CDB-Cherry differentiated to foregut.

(A) ICC of differentiated cells showing staining for HNF1B (green). Images taken using 5X objective (scale bar represents 100μm). **(B)** mRNA expression of *OCT4, HNF1B* and *HNF4A* in differentiated cells. 1μg RNA was used to make cDNA. Expression of all genes normalised to *GAPDH* (shown in Figure at 1-fold) and relative to undifferentiated MS7 hESCs. n=2. Error bars show standard deviation. Significance tested using multiple unpaired t-tests with Holm-Sidak correction.

At the pancreatic progenitor stage of differentiation, there were detectable differences between reporter and WT cells. PDX1 and SOX9 staining looked similar to that seen in WT cells **(Figure 61A)**, although a 426-fold increase in *PDX1* expression compared to undifferentiated cells was significantly lower than that in WT cells (p=0.02), while *SOX9* upregulation of 12-fold was also significantly lower (p=0.02) **(Figure 61B)**.

However, there was no significant difference between reporter and WT cells at the final stage of differentiation to endocrine pancreas progenitors. This, coupled with the fact that PDX1 and SOX9 protein expression appeared similar between cell lines, suggested that variability at the previous stage may be due to stochastic differences between wells or other culture artefacts. MS7 NGN3-GFP/CDB-Cherry upregulated *NGN3* by 314-fold and *NEUROD1* by 850-fold compared to undifferentiated cells **(Figure 62A)**. Furthermore, GFP expression was detected in differentiated reporter cells in three out of three independent culture wells **(Figure 62B)**, although GFP^+ cells were extremely rare and made up an average of only 0.004% of the total population. Taken together, our results suggest that the overall differentiation capacity of MS7 NGN3-GFP/CDB-Cherry is unaltered from parental MS7 hESCs, but the efficiency of differentiation from early pancreas progenitor to endocrine progenitor is poor in both cell lines. A limitation of our flow cytometry analysis is the lack of an undifferentiated NGN3-GFP/CDB-Cherry MS7 control sample, which could have ruled out aberrant GFP expression due to a 'leaky' promoter as a cause of GFP detection in differentiated samples. Unfortunately, it was not possible to perform this experiment due to time constraints and future work using this reporter cell line should seek to address this.

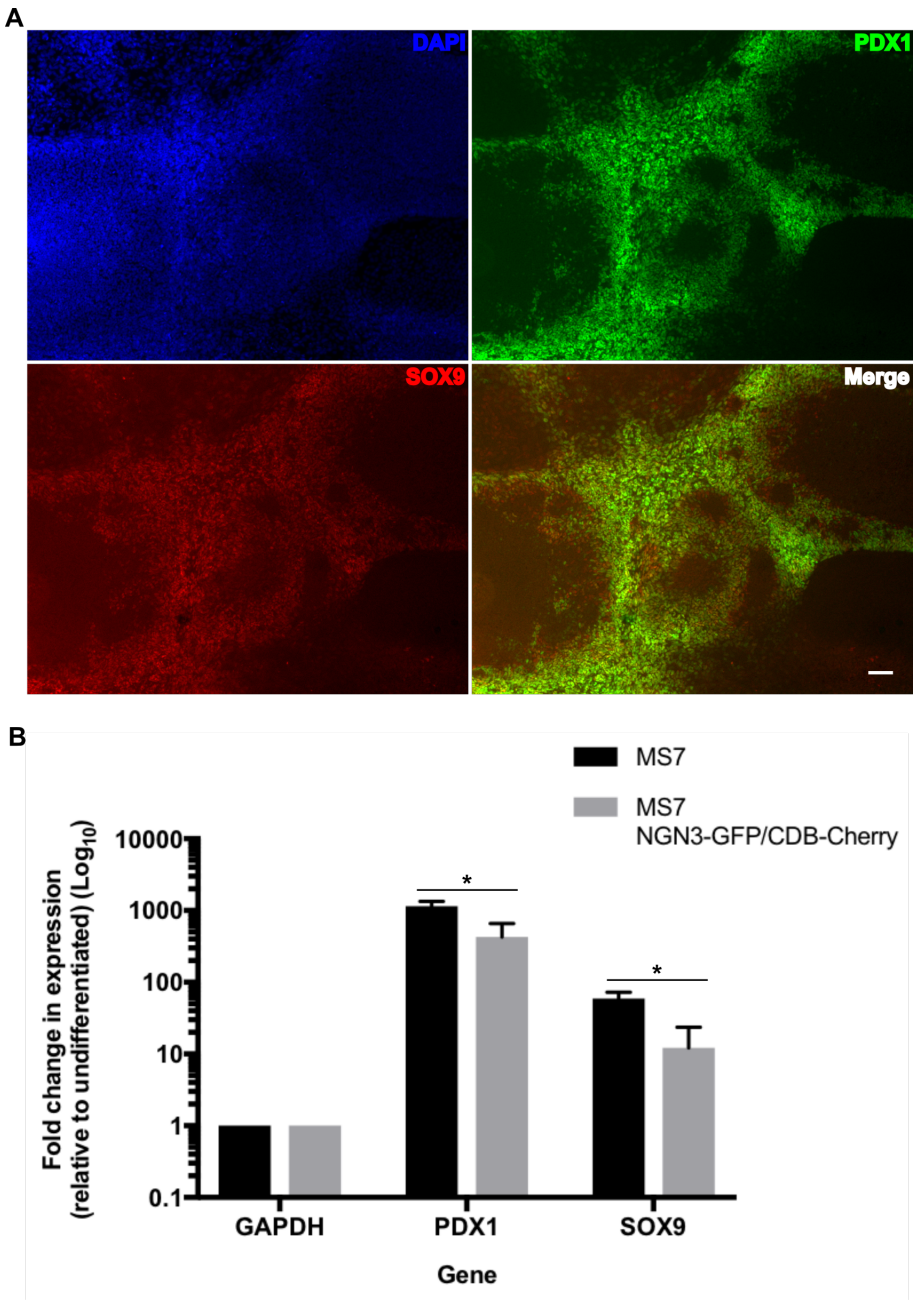

Figure 61. MS7 NGN3-GFP/CycB1-Cherry differentiated to early pancreatic progenitors.

(A) ICC of differentiated cells showing staining for PDX1 (green) and SOX9 (red). Images taken using 5X objective (scale bar represents 100μm). **(B)** mRNA expression of *PDX1* (adjusted p=0.02) and *SOX9* (adjusted p=0.02) in differentiated cells. 1μg RNA was used to make cDNA. Expression of all genes normalised to *GAPDH* (shown in Figure at 1-fold) and relative to undifferentiated MS7 hESCs. n=3. Error bars show standard deviation. Significance tested using multiple unpaired t-tests with Holm-Sidak correction (shown on graph, * = p≤0.05, ** = p≤0.01, *** = p≤0.001, **** = p≤0.0001).

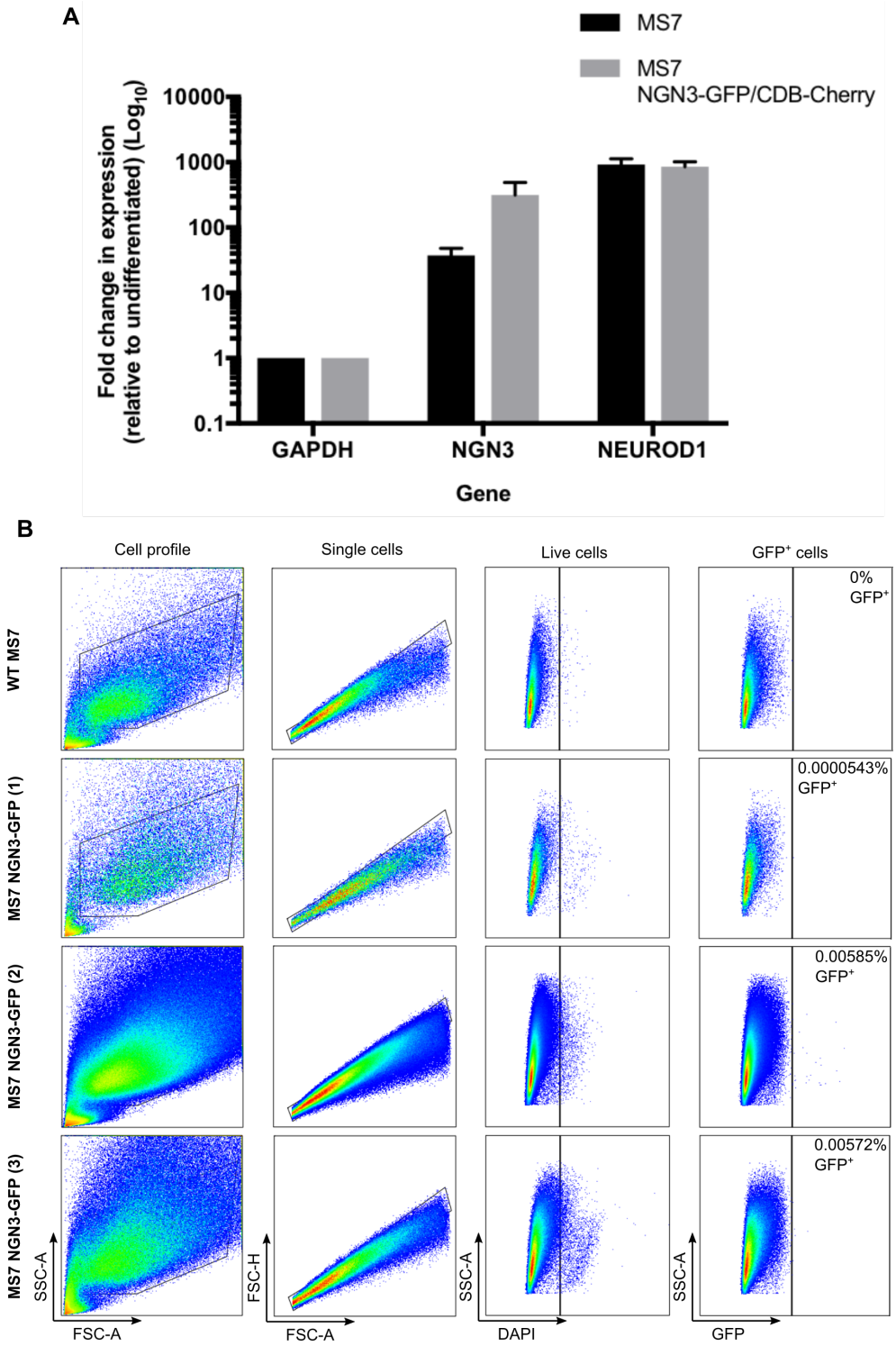

Figure 62. MS7 NGN3-GFP/CycB1-Cherry differentiated to endocrine pancreas progenitors.

(A) mRNA expression of *NGN3* and *NEUROD1* in differentiated cells. 1μg RNA was used to make cDNA. Expression of all genes normalised to *GAPDH* (shown in Figure at 1-fold) and relative to undifferentiated MS7 hESCs. n=3. Error bars show standard deviation. Significance tested using multiple unpaired t-tests with Holm-Sidak correction. **(B)** Analysed cells were gated on cell profile, single cells, and live cells (DAPI), before plotting based on GFP expression (far right plots, proportion of GFP^+ cells indicated). Differentiated WT MS7 cells used as controls.

6.3 Discussion

In this chapter, we have showed that PDX1^{+}/SOX9^{+} pancreas progenitor cells can be efficiently generated in vitro from MS7 hESCs, marrying together the production of potentially therapeutic cells in a clinical-grade hESC line. This marks a step towards the application of cell therapies for diabetes. We also describe the generation of a novel NGN-GFP/CDB-Cherry hESC reporter line, a valuable cellular model, which will allow simple and reliable readouts of endocrine pancreas progenitor production and proliferation. Our NGN3-GFP/CDB-Cherry reporter cell line has proven ability to generate early pancreatic progenitors and provides an excellent platform with which to test compounds to promote the further differentiation toward endocrine progenitors.

Pancreas progenitor generation from a clinical-grade hESC line has been demonstrated once before, by a team at ViaCyte, Inc., a company working towards cellular therapies for treating diabetes [262]. While impressive, the CyT49 hESC line used is proprietary. Furthermore, if immunogenicity of cell therapies is a consideration for the future and alternatives to (presumably also proprietary) encapsulation of transplanted cells are sought, a single clinical-grade hESC line is very unlikely to be suitable for a large proportion of the population. It is estimated that to cover the HLA type of 93% of the UK population, a bank of 150 selected donor pluripotent cells would need to be established [352]. Therefore, our work contributes to an emerging need to demonstrate instances of pancreas progenitor production in clinically relevant pluripotent cell lines.

Early PDX1^{+}/SOX9^{+} pancreas progenitor cells can be used directly for cell therapies, with further differentiation to hormone-producing cells occurring in vivo in diabetic mouse models [265,353]. Mice receiving these grafts were rescued, but analysis of grafted cells revealed an insulin secretory amplitude lower than that of engrafted normal adult

islets. In follow-up studies that further examined the composition of grafts at later time points (50 weeks), the amount of insulin secreted by grafted cells was more similar to normal islet cells, suggesting an extended maturation period is required for implanted pancreas progenitor cells [266]. A further complication of pancreas progenitor implants recognised in this study was the variability in the proportion of endocrine cells produced by grafted cells, which ranged widely from 10-63% of surviving cells. Non-endocrine cells present in the graft comprised $KRT19^+$ ductal cells and VIM^+ cells, possibly indicating mesenchyme formation. $KRT19^+$ cells organized into ductal structures that included ciliated epithelial cells, showing that some engrafted pancreas progenitor cells start to recapitulate pancreas development towards lineages that are not beneficial for treating diabetes.

Grafting endocrine pancreas progenitors instead should, in theory, prevent the in vivo generation of non-endocrine cell types. Unfortunately, the only documented method for capturing and expanding endocrine pancreas progenitors in vitro required co-culture with organ-matched mesenchymal cells [271]. However, the study focused on mouse ES cell differentiation and the data presented on human differentiation was not strong. Even if this study did demonstrate an advance in the in vitro expansion of bona fide $NGN3^+$ endocrine pancreas progenitors, a move towards more defined culture conditions is necessary for cell therapy, and is critical if we are to understand the biology of endocrine specification.

The NGN3-GFP/CDB-Cherry hESC model we have developed here will provide a platform for future research to elucidate defined conditions for the robust and efficient induction of $NGN3^+$ endocrine progenitor cells from hESCs, as well as the conditions amenable to their expansion. Expandable hES-derived $NGN3^+$ endocrine progenitor cells would be an ideal cellular reagent either to be used directly for cell therapy, or further differentiated prior to implantation.

CHAPTER 7
Discussion

Islet cells derived from donated adult human pancreas can be used in cell therapy for diabetes to help achieve independence from exogenous insulin and homeostatic control of blood glucose. Yet islet cell transplants remain under-utilised, tending to be reserved for patients with severe T1D who struggle to manage their blood glucose levels. This is almost exclusively due to an insufficient supply of donor tissue, with successful islet cell therapies often requiring two or more transplants per patient. If cell therapies are ever to become the standard of care for diabetic patients, an alternative source of cells must be found. hESC-derived islet cells have the potential to fill this gap, but significant barriers exist to optimally implementing this technology. Human multipotent pancreas progenitor cell have been tested in animal models and show some function in controlling blood sugar levels, however endocrine cell yield from in vivo differentiation is hugely variable.

We reasoned that because pancreatic endocrine progenitors are restricted to an endocrine cell fate, they constitute the ideal cell stage for use in therapy. However, methods for the efficient induction of endocrine progenitor commitment from hESC-derived pancreas progenitors in vitro require improvement. Furthermore, defined conditions for subsequent stable culture and expansion of endocrine progenitors have not been described. To investigate better methods for in vitro endocrine progenitor induction, culture and expansion, we developed methods for isolating and expanding foetal pancreas progenitor cells from mouse and human tissue. Importantly, we describe defined conditions that allow scalable culture of foetal pancreas progenitors. Cultured cells express key pancreas progenitor markers PDX1 and SOX9, and can be maintained in monolayer conditions that are amenable to unbiased screening of

hundreds of culture conditions in parallel in conjunction with high-content imaging assays.

Foetal pancreas is the only endogenous source of pancreatic progenitors from humans, making their study particularly challenging. PDX1 and SOX9 are expressed in cells in the trunk of the pancreatic ductal tree at multiple stages of development, despite increasing levels of lineage commitment and differentiation as organogenesis proceeds. At what stage does the pool of pancreas progenitors in the human foetal pancreas become depleted? With this in mind, we leveraged our access to fresh human foetal tissue between 10 weeks and 19 weeks gestation to describe expression of key regulators for pancreas progenitor identity PDX1 and SOX9. We showed that $PDX1^{+}/SOX9^{+}$ progenitor cells are proportionally more common in the human foetal pancreas at 12 weeks gestation or earlier. After this stage, SOX9 expression appears to be progressively lost from the progenitor population, and this is associated with reduced PDX1 expression. These data indicate that depletion of the human foetal pancreas progenitor pool begins at approximately 13 weeks gestation. SOX9 regulates expression of more than one third of genes enriched in human foetal pancreas progenitors [135], so its expression is a crucial identifier of true progenitors. Successful isolation and in vitro use of human foetal pancreas progenitors as a cellular model will therefore benefit from – and may even necessitate – harnessing tissue from early in development.

To enable the use of foetal pancreas progenitors as a cellular model, small numbers of freshly isolated cells must be expanded while maintaining their identity in vitro. What culture conditions can promote this? Various culture conditions for foetal pancreas progenitors have been described in the literature, mostly using cells from mice owing to the scarce and precious nature of human foetal material. EGF and FGF7/10 are mainstays of contemporary pancreas progenitor culture media,

identified from their roles in progenitor expansion during organogenesis. Other media components vary between protocols, with no defined conditions having been described that promote progenitor maintenance and expansion in monolayer. Using mouse foetal pancreas due to its availability, we described protocols for isolation and purification of foetal pancreas progenitors. We also developed, for the first time, culture conditions that allow long-term expansion of these cells in vitro in monolayer with continued robust Pdx1/Sox9 expression. The conditions described here have the potential to be widely applied by researchers requiring a cellular model to study pancreatic endocrine progenitor induction and culture. Authentic pancreas progenitor cells can be expanded to a number that enables screening experiments to probe the mechanisms behind endocrine progenitor induction – and importantly we have demonstrated that expanded foetal pancreas progenitors retain the capacity to differentiate to an endocrine fate under suitable conditions.

Endocrine progenitor gene expression may be different between mouse and human. For example, a reduced role of NKX2.2 in human endocrine progenitor specification compared to mouse has been documented [132], and our data support that. In light of this and potential other differences, it may be important to use cellular models from both species to study endocrine commitment. We found that culture conditions that facilitate mouse foetal pancreas progenitor expansion can be applied to human foetal pancreas progenitors with similar results. Our successful implementation of the TGFβ inhibitor A83 for expansion of mouse and human foetal pancreas progenitors can intuitively be explained through its function of blocking EMT and associated differentiation. However, it also calls into question the use of TGFβ inhibitors in the final stages of hESC directed differentiation to endocrine pancreas, where they have been found to increase endocrine yield [252,354]. One possible explanation is that TGFβ signalling dosage affects differentiation outcome – the TGFβ inhibitor Alk5iII is

routinely used at 10μM in differentiations [255,259], compared to the 0.5μM A83 used here for progenitor expansion despite the relatively similar potencies of both inhibitors. Alternatively, the discrepancy could be caused by TGFβ inhibitor specificity, as A83 has broad inhibitory activity on ALK5, but also the Activin/Nodal receptors ALK4 and ALK7 [315], revealing a potential role for inhibition of Activin/Nodal signalling in pancreas progenitors. These, and many other avenues of research in pancreas developmental biology could be explored further using our cellular model system described here.

How can better methods for endocrine progenitor induction be practically applied? Conditions identified by experiments with the foetal progenitor cellular models described here could theoretically be translated to producing hESC-derived endocrine progenitors in vitro in larger quantities than previously possible, and allow maintenance or expansion of these cells in culture. As a means to efficiently test the response of hESC-derived pancreas progenitors to pro-endocrine conditions, we developed a reporter hESC to enable antibody-independent identification of NGN3 expression and simultaneously evaluate proliferative status in live cells. This hESC tool overcomes the problem presented by the lack of a reliable anti-human NGN3 antibody, while also offering a means to investigate the signals required to bypass the cell cycle exit inherent to pancreatic endocrine progenitors.

Moving forward, our foetal pancreas progenitor cellular models could be used in unbiased chemical screens of small molecule libraries (such as the StemSelect® library previously used by our lab) and in parallel to test candidate molecules that may induce endocrine commitment. They would also be well-suited to CRISPR genetic screens. There is direct evidence that histone deacetylase (HDAC) inhibitors aid endocrine progenitor generation [273], and recent research has suggested Hippo signalling inhibitors [355], tyrosine kinase receptor type 2 (TKRB) agonists [356], and

combined protein kinase A (PKA)/mammalian target of rapamycin (mTOR) inhibition [357] as future directions for enhancing endocrine progenitor induction, suggesting that there are many potential gains still to be exploited in this area. Pharmacological modulators for all of these pathways are currently commercially available. A useful addition to these cellular models would be a means of easily assaying *NGN3* expression to provide a simple readout of culture outcomes.

The novel culture conditions we have developed for pancreas progenitor cell expansion in vitro may also be of use in the pancreatic cancer field. Pancreatic adenocarcinoma is thought to feature dedifferentiation of adult exocrine pancreatic cells to a foetal pancreas progenitor-like cell state[360]. Therefore, our culture conditions may be optimal for growth of pancreatic adenocarcinoma cells, which would facilitate their further study.

We have shown here that mouse foetal pancreas progenitors are readily transfectable. Using the pipeline for efficient epitope tagging using Cas9 ribonucleoprotein recently developed by our lab [358], Ngn3 and other endocrine progenitor markers such NeuroD1 and Rfx6 could be tagged in less time and at less expense than previously possible. This would enable the use of effective, reliable and cheap antibodies against epitope tags. More interestingly, it would allow evaluation of whether manipulation of different signalling pathways or proteins in vitro affects expression of pro-endocrine transcription factors independently of each other, giving us a better understanding of how the pancreatic regulatory network is controlled.

In conclusion, the provision of convenient and scalable pancreas progenitor cellular models that genuinely reflect their in vivo counterparts will engender opportunities to improve endocrine progenitor production in vitro. Additionally, these models could allow us to shed light on the mechanisms governing human pancreas development in

a way that has not been possible before. Ultimately, the cellular models described here supply a platform for advancements in pancreatic cell production that could have a significant impact on future cell replacement therapies. An effective cell therapy for diabetes will hugely improve the quality of life for millions of people worldwide, and hopefully alleviate the healthcare burden associated with treating acute and chronic disease complications.

References

1. Falkmer S. Immunocytochemical studies of the evolution of islet hormones. *J Histochem Cytochem*. 1979;27(9):1281-1282. doi:10.1177/27.9.383830.

2. Youson JH, Al-Mahrouki AA. Ontogenetic and phylogenetic development of the endocrine pancreas (islet organ) in fish. *Gen Comp Endocrinol*. 1999;116(3):303-335. doi:10.1006/gcen.1999.7376.

3. Mulley JF, Hargreaves AD, Hegarty MJ, Heller RS, Swain MT. Transcriptomic analysis of the lesser spotted catshark (Scyliorhinus canicula) pancreas, liver and brain reveals molecular level conservation of vertebrate pancreas function. *BMC Genomics*. 2014;15(1):1074. doi:10.1186/1471-2164-15-1074.

4. Kinkel MD, Prince VE. On the diabetic menu: zebrafish as a model for pancreas development and function. *Bioessays*. 2009;31(2):139-152. doi:10.1002/bies.200800123.

5. Wilfinger A, Arkhipova V, Meyer D. Cell type and tissue specific function of islet genes in zebrafish pancreas development. *Developmental Biology*. 2013;378(1):25-37. doi:10.1016/j.ydbio.2013.03.009.

6. Dolenšek J, Rupnik MS, Stožer A. Structural similarities and differences between the human and the mouse pancreas. *Islets*. 2015;7(1):e1024405. doi:10.1080/19382014.2015.1024405.

7. Slack JM. Developmental biology of the pancreas. *Development*. 1995;121(6):1569-1580.

8. Pandol SJ. The Exocrine Pancreas. *Colloquium Series on Integrated Systems Physiology: From Molecule to Function*. 2010;3(1):1-64. doi:10.4199/C00026ED1V01Y201102ISP014.

9. Williams JA. Regulation of acinar cell function in the pancreas. *Curr Opin Gastroenterol*. 2010;26(5):478-483. doi:10.1097/MOG.0b013e32833d11c6.

10. Beer RL, Parsons MJ, Rovira M. Centroacinar cells: At the center of pancreas regeneration. *Developmental Biology*. 2016;413(1):8-15. doi:10.1016/j.ydbio.2016.02.027.

11. Delaspre F, Beer RL, Rovira M, et al. Centroacinar Cells Are Progenitors That Contribute to Endocrine Pancreas Regeneration. *Diabetes*. 2015;64(10):3499-3509. doi:10.2337/db15-0153.

12. Leeson TS, Leeson R. Close association of centroacinar/ductular and insular cells in the rat pancreas. *Histol Histopathol*. 1986;1(1):33-42.

13. Hootman SR, de Ondarza J. Regulation of goblet cell degranulation in isolated pancreatic ducts. *Am J Physiol*. 1995;268(1 Pt 1):G24-G32. doi:10.1152/ajpgi.1995.268.1.G24.

14. Apte MV, Haber PS, Applegate TL, et al. Periacinar stellate shaped cells in rat pancreas: identification, isolation, and culture. *Gut*. 1998;43(1):128-133.

15. Bachem MG, Schneider E, Gross H, et al. Identification, culture, and characterization of pancreatic stellate cells in rats and humans. *Gastroenterology*. 1998;115(2):421-432.

16. Phillips PA, Yang L, Shulkes A, et al. Pancreatic stellate cells produce acetylcholine and may play a role in pancreatic exocrine secretion. *Proc Natl Acad Sci USA*. 2010;107(40):17397-17402. doi:10.1073/pnas.1000359107.

17. Ionescu-Tirgoviste C, Gagniuc PA, Gubceac E, et al. A 3D map of the islet routes throughout the healthy human pancreas. *Sci Rep*. 2015;5(1):14634. doi:10.1038/srep14634.

18. Krejs GJ. Physiological role of somatostatin in the digestive tract: gastric acid secretion, intestinal absorption, and motility. *Scand J Gastroenterol Suppl*. 1986;119:47-53.

19. Hazelwood RL. The pancreatic polypeptide (PP-fold) family: gastrointestinal, vascular, and feeding behavioral implications. *Proc Soc Exp Biol Med*. 1993;202(1):44-63.

20. Hauge-Evans AC, King AJ, Carmignac D, et al. Somatostatin secreted by islet delta-cells fulfills multiple roles as a paracrine regulator of islet function. *Diabetes*. 2009;58(2):403-411. doi:10.2337/db08-0792.

21. Wierup N, Sundler F, Heller RS. The islet ghrelin cell. *J Mol Endocrinol*. 2014;52(1):R35-R49. doi:10.1530/JME-13-0122.

22. Brissova M, Fowler MJ, Nicholson WE, et al. Assessment of human pancreatic islet architecture and composition by laser scanning confocal microscopy. *J Histochem Cytochem*. 2005;53(9):1087-1097. doi:10.1369/jhc.5C6684.2005.

23. Cabrera O, Berman DM, Kenyon NS, Ricordi C, Berggren P-O, Caicedo A. The unique cytoarchitecture of human pancreatic islets has implications for islet cell function. *Proc Natl Acad Sci USA*. 2006;103(7):2334-2339. doi:10.1073/pnas.0510790103.

24. Ichii H, Inverardi L, Pileggi A, et al. A novel method for the assessment of cellular composition and beta-cell viability in human islet preparations. *Am J Transplant*. 2005;5(7):1635-1645. doi:10.1111/j.1600-6143.2005.00913.x.

25. Mojsov S, Heinrich G, Wilson IB, Ravazzola M, Orci L, Habener JF. Preproglucagon gene expression in pancreas and intestine diversifies at the level of post-translational processing. *J Biol Chem*. 1986;261(25):11880-11889.

26. Dey A, Lipkind GM, Rouillé Y, et al. Significance of prohormone convertase 2, PC2, mediated initial cleavage at the proglucagon interdomain site,

Lys70-Arg71, to generate glucagon. *Endocrinology*. 2005;146(2):713-727. doi:10.1210/en.2004-1118.

27. Rorsman P, Hellman B. Voltage-activated currents in guinea pig pancreatic alpha 2 cells. Evidence for Ca2+-dependent action potentials. *J Gen Physiol*. 1988;91(2):223-242.

28. Ahrén B, Lundquist I. Influences of gastro-intestinal polypeptides and glucose on glucagon secretion induced by cholinergic stimulation. *Horm Metab Res*. 1982;14(10):529-532.

29. Ahrén B, Veith RC, Taborsky GJ. Sympathetic nerve stimulation versus pancreatic norepinephrine infusion in the dog: 1). Effects on basal release of insulin and glucagon. *Endocrinology*. 1987;121(1):323-331. doi:10.1210/endo-121-1-323.

30. Adriaenssens AE, Svendsen B, Lam BYH, et al. Transcriptomic profiling of pancreatic alpha, beta and delta cell populations identifies delta cells as a principal target for ghrelin in mouse islets. *Diabetologia*. 2016;59(10):2156-2165. doi:10.1007/s00125-016-4033-1.

31. Segerstolpe Å, Palasantza A, Eliasson P, et al. Single-Cell Transcriptome Profiling of Human Pancreatic Islets in Health and Type 2 Diabetes. *Cell Metab*. 2016;24(4):593-607. doi:10.1016/j.cmet.2016.08.020.

32. Li NX, Brown S, Kowalski T, et al. GPR119 Agonism Increases Glucagon Secretion During Insulin-Induced Hypoglycemia. *Diabetes*. 2018;67(7):1401-1413. doi:10.2337/db18-0031.

33. Overton HA, Babbs AJ, Doel SM, et al. Deorphanization of a G protein-coupled receptor for oleoylethanolamide and its use in the discovery of small-molecule hypophagic agents. *Cell Metab*. 2006;3(3):167-175. doi:10.1016/j.cmet.2006.02.004.

34. Hansen KB, Rosenkilde MM, Knop FK, et al. 2-Oleoyl glycerol is a GPR119 agonist and signals GLP-1 release in humans. *J Clin Endocrinol Metab*. 2011;96(9):E1409-E1417. doi:10.1210/jc.2011-0647.

35. Herzig S, Long F, Jhala US, et al. CREB regulates hepatic gluconeogenesis through the coactivator PGC-1. *Nature*. 2001;413(6852):179-183. doi:10.1038/35093131.

36. Yoon JC, Puigserver P, Chen G, et al. Control of hepatic gluconeogenesis through the transcriptional coactivator PGC-1. *Nature*. 2001;413(6852):131-138. doi:10.1038/35093050.

37. Ciudad C, Camici M, Ahmad Z, Wang Y, DePaoli-Roach AA, Roach PJ. Control of glycogen synthase phosphorylation in isolated rat hepatocytes by epinephrine, vasopressin and glucagon. *Eur J Biochem*. 1984;142(3):511-520.

38. Heimberg H, De Vos A, Pipeleers D, Thorens B, Schuit F. Differences in glucose transporter gene expression between rat pancreatic alpha- and

beta-cells are correlated to differences in glucose transport but not in glucose utilization. *J Biol Chem*. 1995;270(15):8971-8975.

39. MacDonald PE, De Marinis YZ, Ramracheya R, et al. A K ATP channel-dependent pathway within alpha cells regulates glucagon release from both rodent and human islets of Langerhans. Vidal-Puig AJ, ed. *PLoS Biol*. 2007;5(6):e143. doi:10.1371/journal.pbio.0050143.

40. Briant LJB, Reinbothe TM, Spiliotis I, Miranda C, Rodriguez B, Rorsman P. δ-cells and β-cells are electrically coupled and regulate α-cell activity via somatostatin. *J Physiol (Lond)*. 2018;596(2):197-215. doi:10.1113/JP274581.

41. Franklin I, Gromada J, Gjinovci A, Theander S, Wollheim CB. Beta-cell secretory products activate alpha-cell ATP-dependent potassium channels to inhibit glucagon release. *Diabetes*. 2005;54(6):1808-1815.

42. Leung YM, Ahmed I, Sheu L, et al. Insulin regulates islet alpha-cell function by reducing KATP channel sensitivity to adenosine 5'-triphosphate inhibition. *Endocrinology*. 2006;147(5):2155-2162. doi:10.1210/en.2005-1249.

43. Benner C, van der Meulen T, Cáceres E, Tigyi K, Donaldson CJ, Huising MO. The transcriptional landscape of mouse beta cells compared to human beta cells reveals notable species differences in long non-coding RNA and protein-coding gene expression. *BMC Genomics*. 2014;15(1):620. doi:10.1186/1471-2164-15-620.

44. Henckens MJAG, Deussing JM, Chen A. Region-specific roles of the corticotropin-releasing factor-urocortin system in stress. *Nat Rev Neurosci*. 2016;17(10):636-651. doi:10.1038/nrn.2016.94.

45. Huising MO, van der Meulen T, Vaughan JM, et al. CRFR1 is expressed on pancreatic beta cells, promotes beta cell proliferation, and potentiates insulin secretion in a glucose-dependent manner. *Proc Natl Acad Sci USA*. 2010;107(2):912-917. doi:10.1073/pnas.0913610107.

46. Piper K, Brickwood S, Turnpenny LW, et al. Beta cell differentiation during early human pancreas development. *J Endocrinol*. 2004;181(1):11-23.

47. Jeon J, Correa-Medina M, Ricordi C, Edlund H, Diez JA. Endocrine cell clustering during human pancreas development. *J Histochem Cytochem*. 2009;57(9):811-824. doi:10.1369/jhc.2009.953307.

48. Brereton MF, Iberl M, Shimomura K, et al. Reversible changes in pancreatic islet structure and function produced by elevated blood glucose. *Nat Commun*. 2014;5(1):4639. doi:10.1038/ncomms5639.

49. Steiner DJ, Kim A, Miller K, Hara M. Pancreatic islet plasticity: interspecies comparison of islet architecture and composition. *Islets*. 2010;2(3):135-145.

50. Liu M, Lara-Lemus R, Shan S-O, et al. Impaired cleavage of preproinsulin signal peptide linked to autosomal-dominant diabetes. *Diabetes*. 2012;61(4):828-837. doi:10.2337/db11-0878.

51. Wentworth BM, Schaefer IM, Villa-Komaroff L, Chirgwin JM. Characterization of the two nonallelic genes encoding mouse preproinsulin. *J Mol Evol*. 1986;23(4):305-312.

52. Shiao M-S, Liao B-Y, Long M, Yu H-T. Adaptive evolution of the insulin two-gene system in mouse. *Genetics*. 2008;178(3):1683-1691. doi:10.1534/genetics.108.087023.

53. Deltour L, Leduque P, Blume N, et al. Differential expression of the two nonallelic proinsulin genes in the developing mouse embryo. *Proc Natl Acad Sci USA*. 1993;90(2):527-531.

54. Smeekens SP, Montag AG, Thomas G, et al. Proinsulin processing by the subtilisin-related proprotein convertases furin, PC2, and PC3. *Proc Natl Acad Sci USA*. 1992;89(18):8822-8826.

55. Kaufmann JE, Irminger JC, Mungall J, Halban PA. Proinsulin conversion in GH3 cells after coexpression of human proinsulin with the endoproteases PC2 and/or PC3. *Diabetes*. 1997;46(6):978-982.

56. Pinger CW, Entwistle KE, Bell TM, Liu Y, Spence DM. C-Peptide replacement therapy in type 1 diabetes: are we in the trough of disillusionment? *Mol Biosyst*. 2017;13(8):1432-1437. doi:10.1039/c7mb00199a.

57. van de Bunt M, Gloyn AL. A tale of two glucose transporters: how GLUT2 re-emerged as a contender for glucose transport into the human beta cell. *Diabetologia*. 2012;55(9):2312-2315. doi:10.1007/s00125-012-2612-3.

58. Ashcroft FM, Harrison DE, Ashcroft SJ. Glucose induces closure of single potassium channels in isolated rat pancreatic beta-cells. *Nature*. 1984;312(5993):446-448.

59. Cook DL, Hales CN. Intracellular ATP directly blocks K+ channels in pancreatic B-cells. *Nature*. 1984;311(5983):271-273.

60. Rorsman P, Braun M, Zhang Q. Regulation of calcium in pancreatic α- and β-cells in health and disease. *Cell Calcium*. 2012;51(3-4):300-308. doi:10.1016/j.ceca.2011.11.006.

61. Karlsson S, Ahrén B. Cholecystokinin and the regulation of insulin secretion. *Scand J Gastroenterol*. 1992;27(3):161-165.

62. Baggio LL, Drucker DJ. Biology of incretins: GLP-1 and GIP. *Gastroenterology*. 2007;132(6):2131-2157. doi:10.1053/j.gastro.2007.03.054.

63. Huypens P, Ling Z, Pipeleers D, Schuit F. Glucagon receptors on human islet cells contribute to glucose competence of insulin release. *Diabetologia*. 2000;43(8):1012-1019. doi:10.1007/s001250051484.

64. Song G, Pacini G, Ahrén B, D'Argenio DZ. Glucagon increases insulin levels by stimulating insulin secretion without effect on insulin clearance in mice. *Peptides*. 2017;88:74-79. doi:10.1016/j.peptides.2016.12.012.

65. Kern M, Wells JA, Stephens JM, et al. Insulin responsiveness in skeletal muscle is determined by glucose transporter (Glut4) protein level. *Biochem J*. 1990;270(2):397-400.

66. Goodyear LJ, Hirshman MF, Napoli R, et al. Glucose ingestion causes GLUT4 translocation in human skeletal muscle. *Diabetes*. 1996;45(8):1051-1056.

67. Vanhaesebroeck B, Alessi DR. The PI3K-PDK1 connection: more than just a road to PKB. *Biochem J*. 2000;346 Pt 3(Pt 3):561-576.

68. Mîinea CP, Sano H, Kane S, et al. AS160, the Akt substrate regulating GLUT4 translocation, has a functional Rab GTPase-activating protein domain. *Biochem J*. 2005;391(Pt 1):87-93. doi:10.1042/BJ20050887.

69. Cross DA, Alessi DR, Cohen P, Andjelkovich M, Hemmings BA. Inhibition of glycogen synthase kinase-3 by insulin mediated by protein kinase B. *Nature*. 1995;378(6559):785-789. doi:10.1038/378785a0.

70. Brady MJ, Bourbonais FJ, Saltiel AR. The activation of glycogen synthase by insulin switches from kinase inhibition to phosphatase activation during adipogenesis in 3T3-L1 cells. *J Biol Chem*. 1998;273(23):14063-14066.

71. Imai Y, Patel HR, Hawkins EJ, Doliba NM, Matschinsky FM, Ahima RS. Insulin secretion is increased in pancreatic islets of neuropeptide Y-deficient mice. *Endocrinology*. 2007;148(12):5716-5723. doi:10.1210/en.2007-0404.

72. Schwetz TA, Ustione A, Piston DW. Neuropeptide Y and somatostatin inhibit insulin secretion through different mechanisms. *Am J Physiol Endocrinol Metab*. 2013;304(2):E211-E221. doi:10.1152/ajpendo.00374.2012.

73. Lewis K, Li C, Perrin MH, et al. Identification of urocortin III, an additional member of the corticotropin-releasing factor (CRF) family with high affinity for the CRF2 receptor. *Proc Natl Acad Sci USA*. 2001;98(13):7570-7575. doi:10.1073/pnas.121165198.

74. van der Meulen T, Donaldson CJ, Cáceres E, et al. Urocortin3 mediates somatostatin-dependent negative feedback control of insulin secretion. *Nat Med*. 2015;21(7):769-776. doi:10.1038/nm.3872.

75. Braun M, Ramracheya R, Bengtsson M, et al. Gamma-aminobutyric acid (GABA) is an autocrine excitatory transmitter in human pancreatic beta-cells. *Diabetes*. 2010;59(7):1694-1701. doi:10.2337/db09-0797.

76. Wendt A, Birnir B, Buschard K, et al. Glucose inhibition of glucagon secretion from rat alpha-cells is mediated by GABA released from neighboring beta-cells. *Diabetes*. 2004;53(4):1038-1045.

77. Almaça J, Molina J, Menegaz D, et al. Human Beta Cells Produce and Release Serotonin to Inhibit Glucagon Secretion from Alpha Cells. *Cell Rep*. 2016;17(12):3281-3291. doi:10.1016/j.celrep.2016.11.072.

78. Moore CX, Cooper GJ. Co-secretion of amylin and insulin from cultured islet beta-cells: modulation by nutrient secretagogues, islet hormones and hypoglycemic agents. *Biochem Biophys Res Commun*. 1991;179(1):1-9.

79. Mulder H, Ahrén B, Sundler F. Islet amyloid polypeptide and insulin gene expression are regulated in parallel by glucose in vivo in rats. *Am J Physiol*. 1996;271(6 Pt 1):E1008-E1014. doi:10.1152/ajpendo.1996.271.6.E1008.

80. Gedulin BR, Jodka CM, Herrmann K, Young AA. Role of endogenous amylin in glucagon secretion and gastric emptying in rats demonstrated with the selective antagonist, AC187. *Regul Pept*. 2006;137(3):121-127. doi:10.1016/j.regpep.2006.06.004.

81. Rorsman P, Huising MO. The somatostatin-secreting pancreatic δ-cell in health and disease. *Nat Rev Endocrinol*. 2018;14(7):404-414. doi:10.1038/s41574-018-0020-6.

82. Goodman RH, Montminy MR, Low MJ, Habener JF. Biosynthesis of rat preprosomatostatin. *Adv Exp Med Biol*. 1985;188:31-47.

83. Francis BH, Baskin DG, Saunders DR, Ensinck JW. Distribution of somatostatin-14 and somatostatin-28 gastrointestinal-pancreatic cells of rats and humans. *Gastroenterology*. 1990;99(5):1283-1291.

84. de Heer J, Rasmussen C, Coy DH, Holst JJ. Glucagon-like peptide-1, but not glucose-dependent insulinotropic peptide, inhibits glucagon secretion via somatostatin (receptor subtype 2) in the perfused rat pancreas. *Diabetologia*. 2008;51(12):2263-2270. doi:10.1007/s00125-008-1149-y.

85. Hauge-Evans AC, Anderson RL, Persaud SJ, Jones PM. Delta cell secretory responses to insulin secretagogues are not mediated indirectly by insulin. *Diabetologia*. 2012;55(7):1995-2004. doi:10.1007/s00125-012-2546-9.

86. DiGruccio MR, Mawla AM, Donaldson CJ, et al. Comprehensive alpha, beta and delta cell transcriptomes reveal that ghrelin selectively activates delta cells and promotes somatostatin release from pancreatic islets. *Mol Metab*. 2016;5(7):449-458. doi:10.1016/j.molmet.2016.04.007.

87. Patton GS, Ipp E, Dobbs RE, Orci L, Vale W, Unger RH. Pancreatic immunoreactive somatostatin release. *Proc Natl Acad Sci USA*. 1977;74(5):2140-2143.

88. Weir GC, Samols E, Day JA, Patel YC. Glucose and glucagon stimulate the secretion of somatostatin from the perfused canine pancreas. *Metab Clin Exp*. 1978;27(9 Suppl 1):1223-1226.

89. Kieffer TJ, Heller RS, Unson CG, Weir GC, Habener JF. Distribution of glucagon receptors on hormone-specific endocrine cells of rat pancreatic islets. *Endocrinology*. 1996;137(11):5119-5125. doi:10.1210/endo.137.11.8895386.

90. Portela-Gomes GM, Stridsberg M, Grimelius L, Oberg K, Janson ET. Expression of the five different somatostatin receptor subtypes in endocrine cells of the pancreas. *Appl Immunohistochem Mol Morphol*. 2000;8(2):126-132.

91. Strowski MZ, Parmar RM, Blake AD, Schaeffer JM. Somatostatin inhibits insulin and glucagon secretion via two receptors subtypes: an in vitro study of pancreatic islets from somatostatin receptor 2 knockout mice. *Endocrinology*. 2000;141(1):111-117. doi:10.1210/endo.141.1.7263.

92. Ludvigsen E, Olsson R, Stridsberg M, Janson ET, Sandler S. Expression and distribution of somatostatin receptor subtypes in the pancreatic islets of mice and rats. *J Histochem Cytochem*. 2004;52(3):391-400. doi:10.1177/002215540405200310.

93. Wierup N, Svensson H, Mulder H, Sundler F. The ghrelin cell: a novel developmentally regulated islet cell in the human pancreas. *Regul Pept*. 2002;107(1-3):63-69.

94. Date Y, Kojima M, Hosoda H, et al. Ghrelin, a novel growth hormone-releasing acylated peptide, is synthesized in a distinct endocrine cell type in the gastrointestinal tracts of rats and humans. *Endocrinology*. 2000;141(11):4255-4261. doi:10.1210/endo.141.11.7757.

95. Tschöp M, Smiley DL, Heiman ML. Ghrelin induces adiposity in rodents. *Nature*. 2000;407(6806):908-913. doi:10.1038/35038090.

96. Tschöp M, Wawarta R, Riepl RL, et al. Post-prandial decrease of circulating human ghrelin levels. *J Endocrinol Invest*. 2001;24(6):RC19-RC21. doi:10.1007/BF03351037.

97. Chanoine J-P, Wong ACK. Ghrelin gene expression is markedly higher in fetal pancreas compared with fetal stomach: effect of maternal fasting. *Endocrinology*. 2004;145(8):3813-3820. doi:10.1210/en.2004-0053.

98. Walia P, Asadi A, Kieffer TJ, Johnson JD, Chanoine J-P. Ontogeny of ghrelin, obestatin, preproghrelin, and prohormone convertases in rat pancreas and stomach. *Pediatr Res*. 2009;65(1):39-44. doi:10.1203/PDR.0b013e31818bc134.

99. Zhang JV, Ren P-G, Avsian-Kretchmer O, et al. Obestatin, a peptide encoded by the ghrelin gene, opposes ghrelin's effects on food intake. *Science*. 2005;310(5750):996-999. doi:10.1126/science.1117255.

100. Gualillo O, Lago F, Casanueva FF, Dieguez C. One ancestor, several peptides post-translational modifications of preproghrelin generate several peptides with antithetical effects. *Mol Cell Endocrinol*. 2006;256(1-2):1-8. doi:10.1016/j.mce.2006.05.007.

101. Cowan E, Burch KJ, Green BD, Grieve DJ. Obestatin as a key regulator of metabolism and cardiovascular function with emerging therapeutic potential for diabetes. *Br J Pharmacol*. 2016;173(14):2165-2181. doi:10.1111/bph.13502.

102. Mundinger TO, Cummings DE, Taborsky GJ. Direct stimulation of ghrelin secretion by sympathetic nerves. *Endocrinology*. 2006;147(6):2893-2901. doi:10.1210/en.2005-1182.

103. Zhao T-J, Sakata I, Li RL, et al. Ghrelin secretion stimulated by {beta}1-adrenergic receptors in cultured ghrelinoma cells and in fasted mice. *Proc Natl Acad Sci USA*. 2010;107(36):15868-15873. doi:10.1073/pnas.1011116107.

104. Gagnon J, Anini Y. Glucagon stimulates ghrelin secretion through the activation of MAPK and EPAC and potentiates the effect of norepinephrine. *Endocrinology*. 2013;154(2):666-674. doi:10.1210/en.2012-1994.

105. Date Y, Nakazato M, Hashiguchi S, et al. Ghrelin is present in pancreatic alpha-cells of humans and rats and stimulates insulin secretion. *Diabetes*. 2002;51(1):124-129.

106. Egido EM, Rodriguez-Gallardo J, Silvestre RA, Marco J. Inhibitory effect of ghrelin on insulin and pancreatic somatostatin secretion. *Eur J Endocrinol*. 2002;146(2):241-244.

107. Salehi A, Dornonville de la Cour C, Håkanson R, Lundquist I. Effects of ghrelin on insulin and glucagon secretion: a study of isolated pancreatic islets and intact mice. *Regul Pept*. 2004;118(3):143-150. doi:10.1016/j.regpep.2003.12.001.

108. Xin Y, Kim J, Ni M, et al. Use of the Fluidigm C1 platform for RNA sequencing of single mouse pancreatic islet cells. *Proc Natl Acad Sci USA*. 2016;113(12):3293-3298. doi:10.1073/pnas.1602306113.

109. Qader SS, Håkanson R, Rehfeld JF, Lundquist I, Salehi A. Proghrelin-derived peptides influence the secretion of insulin, glucagon, pancreatic polypeptide and somatostatin: a study on isolated islets from mouse and rat pancreas. *Regul Pept*. 2008;146(1-3):230-237. doi:10.1016/j.regpep.2007.09.017.

110. Wang X, Zielinski MC, Misawa R, et al. Quantitative analysis of pancreatic polypeptide cell distribution in the human pancreas. Shi X, ed. *PLoS ONE*. 2013;8(1):e55501. doi:10.1371/journal.pone.0055501.

111. Yamamoto H, Nata K, Okamoto H. Mosaic evolution of prepropancreatic polypeptide. *J Biol Chem*. 1986;261(14):6156-6159.

112. Schwartz TW, Stenquist B, Olbe L, Stadil F. Synchronous oscillations in the basal secretion of pancreatic-polypeptide and gastric acid. Depression by cholinergic blockade of pancreatic-polypeptide concentrations in plasma. *Gastroenterology*. 1979;76(1):14-19.

113. Chen MH, Joffe SN, Magee DF, Murphy RF, Naruse S. Cyclic changes of plasma pancreatic polypeptide and pancreatic secretion in fasting dogs. *J Physiol (Lond)*. 1983;341:453-461. doi:10.1111/(ISSN)1469-7793.

114. Schwartz TW, Holst JJ, Fahrenkrug J, et al. Vagal, cholinergic regulation of pancreatic polypeptide secretion. *J Clin Invest*. 1978;61(3):781-789. doi:10.1172/JCI108992.

115. Okita M, Inui A, Baba S, Kasuga M. Central cholinergic regulation of pancreatic polypeptide secretion in conscious dogs. *J Endocrinol*. 1997;154(2):311-317.

116. Wilson RM, Boden G, Owen OE. Pancreatic polypeptide responses to a meal and to intraduodenal amino acids and sodium oleate. *Endocrinology*. 1978;102(3):859-863. doi:10.1210/endo-102-3-859.

117. Havel PJ, Parry SJ, Curry DL, Stern JS, Akpan JO, Gingerich RL. Autonomic nervous system mediation of the pancreatic polypeptide response to insulin-induced hypoglycemia in conscious rats. *Endocrinology*. 1992;130(4):2225-2229. doi:10.1210/endo.130.4.1347741.

118. Gregor P, Feng Y, DeCarr LB, Cornfield LJ, McCaleb ML. Molecular characterization of a second mouse pancreatic polypeptide receptor and its inactivated human homologue. *J Biol Chem*. 1996;271(44):27776-27781.

119. Larhammar D. Structural diversity of receptors for neuropeptide Y, peptide YY and pancreatic polypeptide. *Regul Pept*. 1996;65(3):165-174.

120. Yulyaningsih E, Loh K, Lin S, et al. Pancreatic polypeptide controls energy homeostasis via Npy6r signaling in the suprachiasmatic nucleus in mice. *Cell Metab*. 2014;19(1):58-72. doi:10.1016/j.cmet.2013.11.019.

121. Asakawa A, Inui A, Yuzuriha H, et al. Characterization of the effects of pancreatic polypeptide in the regulation of energy balance. *Gastroenterology*. 2003;124(5):1325-1336.

122. Batterham RL, Le Roux CW, Cohen MA, et al. Pancreatic polypeptide reduces appetite and food intake in humans. *J Clin Endocrinol Metab*. 2003;88(8):3989-3992. doi:10.1210/jc.2003-030630.

123. Schmidt PT, Näslund E, Grybäck P, et al. A role for pancreatic polypeptide in the regulation of gastric emptying and short-term metabolic control. *J Clin Endocrinol Metab*. 2005;90(9):5241-5246. doi:10.1210/jc.2004-2089.

124. Lin TM, Evans DC, Chance RE, Spray GF. Bovine pancreatic peptide: action on gastric and pancreatic secretion in dogs. *Am J Physiol*. 1977;232(3):E311-E315. doi:10.1152/ajpendo.1977.232.3.E311.

125. Weyer C, Salbe AD, Lindsay RS, Pratley RE, Bogardus C, Tataranni PA. Exaggerated pancreatic polypeptide secretion in Pima Indians: can an increased parasympathetic drive to the pancreas contribute to hyperinsulinemia, obesity, and diabetes in humans? *Metab Clin Exp*. 2001;50(2):223-230. doi:10.1053/meta.2001.20170.

126. Lewis SL, Tam PPL. Definitive endoderm of the mouse embryo: formation, cell fates, and morphogenetic function. *Dev Dyn*. 2006;235(9):2315-2329. doi:10.1002/dvdy.20846.

127. Jennings RE, Berry AA, Strutt JP, Gerrard DT, Hanley NA. Human pancreas development. *Development*. 2015;142(18):3126-3137. doi:10.1242/dev.120063.

128. Li H, Arber S, Jessell TM, Edlund H. Selective agenesis of the dorsal pancreas in mice lacking homeobox gene Hlxb9. *Nat Genet*. 1999;23(1):67-70. doi:10.1038/12669.

129. Jørgensen MC, Ahnfelt-Rønne J, Hald J, Madsen OD, Serup P, Hecksher-Sørensen J. An illustrated review of early pancreas development in the mouse. *Endocr Rev*. 2007;28(6):685-705. doi:10.1210/er.2007-0016.

130. Jennings RE, Berry AA, Kirkwood-Wilson R, et al. Development of the human pancreas from foregut to endocrine commitment. *Diabetes*. 2013;62(10):3514-3522. doi:10.2337/db12-1479.

131. Hebrok M, Kim SK, Melton DA. Notochord repression of endodermal Sonic hedgehog permits pancreas development. *Genes Dev*. 1998;12(11):1705-1713.

132. Jennings RE, Berry AA, Kirkwood-Wilson R, et al. Development of the human pancreas from foregut to endocrine commitment. *Diabetes*. 2013;62(10):3514-3522. doi:10.2337/db12-1479.

133. Deutsch G, Jung J, Zheng M, Lóra J, Zaret KS. A bipotential precursor population for pancreas and liver within the embryonic endoderm. *Development*. 2001;128(6):871-881.

134. Spence JR, Lange AW, Lin S-CJ, et al. Sox17 regulates organ lineage segregation of ventral foregut progenitor cells. *Dev Cell*. 2009;17(1):62-74. doi:10.1016/j.devcel.2009.05.012.

135. Jennings RE, Berry AA, Gerrard DT, et al. Laser Capture and Deep Sequencing Reveals the Transcriptomic Programmes Regulating the Onset of Pancreas and Liver Differentiation in Human Embryos. *Stem Cell Reports*. 2017;9(5):1387-1394. doi:10.1016/j.stemcr.2017.09.018.

136. Seymour PA, Freude KK, Tran MN, et al. SOX9 is required for maintenance of the pancreatic progenitor cell pool. *Proc Natl Acad Sci USA*. 2007;104(6):1865-1870. doi:10.1073/pnas.0609217104.

137. Kawaguchi Y, Cooper B, Gannon M, Ray M, MacDonald RJ, Wright CVE. The role of the transcriptional regulator Ptf1a in converting intestinal to pancreatic progenitors. *Nat Genet*. 2002;32(1):128-134. doi:10.1038/ng959.

138. Willet SG, Hale MA, Grapin-Botton A, Magnuson MA, MacDonald RJ, Wright CVE. Dominant and context-specific control of endodermal organ allocation by Ptf1a. *Development*. 2014;141(22):4385-4394. doi:10.1242/dev.114165.

139. Weedon MN, Cebola I, Patch A-M, et al. Recessive mutations in a distal PTF1A enhancer cause isolated pancreatic agenesis. *Nat Genet*. 2014;46(1):61-64. doi:10.1038/ng.2826.

140. Evliyaoğlu O, Ercan O, Ataoğlu E, et al. Neonatal Diabetes: Two Cases with Isolated Pancreas Agenesis due to Homozygous PTF1A Enhancer Mutations and One with Developmental Delay, Epilepsy, and Neonatal Diabetes Syndrome due to KCNJ11 Mutation. *J Clin Res Pediatr Endocrinol*. 2018;10(2):168-174. doi:10.4274/jcrpe.5162.

141. Sussel L, Kalamaras J, Hartigan-O'Connor DJ, et al. Mice lacking the homeodomain transcription factor Nkx2.2 have diabetes due to arrested differentiation of pancreatic beta cells. *Development*. 1998;125(12):2213-2221.

142. Chiang M-K, Melton DA. Single-cell transcript analysis of pancreas development. *Dev Cell*. 2003;4(3):383-393.

143. Villasenor A, Chong DC, Cleaver O. Biphasic Ngn3 expression in the developing pancreas. *Dev Dyn*. 2008;237(11):3270-3279. doi:10.1002/dvdy.21740.

144. Shih HP, Panlasigui D, Cirulli V, Sander M. ECM Signaling Regulates Collective Cellular Dynamics to Control Pancreas Branching Morphogenesis. *Cell Rep*. 2016;14(2):169-179. doi:10.1016/j.celrep.2015.12.027.

145. Afelik S, Pool B, Schmerr M, Penton C, Jensen J. Wnt7b is required for epithelial progenitor growth and operates during epithelial-to-mesenchymal signaling in pancreatic development. *Developmental Biology*. 2015;399(2):204-217. doi:10.1016/j.ydbio.2014.12.031.

146. Pujadas G, Cervantes S, Tutusaus A, et al. Wnt9a deficiency discloses a repressive role of Tcf7l2 on endocrine differentiation in the embryonic pancreas. *Sci Rep*. 2016;6:19223. doi:10.1038/srep19223.

147. Apelqvist A, Li H, Sommer L, et al. Notch signalling controls pancreatic cell differentiation. *Nature*. 1999;400(6747):877-881. doi:10.1038/23716.

148. Jensen J, Pedersen EE, Galante P, et al. Control of endodermal endocrine development by Hes-1. *Nat Genet*. 2000;24(1):36-44. doi:10.1038/71657.

149. Miralles F, Czernichow P, Ozaki K, Itoh N, Scharfmann R. Signaling through fibroblast growth factor receptor 2b plays a key role in the development of the exocrine pancreas. *Proc Natl Acad Sci USA*. 1999;96(11):6267-6272.

150. Gao N, LeLay J, Vatamaniuk MZ, Rieck S, Friedman JR, Kaestner KH. Dynamic regulation of Pdx1 enhancers by Foxa1 and Foxa2 is essential for pancreas development. *Genes Dev*. 2008;22(24):3435-3448. doi:10.1101/gad.1752608.

151. Pan FC, Wright C. Pancreas organogenesis: from bud to plexus to gland. *Dev Dyn*. 2011;240(3):530-565. doi:10.1002/dvdy.22584.

152. Stanger BZ, Tanaka AJ, Melton DA. Organ size is limited by the number of embryonic progenitor cells in the pancreas but not the liver. *Nature*. 2007;445(7130):886-891. doi:10.1038/nature05537.

153. Decker K, Goldman DC, Grasch CL, Sussel L. Gata6 is an important regulator of mouse pancreas development. *Developmental Biology*. 2006;298(2):415-429. doi:10.1016/j.ydbio.2006.06.046.

154. Zhou Q, Law AC, Rajagopal J, Anderson WJ, Gray PA, Melton DA. A multipotent progenitor domain guides pancreatic organogenesis. *Dev Cell*. 2007;13(1):103-114. doi:10.1016/j.devcel.2007.06.001.

155. Schaffer AE, Freude KK, Nelson SB, Sander M. Nkx6 transcription factors and Ptf1a function as antagonistic lineage determinants in multipotent pancreatic progenitors. *Dev Cell*. 2010;18(6):1022-1029. doi:10.1016/j.devcel.2010.05.015.

156. Solar M, Cardalda C, Houbracken I, et al. Pancreatic exocrine duct cells give rise to insulin-producing beta cells during embryogenesis but not after birth. *Dev Cell*. 2009;17(6):849-860. doi:10.1016/j.devcel.2009.11.003.

157. Briscoe J, Pierani A, Jessell TM, Ericson J. A homeodomain protein code specifies progenitor cell identity and neuronal fate in the ventral neural tube. *Cell*. 2000;101(4):435-445.

158. Afelik S, Qu X, Hasrouni E, et al. Notch-mediated patterning and cell fate allocation of pancreatic progenitor cells. *Development*. 2012;139(10):1744-1753. doi:10.1242/dev.075804.

159. Gradwohl G, Dierich A, LeMeur M, Guillemot F. neurogenin3 is required for the development of the four endocrine cell lineages of the pancreas. *Proc Natl Acad Sci USA*. 2000;97(4):1607-1611.

160. Schwitzgebel VM, Scheel DW, Conners JR, et al. Expression of neurogenin3 reveals an islet cell precursor population in the pancreas. *Development*. 2000;127(16):3533-3542.

161. Gu G, Dubauskaite J, Melton DA. Direct evidence for the pancreatic lineage: NGN3+ cells are islet progenitors and are distinct from duct progenitors. *Development*. 2002;129(10):2447-2457.

162. Wang S, Yan J, Anderson DA, et al. Neurog3 gene dosage regulates allocation of endocrine and exocrine cell fates in the developing mouse pancreas. *Developmental Biology*. 2010;339(1):26-37. doi:10.1016/j.ydbio.2009.12.009.

163. Wang S, Jensen JN, Seymour PA, et al. Sustained Neurog3 expression in hormone-expressing islet cells is required for endocrine maturation and function. *Proc Natl Acad Sci USA*. 2009;106(24):9715-9720. doi:10.1073/pnas.0904247106.

164. Magenheim J, Klein AM, Stanger BZ, et al. Ngn3(+) endocrine progenitor cells control the fate and morphogenesis of pancreatic ductal epithelium. *Developmental Biology*. 2011;359(1):26-36. doi:10.1016/j.ydbio.2011.08.006.

165. Bankaitis ED, Bechard ME, Wright CVE. Feedback control of growth, differentiation, and morphogenesis of pancreatic endocrine progenitors in an epithelial plexus niche. *Genes Dev*. 2015;29(20):2203-2216. doi:10.1101/gad.267914.115.

166. Shih HP, Kopp JL, Sandhu M, et al. A Notch-dependent molecular circuitry initiates pancreatic endocrine and ductal cell differentiation. *Development*. 2012;139(14):2488-2499. doi:10.1242/dev.078634.

167. Rukstalis JM, Habener JF. Snail2, a mediator of epithelial-mesenchymal transitions, expressed in progenitor cells of the developing endocrine pancreas. *Gene Expr Patterns*. 2007;7(4):471-479. doi:10.1016/j.modgep.2006.11.001.

168. Gouzi M, Kim YH, Katsumoto K, Johansson K, Grapin-Botton A. Neurogenin3 initiates stepwise delamination of differentiating endocrine cells during pancreas development. *Dev Dyn*. 2011;240(3):589-604. doi:10.1002/dvdy.22544.

169. Metzger DE, Gasperowicz M, Otto F, Cross JC, Gradwohl G, Zaret KS. The transcriptional co-repressor Grg3/Tle3 promotes pancreatic endocrine progenitor delamination and β-cell differentiation. *Development*. 2012;139(8):1447-1456. doi:10.1242/dev.072892.

170. Barrallo-Gimeno A, Nieto MA. The Snail genes as inducers of cell movement and survival: implications in development and cancer. *Development*. 2005;132(14):3151-3161. doi:10.1242/dev.01907.

171. Kaul A, Schuster E, Jennings BH. The Groucho co-repressor is primarily recruited to local target sites in active chromatin to attenuate transcription. Russell S, ed. *PLoS Genet*. 2014;10(8):e1004595. doi:10.1371/journal.pgen.1004595.

172. Salisbury RJ, Blaylock J, Berry AA, et al. The window period of NEUROGENIN3 during human gestation. *Islets*. 2014;6(3):e954436. doi:10.4161/19382014.2014.954436.

173. Naya FJ, Huang HP, Qiu Y, et al. Diabetes, defective pancreatic morphogenesis, and abnormal enteroendocrine differentiation in BETA2/neuroD-deficient mice. *Genes Dev*. 1997;11(18):2323-2334.

174. Mellitzer G, Bonné S, Luco RF, et al. IA1 is NGN3-dependent and essential for differentiation of the endocrine pancreas. *EMBO J*. 2006;25(6):1344-1352. doi:10.1038/sj.emboj.7601011.

175. Du A, Hunter CS, Murray J, et al. Islet-1 is required for the maturation, proliferation, and survival of the endocrine pancreas. *Diabetes*. 2009;58(9):2059-2069. doi:10.2337/db08-0987.

176. Smith SB, Qu H-Q, Taleb N, et al. Rfx6 directs islet formation and insulin production in mice and humans. *Nature*. 2010;463(7282):775-780. doi:10.1038/nature08748.

177. Prado CL, Pugh-Bernard AE, Elghazi L, Sosa-Pineda B, Sussel L. Ghrelin cells replace insulin-producing beta cells in two mouse models of pancreas development. *Proc Natl Acad Sci USA*. 2004;101(9):2924-2929. doi:10.1073/pnas.0308604100.

178. St-Onge L, Sosa-Pineda B, Chowdhury K, Mansouri A, Gruss P. Pax6 is required for differentiation of glucagon-producing alpha-cells in mouse pancreas. *Nature*. 1997;387(6631):406-409. doi:10.1038/387406a0.

179. Collombat P, Mansouri A, Hecksher-Sørensen J, et al. Opposing actions of Arx and Pax4 in endocrine pancreas development. *Genes Dev*. 2003;17(20):2591-2603. doi:10.1101/gad.269003.

180. Sosa-Pineda B, Chowdhury K, Torres M, Oliver G, Gruss P. The Pax4 gene is essential for differentiation of insulin-producing beta cells in the mammalian pancreas. *Nature*. 1997;386(6623):399-402. doi:10.1038/386399a0.

181. Collombat P, Hecksher-Sørensen J, Broccoli V, et al. The simultaneous loss of Arx and Pax4 genes promotes a somatostatin-producing cell fate specification at the expense of the alpha- and beta-cell lineages in the mouse endocrine pancreas. *Development*. 2005;132(13):2969-2980. doi:10.1242/dev.01870.

182. Scharfmann R, Xiao X, Heimberg H, Mallet J, Ravassard P. Beta cells within single human islets originate from multiple progenitors. Chan-Ling T, ed. *PLoS ONE*. 2008;3(10):e3559. doi:10.1371/journal.pone.0003559.

183. Desgraz R, Herrera PL. Pancreatic neurogenin 3-expressing cells are unipotent islet precursors. *Development*. 2009;136(21):3567-3574. doi:10.1242/dev.039214.

184. Miller K, Kim A, Kilimnik G, et al. Islet formation during the neonatal development in mice. Maedler K, ed. *PLoS ONE*. 2009;4(11):e7739. doi:10.1371/journal.pone.0007739.

185. Chen H, Gu X, Liu Y, et al. PDGF signalling controls age-dependent proliferation in pancreatic β-cells. *Nature*. 2011;478(7369):349-355. doi:10.1038/nature10502.

186. Gregg BE, Moore PC, Demozay D, et al. Formation of a human β-cell population within pancreatic islets is set early in life. *J Clin Endocrinol Metab*. 2012;97(9):3197-3206. doi:10.1210/jc.2012-1206.

187. Arda HE, Li L, Tsai J, et al. Age-Dependent Pancreatic Gene Regulation Reveals Mechanisms Governing Human β Cell Function. *Cell Metab*. 2016;23(5):909-920. doi:10.1016/j.cmet.2016.04.002.

188. Miyatsuka T, Kosaka Y, Kim H, German MS. Neurogenin3 inhibits proliferation in endocrine progenitors by inducing Cdkn1a. *Proc Natl Acad Sci USA*. 2011;108(1):185-190. doi:10.1073/pnas.1004842108.

189. Bechard ME, Bankaitis ED, Ustione A, Piston DW, Magnuson MA, Wright CVE. FUCCI tracking shows cell-cycle-dependent Neurog3 variation in pancreatic progenitors. *Genesis*. 2017;55(9):e23050. doi:10.1002/dvg.23050.

190. Greiner TU, Kesavan G, Ståhlberg A, Semb H. Rac1 regulates pancreatic islet morphogenesis. *BMC Dev Biol*. 2009;9(1):2. doi:10.1186/1471-213X-9-2.

191. Riedel MJ, Asadi A, Wang R, Ao Z, Warnock GL, Kieffer TJ. Immunohistochemical characterisation of cells co-producing insulin and glucagon in the developing human pancreas. *Diabetologia*. 2012;55(2):372-381. doi:10.1007/s00125-011-2344-9.

192. Pierreux CE, Poll AV, Kemp CR, et al. The transcription factor hepatocyte nuclear factor-6 controls the development of pancreatic ducts in the mouse. *Gastroenterology*. 2006;130(2):532-541. doi:10.1053/j.gastro.2005.12.005.

193. Rovira M, Scott S-G, Liss AS, Jensen J, Thayer SP, Leach SD. Isolation and characterization of centroacinar/terminal ductal progenitor cells in adult mouse pancreas. *Proc Natl Acad Sci USA*. 2010;107(1):75-80. doi:10.1073/pnas.0912589107.

194. Douville J, Beaulieu R, Balicki D. ALDH1 as a functional marker of cancer stem and progenitor cells. *Stem Cells Dev*. 2009;18(1):17-25. doi:10.1089/scd.2008.0055.

195. Masui T, Swift GH, Deering T, et al. Replacement of Rbpj with Rbpjl in the PTF1 complex controls the final maturation of pancreatic acinar cells. *Gastroenterology*. 2010;139(1):270-280. doi:10.1053/j.gastro.2010.04.003.

196. Hoang CQ, Hale MA, Azevedo-Pouly AC, et al. Transcriptional Maintenance of Pancreatic Acinar Identity, Differentiation, and Homeostasis by PTF1A. *Mol Cell Biol*. 2016;36(24):3033-3047. doi:10.1128/MCB.00358-16.

197. Pin CL, Rukstalis JM, Johnson C, Konieczny SF. The bHLH transcription factor Mist1 is required to maintain exocrine pancreas cell organization and

acinar cell identity. *J Cell Biol*. 2001;155(4):519-530. doi:10.1083/jcb.200105060.

198. Jiang M, Azevedo-Pouly A, Deering TG, et al. MIST1 and PTF1 Collaborate in Feed-forward Regulatory Loops that Maintain the Pancreatic Acinar Phenotype in Adult Mice. *Mol Cell Biol*. 2016;36(23):2945-2955. doi:10.1128/MCB.00370-16.

199. NCD Risk Factor Collaboration (NCD-RisC). Worldwide trends in diabetes since 1980: a pooled analysis of 751 population-based studies with 4.4 million participants. *Lancet*. 2016;387(10027):1513-1530. doi:10.1016/S0140-6736(16)00618-8.

200. Mathers CD, Loncar D. Projections of global mortality and burden of disease from 2002 to 2030. Samet J, ed. *PLoS Med*. 2006;3(11):e442. doi:10.1371/journal.pmed.0030442.

201. Katsarou A, Gudbjörnsdottir S, Rawshani A, et al. Type 1 diabetes mellitus. *Nat Rev Dis Primers*. 2017;3:17016. doi:10.1038/nrdp.2017.16.

202. DeFronzo RA, Ferrannini E, Groop L, et al. Type 2 diabetes mellitus. *Nat Rev Dis Primers*. 2015;1:15019. doi:10.1038/nrdp.2015.19.

203. Gilmartin ABH, Ural SH, Repke JT. Gestational diabetes mellitus. *Rev Obstet Gynecol*. 2008;1(3):129-134.

204. Yang Q, Yamagata K, Fukui K, et al. Hepatocyte nuclear factor-1alpha modulates pancreatic beta-cell growth by regulating the expression of insulin-like growth factor-1 in INS-1 cells. *Diabetes*. 2002;51(6):1785-1792.

205. Gardner DS, Tai ES. Clinical features and treatment of maturity onset diabetes of the young (MODY). *Diabetes Metab Syndr Obes*. 2012;5:101-108. doi:10.2147/DMSO.S23353.

206. Rawshani A, Landin-Olsson M, Svensson A-M, et al. The incidence of diabetes among 0-34 year olds in Sweden: new data and better methods. *Diabetologia*. 2014;57(7):1375-1381. doi:10.1007/s00125-014-3225-9.

207. Velthuis JH, Unger WW, Abreu JRF, et al. Simultaneous detection of circulating autoreactive CD8+ T-cells specific for different islet cell-associated epitopes using combinatorial MHC multimers. *Diabetes*. 2010;59(7):1721-1730. doi:10.2337/db09-1486.

208. Oling V, Reijonen H, Simell O, Knip M, Ilonen J. Autoantigen-specific memory CD4+ T cells are prevalent early in progression to Type 1 diabetes. *Cell Immunol*. 2012;273(2):133-139. doi:10.1016/j.cellimm.2011.12.008.

209. Patterson CC, Dahlquist GG, Gyürüs E, Green A, Soltész G, EURODIAB Study Group. Incidence trends for childhood type 1 diabetes in Europe during 1989-2003 and predicted new cases 2005-20: a multicentre prospective registration study. *Lancet*. 2009;373(9680):2027-2033. doi:10.1016/S0140-6736(09)60568-7.

210. Mayer-Davis EJ, Lawrence JM, Dabelea D, et al. Incidence Trends of Type 1 and Type 2 Diabetes among Youths, 2002-2012. *N Engl J Med*. 2017;376(15):1419-1429. doi:10.1056/NEJMoa1610187.

211. You W-P, Henneberg M. Type 1 diabetes prevalence increasing globally and regionally: the role of natural selection and life expectancy at birth. *BMJ Open Diabetes Res Care*. 2016;4(1):e000161. doi:10.1136/bmjdrc-2015-000161.

212. Beyerlein A, Donnachie E, Jergens S, Ziegler A-G. Infections in Early Life and Development of Type 1 Diabetes. *JAMA*. 2016;315(17):1899-1901. doi:10.1001/jama.2016.2181.

213. Mustonen N, Siljander H, Peet A, et al. Early childhood infections precede development of beta-cell autoimmunity and type 1 diabetes in children with HLA-conferred disease risk. *Pediatr Diabetes*. 2018;19(2):293-299. doi:10.1111/pedi.12547.

214. La Torre D, Seppänen-Laakso T, Larsson HE, et al. Decreased cord-blood phospholipids in young age-at-onset type 1 diabetes. *Diabetes*. 2013;62(11):3951-3956. doi:10.2337/db13-0215.

215. Oresic M, Gopalacharyulu P, Mykkänen J, et al. Cord serum lipidome in prediction of islet autoimmunity and type 1 diabetes. *Diabetes*. 2013;62(9):3268-3274. doi:10.2337/db13-0159.

216. Hu Y, Wong FS, Wen L. Antibiotics, gut microbiota, environment in early life and type 1 diabetes. *Pharmacol Res*. 2017;119:219-226. doi:10.1016/j.phrs.2017.01.034.

217. Giacco F, Brownlee M. Oxidative stress and diabetic complications. *Circ Res*. 2010;107(9):1058-1070. doi:10.1161/CIRCRESAHA.110.223545.

218. de Ferranti SD, de Boer IH, Fonseca V, et al. Type 1 diabetes mellitus and cardiovascular disease: a scientific statement from the American Heart Association and American Diabetes Association. *Circulation*. 2014;130(13):1110-1130. doi:10.1161/CIR.0000000000000034.

219. Lind M, Svensson A-M, Kosiborod M, et al. Glycemic control and excess mortality in type 1 diabetes. *N Engl J Med*. 2014;371(21):1972-1982. doi:10.1056/NEJMoa1408214.

220. Livingstone SJ, Levin D, Looker HC, et al. Estimated life expectancy in a Scottish cohort with type 1 diabetes, 2008-2010. *JAMA*. 2015;313(1):37-44. doi:10.1001/jama.2014.16425.

221. Rahier J, Guiot Y, Goebbels RM, Sempoux C, Henquin JC. Pancreatic beta-cell mass in European subjects with type 2 diabetes. *Diabetes, Obesity and Metabolism*. 2008;10 Suppl 4(Suppl. 1):32-42. doi:10.1111/j.1463-1326.2008.00969.x.

222. Masini M, Bugliani M, Lupi R, et al. Autophagy in human type 2 diabetes pancreatic beta cells. *Diabetologia*. 2009;52(6):1083-1086. doi:10.1007/s00125-009-1347-2.

223. Marselli L, Bugliani M, Suleiman M, et al. β-Cell inflammation in human type 2 diabetes and the role of autophagy. *Diabetes, Obesity and Metabolism*. 2013;15 Suppl 3(s3):130-136. doi:10.1111/dom.12152.

224. Henquin JC, Rahier J. Pancreatic alpha cell mass in European subjects with type 2 diabetes. *Diabetologia*. 2011;54(7):1720-1725. doi:10.1007/s00125-011-2118-4.

225. Nguyen QM, Xu J-H, Chen W, Srinivasan SR, Berenson GS. Correlates of age onset of type 2 diabetes among relatively young black and white adults in a community: the Bogalusa Heart Study. *Diabetes Care*. 2012;35(6):1341-1346. doi:10.2337/dc11-1818.

226. Wang YC, McPherson K, Marsh T, Gortmaker SL, Brown M. Health and economic burden of the projected obesity trends in the USA and the UK. *Lancet*. 2011;378(9793):815-825. doi:10.1016/S0140-6736(11)60814-3.

227. Hu FB. Globalization of diabetes: the role of diet, lifestyle, and genes. *Diabetes Care*. 2011;34(6):1249-1257. doi:10.2337/dc11-0442.

228. Grøntved A, Rimm EB, Willett WC, Andersen LB, Hu FB. A prospective study of weight training and risk of type 2 diabetes mellitus in men. *Arch Intern Med*. 2012;172(17):1306-1312. doi:10.1001/archinternmed.2012.3138.

229. Ley SH, Hamdy O, Mohan V, Hu FB. Prevention and management of type 2 diabetes: dietary components and nutritional strategies. *Lancet*. 2014;383(9933):1999-2007. doi:10.1016/S0140-6736(14)60613-9.

230. Gerstein HC, Santaguida P, Raina P, et al. Annual incidence and relative risk of diabetes in people with various categories of dysglycemia: a systematic overview and meta-analysis of prospective studies. *Diabetes Res Clin Pract*. 2007;78(3):305-312. doi:10.1016/j.diabres.2007.05.004.

231. Copps KD, White MF. Regulation of insulin sensitivity by serine/threonine phosphorylation of insulin receptor substrate proteins IRS1 and IRS2. *Diabetologia*. 2012;55(10):2565-2582. doi:10.1007/s00125-012-2644-8.

232. Krssak M, Falk Petersen K, Dresner A, et al. Intramyocellular lipid concentrations are correlated with insulin sensitivity in humans: a 1H NMR spectroscopy study. *Diabetologia*. 1999;42(1):113-116. doi:10.1007/s001250051123.

233. Yu C, Chen Y, Cline GW, et al. Mechanism by which fatty acids inhibit insulin activation of insulin receptor substrate-1 (IRS-1)-associated phosphatidylinositol 3-kinase activity in muscle. *J Biol Chem*. 2002;277(52):50230-50236. doi:10.1074/jbc.M200958200.

234. Patti M-E, Corvera S. The role of mitochondria in the pathogenesis of type 2 diabetes. *Endocr Rev*. 2010;31(3):364-395. doi:10.1210/er.2009-0027.

235. Eizirik DL, Cardozo AK, Cnop M. The role for endoplasmic reticulum stress in diabetes mellitus. *Endocr Rev*. 2008;29(1):42-61. doi:10.1210/er.2007-0015.

236. Arkan MC, Hevener AL, Greten FR, et al. IKK-beta links inflammation to obesity-induced insulin resistance. *Nat Med*. 2005;11(2):191-198. doi:10.1038/nm1185.

237. Lebrun P, Van Obberghen E. SOCS proteins causing trouble in insulin action. *Acta Physiol (Oxf)*. 2008;192(1):29-36. doi:10.1111/j.1748-1716.2007.01782.x.

238. Lyssenko V, Jonsson A, Almgren P, et al. Clinical risk factors, DNA variants, and the development of type 2 diabetes. *N Engl J Med*. 2008;359(21):2220-2232. doi:10.1056/NEJMoa0801869.

239. Villareal DT, Robertson H, Bell GI, et al. TCF7L2 variant rs7903146 affects the risk of type 2 diabetes by modulating incretin action. *Diabetes*. 2010;59(2):479-485. doi:10.2337/db09-1169.

240. Adler AI, Stratton IM, Neil HA, et al. Association of systolic blood pressure with macrovascular and microvascular complications of type 2 diabetes (UKPDS 36): prospective observational study. *BMJ*. 2000;321(7258):412-419.

241. Holman RR, Farmer AJ, Davies MJ, et al. Three-year efficacy of complex insulin regimens in type 2 diabetes. *N Engl J Med*. 2009;361(18):1736-1747. doi:10.1056/NEJMoa0905479.

242. Schellenberg ES, Dryden DM, Vandermeer B, Ha C, Korownyk C. Lifestyle interventions for patients with and at risk for type 2 diabetes: a systematic review and meta-analysis. *Ann Intern Med*. 2013;159(8):543-551. doi:10.7326/0003-4819-159-8-201310150-00007.

243. Tancredi M, Rosengren A, Svensson A-M, et al. Excess Mortality among Persons with Type 2 Diabetes. *N Engl J Med*. 2015;373(18):1720-1732. doi:10.1056/NEJMoa1504347.

244. Loukine L, Waters C, Choi BC, Ellison J. Impact of diabetes mellitus on life expectancy and health-adjusted life expectancy in Canada. *Popul Health Metr*. 2012;10(1):7. doi:10.1186/1478-7954-10-7.

245. Tzakis AG, Ricordi C, Alejandro R, et al. Pancreatic islet transplantation after upper abdominal exenteration and liver replacement. *Lancet*. 1990;336(8712):402-405.

246. Shapiro AM, Lakey JR, Ryan EA, et al. Islet transplantation in seven patients with type 1 diabetes mellitus using a glucocorticoid-free immunosuppressive regimen. *N Engl J Med*. 2000;343(4):230-238. doi:10.1056/NEJM200007273430401.

247. Shapiro AMJ, Pokrywczynska M, Ricordi C. Clinical pancreatic islet transplantation. *Nat Rev Endocrinol*. 2017;13(5):268-277. doi:10.1038/nrendo.2016.178.

248. Bruin JE, Erener S, Vela J, et al. Characterization of polyhormonal insulin-producing cells derived in vitro from human embryonic stem cells. *Stem Cell Res*. 2014;12(1):194-208. doi:10.1016/j.scr.2013.10.003.

249. D'Amour KA, Bang AG, Eliazer S, et al. Production of pancreatic hormone–expressing endocrine cells from human embryonic stem cells. *Nat Biotechnol*. 2006;24(11):1392-1401. doi:10.1038/nbt1259.

250. Hrvatin S, O'Donnell CW, Deng F, et al. Differentiated human stem cells resemble fetal, not adult, β cells. *Proc Natl Acad Sci USA*. 2014;111(8):3038-3043. doi:10.1073/pnas.1400709111.

251. Pagliuca FW, Millman JR, Gürtler M, et al. Generation of functional human pancreatic β cells in vitro. *Cell*. 2014;159(2):428-439. doi:10.1016/j.cell.2014.09.040.

252. Rezania A, Bruin JE, Arora P, et al. Reversal of diabetes with insulin-producing cells derived in vitro from human pluripotent stem cells. *Nat Biotechnol*. September 2014. doi:10.1038/nbt.3033.

253. Taylor BL, Liu F-F, Sander M. Nkx6.1 is essential for maintaining the functional state of pancreatic beta cells. *Cell Rep*. 2013;4(6):1262-1275. doi:10.1016/j.celrep.2013.08.010.

254. Russ HA, Parent AV, Ringler JJ, et al. Controlled induction of human pancreatic progenitors produces functional beta-like cells in vitro. *EMBO J*. April 2015. doi:10.15252/embj.201591058.

255. Massumi M, Pourasgari F, Nalla A, et al. An Abbreviated Protocol for In Vitro Generation of Functional Human Embryonic Stem Cell-Derived Beta-Like Cells. Maedler K, ed. *PLoS ONE*. 2016;11(10):e0164457. doi:10.1371/journal.pone.0164457.

256. Ameri J, Borup R, Prawiro C, et al. Efficient Generation of Glucose-Responsive Beta Cells from Isolated GP2+ Human Pancreatic Progenitors. *Cell Rep*. 2017;19(1):36-49. doi:10.1016/j.celrep.2017.03.032.

257. Teo AKK, Lim CS, Cheow LF, et al. Single-cell analyses of human islet cells reveal de-differentiation signatures. *Cell Death Discov*. 2018;4(1):14. doi:10.1038/s41420-017-0014-5.

258. Kroon E, Martinson LA, Kadoya K, et al. Pancreatic endoderm derived from human embryonic stem cells generates glucose-responsive insulin-secreting cells in vivo. *Nat Biotechnol*. 2008;26(4):443-452. doi:10.1038/nbt1393.

259. Rostovskaya M, Bredenkamp N, Smith A. Towards consistent generation of pancreatic lineage progenitors from human pluripotent stem cells. *Philos*

Trans R Soc Lond, B, Biol Sci. 2015;370(1680):20140365. doi:10.1098/rstb.2014.0365.

260. Wang P, Fiaschi-Taesch NM, Vasavada RC, Scott DK, García-Ocaña A, Stewart AF. Diabetes mellitus-advances and challenges in human β-cell proliferation. *Nat Rev Endocrinol*. February 2015. doi:10.1038/nrendo.2015.9.

261. Trott J, Tan E-K, Ong S, et al. Long-Term Culture of Self-renewing Pancreatic Progenitors Derived from Human Pluripotent Stem Cells. *Stem Cell Reports*. 2017;8(6):1675-1688. doi:10.1016/j.stemcr.2017.05.019.

262. Schulz TC, Young HY, Agulnick AD, et al. A Scalable System for Production of Functional Pancreatic Progenitors from Human Embryonic Stem Cells. Lynn FC, ed. *PLoS ONE*. 2012;7(5):e37004. doi:10.1371/journal.pone.0037004.

263. Bruin JE, Rezania A, Xu J, et al. Maturation and function of human embryonic stem cell-derived pancreatic progenitors in macroencapsulation devices following transplant into mice. *Diabetologia*. 2013;56(9):1987-1998. doi:10.1007/s00125-013-2955-4.

264. van der Torren CR, Zaldumbide A, Duinkerken G, et al. Immunogenicity of human embryonic stem cell-derived beta cells. *Diabetologia*. 2017;60(1):126-133. doi:10.1007/s00125-016-4125-y.

265. Motté E, Szepessy E, Suenens K, et al. Composition and function of macroencapsulated human embryonic stem cell-derived implants: comparison with clinical human islet cell grafts. *Am J Physiol Endocrinol Metab*. 2014;307(9):E838-E846. doi:10.1152/ajpendo.00219.2014.

266. Robert T, De Mesmaeker I, Stangé GM, et al. Functional Beta Cell Mass from Device-Encapsulated hESC-Derived Pancreatic Endoderm Achieving Metabolic Control. *Stem Cell Reports*. 2018;10(3):739-750. doi:10.1016/j.stemcr.2018.01.040.

267. Lemaire LA, Goulley J, Kim YH, et al. Bicaudal C1 promotes pancreatic NEUROG3+ endocrine progenitor differentiation and ductal morphogenesis. *Development*. 2015;142(5):858-870. doi:10.1242/dev.114611.

268. Henley KD, Stanescu DE, Kropp PA, et al. Threshold-Dependent Cooperativity of Pdx1 and Oc1 in Pancreatic Progenitors Establishes Competency for Endocrine Differentiation and β-Cell Function. *Cell Rep*. 2016;15(12):2637-2650. doi:10.1016/j.celrep.2016.05.040.

269. Krentz NAJ, van Hoof D, Li Z, et al. Phosphorylation of NEUROG3 Links Endocrine Differentiation to the Cell Cycle in Pancreatic Progenitors. *Dev Cell*. 2017;41(2):129–142.e6. doi:10.1016/j.devcel.2017.02.006.

270. Azzarelli R, Hurley C, Sznurkowska MK, et al. Multi-site Neurogenin3 Phosphorylation Controls Pancreatic Endocrine Differentiation. *Dev Cell*. 2017;41(3):274-286.e275. doi:10.1016/j.devcel.2017.04.004.

271. Sneddon JB, Borowiak M, Melton DA. Self-renewal of embryonic-stem-cell-derived progenitors by organ-matched mesenchyme. *Nature*. 2012;491(7426):765-768. doi:10.1038/nature11463.

272. Jiang F-X, Morahan G. Pancreatic stem cells: from possible to probable. *Stem Cell Rev*. 2012;8(3):647-657. doi:10.1007/s12015-011-9333-8.

273. Haumaitre C, Lenoir O, Scharfmann R. Histone deacetylase inhibitors modify pancreatic cell fate determination and amplify endocrine progenitors. *Mol Cell Biol*. 2008;28(20):6373-6383. doi:10.1128/MCB.00413-08.

274. Loh KM, Ang LT, Zhang J, et al. Efficient endoderm induction from human pluripotent stem cells by logically directing signals controlling lineage bifurcations. *Cell Stem Cell*. 2014;14(2):237-252. doi:10.1016/j.stem.2013.12.007.

275. Edlund H. Organogenesis: Pancreatic organogenesis — developmental mechanisms and implications for therapy. *Nat Rev Genet*. 2002;3(7):524-532. doi:10.1038/nrg841.

276. Carolan PJ, Melton DA. New findings in pancreatic and intestinal endocrine development to advance regenerative medicine. *Curr Opin Endocrinol Diabetes Obes*. 2013;20(1):1-7. doi:10.1097/MED.0b013e32835bc380.

277. Tiso N, Moro E, Argenton F. Zebrafish pancreas development. *Mol Cell Endocrinol*. 2009;312(1-2):24-30. doi:10.1016/j.mce.2009.04.018.

278. King A, Bowe J. Animal models for diabetes: Understanding the pathogenesis and finding new treatments. *Biochem Pharmacol*. 2016;99:1-10. doi:10.1016/j.bcp.2015.08.108.

279. Lyttle BM, Li J, Krishnamurthy M, et al. Transcription factor expression in the developing human fetal endocrine pancreas. *Diabetologia*. 2008;51(7):1169-1180. doi:10.1007/s00125-008-1006-z.

280. Liu Y, Beyer A, Aebersold R. On the Dependency of Cellular Protein Levels on mRNA Abundance. *Cell*. 2016;165(3):535-550. doi:10.1016/j.cell.2016.03.014.

281. Bechard ME, Bankaitis ED, Hipkens SB, et al. Precommitment low-level Neurog3 expression defines a long-lived mitotic endocrine-biased progenitor pool that drives production of endocrine-committed cells. *Genes Dev*. 2016;30(16):1852-1865. doi:10.1101/gad.284729.116.

282. Offield MF, Jetton TL, Labosky PA, et al. PDX-1 is required for pancreatic outgrowth and differentiation of the rostral duodenum. *Development*. 1996;122(3):983-995.

283. Ahlgren U, Jonsson J, Edlund H. The morphogenesis of the pancreatic mesenchyme is uncoupled from that of the pancreatic epithelium in IPF1/PDX1-deficient mice. *Development*. 1996;122(5):1409-1416.

284. Stoffers DA, Zinkin NT, Stanojevic V, Clarke WL, Habener JF. Pancreatic agenesis attributable to a single nucleotide deletion in the human IPF1 gene coding sequence. *Nat Genet*. 1997;15(1):106-110. doi:10.1038/ng0197-106.

285. Seymour PA, Freude KK, Dubois CL, Shih HP, Patel NA, Sander M. A dosage-dependent requirement for Sox9 in pancreatic endocrine cell formation. *Developmental Biology*. 2008;323(1):19-30. doi:10.1016/j.ydbio.2008.07.034.

286. Lynn FC, Smith SB, Wilson ME, Yang KY, Nekrep N, German MS. Sox9 coordinates a transcriptional network in pancreatic progenitor cells. *Proc Natl Acad Sci USA*. 2007;104(25):10500-10505. doi:10.1073/pnas.0704054104.

287. Jonsson J, Carlsson L, Edlund T, Edlund H. Insulin-promoter-factor 1 is required for pancreas development in mice. *Nature*. 1994;371(6498):606-609. doi:10.1038/371606a0.

288. Shih HP, Seymour PA, Patel NA, et al. A Gene Regulatory Network Cooperatively Controlled by Pdx1 and Sox9 Governs Lineage Allocation of Foregut Progenitor Cells. *Cell Rep*. 2015;13(2):326-336. doi:10.1016/j.celrep.2015.08.082.

289. Seymour PA, Shih HP, Patel NA, et al. A Sox9/Fgf feed-forward loop maintains pancreatic organ identity. *Development*. 2012;139(18):3363-3372. doi:10.1242/dev.078733.

290. Tiedemann HB, Schneltzer E, Beckers J, Przemeck GKH, Hrabě de Angelis M. Modeling coexistence of oscillation and Delta/Notch-mediated lateral inhibition in pancreas development and neurogenesis. *J Theor Biol*. 2017;430:32-44. doi:10.1016/j.jtbi.2017.06.006.

291. Moffat JG, Rudolph J, Bailey D. Phenotypic screening in cancer drug discovery - past, present and future. *Nat Rev Drug Discov*. 2014;13(8):588-602. doi:10.1038/nrd4366.

292. Swinney DC, Anthony J. How were new medicines discovered? *Nat Rev Drug Discov*. 2011;10(7):507-519. doi:10.1038/nrd3480.

293. Sato T, Vries RG, Snippert HJ, et al. Single Lgr5 stem cells build crypt-villus structures in vitro without a mesenchymal niche. *Nature*. 2009;459(7244):262-265. doi:10.1038/nature07935.

294. Conti L, Pollard SM, Gorba T, et al. Niche-independent symmetrical self-renewal of a mammalian tissue stem cell. Lovell-Badge R, ed. *PLoS Biol*. 2005;3(9):e283. doi:10.1371/journal.pbio.0030283.

295. Ullah I, Subbarao RB, Rho GJ. Human mesenchymal stem cells - current trends and future prospective. *Biosci Rep*. 2015;35(2):1-18. doi:10.1042/BSR20150025.

296. Zhao Y, Ding S. A high-throughput siRNA library screen identifies osteogenic suppressors in human mesenchymal stem cells. *Proc Natl Acad Sci USA*. 2007;104(23):9673-9678. doi:10.1073/pnas.0703407104.

297. Huang AH, Motlekar NA, Stein A, Diamond SL, Shore EM, Mauck RL. High-throughput screening for modulators of mesenchymal stem cell chondrogenesis. *Ann Biomed Eng*. 2008;36(11):1909-1921. doi:10.1007/s10439-008-9562-4.

298. Brey DM, Motlekar NA, Diamond SL, Mauck RL, Garino JP, Burdick JA. High-throughput screening of a small molecule library for promoters and inhibitors of mesenchymal stem cell osteogenic differentiation. *Biotechnol Bioeng*. 2011;108(1):163-174. doi:10.1002/bit.22925.

299. Dor Y, Brown J, Martinez OI, Melton DA. Adult pancreatic beta-cells are formed by self-duplication rather than stem-cell differentiation. *Nature*. 2004;429(6987):41-46. doi:10.1038/nature02520.

300. Teta M, Rankin MM, Long SY, Stein GM, Kushner JA. Growth and regeneration of adult beta cells does not involve specialized progenitors. *Dev Cell*. 2007;12(5):817-826. doi:10.1016/j.devcel.2007.04.011.

301. Meier JJ, Butler AE, Saisho Y, et al. Beta-cell replication is the primary mechanism subserving the postnatal expansion of beta-cell mass in humans. *Diabetes*. 2008;57(6):1584-1594. doi:10.2337/db07-1369.

302. Miki R, Tatsumi N, Matsumoto K, Yokouchi Y. New primary culture systems to study the differentiation and proliferation of mouse fetal hepatoblasts. *Am J Physiol Gastrointest Liver Physiol*. 2008;294(2):G529-G539. doi:10.1152/ajpgi.00412.2007.

303. Sugiyama T, Benitez CM, Ghodasara A, et al. Reconstituting pancreas development from purified progenitor cells reveals genes essential for islet differentiation. *Proc Natl Acad Sci USA*. 2013;110(31):12691-12696. doi:10.1073/pnas.1304507110.

304. Greggio C, De Franceschi F, Figueiredo-Larsen M, et al. Artificial three-dimensional niches deconstruct pancreas development in vitro. *Development*. 2013;140(21):4452-4462. doi:10.1242/dev.096628.

305. Bonfanti P, Nobecourt E, Oshima M, et al. Ex Vivo Expansion and Differentiation of Human and Mouse Fetal Pancreatic Progenitors Are Modulated by Epidermal Growth Factor. *Stem Cells Dev*. 2015;24(15):1766-1778. doi:10.1089/scd.2014.0550.

306. Noguchi H, Saitoh I, Kataoka HU, Watanabe M, Noguchi Y, Fujiwara T. Culture Conditions for Mouse Pancreatic Stem Cells. *Cell Med*. 2013;5(2-3):63-68. doi:10.3727/215517913X666495.

307. Noguchi H, Oishi K, Ueda M, et al. Establishment of mouse pancreatic stem cell line. *Cell Transplant*. 2009;18(5):563-571.

308. Georgia S, Soliz R, Li M, Zhang P, Bhushan A. p57 and Hes1 coordinate cell cycle exit with self-renewal of pancreatic progenitors. *Developmental Biology*. 2006;298(1):22-31. doi:10.1016/j.ydbio.2006.05.036.

309. Miralles F, Serup P, Cluzeaud F, Vandewalle A, Czernichow P, Scharfmann R. Characterization of beta cells developed in vitro from rat embryonic pancreatic epithelium. *Dev Dyn*. 1999;214(2):116-126. doi:10.1002/(SICI)1097-0177(199902)214:2<116::AID-AJA2>3.0.CO;2-M.

310. Attali M, Stetsyuk V, Basmaciogullari A, et al. Control of beta-cell differentiation by the pancreatic mesenchyme. *Diabetes*. 2007;56(5):1248-1258. doi:10.2337/db06-1307.

311. Cras-Méneur C, Elghazi L, Czernichow P, Scharfmann R. Epidermal growth factor increases undifferentiated pancreatic embryonic cells in vitro: a balance between proliferation and differentiation. *Diabetes*. 2001;50(7):1571-1579.

312. Elghazi L, Cras-Méneur C, Czernichow P, Scharfmann R. Role for FGFR2IIIb-mediated signals in controlling pancreatic endocrine progenitor cell proliferation. *Proc Natl Acad Sci USA*. 2002;99(6):3884-3889. doi:10.1073/pnas.062321799.

313. Duvillie B, Attali M, Bounacer A, Ravassard P, Basmaciogullari A, Scharfmann R. The mesenchyme controls the timing of pancreatic beta-cell differentiation. *Diabetes*. 2006;55(3):582-589.

314. Ornitz DM, Itoh N. The Fibroblast Growth Factor signaling pathway. *Wiley Interdiscip Rev Dev Biol*. 2015;4(3):215-266. doi:10.1002/wdev.176.

315. Tojo M, Hamashima Y, Hanyu A, et al. The ALK-5 inhibitor A-83-01 inhibits Smad signaling and epithelial-to-mesenchymal transition by transforming growth factor-beta. *Cancer Sci*. 2005;96(11):791-800. doi:10.1111/j.1349-7006.2005.00103.x.

316. Zhu S, Russ HA, Wang X, et al. Human pancreatic beta-like cells converted from fibroblasts. *Nat Commun*. 2016;7:10080. doi:10.1038/ncomms10080.

317. Gasca S, Canizares J, De Santa Barbara P, et al. A nuclear export signal within the high mobility group domain regulates the nucleocytoplasmic translocation of SOX9 during sexual determination. *Proc Natl Acad Sci USA*. 2002;99(17):11199-11204. doi:10.1073/pnas.172383099.

318. Malki S, Nef S, Notarnicola C, et al. Prostaglandin D2 induces nuclear import of the sex-determining factor SOX9 via its cAMP-PKA phosphorylation. *EMBO J*. 2005;24(10):1798-1809. doi:10.1038/sj.emboj.7600660.

319. Pieper FR, Van de Klundert FA, Raats JM, et al. Regulation of vimentin expression in cultured epithelial cells. *Eur J Biochem*. 1992;210(2):509-519.

320. Landsman L, Nijagal A, Whitchurch TJ, et al. Pancreatic mesenchyme regulates epithelial organogenesis throughout development. Vidal-Puig AJ, ed. *PLoS Biol*. 2011;9(9):e1001143. doi:10.1371/journal.pbio.1001143.

321. Nostro MC, Sarangi F, Ogawa S, et al. Stage-specific signaling through TGF family members and WNT regulates patterning and pancreatic specification of human pluripotent stem cells. *Development*. 2011;138(7):1445-1445. doi:10.1242/dev.065904.

322. Sanvito F, Herrera PL, Huarte J, et al. TGF-beta 1 influences the relative development of the exocrine and endocrine pancreas in vitro. *Development*. 1994;120(12):3451-3462.

323. Miralles F, Battelino T, Czernichow P, Scharfmann R. TGF-beta plays a key role in morphogenesis of the pancreatic islets of Langerhans by controlling the activity of the matrix metalloproteinase MMP-2. *J Cell Biol*. 1998;143(3):827-836.

324. Tulachan SS, Tei E, Hembree M, et al. TGF-beta isoform signaling regulates secondary transition and mesenchymal-induced endocrine development in the embryonic mouse pancreas. *Developmental Biology*. 2007;305(2):508-521. doi:10.1016/j.ydbio.2007.02.033.

325. Vincent SD, Dunn NR, Hayashi S, Norris DP, Robertson EJ. Cell fate decisions within the mouse organizer are governed by graded Nodal signals. *Genes Dev*. 2003;17(13):1646-1662. doi:10.1101/gad.1100503.

326. McLean AB, D'Amour KA, Jones KL, et al. Activin a efficiently specifies definitive endoderm from human embryonic stem cells only when phosphatidylinositol 3-kinase signaling is suppressed. *STEM CELLS*. 2007;25(1):29-38. doi:10.1634/stemcells.2006-0219.

327. Agren A, Andersson A, Björkén C, et al. Human fetal pancreas: culture and function in vitro. *Diabetes*. 1980;29 Suppl 1:64-69.

328. Sandler S, Andersson A, Schnell A, et al. Tissue culture of human fetal pancreas. Development and function of B-cells in vitro and transplantation of explants to nude mice. *Diabetes*. 1985;34(11):1113-1119.

329. Sandler S, Andersson A, Korsgren O, et al. Tissue culture of human fetal pancreas: growth hormone stimulates the formation and insulin production of islet-like cell clusters. *J Clin Endocrinol Metab*. 1987;65(6):1154-1158. doi:10.1210/jcem-65-6-1154.

330. Sandler S, Andersson A, Korsgren O, et al. Tissue culture of human fetal pancreas. Effects of nicotinamide on insulin production and formation of isletlike cell clusters. *Diabetes*. 1989;38 Suppl 1:168-171.

331. Huang H, Tang X. Phenotypic determination and characterization of nestin-positive precursors derived from human fetal pancreas. *Lab Invest*. 2003;83(4):539-547.

332. Zhang W-J, Xu S-Q, Cai H-Q, et al. Evaluation of islets derived from human fetal pancreatic progenitor cells in diabetes treatment. *Stem Cell Res Ther*. 2013;4(6):141. doi:10.1186/scrt352.

333. Lopez AD, Kayali AG, Hayek A, King CC. Isolation, culture, and imaging of human fetal pancreatic cell clusters. *J Vis Exp*. 2014;(87):e50796-e50796. doi:10.3791/50796.

334. Kemler R, Ozawa M, Ringwald M. Calcium-dependent cell adhesion molecules. *Curr Opin Cell Biol*. 1989;1(5):892-897.

335. Leitinger B, McDowall A, Stanley P, Hogg N. The regulation of integrin function by Ca(2+). *Biochim Biophys Acta*. 2000;1498(2-3):91-98.

336. Beers J, Gulbranson DR, George N, et al. Passaging and colony expansion of human pluripotent stem cells by enzyme-free dissociation in chemically defined culture conditions. *Nat Protoc*. 2012;7(11):2029-2040. doi:10.1038/nprot.2012.130.

337. OTIS EM, BRENT R. Equivalent ages in mouse and human embryos. *Anat Rec*. 1954;120(1):33-63.

338. Ramond C, Glaser N, Berthault C, et al. Reconstructing human pancreatic differentiation by mapping specific cell populations during development. *Elife*. 2017;6:36. doi:10.7554/eLife.27564.

339. Canham MA, Van Deusen A, Brison DR, et al. The Molecular Karyotype of 25 Clinical-Grade Human Embryonic Stem Cell Lines. *Sci Rep*. 2015;5(1):17258. doi:10.1038/srep17258.

340. Self-Renewing Endodermal Progenitor Lines Generated from Human Pluripotent Stem Cells. 2012;10(4):371-384. doi:10.1016/j.stem.2012.02.024.

341. Ameri J, Ståhlberg A, Pedersen J, et al. FGF2 specifies hESC-derived definitive endoderm into foregut/midgut cell lineages in a concentration-dependent manner. *STEM CELLS*. 2010;28(1):45-56. doi:10.1002/stem.249.

342. Hannan NRF, Fordham RP, Syed YA, et al. Generation of multipotent foregut stem cells from human pluripotent stem cells. *Stem Cell Reports*. 2013;1(4):293-306. doi:10.1016/j.stemcr.2013.09.003.

343. Rezania A, Bruin JE, Riedel MJ, et al. Maturation of human embryonic stem cell-derived pancreatic progenitors into functional islets capable of treating pre-existing diabetes in mice. *Diabetes*. 2012;61(8):2016-2029. doi:10.2337/db11-1711.

344. Haldorsen IS, Vesterhus M, Raeder H, et al. Lack of pancreatic body and tail in HNF1B mutation carriers. *Diabet Med*. 2008;25(7):782-787. doi:10.1111/j.1464-5491.2008.02460.x.

345. Kotalova R, Dusatkova P, Cinek O, et al. Hepatic phenotypes of HNF1B gene mutations: a case of neonatal cholestasis requiring portoenterostomy and literature review. *World J Gastroenterol*. 2015;21(8):2550-2557. doi:10.3748/wjg.v21.i8.2550.

346. Cai Q, Bonfanti P, Sambathkumar R, et al. Prospectively isolated NGN3-expressing progenitors from human embryonic stem cells give rise to pancreatic endocrine cells. *Stem Cells Transl Med*. 2014;3(4):489-499. doi:10.5966/sctm.2013-0078.

347. Qu X, Afelik S, Jensen JN, et al. Notch-mediated post-translational control of Ngn3 protein stability regulates pancreatic patterning and cell fate commitment. *Developmental Biology*. 2013;376(1):1-12. doi:10.1016/j.ydbio.2013.01.021.

348. Klochendler A, Weinberg-Corem N, Moran M, et al. A transgenic mouse marking live replicating cells reveals in vivo transcriptional program of proliferation. *Dev Cell*. 2012;23(4):681-690. doi:10.1016/j.devcel.2012.08.009.

349. Yu H, Yao X. Cyclin B1: conductor of mitotic symphony orchestra. *Cell Res*. 2008;18(2):218-220. doi:10.1038/cr.2008.20.

350. Pines J, Hunter T. Isolation of a human cyclin cDNA: evidence for cyclin mRNA and protein regulation in the cell cycle and for interaction with p34cdc2. *Cell*. 1989;58(5):833-846.

351. Wolf F, Sigl R, Geley S. “... The end of the beginning”: cdk1 thresholds and exit from mitosis. *Cell Cycle*. 2007;6(12):1408-1411.

352. Taylor CJ, Peacock S, Chaudhry AN, Bradley JA, Bolton EM. Generating an iPSC bank for HLA-matched tissue transplantation based on known donor and recipient HLA types. *Cell Stem Cell*. 2012;11(2):147-152. doi:10.1016/j.stem.2012.07.014.

353. Human embryonic stem cell derived islet progenitors mature inside an encapsulation device without evidence of increased biomass or cell escape. 2014;12(3):807-814. doi:10.1016/j.scr.2014.03.003.

354. Rezania A, Riedel MJ, Wideman RD, et al. Production of functional glucagon-secreting α-cells from human embryonic stem cells. *Diabetes*. 2011;60(1):239-247. doi:10.2337/db10-0573.

355. Cebola I, Rodríguez-Seguí SA, Cho CH-H, et al. TEAD and YAP regulate the enhancer network of human embryonic pancreatic progenitors. *Nat Cell Biol*. 2015;17(5):615-626. doi:10.1038/ncb3160.

356. Shamblott MJ, O'Driscoll ML, Gomez DL, McGuire DL. Neurogenin 3 is regulated by neurotrophic tyrosine kinase receptor type 2 (TRKB) signaling in the adult human exocrine pancreas. *Cell Commun Signal*. 2016;14(1):23. doi:10.1186/s12964-016-0146-x.

357. Cheng C-W, Villani V, Buono R, et al. Fasting-Mimicking Diet Promotes Ngn3-Driven β-Cell Regeneration to Reverse Diabetes. *Cell*. 2017;168(5):775–788.e12. doi:10.1016/j.cell.2017.01.040.

358. Dewari PS, Southgate B, Mccarten K, et al. An efficient and scalable pipeline for epitope tagging in mammalian stem cells using Cas9 ribonucleoprotein. *Elife*. 2018;7:87. doi:10.7554/eLife.35069.